The Performance of Jacked Pipes

by

Kevin John Ripley

A Thesis submitted for the
Degree of Doctor of Philosophy
at the University of Oxford

Magdalen College   Hilary Term, 1989.

The Performance of Jacked Pipes.

Kevin J. Ripley

Magdalen College, University of Oxford.

A Thesis submitted for the Degree of Doctor of Philosophy.

Hilary Term, 1989.

ABSTRACT

Pipejacking is a tunnel construction technique which is increasing in popularity, but fundamental research is necessary to fully understand the extent of its possible uses and limitations. This dissertation reports on laboratory research into the performance of reinforced concrete pipes, assessment of pipe joints and the use of joint packing materials.

The research has addressed specific problems which the tunnelling fraternity have raised. Model pipes have been constructed at scales of 1:6 and 1:10.5 using reinforced microconcrete and they have been tested in either a sand filled chamber or between supporting yokes. Current British Standard tests have been used as a control on the quality of pipe manufacture. Data have been recorded of changes in soil pressures, pipe geometry and strains induced in the pipes. The tests have investigated deformation of pipes, deflection angles between consecutive pipes, distribution of stress concentrations and the effects of the use of joint packing materials on allowable jacking loads and induced stress magnitudes in the pipes.

A review of current pipejacking practice is presented and recommendations for the control and supervision of pipejacking operations are made. The conclusions include recommendations for fieldwork monitoring and implications of this stage of the research to industry. Recommendations are made for maximum installation jacking loads for any given deflection angle between pipes. The prediction of friction angles at the pipe soil interface have been assessed at different soil stress levels and new recommendations are made. The effects of cyclic loading on the pipejacking system and transfer from jacking load to ground loading once the pipes are installed are presented. The criteria used in the selection of a recommended joint packing material for use in jacking operations have been included. Failure modes of pipes are stated and recommendations are made for pipe design, installation and monitoring to predict and prevent such failures.

This dissertation is the report on the first stage of an overall programme of research which is now set to progress with monitoring of pipejacking operations on several construction sites.

Contents

ABSTRACT

Acknowledgements

Symbols

a	Initial packing material thickness
Δa	Packing material compression
b	Contact breadth of packing material
D	Pipe external diameter
d	Radius of pipe end profile
E	Elastic modulus
e_{min}	Minimum voids ratio
e_{max}	Maximum voids ratio
F	Applied jacking load
H	Horizontal pipe movement
I_D	Relative density
I_R	Relative dilatancy index
K_0	Coefficient of earth pressure at rest
L	Pipe length
M_c	Bending moment at crown
M_s	Bending moment at springing point
P	Total soil load on pipe
p'	Mean effective soil stress
R	External radius of pipe
r	Internal radius of pipe
t	Wall thickness of pipe
V	Vertical pipe movement
z	Diametrical contact width at pipe joint
α	Radial angle around pipe
β	Angular deflection at pipe joints
γ	Unit weight of soil

δ	Angle of friction between pipe and soil
$\varepsilon 1$	Major principal strain
$\varepsilon 2$	Minor principal strain
ν	Poisson's ratio
σ_c	Maximum induced stress
σ_h	Total horizontal soil stress
σ_j	Maximum stress at pipe joint
σ_p	Radial stress on outside of pipe
σ_v	Total vertical soil stress
ϕ	Internal angle of friction of the sand
ϕ'_{crit}	Critical state friction angle
ω	Direction of principal strain

CHAPTER 1

INTRODUCTION

Jacked pipes are used in the Civil Engineering industry for the installation of underground pipelines by tunnelling using a trenchless construction technique called pipejacking. The system has been used for many years but its increasing world-wide popularity and use over the last decade has led to the need for a fundamental assessment of its uses and limitations. A programme of research, beginning with the laboratory modelling presented in this dissertation, has been instigated. It will lead onto correlation with fieldwork and monitoring of prototype pipejacks.

Problems with pipejacking were reported by Shullock (1982) when a contract encountered unexpected ground conditions which eventually resulted in failure of some of the pipes being used for construction by pipejacking. The Pipe Jacking Association (PJA) and Construction Industries Research and Information Association (CIRIA) had already undertaken a review of pipejacking which was published by Craig (1983). This outlined some specific topics for investigation and research which were taken up by the PJA with the commencement of this research programme. The principal topics for investigation were outlined as: friction loads in different ground conditions; behaviour of pipe joints; cyclic loading effects; reduction of frictional resistance and prediction of installation forces. Research began with investigations into load capacities and distribution of loads in model pipes.

The laboratory work reported here has concentrated on the first three points. Prediction and reduction of friction forces will become more clear as a result of the overall programme. The use of scale models and testing in the laboratory has enabled conditions during tests to be controlled and has led to reproduction of the pipe failure modes occasionally experienced on pipejacking contracts. This has enabled assessment of the reasons for failures and conclusions as to how they can be prevented.

The report of the laboratory research begins with Chapter 2 which gives a background to the pipejacking method of construction and its uses. It continues to explain the reasons for the research, what it is hoped might be achieved and a review of previous microconcrete modelling techniques. A section in the Chapter presents information about current practice in pipe design and manufacture and literature about load transfer at joints between pipes. Chapter 3 continues to introduce the design of the apparatus used in the laboratory and how tests were controlled and monitored.

The techniques of modelling investigated for manufacture of jacking pipes are presented in Chapter 4. Methods of controlling standards and quality in model preparation are reviewed and reasons for the selection of the microconcrete mix and reinforcement are stated.

Chapters 5 to 8 deal in turn with four different test series. Chapter 5 presents tests and results carried out on model pipes in a sand filled stress controlled chamber. Results are included assessing how pipes move and interact with the sand when axial load is applied to them. As a result of some of the findings in this test series, apparatus was designed to maintain pipes in misaligned positions while axial load was applied. Results from this test series are presented in Chapter 6 which reports on the results of tests modelling the two most common modes of load application. Diagonal loading and edge loading of the pipes were used in the tests.

Joint packing materials and their changing characteristics when subjected to cyclic loading are the subject of Chapter 7. Predictions of axial load capacities of prototype pipes can begin to be made as a result of these tests. Recommendations are made for the most suitable packing material to be used in pipejacking. Chapter 8 assesses interaction at the pipe/soil interface and how the friction angle at the interface affects predictions of jacking load.

The results from all the test series are reviewed and discussed in Chapter 9. Distribution of soil stresses on the pipe are analysed. Changes of pipe alignments during misaligned tests are related to changes in the orientation of pipes during prototype pipejacking. Axial load capacities of pipes are assessed and figures tabulated for capacities at various angular deflections. The use of profiled joint packing materials is reviewed and results of the angle of friction between the pipe and sand are discussed. British Standard tests on pipes are presented and results are assessed for improved control and specification of the tests.

The conclusions from the research are drawn together in Chapter 10 where recommendations for the future fieldwork monitoring in the project are made. Control and management of pipejacking operations are assessed and how, if at all, the pipejackers' and designers' philosophies might be encouraged to change as a result of the continuing research programme.

CHAPTER 2

BACKGROUND

2.1 Introduction

Pipejacking is a tunnel construction technique used to install pipes into a near horizontally excavated hole. It is being used more frequently in preference to trenching or segmental tunnelling; pipejacks have increased their United Kingdom market share from 10% to over 30% during the last five years. The advent of microtunnelling and its increasing use will increase this figure. Pipejacking is used to avoid interference with surface traffic, services and the environment. Increasing pressure is being brought upon authorities to use the technique as it is a 'minimum disruption' method and popular in urban areas for infrastructure renewal. Pipejacking techniques are used to provide pipelines, conduits or access for sewers, gas and water mains, electric and telephone cables, sewer relining, subways and land drainage.

Installation of pipes by jacking requires large forces to be provided by hydraulic powerpacks and rams. A thrust ring distributes these forces around the circumference of the pipe being jacked. Jacking equipment is accommodated in a thrust pit, shown in Plate 2.1, with a thrust wall to provide a reaction against which jacking forces can be applied, as depicted in Figure 2.1.

Key

① Jacking Shield
② Concrete Lead Pipe
③ Interjack Station
④ Interjack Pipe
⑤ Steel Thrust Ring
⑥ Hydraulic Jacks
⑦ Steel Pressure Plates
⑧ Concrete Thrust Wall
⑨ Guide Rails
⑩ Power Pack

(Note: The above is only a diagrammatic representation)
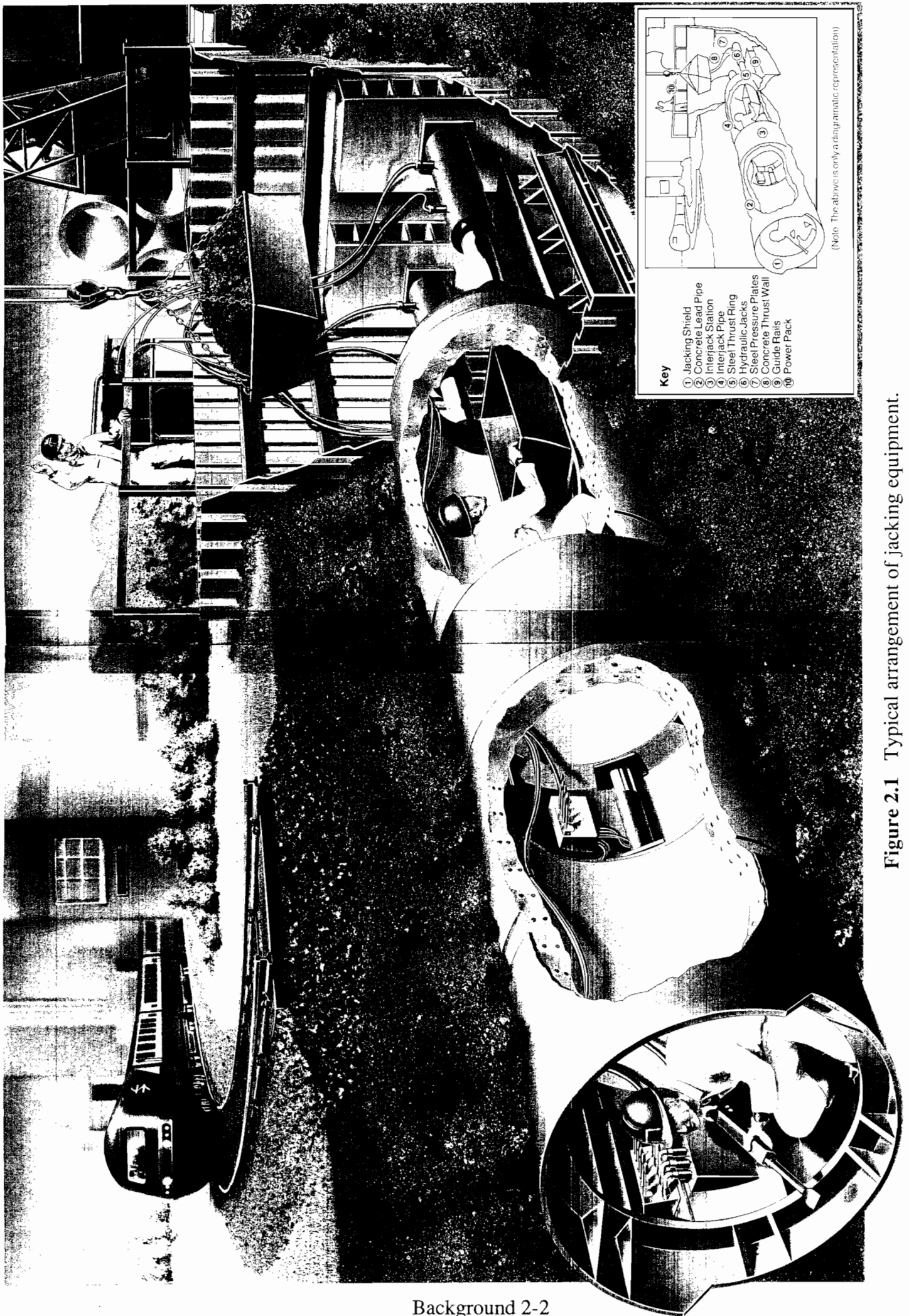
Figure 2.1 Typical arrangement of jacking equipment.
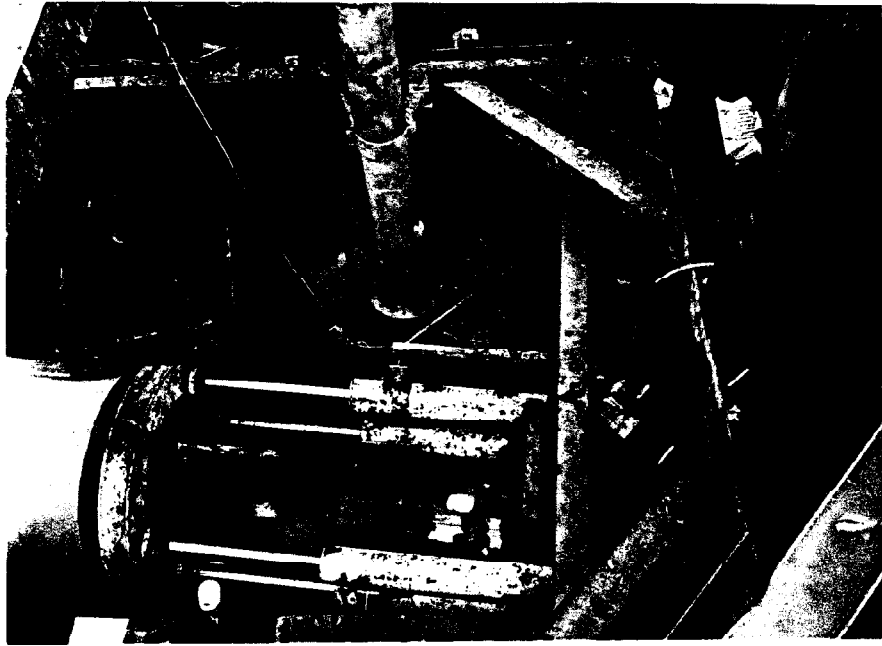
Plate 2.1 A view of a typical pipejacking thrust pit.

Excavation is normally carried out within a shield in front of the pipeline being jacked. The ground is excavated using pneumatic tools, hydraulic shovels or boring machines, the soil being transported along the pipeline to the surface and pipes advanced as the ground is mined. Corrections to the alignment of the pipes are made using hydraulic rams in the shield in conjunction with frequent surveying to fixed reference points.

2.2 Pipejacking

The use of pipejacking has become common place during the last two decades. The earliest recorded use of the pipejacking method was in America about 1910, Richardson and Mayo (1941). The basic principles of the technique have been presented in detail by the American Pipe Jacking Association (1960), Richardson (1970), Hough (1974), Drennon (1979) and Clark and Thompson (1983). The British Pipe Jacking Association publish notes giving guidance on design and practice (Pipe Jacking Association 1981 and 1986). The increasing use of modern technology and a competitive tendering market have led to many innovative methods being introduced in recent years. Advances in technology have been particularly significant in Japan and West Germany, where pipes from 200mm to 4000mm diameter are jacked in almost any ground conditions, to alignments which include horizontal and vertical curves, over ever increasing distances.

The introduction of mechanised excavation has increased jacking distances. In Great Britain, Wallis (1982) reports an 1800mm diameter pipejack, 460m long in London Clay; Byles (1983) reports an increase in length to 560m in water bearing sands and gravels; Winfield (1986) records 690m of 1950mm diameter pipes jacked through sandstone and siltstone, whilst in 1988, 1500m of 3300mm external diameter pipes were jacked in mixed ground conditions around a number of curves, Dumbleton (1988). A point is reached in most construction contracts when it becomes more economic to excavate a thrust shaft and commence a new pipejack, rather than be delayed by increasing muck haulage distances and costs, but improvements in techniques are constantly increasing this distance.

New methods of construction and new materials are constantly being developed and implemented. Richardson and Scruby (1981) reported on the development of the Uni-Tunnel system in which pipes are jacked forward by inflatable bladders positioned between successive pipes. A new jointing profile is reported by Cole (1986) used for pipejacking in

Greenwich and Newman (1986) reports on the use of vitrified clay pipes in Newcastle. White et al. (1988) presented details of the use of new joint packing materials, and microtunnel technology using unreinforced concrete pipes in a joint venture project based in Yorkshire.

A new British Standard for concrete pipejacking pipes in Great Britain is to be published shortly as BS 5911: part 4 (1986 draft). Concrete jacking pipes are generally manufactured by centrifugal spinning or vertical casting using concrete with a 28 day characteristic crushing strength greater than $50N/mm^2$. Pipes are normally reinforced with spiral and longitudinal steel spot welded to form internal and external cages. The specific method of manufacture and material characteristics are dependent upon the manufacturer.

Materials used for manufacturing jacking pipes include:-

1   Unreinforced concrete.

2   Reinforced concrete.

3   Vitrified clay.

4   Glass reinforced plastic.

5   Asbestos cement.

6   Steel and ductile iron.

7   Concrete and resin laminates or composites.

Manufacturers of concrete pipes design their pipes to comply with BS 8110: 1985 and BS 5911: part 4 (1986 draft). The pipes must withstand loadings imposed under the various tests of BS 5911. They are designed to higher standards and strengths if ground conditions or clients' specifications impose more onerous design requirements.

2.3 The need for research

Until 1980, any research carried out into pipejacking was commissioned by individual companies to meet their specific requirements. No attempt was made to collate this research and in the course of time their documentation has been mislaid. The Pipe Jacking Association (PJA) and Construction Industries Research and Information Association (CIRIA) have been instrumental in establishing a research programme with full support from all interested parties. CIRIA undertook a review of pipejacking and published a Technical Note 112, Craig (1983), as a state of the art review, which recommended that the following areas required research:-

1 Friction loads in different ground conditions.

2 Characteristics of joints and joint packing materials.

3 Effects of cyclic loading on pipes.

4 Effects of lubricants in reducing friction.

5 Development of a site investigation test to predict friction forces.

Kirkland (1982) had previously reported on the requirements for pipejacking research when he stated the need for researchers to establish more scientific facts to support a sound concept.

Following publication of the Technical Note 112, a second phase of CIRIA's work involves the collection and analysis of pipejacking data. This relies on contractors answering questionnaires about their jacking contracts. No details of the survey have been published.

CIRIA have published a Technical Note 127, Watson (1987), which is a survey of trenchless construction for underground services. The Note recommends future work in full scale field trials, monitoring by an independent body and recording of detailed statistics relating particularly to the method of installation, materials used and costs. Many of the other techniques

used in trenchless construction have been adopted from the principles of pipejacking. The findings of pipejacking research are often equally applicable to the other trenchless techniques.

Following the recommendations of CIRIA and enthusiasm of the PJA in promoting and supporting research, a project commenced at Oxford University during 1986 and is the subject of this thesis. Milligan (1986), reports on current research programmes being undertaken.

Failures of clayware jacking pipes have been reported (Winney 1987) as occurring on a Scottish contract. Large numbers of pipes were cracking, prompting research into joint details for clayware pipes. More recently in Germany, pipes were seen to crack due to excess jacking load and poor control of alignment (Winney 1988a and Winney 1988b). It should be noted that current production techniques do not permit reinforcement of clay pipes. Clayware pipes are only used on pipejacks less than 600mm in diameter. It is understood that allowable jacking stresses for clay pipes are less than for concrete pipes and economic considerations most often rule out their use.

2.4 Oxford research

Pipejacking research at Oxford University was commenced by the author with support from the Science and Engineering Research Council (SERC) for equipment and supervision and with the PJA and Concrete Pipe Association (CPA) providing further finance for staff, together with invaluable guidance, advice and industrial involvement. There was limited knowledge about the behaviour of jacked pipes during installation and disagreement on the explanations of some failures in the field. Research proposals were broadly based to allow a specific direction to be chosen once a basic understanding of the problems had been achieved. The initial research programme presented in this thesis is based on laboratory testing of scale models.

The overall objectives of the research are to improve understanding of the loads applied to jacked pipes, both during and after installation and to establish a fieldwork programme. It is intended to make recommendations of the most suitable and economic data collection for the exercise of monitoring performance of full-scale pipejacking operations.

Model test results have a limited application to the prototype behaviour due to the difficulties of modelling precisely many aspects of the problem such as self weight, stress level, stress path and dilation behaviour. Theoretical calculations can be carried out before results of model tests are applied to prototype predictions. Tests can later be carried out on prototype pipejacks to correlate to model test results, but with a large saving in cost.

Bassett (1979), outlines the advantages of small scale physical models for studying soil mechanics problems:-

1   Testing models is relatively cheap, easily modified and quick to conduct.
2   Soil properties can be chosen within known limits.
3   Simple controlled variations can be introduced one by one as required.
4   Internal movements of soil or rupture lines can be observed.
5   Homogeneity of soil provides easier analysis.
6   Tests are repeatable to provide data for experimental and statistical scatter.

The scale model testing programme at Oxford has been used to investigate the following points:-

1   The distribution of concrete strains during pipejacking and how these change when soil loading transfers to the pipe as it is installed in its final position.
2   Parameters relating the allowable jacking load to the soil type and angular misalignments between consecutive pipes.

3 The distribution of stress concentrations between misaligned pipes, the use of a packing material to reduce these concentrations and to find a suitable joint profile to minimise stresses and retain pipeline watertightness and integrity.

4 The possibility of using a suitable jacking strength test to supplement the existing British Standard tests and to test the compliance of model pipes with BS 5911: part 4 (1986 draft).

5 The effect of soil stress level on the behaviour of the pipes during installation, in particular changes in shape and orientation of the pipes with different applied jacking loads.

6 The most suitable and economic measurements to be made to monitor performance of a full-scale pipe jacking operation.

7 The various failure modes occurring in jacked pipes and how pipes can be designed, installed and monitored to predict and prevent such failures.

2.5 Jacked pipes and their design

The primary loads imposed on a pipejack are:-

1 Installation jacking load.

2 Face resistance during jacking.

3 Ground load, both surcharge and transient.

4 Loads from footings and buildings.

5 Fluid pressure, internal and external.

British manufacturers' design calculations assess compliance of the pipes' strength to withstand loadings imposed on the installed pipe. Allowance for installation loads receives scant attention, possibly due to the uncertainty surrounding loads, stresses and their distribution throughout the jacking cycle.

The British Standard 5911: part 4 (1986 draft) details the test requirements for jacked concrete pipes. The drafting committee were aware at the time of writing that research was required to establish a suitable test to assess a pipe's ability to sustain installation end loads. The forward to the Standard states "The joint face strength test is included in the absence of a suitable jacking strength test. Research is presently being undertaken in order to devise such a test and this may be incorporated in a future revision." The British Standard Institute is looking towards the results of this research programme to provide guidance on a more suitable test.

2.5.1 Joints

The functional requirements of a joint on a jacked pipe are adapted from Clarke (1968) as:-

1 It should be constructed to the standards laid down in BS 5911: part 4 (1986 draft).

2 It should be designed to permit angular and axial movement large enough to tolerate maximum displacement likely to occur, without damage or loss of watertightness.

3 It should be designed to withstand the force applied during installation without detrimental damage.

4 It should remain efficient throughout its working life i.e. use materials that do not change with time or within the exposed environments.

5   It should be simple to make and dismantle in the limited space of the jacking thrust pit.

6   It should remain effective under vibration.

7   It should be capable of withstanding the service loading conditions.

Traditionally jacked pipe joints in the United Kingdom have been an in wall spigot and socket as shown in Figure 2.2a. Disquiet in the industry about the performance of the in wall joint and its ability to transmit longitudinal loads has led to the introduction of new joint details. The most often used of the new joints is shown in Figure 2.2b; the steel collar joint. The main reason for its introduction was the belief that jacking loads would be better transmitted through the centre of the jacked pipe wall rather than its edges. An increase of available end area would improve the pipe's jacking load carrying capacity. Limited design or research was carried out to ascertain the parameters for configuration and performance of the steel collar joint detail. The CIRIA Technical Notes 112 and 127 give many more examples of joint profiles and arrangements used both in the United Kingdom and around the world. The more common of these details are reproduced in Figure 2.3.

RUBBER RING

JOINT PACKING MATERIAL

EXTERNAL DIAMETER

INTERNAL DIAMETER
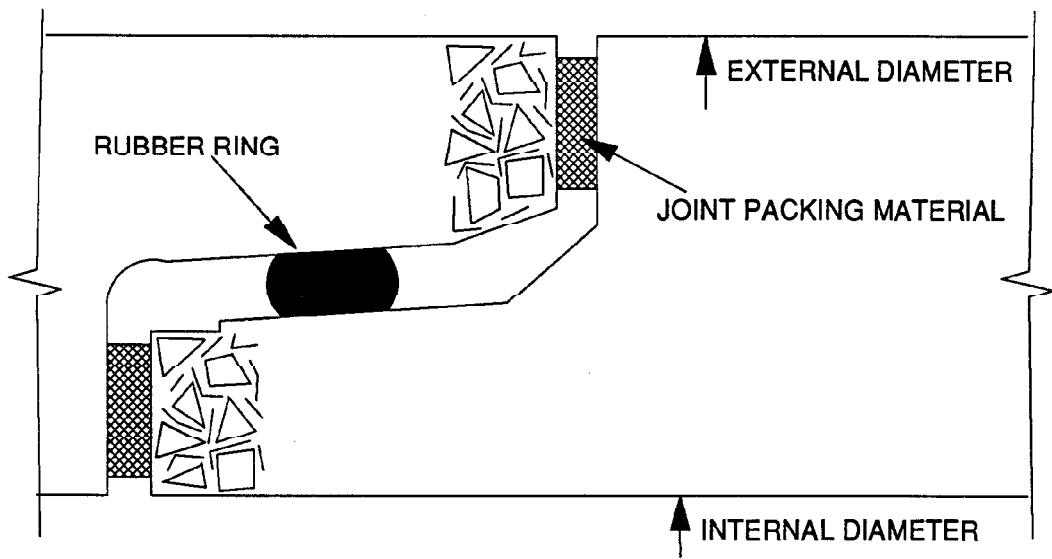
a) IN WALL SPIGOT AND SOCKET JOINT

STEEL COLLAR

EXTERNAL DIAMETER

RUBBER SEAL

JOINT PACKING MATERIAL

INTERNAL DIAMETER
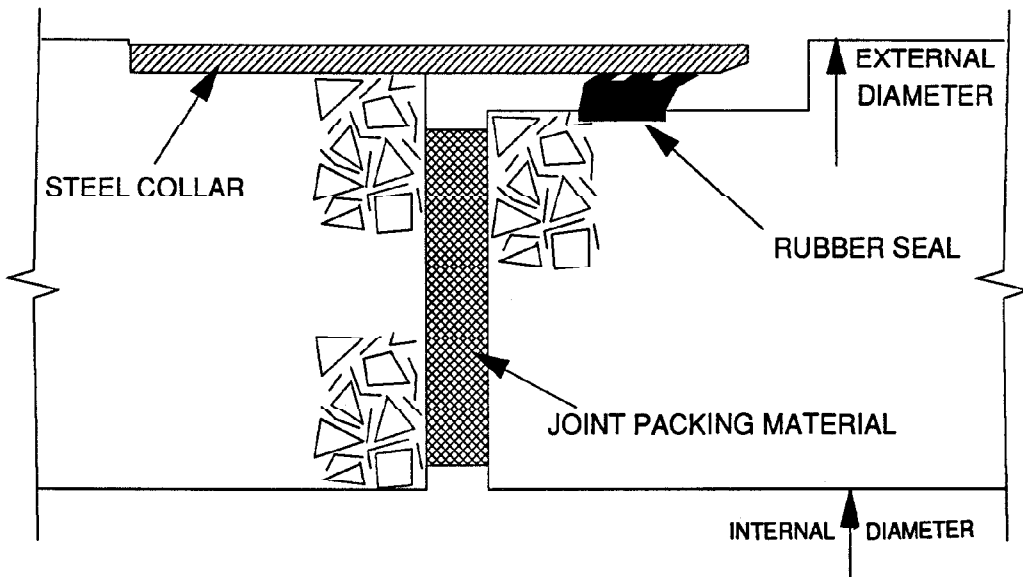
b) STEEL COLLAR JOINT

Figure 2.2 Types of pipe joint common in Britain.

GRP COLLAR

SEALING RING

ADHESIVE

INTERNAL DIAMETER

PACKING RING

JOINT FOR GRP JACKING PIPE

SOFT RUBBER RING

STAINLESS STEEL COLLAR

PROFILED SEAL

PACKING RING

INTERNAL DIAMETER

GERMAN CLAYWARE JACKING PIPE JOINT

PACKING

DOWEL

SEAL

DOWEL JOINT (SWISS ORIGIN)
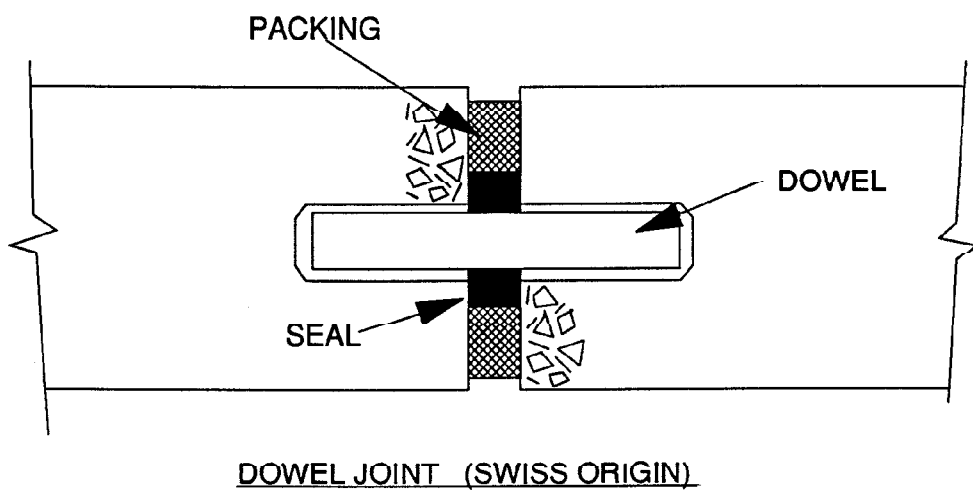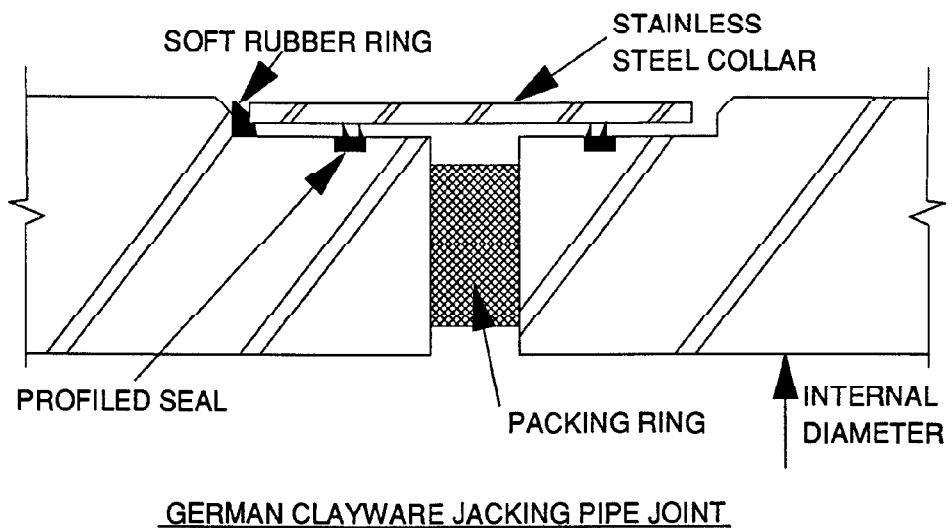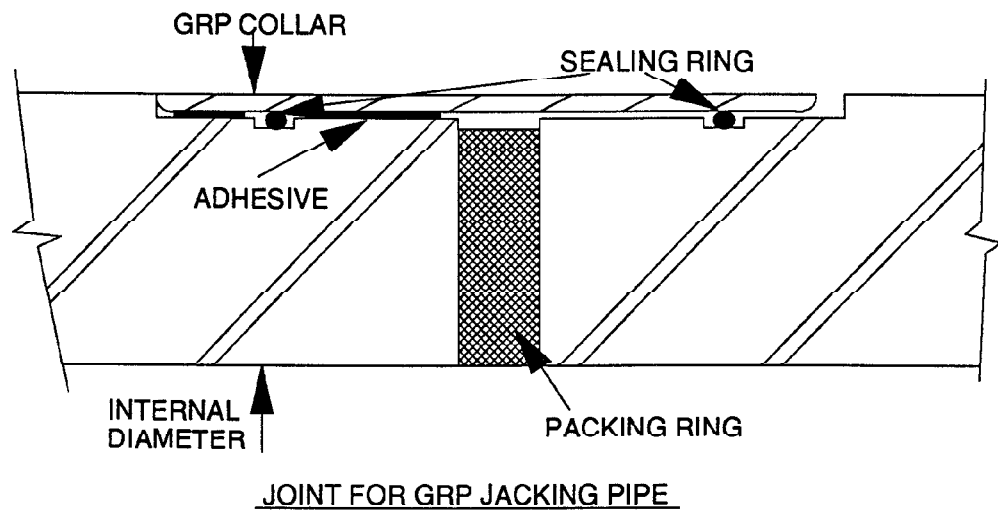
Figure 2.3 Other common pipe joint details.

2.5.2 Pipes

Jacking pipes are designed to withstand the Class H proof load of BS 5911. Pipes are also designed to CP 110: 1972 and BS 8110: 1985 to withstand ground loading conditions only. No specific calculations are carried out to assess a pipe's axial loading capacity.

For the purposes of design it is usual to make the assumption that in ideal jacking conditions the pipes are subjected to an axial load evenly distributed around the circumference of the pipe. A view along a pipejack is shown in Plate 2.2. The worst case is assumed to be the pipe nearest the thrust ring which will be subjected to the maximum jacking force from the rams.
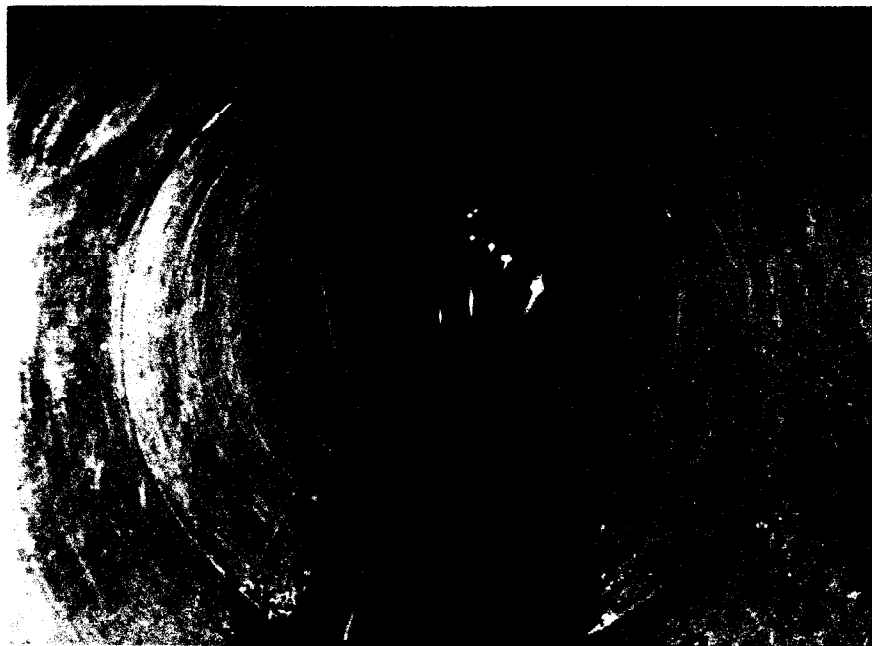
Plate 2.2 General view along a pipejack during construction.

In a typical design example for an 1800mm internal diameter pipe, a jacking load of 10,000kN produces an average direct compression at a pipe's spigot face of $11N/mm^2$ and an average direct compression in the full pipe section of $9N/mm^2$. A manufacturer's qualifying statement might be along the lines that "excessive departure from uniform jacking conditions will reduce the acceptable load. Equally some increase in jacking load may be practicable under uniform conditions. Experience rather than theoretical calculations will be the ultimate guide." No data are quoted, and it is one of the aims of the pipejacking research programme to enable manufacturers and contractors to offer clients and design engineers a theoretically based method for axial load design of pipes for jacking.

British pipe manufacturers specify their pipes as capable of sustaining a uniformly distributed end stress of between 10 and $15N/mm^2$ (dependent on manufacturer and pipe diameter). These figures appear conservative if loads are applied to the full end area of the pipe, but allow for end tolerances and jacking misalignment in an arbitrary fashion.

2.5.3 Manufacture

Until recently the majority of pipes used in the United Kingdom were manufactured with reinforced concrete by centrifugal spinning. During spinning, concrete is poured into pipe moulds in two operations. The centrifugal forces drive out entrained air, but also cause some particle segregation. Two distinct layers can be seen with a layer of cement paste separating them, when a completed pipe is cut.

Pipes are now commonly cast vertically with concrete poured between inner and outer moulds from one end because this method of construction is much safer and cleaner, and requires less skilled personnel for the operation. The moulds have vibrators attached to them which are operated in sequence as the moulds are filled. Some segregation occurs due to the dif-

ference in vibration times from bottom to top of the mould. The top end of the pipe, when cast, has to be hand finished using a trowel which results in a less smooth end profile to the pipe than could have been achieved with the use of end moulds.

2.5.4 Joint packing materials

Compressible joint packing material is recommended by all jacking pipe manufacturers. However, not all are prepared to specify the type of material or advise in any detail on its use. This research project has been investigating various packing materials, to what extent pipe misalignment can be accepted with each type, and where the packing should be positioned.

The purpose of the packing materials is to provide a compressible medium between the two adjacent concrete faces. This aids distribution of stress concentrations over larger areas and avoids concentrations of stress induced by unevenness on the pipe's ends. It should be noted that misalignment between consecutive pipes can result from a lack of pipe end squareness even though they comply with manufacturing tolerances. It is therefore important to be aware of the end squareness of pipes.

2.5.5 Load transfer at joints

The design of joints and distribution of load across their faces has not been investigated in any detail. The Concrete Pipe Association of Australia (1983) published a theory based on material properties, their stress/strain relationship and compressive strengths (Figure 2.4). Since commencement of research at Oxford, Hornung et al. (1987) presented a guide for calculation and design of jacking pipes according to German codes and specifications. It presents the authors' considerations for loading, calculation and dimensioning criteria. The

guide details information considered on a particular contract and presents the design considerations for pipe deflections and a suitable packing material. A summary of this guide's recommendations on packing material and stress distribution at the pipe joint is presented in Figure 2.5 and relates them to jacking pipes around curves. No allowance has been made for pipe elasticity and only the material properties of the timber packing and orientation of the pipe are considered.

Clarke (1968) wrote a manual about buried pipelines which noted some points that are relevant to pipejacking. Clarke wrote that radial compression of a joint sealing ring induces circumferential stress in the pipe's socket and collar. The intensity of the stress is dependent on the hardness of the rubber and the degree of its compression. The load is additional to the stresses induced by internal and external service loads and jacking loads imposed during installation. Tests on the jointing rubber ring show a rapid increase in socket loading as compression of the jointing ring is increased. The compression needs to be sufficient to maintain a watertight seal during testing and service life, whilst allowing for stress relaxation of the rubber.

The analysis presented by the Concrete Pipe Association of Australia is summarised as follows:-

$$\beta = \tan^{-1}\frac{\Delta a}{z} \qquad = \qquad \tan^{-1}\frac{a\,\max\sigma_j}{z\,E} \qquad since\ \frac{\Delta a}{a} = \frac{\sigma}{E}$$

Total deformation $\sum \Delta a = \Delta a + \Delta L$

$$\frac{\sigma_j a}{E_j} \quad = \quad \frac{\sigma_j a}{E_p} \quad + \quad \frac{\sigma L}{E_c}$$

Joint   Packer   Concrete

but $\sigma = \frac{\sigma_j t_j}{t}$ where t = wall thickness and t_j = wall thickness at joint

$$\frac{a}{E_j} = \frac{a}{E_p} + \frac{t_j L}{t E_c}$$

$$E_j = \frac{a t E_p E_c}{a t E_c + L t_j E_p}$$

Permissible joint deflection:- $\beta = \tan^{-1}\dfrac{a}{E_j}\dfrac{\sigma_{jo}}{R}\dfrac{\max\frac{\sigma_j}{\sigma_{jo}}}{\frac{z}{R}}$ $\frac{z}{R}$ *from* *tables*
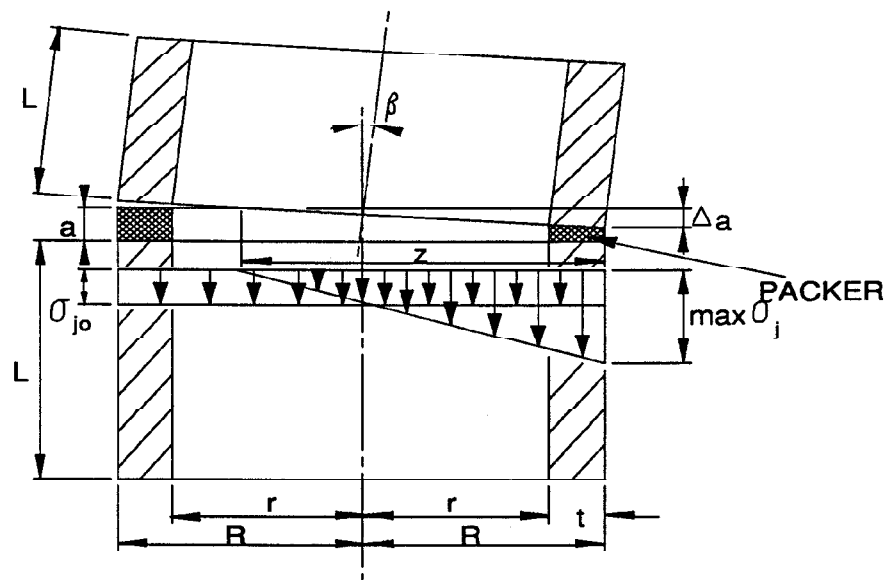
Figure 2.4 Australian joint stress distribution.

$$\frac{2r}{L+a} = \frac{2Z}{\Delta a}$$

$$\text{as } \Delta a = \frac{a\,\sigma_j}{E_t} \qquad r = \frac{Z(L+a)E_t}{a\,\sigma_j}$$
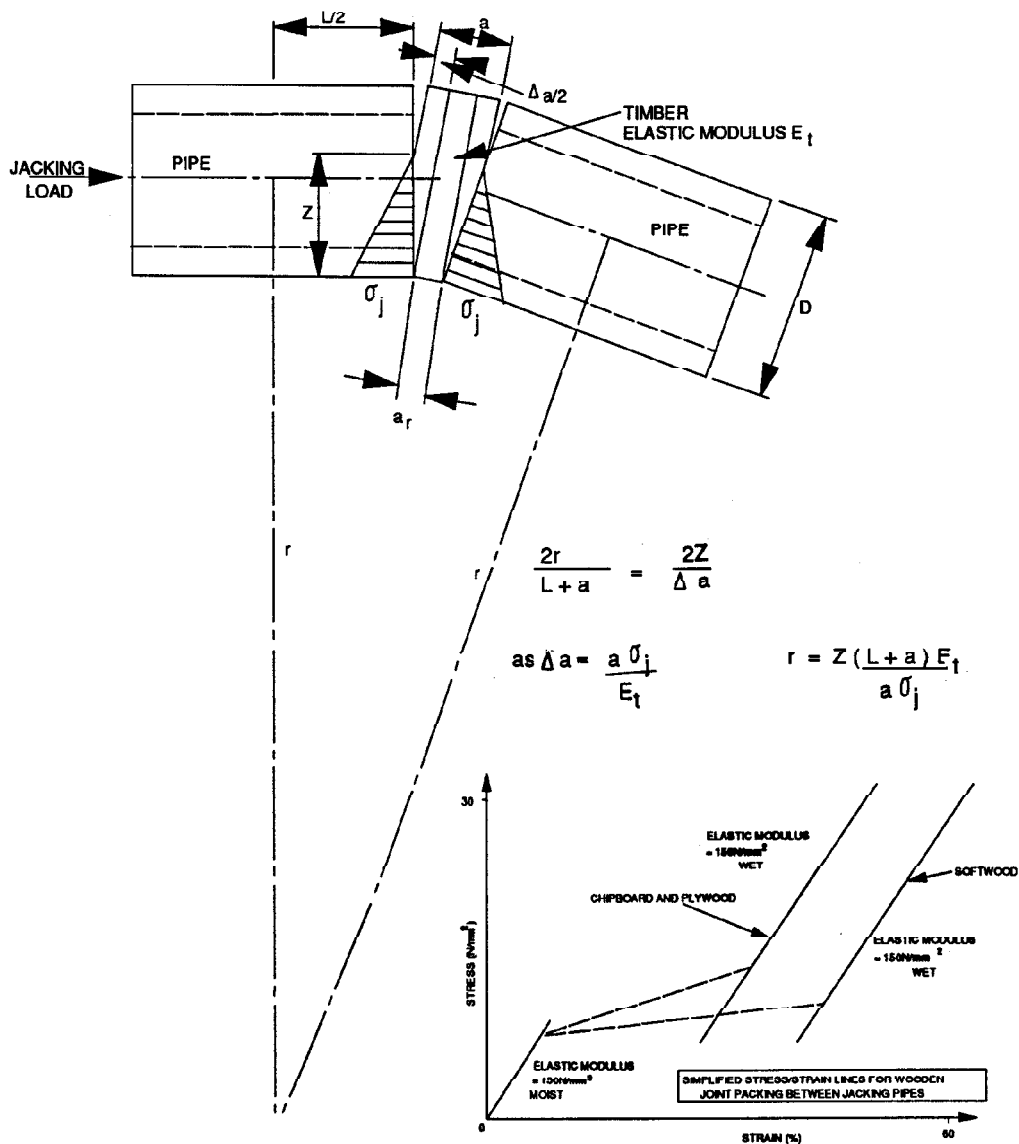
Figure 2.5 German joint stress distribution (Hornung et al. 1987).

2.6 Prediction of jacking forces

Pipejacking contractors use empirical methods to predict jacking forces and allow for pipe/soil friction forces in different ground conditions. Typical values of friction loads are listed in Table 2.1 below, Craig (1983).

Ground Type	External Load (kN/m^2)
Rock	2-3
Boulder Clay	5-18
Firm Clay	5-20
Wet Sand	10-15
Silt	5-20
Dry Loose Sand	25-45
Fill	-45

Table 2.1 Typical values of Friction Loads on Pipes

Prediction of jacking forces is obtained by multiplying figures from Table 2.1 by the total external surface area of the pipes being installed. Jacking forces can be reduced, Durden (1982), by the use of injected lubricants, intermediate jacking stations (shown in Plate 2.3), jacking in two directions and making underground connections and using mechanised jacking methods which speed up construction operations.

Analytical predictions of jacking forces are detailed by Auld (1982) based on standard soil properties and theories and are discussed later in this Section. Auld's predictions of jacking loads are based on ground pressures, the angle of internal friction of the surrounding soil and an "experienced guess". The following points are listed as influencing jacking loads:-

1   Resistance at excavation face.

2   Amount of overcut during excavation.

3   Variations in ground conditions.

4   Recommencement of jacking after a weekend stoppage.

5   Steps at joint.

6   Joint deformation.

Plate 2.3 An intermediate jacking station installed between pipes.

7 Misalignment of jacking pipe.

8 Jacking around curves.

9 Injection of a lubricant into the overbreak void.

10 The use of interjack stations.

Haslem (1986) and O'Reilly and Rogers (1987) have presented papers proposing new approaches to predictions of jacking forces based on the analysis of field data from selected pipejacks. Haslem's analysis was for pipejacks in London Clay and O'Reilly's for pipejacks

in sandstone. Both authors presented methods for dealing with misalignment of pipes. More work is required for predictions in different and variable ground conditions; a series of analyses applicable to each type of ground condition would be an ideal outcome.

The paper presented by Haslem studied the behaviour of an elastic cylinder resting in a cylindrical void in an elastic continuum. Comparisons made between the predicted jacking forces and those experienced in the field were found to give an under estimate of jacking forces. Adjustments were made to allow for misalignment of pipes but were found to be negligible. Haslem concluded that the differences he found between predicted jacking forces and those encountered on the studied pipejacks may have been from another cause. It is interesting to compare these remarks with the values of the angle of friction between the pipe and soil discussed in Section 9.5.

O'Reilly and Rogers used the same techniques to compare predicted and field measurements and find a similar low estimate for pipejacks through cohesive materials. However, predictions for pipejacks through rock produced comparable results if the site conditions were uniform. Laboratory tests were carried out to assess the contact area between pipes and clay and the results from the experimental data confirmed a need to account for plastic behaviour of clay and the effect of time.

The commonly used empirical approach predicts jacking forces with reasonable accuracy. Errors encountered using this approach are most likely due to variation in soil properties or large misalignments of the pipejack. The presentations of Haslem and O'Reilly only allow for small misalignments of the pipejacks and one consistent ground condition.

The analysis of each author is relevant to the ground conditions and contractor of the specific contract. Variations between the jacking loads experienced by the different contractors can

be due to the method of working, labour employed, amount of supervision, jacking arrangement, pressure of lubricant injection and excavation method (type of machine or hand excavation).

Auld (1982) presented theories for calculation of pressure distribution due to cohesionless ground loading onto a jacked pipe. Auld stated that he was not satisfied with the pressure distribution obtained from the analysis. The approach is ambiguous because no allowance is made for changing depth below ground level (see Section 9.4).

The author of this thesis has taken a simplistic approach at this stage in assuming no change of vertical or horizontal stress with the changing depth below ground level (Figure 2.6). Using Mohr's circle for stress in the soil, the radial stress at any point on the pipe is given by :-

$$\sigma_p = \frac{(\sigma_v + \sigma_h)}{2} + \frac{(\sigma_v - \sigma_h)}{2} \cos 2\alpha \qquad \text{...Eq 2.1}$$

where σ_p = total stress on pipe

σ_h = total horizontal soil stress

σ_v = total vertical soil stress

α = vertical angle to position of stress calculation

The total load on the pipe can be obtained by integrating.

$$P_{total} = 2 \int_0^{\pi} \left(\frac{(\sigma_v + \sigma_h)}{2} + \frac{(\sigma_v - \sigma_h)}{2} \cos 2\alpha \right) R \, d\alpha$$

where R = pipe external radius.

$$P_{total} = \pi R (\sigma_v + \sigma_h) \qquad \text{...Eq 2.2}$$

The frictional resistance which needs to be overcome along the pipeline being pushed into the ground is

$$F = P_{total} \tan \delta$$

...Eq 2.3

where δ is the angle of friction between the pipe and soil. δ is generally taken as 0.7 of the angle of internal friction, ϕ, of the soil.

$$\sigma_p = \frac{(\sigma_v + \sigma_h)}{2} + \frac{(\sigma_v - \sigma_h)}{2}\cos 2\alpha$$
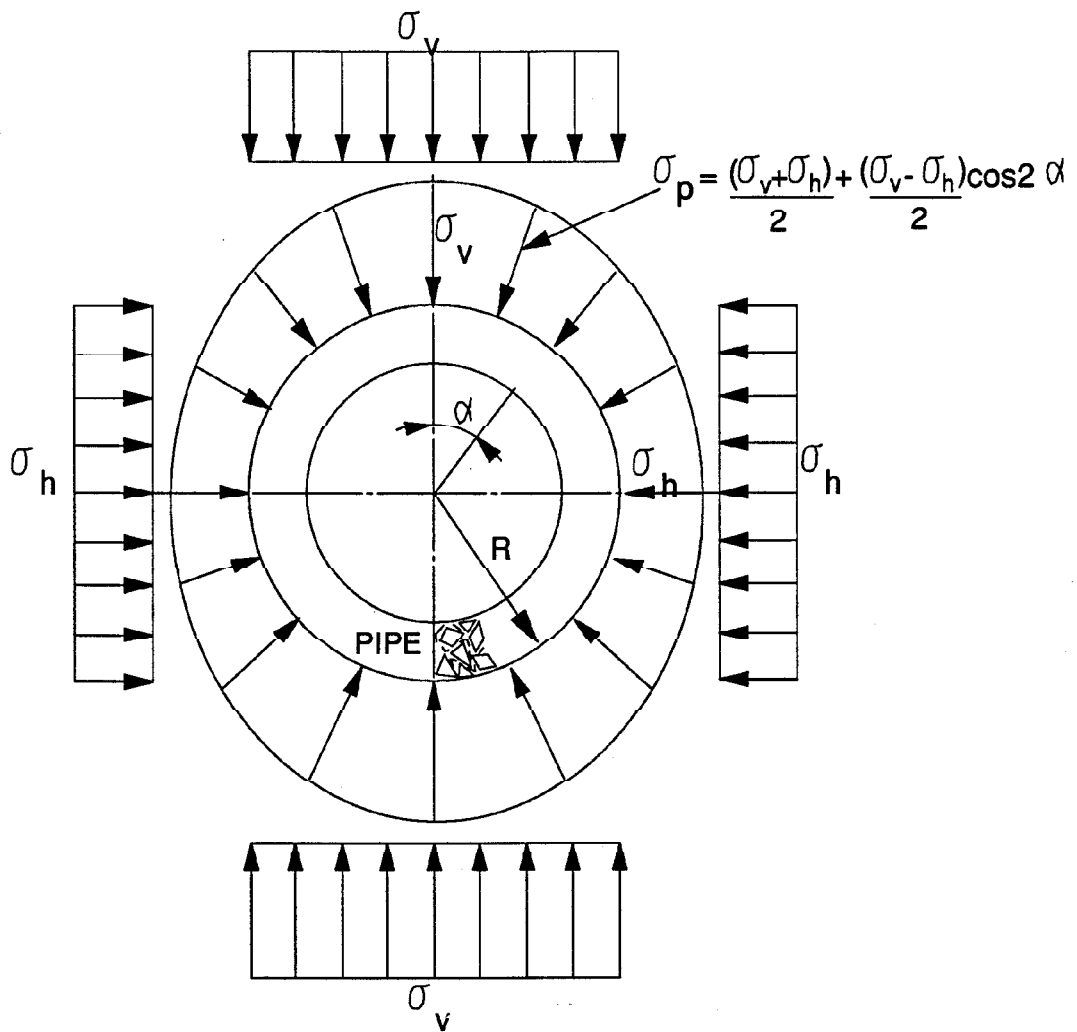
Figure 2.6 Proposed stress distribution on a pipe.

More detailed analysis is presented in Chapter 9 which allows for soil stress variations with depth.

2.7 Reinforced microconcrete

The use of reinforced microconcrete for scale model testing of reinforced concrete structures has been frequently used and developed. The principles of the use of microconcrete have been reviewed and the more influential characteristics investigated to enable selection of a suitable design mix and reinforcement material to model the jacking pipes.

Concrete is highly inelastic in compression and tension. This creates problems in attempting to model a reinforced concrete structure to fail at the modelled capacity and in the correct mode. The reinforcement also presents a major difficulty; its strength and bond characteristics must be given careful attention for correct modelling.

The failure criteria for model concrete should be identical to that for the prototype concrete. However, concrete does not have a well defined failure criterion. Therefore, model concrete should have geometrically similar stress/strain curves for uniaxial compression and tension and the model and prototype strains at failure should be the same (Sabnis et al. 1983). The current research has placed emphasis on reproduction of failure mode and correlation between model and prototype British Standard tests.

2.7.1 Model concrete

A well graded aggregate is recommended to produce concrete with minimum voids, maximum strength and minimum volume change during curing. The maximum aggregate size is determined by geometric scaling.

The engineering properties of concrete are influenced by:-

1   Water/cement ratio.

2   Aggregate/cement ratio.

3   Aggregate dimensions and properties.

4   Cement type.

5   History of moisture available and temperature during curing.

6   Test age.

7   Type of stress caused by loading.

8   Duration and rate of loading.

The influence of aggregate size on deformation of concrete was investigated by the Cement and Concrete Association, Hughes and Chapman (1966). It was concluded that as the size of aggregate increased so compressive strength and elastic modulus in compression decreased. Tensile strength and elastic modulus in tension decreased with increased aggregate size and roundness.

More recent investigations have been conducted into the effects of size on microconcrete behaviour, Sabnis and Mirza (1979), the modelling of stress/strain relationships of structural concrete, Noor and Wijayasri (1982), and the comparative flexural behaviour of model and prototype beams, Evans and Clarke (1981). The conclusions reached in each of the studies have influenced the tests and choice of microconcrete and model reinforcement used for this research. Each of the investigators used Rapid Hardening Portland Cement (RHPC) to enable results to be obtained in the laboratory more quickly. RHPC produces concrete with a seven day compressive strength comparable to the twenty eight day strength if Ordinary Portland Cement (OPC) were used. Previous investigators have used a variety of different aggregates in concrete mixes. The results of their tests gave some indication as to how sensitive mixes are to the influence of aggregate properties, mix proportions and test procedures upon the

compressive strengths obtained, Figure 2.7. Maintenance of standards and procedures throughout a test series is essential to the manufacture of concrete with consistent quality and to enable valid comparisons to be made.

2.7.2 Model reinforcement

The properties requiring investigation during the choice of a reinforcement to model the behaviour of prototype reinforcements are summarised as follows:-

1 Yield and ultimate strengths are to be duplicated.

2 Bond at the steel/concrete interface is to be similar.

3 Ductility of reinforcement is to be the same as in the prototype.

The author's review encountered many types of bar and wire having been investigated for use as a model reinforcement. These included:-

1 Round steel wire and bar.

2 Square steel wire.

3 Custom deformed wire.

4 Threaded rod.

5 Commercially deformed wire.

It was apparent that one of the modelling problems would be to reproduce a similar number and pattern of cracks to the prototype. The conclusions as to the most suitable wire to use pointed to a black annealed steel with deformations somewhere between those produced by knurled wheels and those of a threaded bar (White and Clark (1980), Noor and Khalid (1980) and Evans and Clarke (1981)).

MIX REFERENCE	MIX PROPORTIONS W/C RATIO	A/C RATIO	AGGREGATE TYPE	COMPRESSIVE STRENGTH (N/mm²)	REFERENCE
A	0.8	3.25	2mm DOWN	21	WHITE (1983)
B	0.7	3.6	6mm DOWN	23	SABNIS & MIRZA (1979)
C	0.54	2.1	3mm DOWN	27	HUGHES & CHAPMAN (1966)
D	0.7	3.5	10mm DOWN	34	TSUI & MIRZA (1969)
E	0.6	4	2.4mm DOWN	35	EVANS & CLARK (1978)
F	0.44	2.8	2mm DOWN	40	NOOR & WIJAYASRI (1982)
G	0.63	5.6	10mm DOWN	42	WHITE & CLARK (1980)
H	0.515	2.75	2.36mm DOWN	43	WALDRON, PINKNEY & PERRY (1980)
I	0.5	3.8	7mm DOWN	69	WHITE (1983)
J	0.4	2.5	10mm DOWN	74	WHITE & CLARK (1980)
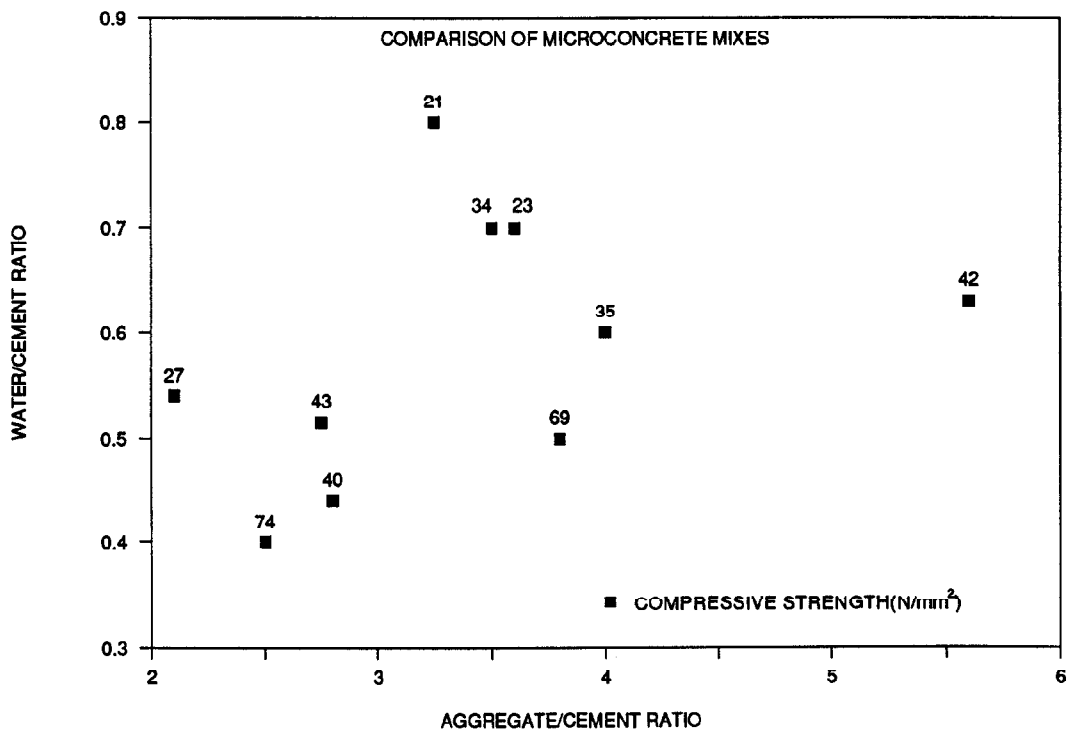
Figure 2.7 Comparison of mix proportions and compressive strengths.

Background 2-28

2.7.3 Joint sealing rings.

Pipes with in wall joints have always used a circular section rolling rubber ring to provide water tightness and integrity of joints. The development of other joint profiles has led to changes of the cross section of the rubber ring and to its material properties. The most commonly used joint sealing ring for steel collar joints is shown in Figure 2.2b. It is a rectangular section, located in a groove on the pipe spigot and uses two fins to locate and seal in the steel collar. The first fin is lower than the second fin and positions the jointing pipes into their correct central alignment. The steel collar then meets the second fin which provides watertightness and sealing as it is compressed and bent.

CHAPTER 3

APPARATUS DESIGN

3.1 Introduction

Details of the design for the testing apparatus, instrumentation and systems incorporated in the test rig are presented in this Chapter.Design calculations are not included but were carried out with reference to British Standard 5500 (1985), Donnel (1976), Williams and Aalami (1979) and Structural Steelwork Properties and Safe Load Tables (1978). The equipment was designed to enable modelling of pipejacking through a stress controlled soil chamber. Later modifications allowed for testing of pipes in free air and cyclic load testing of joint packing materials. Pipes were manufactured to dimensions sufficiently large to allow access for measurement of deflections, deformations and concrete strains.

3.2 Chamber and reaction frame

The aim of the research was to improve understanding of the factors controlling the behaviour of jacked pipes during installation and after completion of jacking operations. The apparatus was designed to enable various end loads to be applied to static and moving pipes. Vertical stress (due to overburden), can be applied and varied independently of horizontal stress.

The outside diameter of all model pipes was standardised at 200mm. Model pipes were constructed with wall thickness to internal diameter ratios of 1:6 and 1:12. These represent true scale models of 900mm and 1800mm internal diameter prototype pipes at scales of 1:6 and 1:10.5 respectively. Further details of pipe manufacture and material selection are presented in the nextChapter. The minimum internal diameter of model pipes was 150mm, which allowed adequate space for mounting transducers to record pipe movements and concrete strains.

The soil testing chamber is cubical with internal dimensions of 600mm and is shown in Plate 3.1. This allows for the pipes to be surrounded by sand equal in thickness to one pipe diameter. Transducers were mounted in the chamber wall to monitor changes in sand stress at the boundary of the chamber, as it was evident from previous research that boundary conditions were going to influence the behaviour of the pipes. The chamber was sufficiently long to enable two pipe sections to be completely retained within the chamber. The common joint between the two pipes was approximately central within the chamber during static testing and this was the position where most monitoring was carried out.

The test chamber clamped into a compressive testing framework which both supported the chamber and provided a reaction frame. The general arrangement can be seen in Figure 3.1. Jacking forces were transmitted to model pipes by hydraulic jacks.

Plate 3.1 A general view of the test apparatus.

The test chamber was filled with Leighton Buzzard 14-25 sand. To do this, the chamber was rotated ninety degrees from its test orientation and the top removed. Model pipes were set vertically in their test attitude before placing sand around them, thus enabling a uniformly dense sample to be obtained.

The sand pouring technique was chosen after discussions with research colleagues at Oxford University who have worked with the same sand poured into various test chambers. Reference was made to Bieganousky and Marcuson (1976) and to seminar notes of a Calibration Chamber Conference at Southampton University, Last (1985). The sand was poured through a steel plate perforated with 6mm holes on a 90mm grid. Below the steel plate were two 4mm sieve grids to act as diffusers of the jets of sand. The sieves were maintained at least 550mm above the sand surface as shown in Figure 3.2 and a dense sand sample was produced.
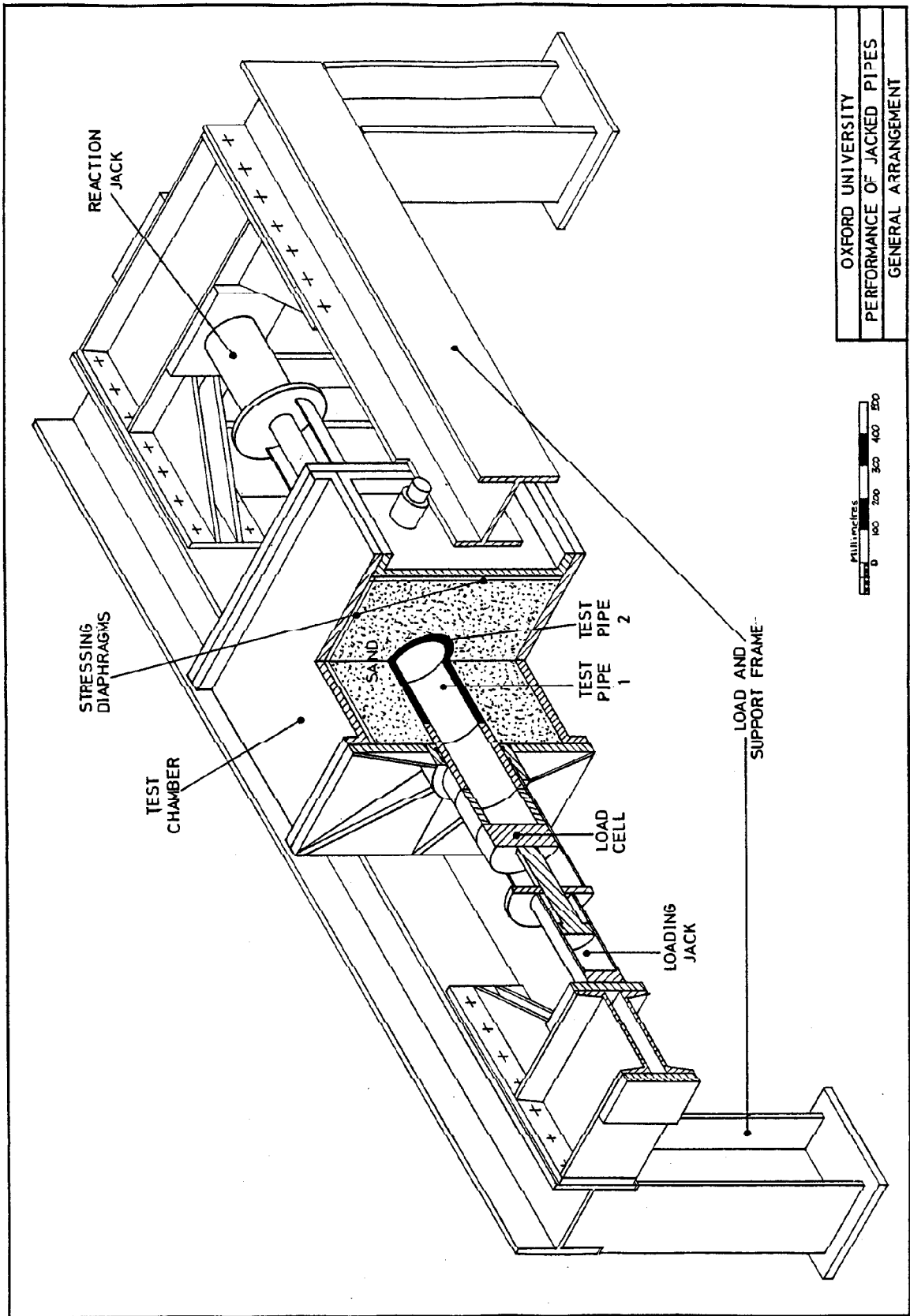
Figure 3.1 General arrangement of test apparatus.

Apparatus Design 3-4

Tests on the pouring technique indicated a sample with a relative density of 85%. It was necessary to include a 2mm stainless steel wire sieve mesh above the perforated plate. This enabled larger pieces of microconcrete contaminating the sand to be removed.
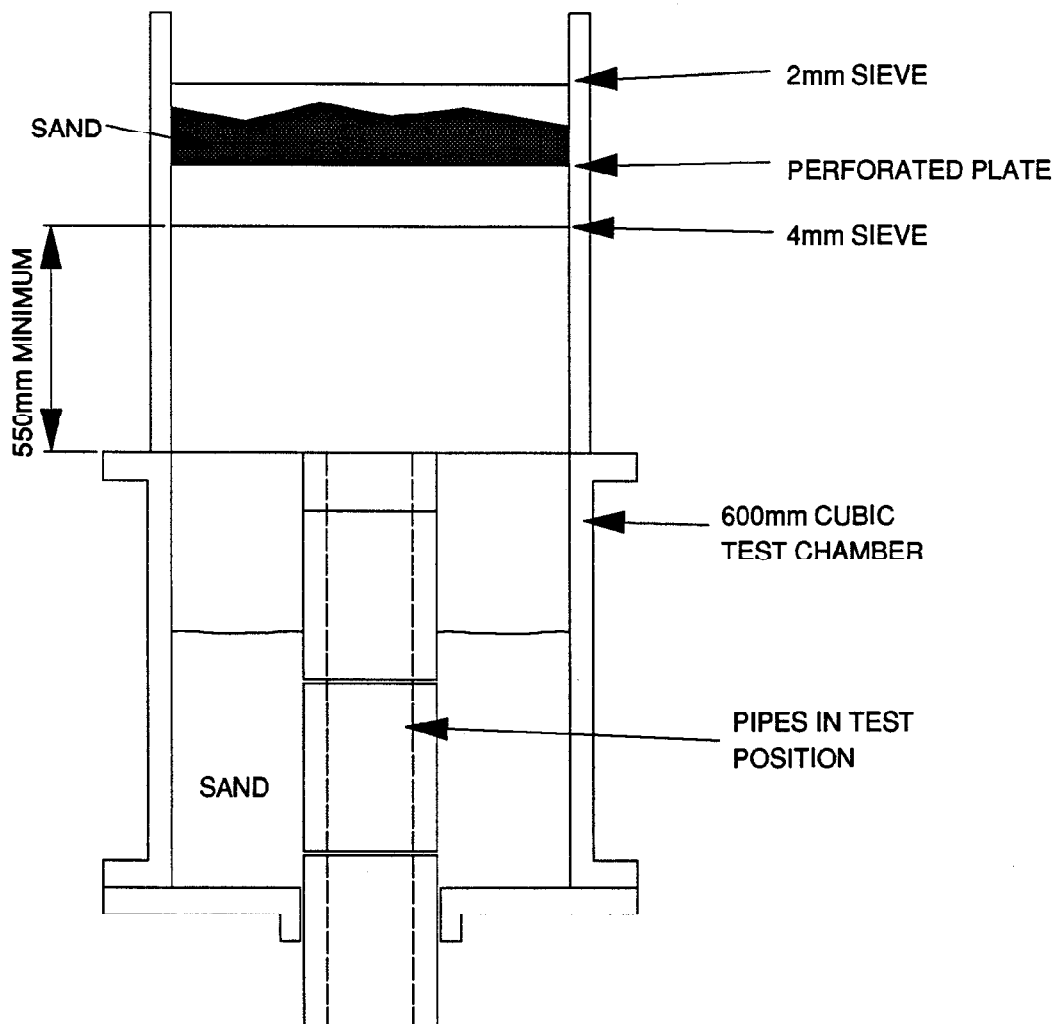
Figure 3.2   Sand pouring.

Pipes could be placed in the chamber at various alignments prior to pouring the sand. Pipes were aligned with the use of wedges placed in the joint gaps. The wedges enabled the pipes to be set up either in a straight line or with deflection at the joint. The wedges were removed once the sand had been placed, but before commencement of testing. The sand provided sufficient restraint to maintain pipe position before testing started.

Specifications for pipejacking normally require the contractor to maintain records of ground conditions, line and level alignment of the pipeline, installation jacking forces and other relevant information. These can typically be recorded as illustrated in Figure 3.3. Any deviations from the intended centreline result in deflections at pipe joints. These are magnified if the pipes'ends are not square to each other.

The importance of directional control of a pipejack is illustrated in Figure 3.4. Specifications often state ± 50mm as the allowable tolerances on line and level. However, the example presented by Hough (1986) showed how large deflections can become. Two 2.5 metre long pipes can have a maximum deflection angle of 4.6° and yet still be within tolerance. Deflections of this magnitude would produce a joint gap of 96mm across a 900mm diameter pipe and the pipe joint would be incapable of performing its required functions. Hough suggested a maximum 0.5° deflection as acceptable, but also illustrated how care must be exercised in directional control to remain within tolerance. This research project has addressed the problems of joint deflections on pipes and presents conclusions in Chapter 9 on acceptable magnitudes of deflection and their relationship to allowable jacking loads.

Once sand had been placed around the pipes, the lid was replaced on the test chamber, which was rotated back through ninety degrees to its test position as depicted in Figure 3.5. The pipes were then orientated in a horizontal direction. Instrumentation and transducers were connected to record initial data. Concrete strain readings had been previously recorded, to obtain zero values before sand was poured around the pipes.
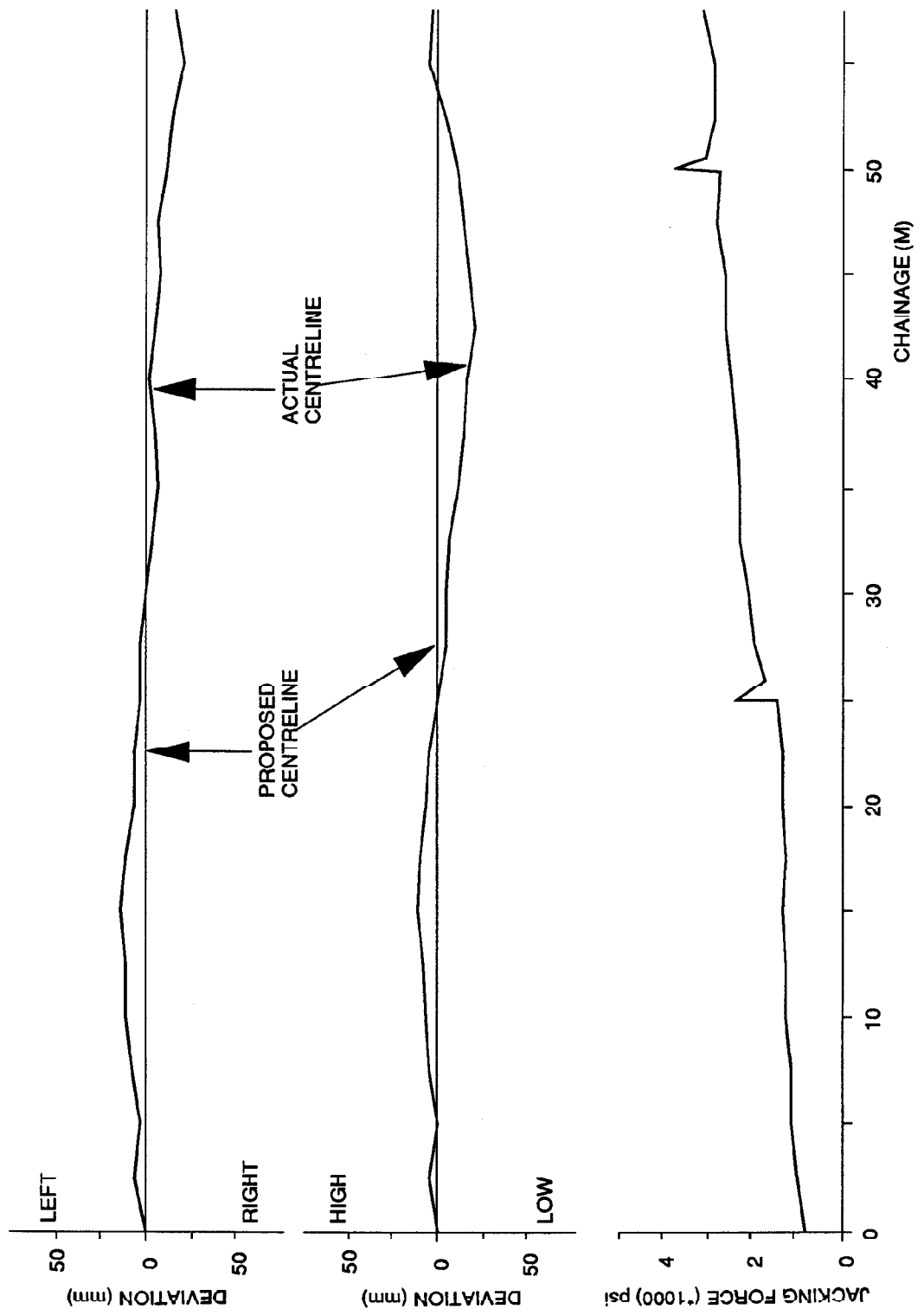
Figure 3.3 Typical jacking records.
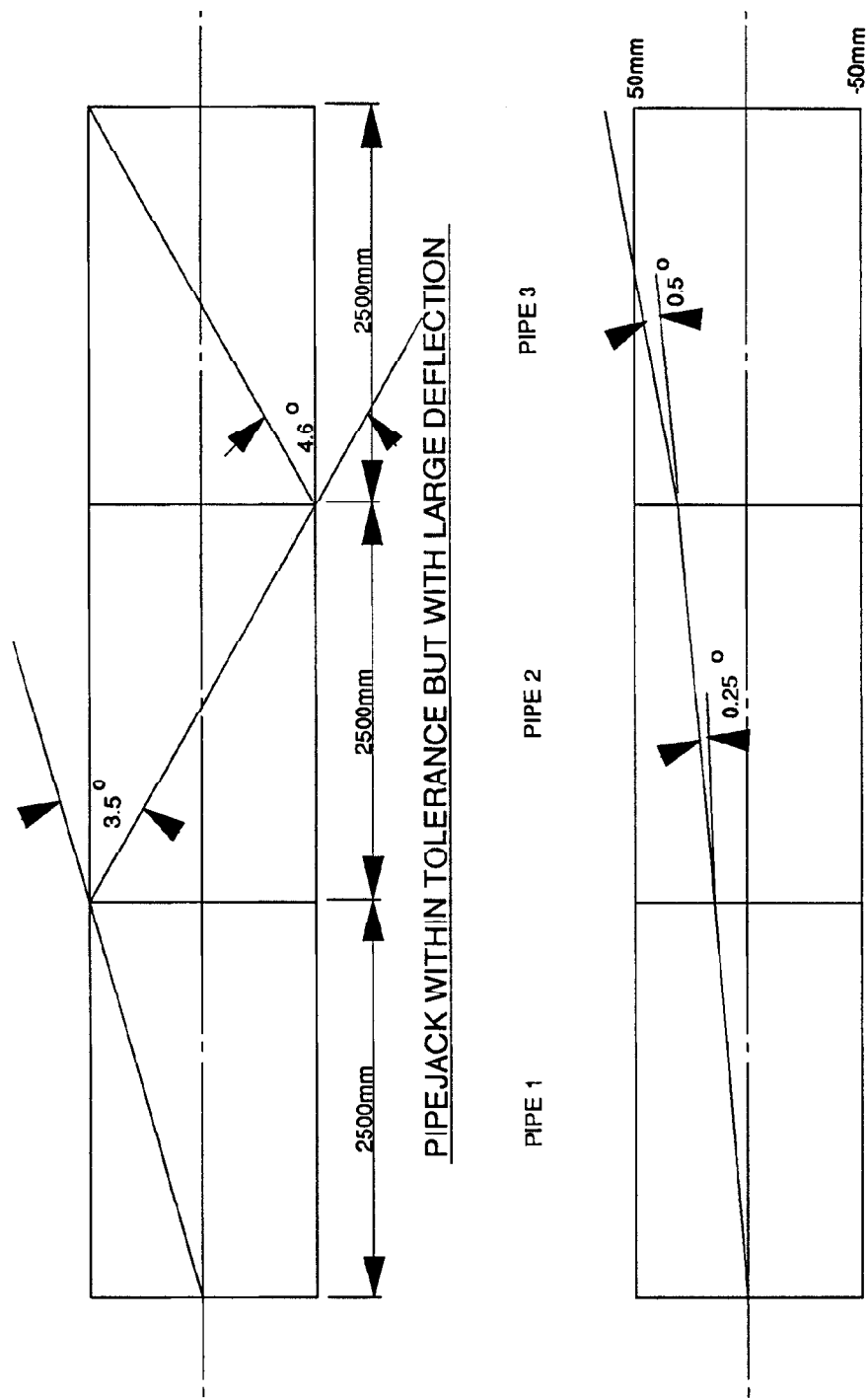
Figure 3.4 Deflections at pipe joints and tolerance allowances.

SAND POURING
POSITION

LOADING
JACK

ENCLOSE CHAMBER

REACTION
JACK

TURNING TO
TEST POSITION

TEST POSITION
JACKS EXTENDED AS REQUIRED
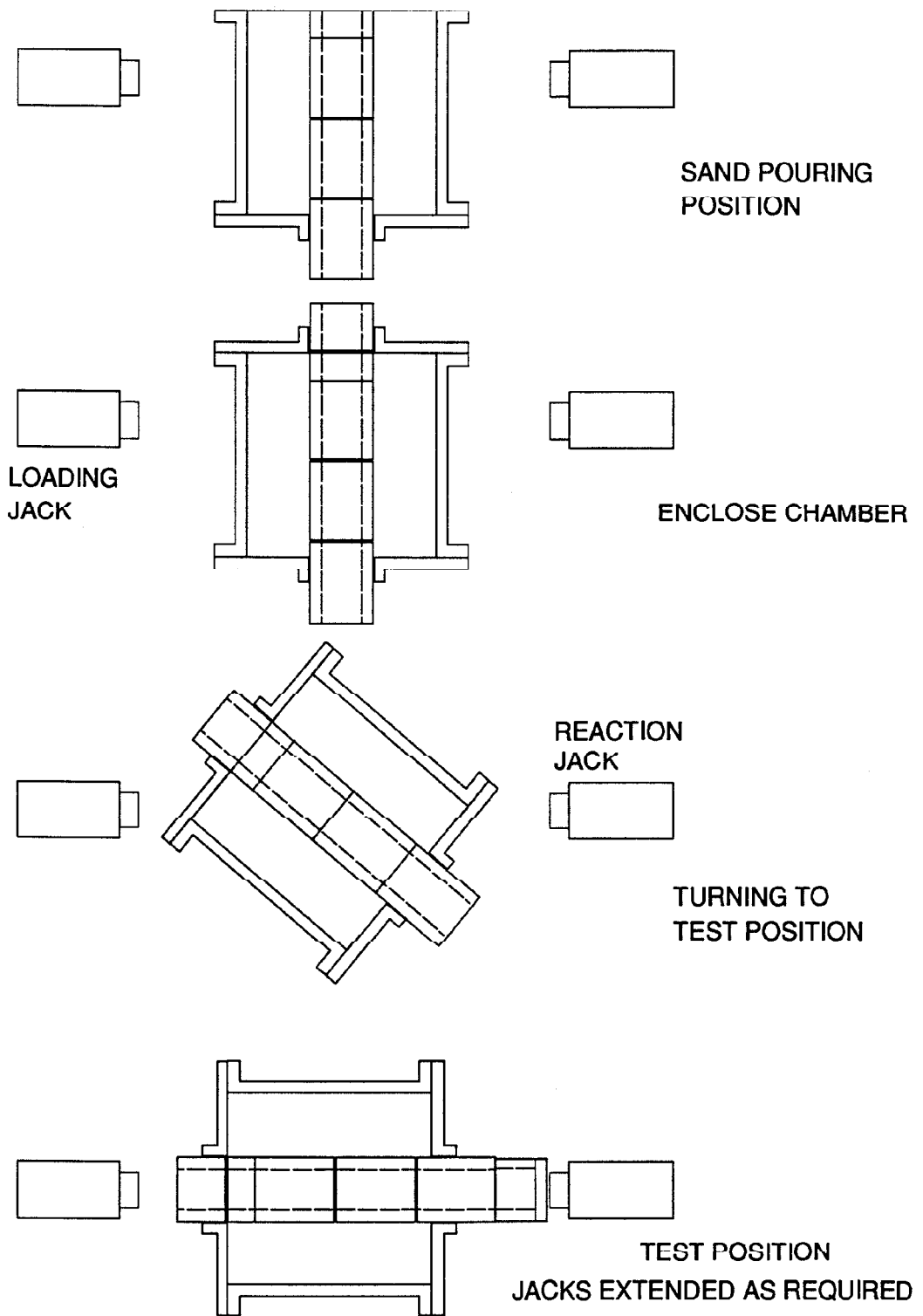
Figure 3.5 Set up and turning of the chamber.

3.3 Hydraulics

Jacking loads were applied to the model pipes using hydraulic rams. The hydraulic system was designed with two rams, one each end of the pipe string. The rams had a maximum capacity of 20 tonnes and were driven by an electrically powered hydraulic powerpack. Controls had been incorporated in the system (Figure 3.6) to allow variable ram extension speed and control of maximum loads below 20 tonnes.
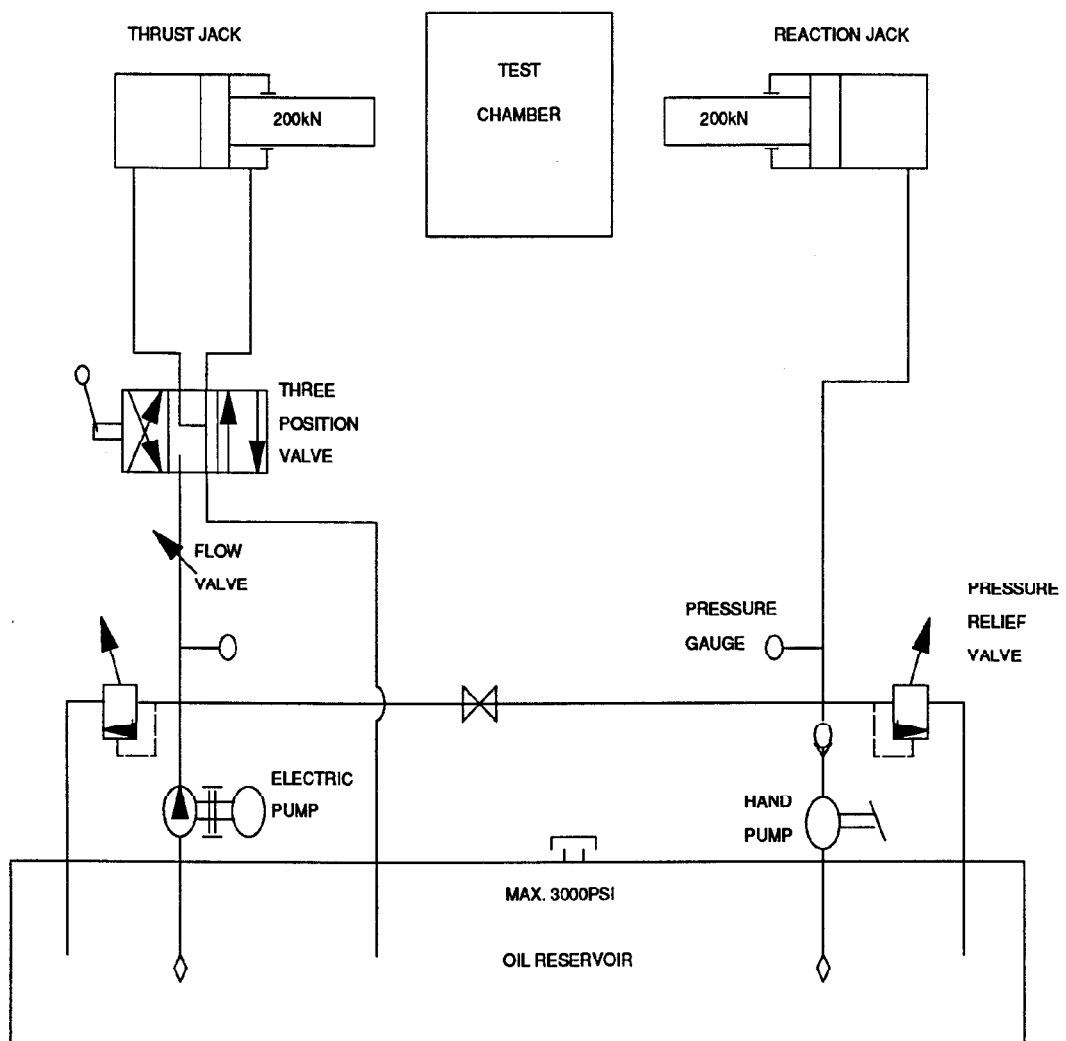
Figure 3.6 Hydraulic circuit.

The jacks were used in three operating modes. Initially the system was used with one jack applying load to the pipe strings and the second jack redundant apart from being used as a fixed reaction against which to push.

Secondly, the jacks were used to model resistance to movement in order to model pipes at different positions along a pipejack. One jack provided pushing load to the pipe string, whilst the second jack resisted movement until a preset force was applied when this jack began to retract and hence the pipe string began to move through the sand

For the third mode, the equipment was modified during the research to provide cyclic loading. This was used for the testing of prototype joint packing materials. The load/unload cycle was provided by moving the control lever backwards and forwards with a linkage attached to a cam and motor. The modifications are shown in Figure 7.2 together with the cyclic loading movements the cam was designed to provide.

The second mode of operating the hydraulic testing rams was able to model four very different installation conditions. The different modes of axial loading during a pipejack installation can be illustrated with the following examples:-

1   The first pipes to be installed in the pipejack sequence are pushed through to the reception end of a pipejack. They are installed with the use of a large number of axial load applications but the magnitude is always relatively small (at the front end of the pipe string). The load remains small unless the pipejack shield is being buried into the soil. The first few pipes in the string are subject to larger deflections than those further behind as the pipes tend to straighten as more axial load is applied.

2   The last pipes to be installed have the largest loads applied to them. They are not moved very far and axial forces are applied a small number of times.

3   The pipes whose final position is halfway along a pipejack have a large number of sizeable axial load applications applied for their installation. The difference with these is that load is permanently applied to the pipes as the ground frictional resistance along the pipeline prevents full release of the load.

4   If an interjack station is used, the pipes close to it will be subjected to a large number of large magnitude load and unload cycles.

The 20 tonnes maximum capacity of the jacks could apply up to $24N/mm^2$ to the ends of model pipes if the load was evenly distributed over the full cross sectional area. This compares with manufacturers' current recommendation of 10 to $15N/mm^2$. As misalignment between the pipes was introduced so concrete stress at the joint between consecutive pipes increased for any given load application. Load was transferred from the hydraulic rams to the pipes using hollow cylindrical blocks.

3.4 Transducers and instrumentation

Measurements were taken during testing using a number of different types of transducer; linear variable differential transformers (LVDT's), load cells, pressure transducers and electrical resistance strain gauges. Data logging was controlled by an Olivetti M21 micro-computer and carried out by an E500 Translog datalogger. Software was written to record data during the various tests and to process the data into engineering units, suitably formatted for analysis using spreadsheets. Generally, the programmes continually monitored the load cell for axial load on the pipes and recorded data at specific increments of load. Data from cyclic load tests were recorded during specific time intervals coinciding with an application of load. Positions at which transducers were mounted will be presented with each test series in the following chapters.

A load cell supplied by Maywood instruments was used to measure the axial jacking force applied to the system. It had a capacity in tension or compression of up to 250kN with measurement accuracy of 0.01kN. The load cell was mounted, using a ball and cup connector, to the end of the thrust ram. This ensured load was applied uniformly around the circumference to the end of the pipe string.

Five pressure transducers were used to monitor the stress normal to the soil chamber surface. These transducers were used to measure any changes in boundary stress that occurred during testing in order that any necessary corrections could be made for edge effects. They could be located with their measuring face flush to the internal wall of the chamber at a number of different positions. Following recommendations of Weiler and Kulhawy (1982) that the transducer diaphragm diameter should be at least ten times the mean particle size of the sand, these transducers were selected to have 19mm diameter. The transducers were P310 type supplied by Maywood Instruments and had a working range of 0 to 140 kPa and an accuracy of 0.003 kPa.

Electrical resistance strain gauges supplied by Techni Measure were used to record surface strains on the model pipes; strain gauges PR10 were used. These were supplied as a forty five degree three gauge rosette, enabling major and minor strains to be calculated. Recommendations are that gauge length should be at least five times the maximum aggregate size to avoid effects of stress concentrations. At the same time use of long gauge lengths is not good practice in areas with a high strain gradient; the gauges used were 10mm long. The strain gauges were connected to electrical circuits in the datalogger which provided resistors to complete a full Wheatstone bridge circuit.

LVDT's were mounted inside the model pipes to monitor changes of alignment during testing, and to measure changes in the longitudinal distance between pipes at their common joint. The transducers were supplied by RDP Electronics and Sangamo Electronics. They could measure displacements of up to 10mm to within 0.005mm. Eight of the transducers

were secured to a beam, positioned in pairs at ninety degrees to each other. Each pair was positioned near the end of a model pipe and measured the horizontal and vertical position of the pipe, as shown in Figure 5.3. The eight transducers accordingly gave information on the alignments of two consecutive pipes relative to their start position and to each other. The LVDT's could be rearranged to measure changes of internal diameter during loading. (It may be possible to use this information to correlate with future fieldwork testing). Three transducers measured changes in the gap between common pipe joints. They were mounted at 120^{0} intervals around the circumference of the pipe as can be seen in Plate 3.2 and measured changes of the joint alignment and compression of packing materials.
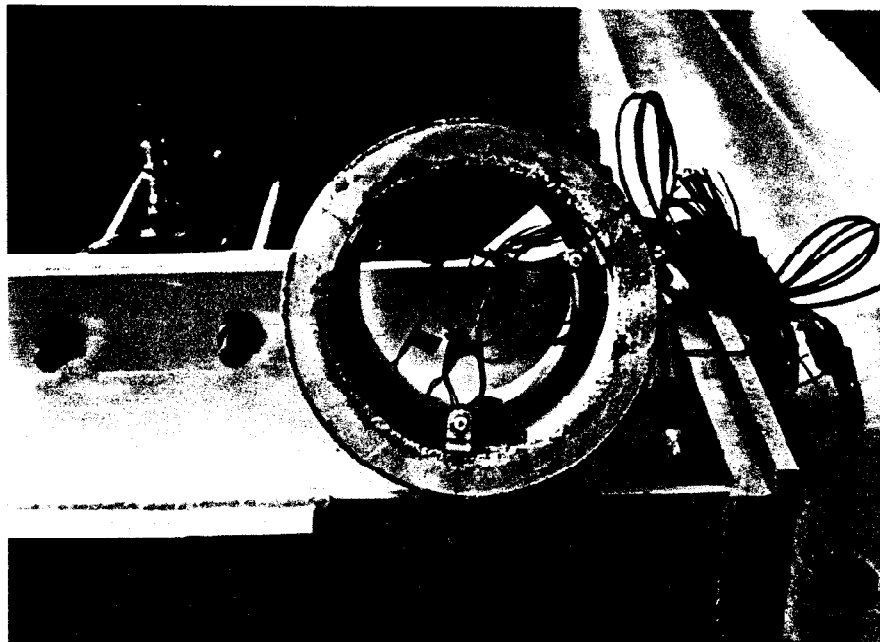
Plate 3.2   An instrumented pipe.

A P102 type pressure transducer supplied by Maywood Instruments was used to monitor hydraulic oil pressure in the second reaction ram. This had been calibrated to enable assessment of the reaction load to be made.

All data were recorded through an E500 Translog datalogger, manufactured and supplied by RDP Electronics. It had facilities for recording 64 transducers at speeds of up to 100 individual readings each second. It could be used in a stand alone operation (away from the micro computer) or controlled in real time. Software was supplied with the datalogger but was not suitable for recording data during this test programme because it could only record at given time increments. The datalogger records transducer readings with the sensitivity shown in the table below:-

		required	achieved	maximum working range
a	Axial load cell	±0.5kN	±0.1kN	250kN
b	Pressure transducer P310	±0.1kPa	±0.1kPa	140kPa
c	Electrical resistance strain gauge	±1$\mu\varepsilon$	±1$\mu\varepsilon$	3000$\mu\varepsilon$
d	LVDT	±0.01mm	±0.01mm	10mm
e	Pressure transducer P102	±50kPa	±5kPa	69MPa

Table 3.1   Accuracy of transducers.

Calibration was carried out in the laboratory to obtain calibration factors and working range limits for the transducers and to allow for any variables that were specific to the system into which they were wired. The calibration procedure also confirmed the accuracy of the transducers.

Total stress cell readings may be underestimates and stresses vary throughout the chamber due to friction at the side walls.

3.5 Soil stressing system

A general arrangement of the soil stressing system is shown in Figure 3.7. The system operated using compressed air from the laboratory ring supply and an air-water interface. The interface stabilised pressure fluctuations and allowed water to be used to apply stresses to the soil sample. Consequently the test chamber did not require designing as a pressure vessel and did not require a pressure vessel test certificate.
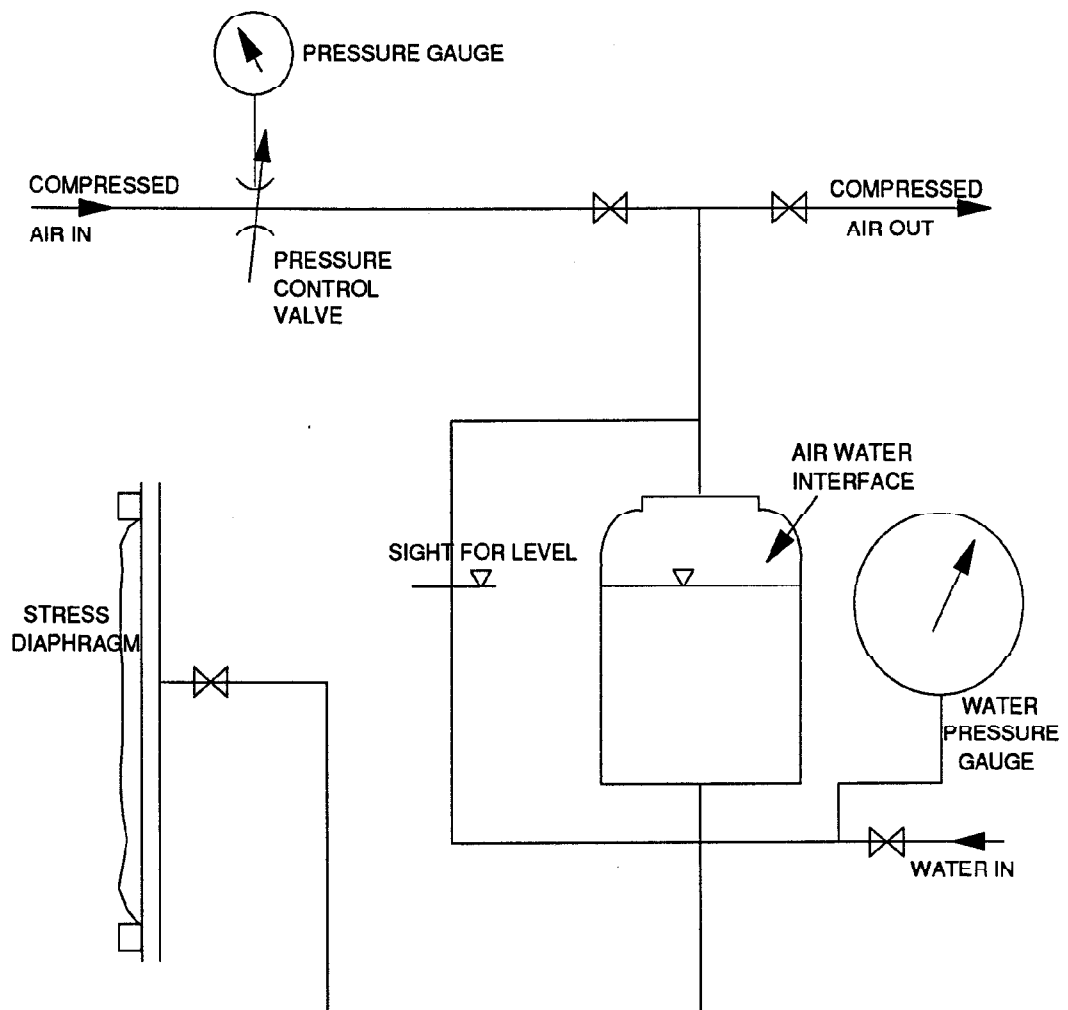
Figure 3.7 General arrangement of sand stressing system.

Two separate systems were operated, one controlling vertical soil stress and the other horizontal soil stress. These could be varied independently. Stresses were induced into the soil sample through rubber membranes with the pressurised water behind them.

CHAPTER 4

MODELLING

4.1 Microconcrete

4.1.1 Trial mixes

It was necessary to manufacture a microconcrete with a 28 day compressive cube strength of $65N/mm^2$ in order to model prototype concrete strengths. There were no records of any previous microconcrete research at Oxford University.

Rapid Hardening Portland Cement (RHPC) was used to produce the 28 day strength when samples were 7 days old, so that results could be obtained more quickly from the laboratory. An initial estimate of water/cement and aggregate/cement ratios were obtained by reference to Figure 2.7 and four mixes were produced. From the results of tests on these mixes, refinements to the mix ratios could be made to produce the desired concrete workability and crushing strength.

Modelling of the prototype concrete aggregate size was made using sharp sand which was dried and sieved in the laboratory. The particle size distribution of the unsieved sharp sand is shown in Figure 4.1, and indicates grain sizes up to 5mm. The prototype concrete has a maximum particle size of 10mm which scaled for use in the models to 1.0mm and 1.7mm
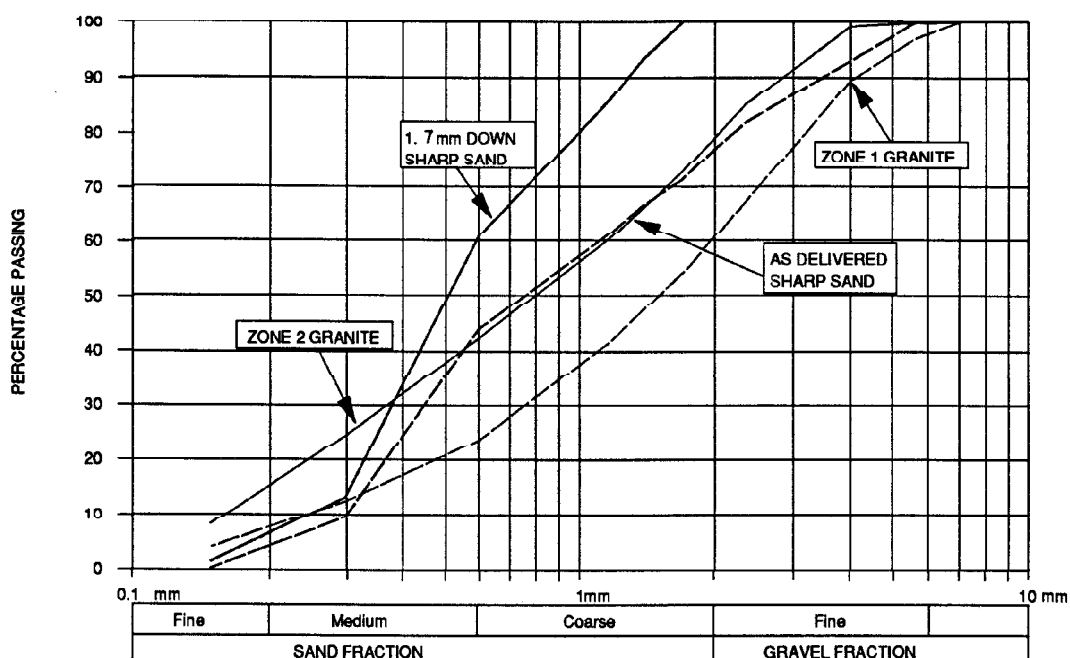
Figure 4.1   Particle Size Distribution

size sand. The particle size distribution curves in Figure 4.1 indicate the range of grain size obtained by sieving the sharp sand through a 1.7mm sieve. Table 4.1 lists the aggregate and water/cement ratios of the trial mixes. It details changes of aggregate type and size, the use of additives and compressive cube strengths obtained.

4.1.2 Characteristic tests

Tests on the compressive cube strength were carried out on three sample sizes; 150mm cubes, 100mm cubes and cylinders 50mm diameter by 100mm long. The 150mm cube tests are identical to those carried out by British pipe manufacturers on full-size pipe concrete. Testing of microconcrete should be conducted on scaled cubes to model the effects of hydration, scaling and the ratio of concrete volume to surface area as reported by Pomeroy (1972).

The results of these tests showed that 150mm cubes resulted in crushing strengths 5% less than those obtained from 100mm cubes. The crushing strengths of the cylinders were 15%

MIX REFERENCE	WATER/ CEMENT RATIO	AGGREGATE/ CEMENT RATIO	7 DAY COMPRESSIVE STRENGTH (N/mm^2)	REMARKS
A	0.4	2.0	58.0	Unsieved
B	0.4	2.5	---	Sharp
C	0.35	2.0	73.0	Sand
D	0.35	2.5	63.0	
E	0.30	1.5	83.0	14-25 Leighton Buzzard Sand
F	0.30	1.5	91.0	Mixes F to M
G1	0.35	2.0	72.0	sharp sand
G2	0.35	2.0	74.0	maximum
H1	0.325	1.75	75.0	aggregate
H2	0.325	1.75	73.5	size 1.7mm
H3	0.325	1.75	73.5	
H4	0.325	1.75	81.5	(89.5N/mm^2@ 28
H5	0.325	1.75	81.5	days)
I	0.325	2.0	71.0	
J1	0.375	2.25	61.0	
J2	0.375	2.25	61.0	(Plasticiser)
K1	0.392	2.2	61.5	
K2	0.392	2.2	56.0	(Plasticiser)
K3	0.392	2.2	56.5	(Plasticiser)
L	0.4	1.75	62.5	
M1	0.43	1.75	56.0	
M2	0.43	1.75	54.0	

Table 4.1 Microconcrete mix proportions and compressive strengths.

less than 100mm cubes. These differences are similar to those quoted by Erntroy (1960) who also highlighted the importance of consistent concrete mix practice in order to obtain reliable results and discussed the variations found between various mixing sites. Corrections were carried out on results from the cylindrical specimens in accordance with BS 1881 Part 120: 1983 to allow for their different height to breadth ratio. However, results from cylinder tests were scattered and consistent results were not obtainable. It was decided to use 100mm cubes to test for compressive strengths during pipe manufacture and correct the test results to make correct comparisons between the concrete in the models and prototypes.

A compressive cube strength of 65N/mm^2 was required in the model pipes. Further characteristic tests were carried out on mix reference H which had a crushing strength of 67.5N/mm^2 at 7 days old. Details of all cube strengths obtained for this mix are presented in Figure 4.2.

Comparisons of the mix ratios and compressive strengths from the trial mixes are presented in Figure 4.3. They clearly show the following relationships which are both as expected:-

1   As water/cement ratio increases, compressive strength decreases.

2   As aggregate/cement ratio increases, compressive strength decreases.

After consideration and examination of the results, mix reference H was chosen as the design microconcrete mix for pipe manufacture and testing. This mix had the closest correspondence to the required compressive and tensile strengths, together with a suitable workability for placing concrete in the pipe moulds.
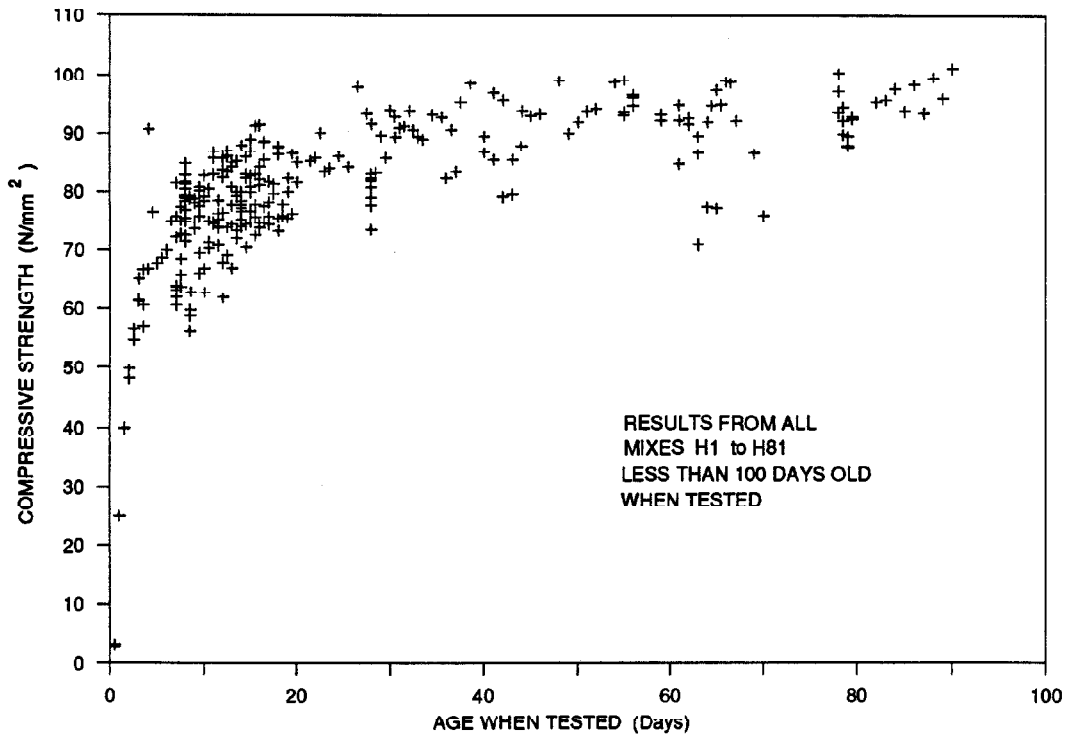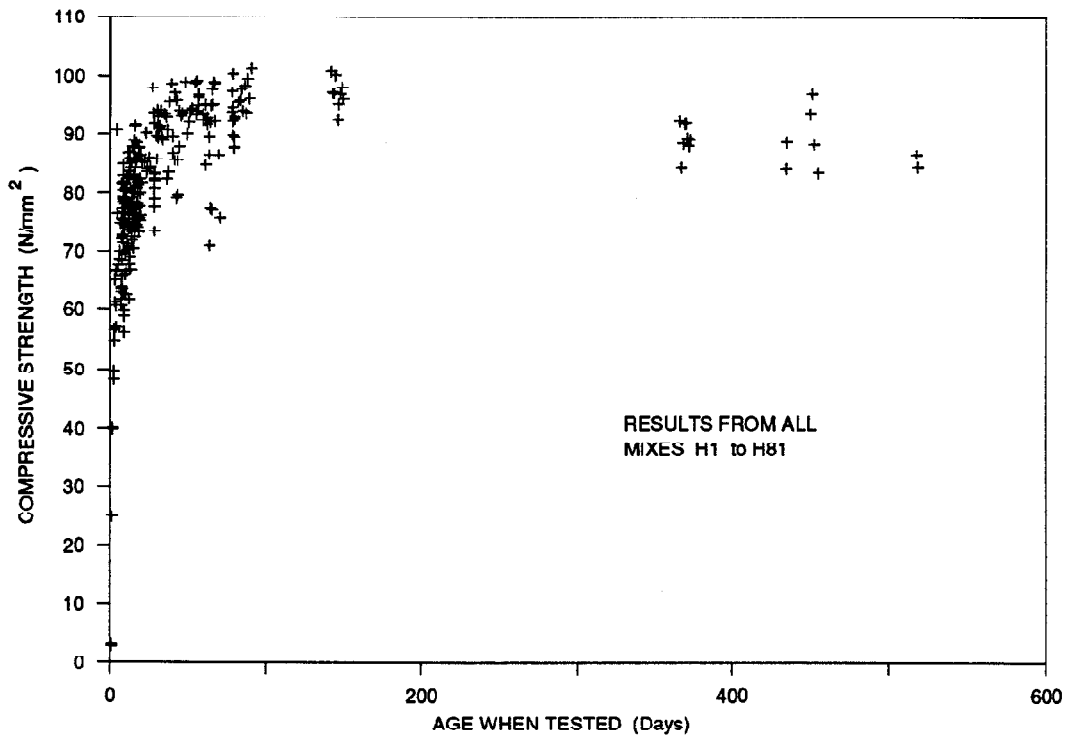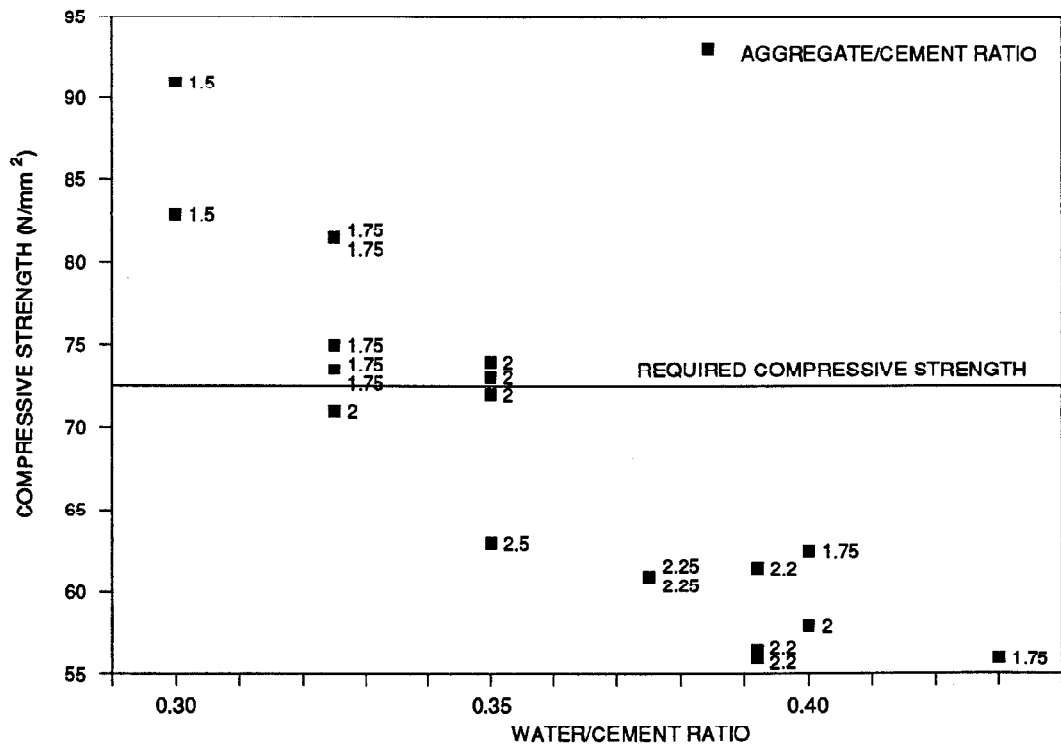
Figure 4.2 Crushing test results.
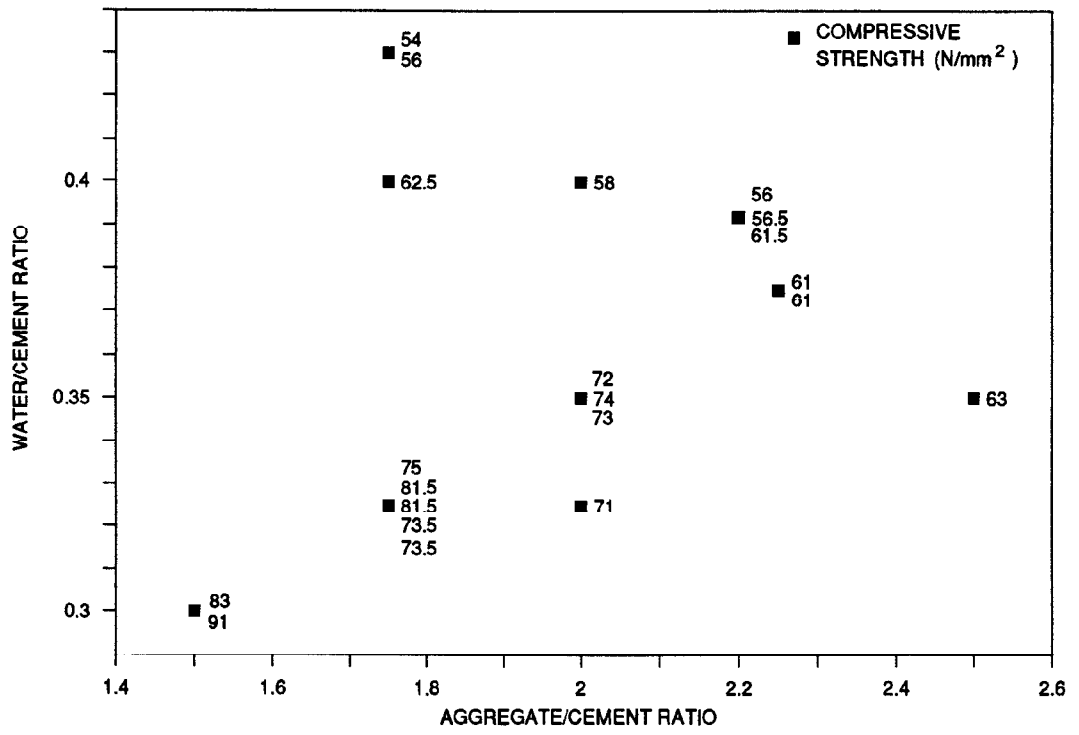
Figure 4.3 Affect of aggregate and water quantities on compressive strengths.

Tests were conducted to determine the tensile strength of the microconcrete in accordance with BS 1881 Part 117: 1983. They gave results of a tensile splitting strength of $4.65N/mm^2$. Testing the flexural strength of the microconcrete gave results of $5.40N/mm^2$. The conclusions stated by Dewar (1964) for testing of indirect tensile strength of high compressive strength concretes are that the tensile strength may be as low as 5% of the compressive strength, and the flexural strength can be expected to be 40% higher than the tensile strength. The results obtained from the tests on the microconcrete mixes agree with the conclusions of Dewar.

A number of prisms and cylinders were loaded with strain gauges attached to their faces as shown in Figure 4.4. This enabled computation of the elastic modulus and Poisson's ratio of the concrete. The elastic modulus was calculated as $31.7kN/mm^2$ and Poisson's ratio as 0.22.

Whilst testing trial mixes, model pipes were also manufactured to experiment with manufacturing methods, vibration techniques, pipe quality, most suitable workability and adherence to British Standards. This enabled the pipe manufacturing technique to be perfected before production of model test pipes commenced.

Discussions with the Concrete Pipe Association resulted in tests being carried out using a granite sand in an attempt to reduce cement contents. Granite sand has an angular sand grain which should improve the crushing strength and is more akin to the shape and quality of prototype aggregates, rather than the rounded particles of sharp sand. Results of the tests are compared in Table 4.2. They indicated that no significant saving of cement content would be possible by using granite sand.

AXIAL LOAD

DEMEC PIPS AT 100mm
VERTICAL CENTRES
FOR CALCULATION OF
ELASTIC MODULUS IN COMPRESSION

BS 1881 : Part 121 : 1983

DEMEC PIPS AT 50mm
HORIZONTAL CENTRES
FOR CALCULATION OF
POISSON'S RATIO

150mm x 150mm x 300mm PRISM
or 150mm DIA. x 300mm CYLINDER

COMPRESSIVE LOAD

SPLIT CYLINDER TEST
USING 150mm DIA. x 300mm LONG CYLINDER

BS 1881 : Part 117 : 1983

F/2 F/2

L/3 L/3 L/3

L

BS 1881 : Part 118 : 1983

FLEXURAL TEST
USING 100mm x 100mm x 500mm PRISM

Figure 4.4 British Standard test arrangements.

	SHARP SAND	GRANITE ZONE	GRANITE ZONE
	< 1.7mm	1	2
		< 1.7mm	< 1.7mm
Aggregate/cement Ratio	1.75	1.75	1.75
Water/cement Ratio	0.375	0.375	0.375
Mean cube strength			
150mm cubes	63.8N/mm^2	68.5N/mm^2	59.8N/mm^2
100mm cubes	72.8N/mm^2	75.0N/mm^2	60.9N/mm^2
Tensile splitting strength	4.65N/mm^2	5.27N/mm^2	4.73N/mm^2
Tensile stress in bending	5.40N/mm^2		5.52N/mm^2
Density	2229kg/m^3	2283kg/m^3	2249kg/m^3
Supplier	J. Curtis & Sons, Abingdon	ARC., Judkins, Nuneaton	
Sieve Tests (see Figure 4.1)	percentage passing		
5.60mm	99.9	97.2	99.7
4.00mm		89.5	99.1
2.36mm	82.5	67.8	85.0
1.70mm	71.8	54.2	72.6
1.18mm	61.5	41.6	60.4
600μm	43.5	23.7	42.2
300μm	10.1	12.4	24.6
150μm	1.2	4.1	8.2

Table 4.2 Comparison of effects of different sand types.

4.1.3 Pipe manufacture

Moulds for model pipe construction were manufactured to the dimensions listed below in Table 4.3. Construction details of the moulds are illustrated in Figure 4.5 and Plate 4.1 together with the end plates used to manufacture different joint profiles.

TOP END
PLATE TO
BE USED
WITH JOINT
PROFILE

OUTER MOULD
200mm I.D.

MICROCONCRETE

INNER
MOULD

VARIABLE
END PLATE
WITH JOINT
PROFILE
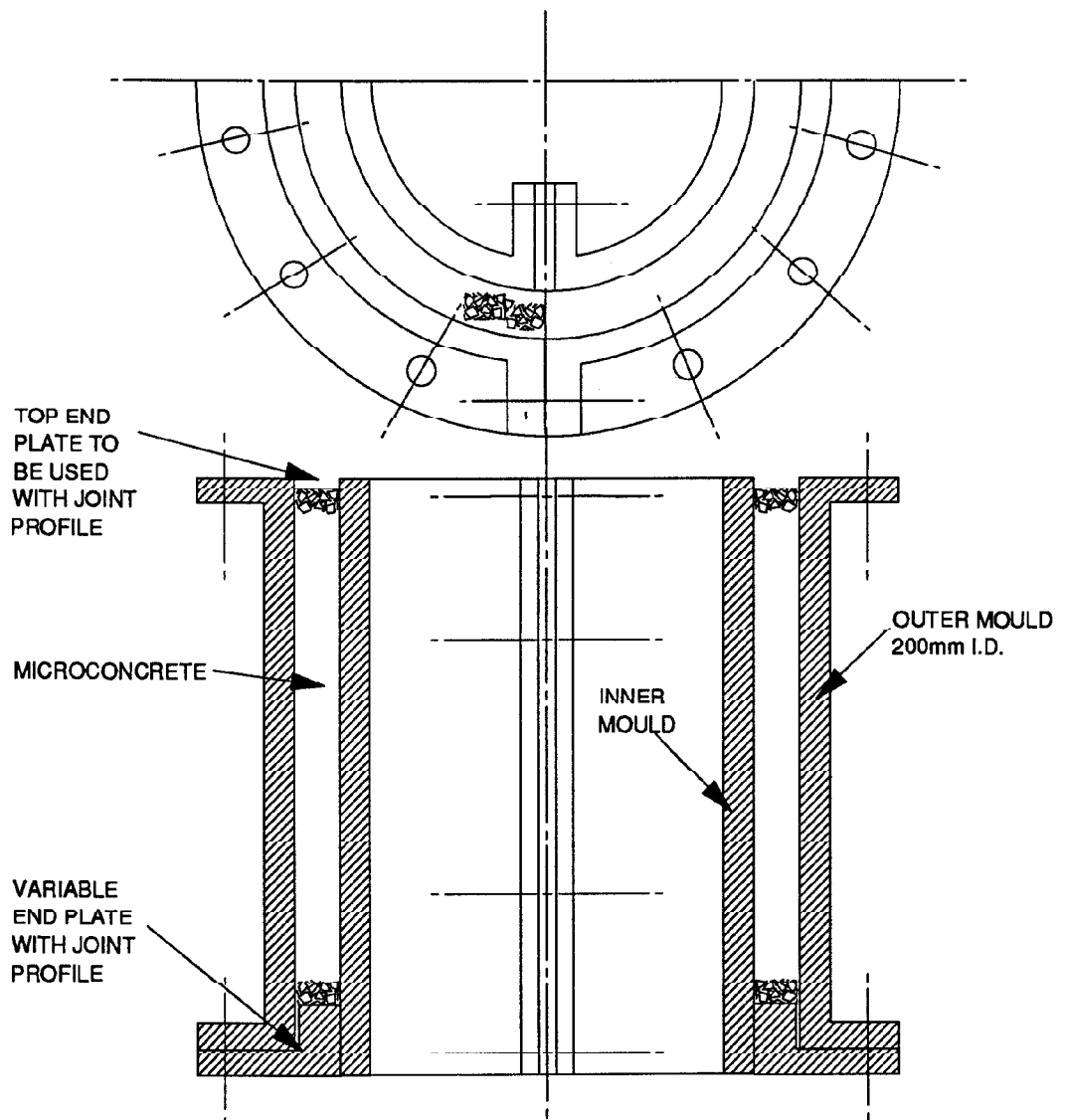
Figure 4.5 Model pipe moulds.
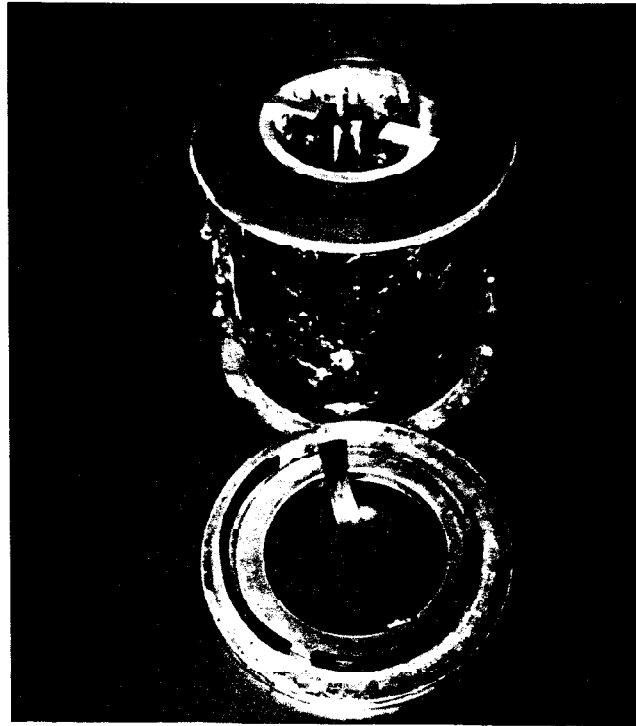
Plate 4.1 Moulds used for construction of model pipes.

Figure 4.6 presents a comparison of model and prototype pipe external diameter to wall thickness ratios. Manufacture of model pipes was carried out by vertical casting. Particle segregation was experienced with some of the wetter trial mixes. The pipe moulds were vibrated on a vibrating table whilst microconcrete was added in approximately four layers. Large air voids were sometimes experienced at layer interfaces. To overcome these voids it was found necessary to use a 4mm diameter rod as a vibrating poker and to control carefully the quantity of mould release oil used. This manufacturing method together with microconcrete mix II produces good quality model pipes with few air voids and no visible particle segregation.

MOULD		PROTOTYPE DIMENSION	MODEL DIMENSION	SCALE
1	Outside Diameter	1200mm	200mm	1:6
	Inside Diameter	900mm	150mm	1:6
	Length	2500-1100mm	232mm	varies
2	Outside Diameter	2100mm	200mm	1:10.5
	Inside Diameter	1800mm	171.4mm	1:10.5
	Length	2440-2500mm	232mm	approx. 1:10.5

Table 4.3 Model and prototype pipe dimensions.
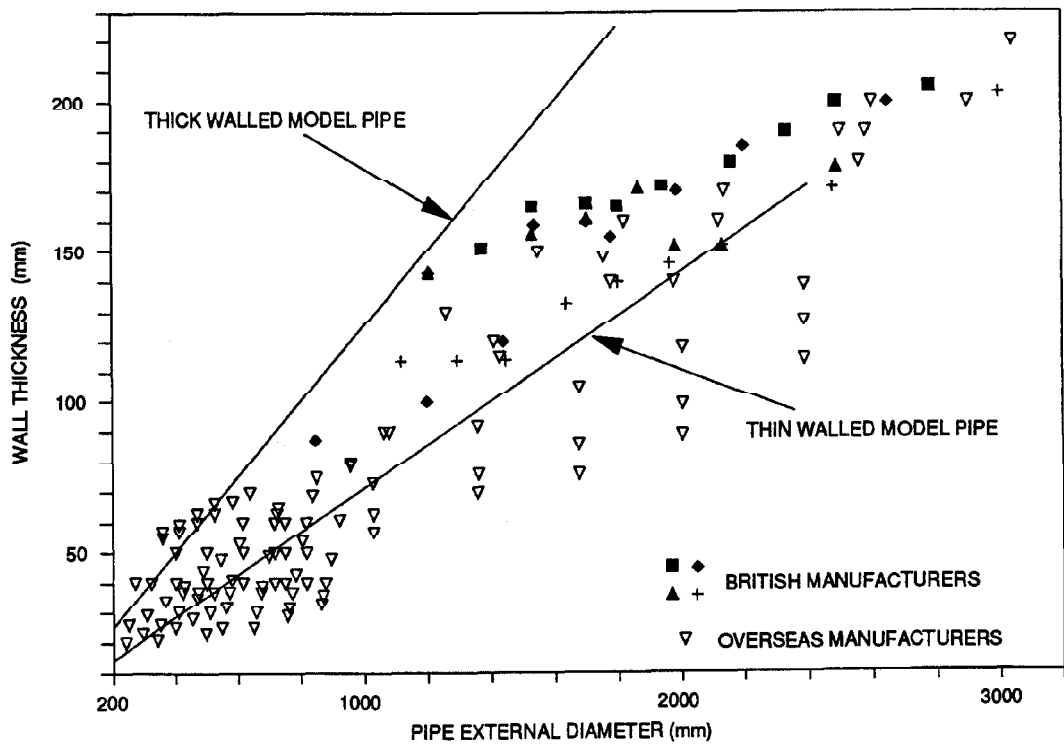
Figure 4.6 Comparison of model and prototype diameter to wall thickness ratios.

Initially pipes were manufactured as unreinforced with plain ends. This approach was chosen to obtain an understanding of hollow microconcrete cylinder behaviour under typical jacking loads. Reinforcement and joint profiles could be introduced as testing progressed and changes in readings or behaviour as a result of their addition could be assessed. Commencing with a pipe which will fail during tests allows joint profiles and reinforcement to be developed. Their ability to prevent failures, improve the pipes' performance and help establish design criteria can be assessed. Exact scale models of prototype pipes have been manufactured to test their behaviour and make the most valid comparisons and predictions.

Manufacture of pipes with joint profiles was carried out to model the in wall and steel collar joints; the pipes can be seen in Plates 4.2 and 4.3. It was necessary to take care in removing moulds. Pipe moulds were stripped eleven hours after concrete placing to avoid damage to the joint profiles. Steel collars were attached to the microconcrete pipe by short lengths of model reinforcement, in a manner similar to that used on prototype pipes.
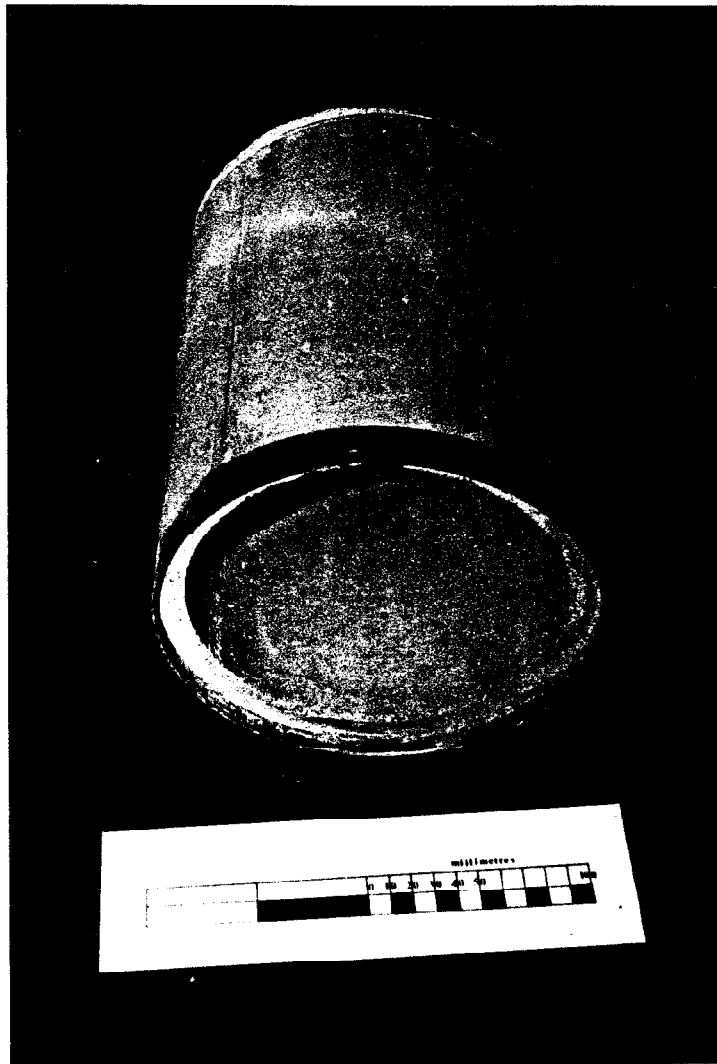
Plate 4.2 A steel collar jointed thin walled model pipe.
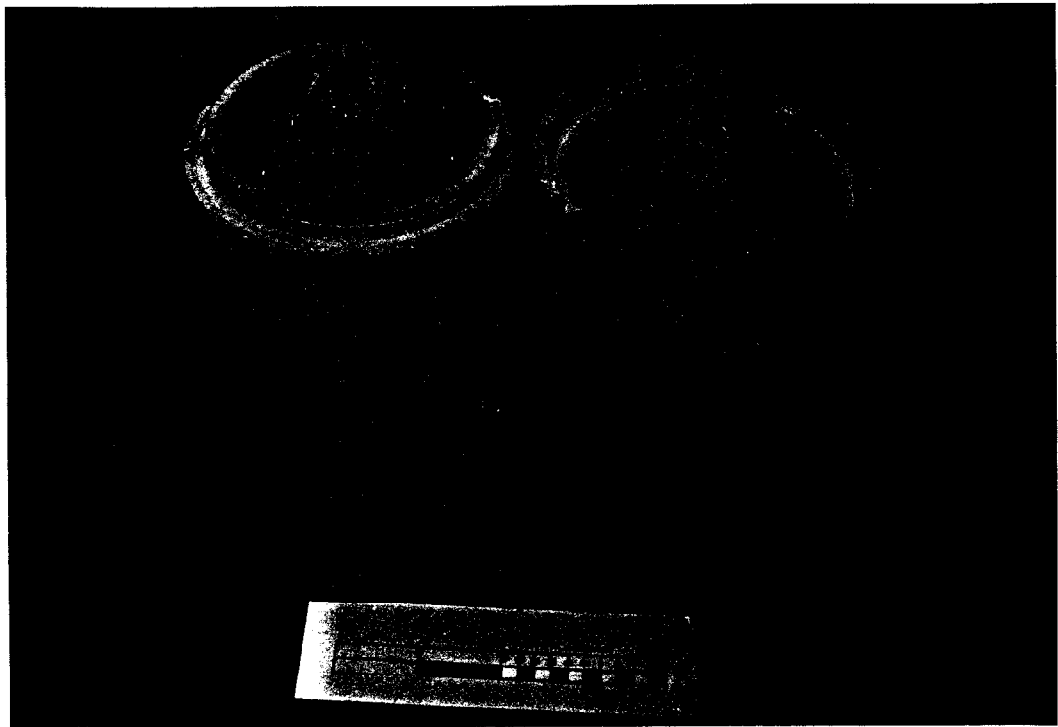
Plate 4.3 In wall jointed thick walled model pipes.

4.1.4 Pipe tests

Pipes were tested for compliance with BS 5911: part 4 crushing test requirements. The test procedure involves loading a horizontal pipe along the top edge through a bearing strip the full length of the pipe. The underside of the pipe was supported on two parallel bearing strips as shown in Figure 4.7 and Plate 4.4. The British Standard specifies dimensions for the bearing strips which have been accurately scaled to test the model concrete pipes. The pipes must pass three stage requirements to pass the test. Firstly, a 'no crack' load must be sustained for one minute and secondly a works proof load for a further minute, both with a requirement for maximum allowable crack widths. Finally, the pipe must carry a maximum load. The

'No crack' load is 50% of maximum and the works proof load is 80% of the maximum load. Modelled maximum loads for the pipes were 4.25kN/pipe(232mm) for the 1:6 thicker walled pipe and 4.42kN/pipe(232mm) for the thinner walled pipes at a scale of 1:10.5.
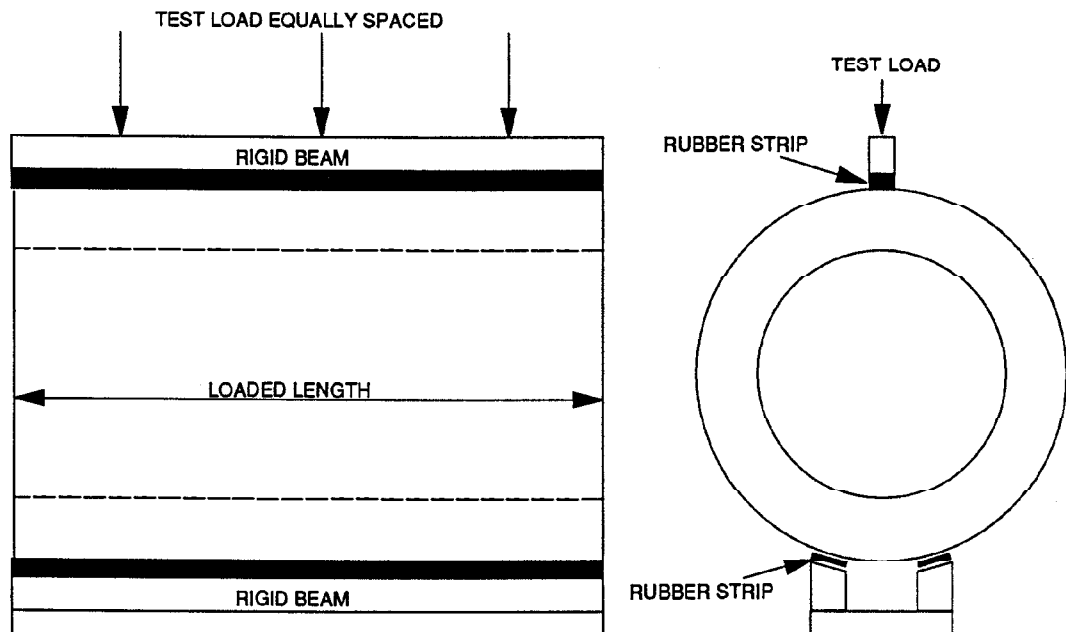
Figure 4.7 BS 5911 crushing test arrangement.

Results from the earlier crushing tests have shown that thick walled unreinforced model pipes surpass the British Standard requirements for this test and thin walled pipes need reinforcement in order to reach the necessary standard. During the course of the research, pipe manufacturers' works have been visited, where manufacture and testing of prototype pipes have been witnessed.

The British Standard makes no specification as to the placement of loading platens on the pipes with steel collar joints and whether the steel collar should or should not be loaded. Loading of the socket is left to the discretion of the manufacturer. During laboratory modelling a number of tests was conducted with the platen placed at different positions relative to the steel collar ring and results are reported in Section 9.9.

Plate 4.4 A view of loading platen positions for a British Standard test.

Regular testing has been carried out as research progressed to ensure British Standards have been maintained. These have included measurements of the dimensions of pipes to comply with allowable tolerances and the joint face strength test (Peckham 1987). At the commencement of this research a realistic axial load capacity test was being called for by the pipejacking industry. It is hoped that results reported in Chapter 6 will lead to a more realistic test that will produce the same types of failure as those experienced in the field under eccentric loading.

4.1.5 Manufacturing tolerances

Measurements for compliance of model pipes with the dimension requirements of BS 5911: part 4 (1986 draft) have been carried out. The requirements of the various Clauses are summarised in Table 4.4 for comparisons between model and prototype pipes.

Measurement of squareness of end is of particular importance. The British Standard does not state what part of the pipe the squareness should be measured in relation to.

Data recorded during the experimental period confirmed that the pipes complied with the scaled dimensions of the British Standard. It was noted that extreme care was required to maintain squareness of pipe ends; some pipes manufactured were not within the squareness tolerance and were used for British Standard crushing tests. The model pipes were invariably a slightly different external diameter at each end. The greater diameter was always the bottom end of the pipe as it was cast due to the constraint imposed on the pipe mould by the mould for the pipe end profile.

4.2 Reinforcement

A review of materials used for model reinforcement was presented in Section 2.7.2 and led to a choice between two suitable wires. Selection was made on economic grounds; threaded bar was very costly, so custom deformed black annealed wire was chosen.

The reinforcement used in the manufacture of prototype pipes is 9-12mm diameter high yield steel rebar for circumferential bars and 6-12mm diameter for longitudinal bars. Scaling required reinforcement from 1.14mm to 2.0mm diameter. Black annealed wire is commercially available in diameters of 1.25mm, 1.6mm and 2.0mm. The 1.25mm and 2.0mm diameter wires were chosen to give correct cross sectional areas once deformed. The patterns
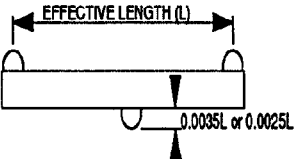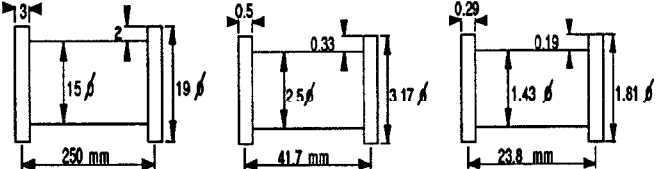
Clause	Dimension	Prototype	Scale Model 1:6 D/T = 8	Scale Model 1:10.5 D/T = 14
10	Internal Diameter Permissible Deviation	+50mm -20mm 900mm ±6mm 1800mm ±10mm	+8.3mm -3.3mm 150mm ±1mm	+4.8mm -1.9mm 171.4mm ±0.95mm
11	External Diameter	900 I.D. ±3mm 1800 I.D. ±5mm	200mm O.D. ±0.5mm	200mm O.D. ±0.48mm
12	Wall Thickness Variation	900mm ±6mm 1800mm ±10mm	±1mm	±0.95mm
13	Squareness of End	900mm ±4mm 1800mm ±5.5mm	±0.67mm	±0.52mm
14	Straightness	3.5mm/M I.D. 2.5mm/M O.D.	For pipe length = 232mm I.D. 0.812mm/pipe O.D. 0.58mm/pipe	

Clause	Dimension	Prototype	Scale Model 1:6 D/T = 8	Scale Model 1:10.5 D/T = 14
15	Surface Regularity			

Clause	Dimension	Prototype	Scale Model 1:6 D/T = 8	Scale Model 1:10.5 D/T = 14
18.3	Crushing Test Loads			
	900mm I.D. No Crack	55kN/M	2.13kN/232mm	
	Works Proof	88kN/M	3.40kN/232mm	
	Maximum	110kN/M	4.25kN/232mm	
	1800mm I.D. No Crack	100kN/M		2.21kN/232mm
	Works Proof	160kN/M		3.54kN/232mm
	Maximum	200kN/M		4.42kN/232mm

Table 4.4   BS 5911: Part 4. Dimensional requirements for model and prototype pipes.

of deformations have previously been studied by Sabnis et al. (1983) who have used a hand operated device with two sets of knurling wheels, and Noor and Khalid (1980) and Evans and Clarke (1981) have used a machine that produces ribs rather than indentations. Personal communication with Evans suggested that the machine he had been using was unreliable and prone to breakdowns and the model reinforcement produced did not have enough surface deformation to produce adequate bond or crack simulation. In the light of the drawbacks with each type of wire, the knurling machine was chosen with the most regularly knurled wheels commercially available. The wire deforming machine is drawn in Figure 4.8 and was designed and constructed from a photograph, Sabnis et al. (1983), after a technique developed at Cornell Structural Laboratory, U.S.A.

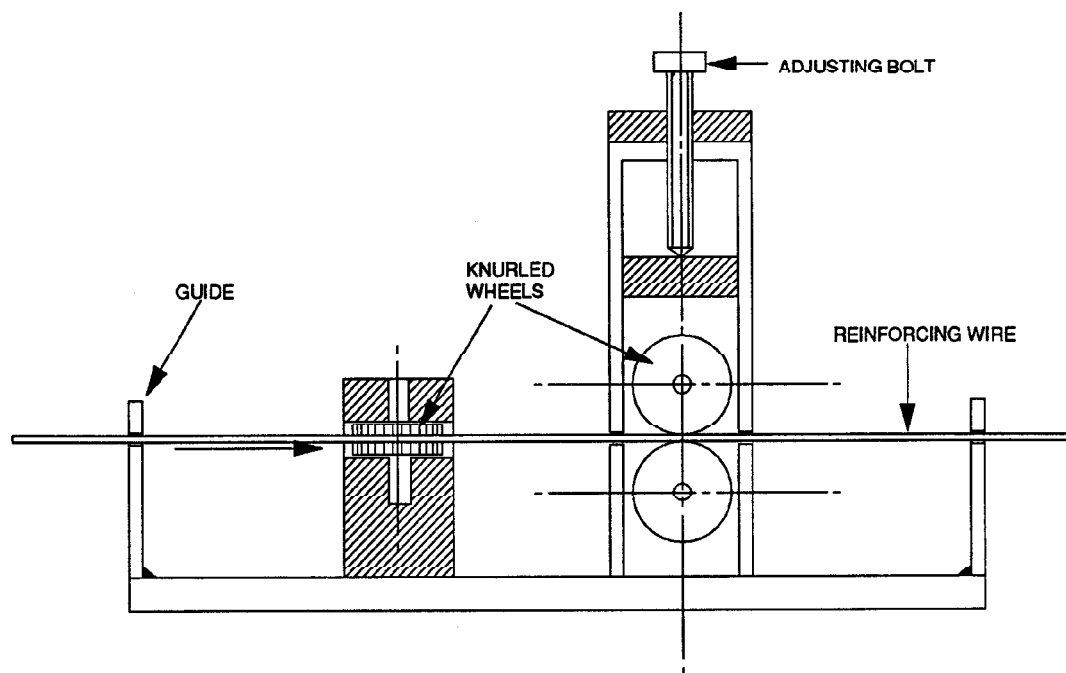**Figure 4.8** Model reinforcement deforming machine.

Black annealed wire is work hardened by the knurling wheels which increases its yield strength. Tests were carried out on the wire before and after deforming using an Instron loading machine and load extension graphs were plotted (Figure 4.9). The deformed wire was found to have an elastic modulus of $240kN/mm^2$ which is close to that of the prototype

steel. Deformed wire was also tested for its bond characteristics. It was established that the bond stress developed between the steel and microconcrete was 2.0N/mm^2 before failure due to slipping. This indicated that a bond length of 34mm for the 1.25mm diameter wire and 55mm for the 2.0mm diameter wire was required compared with the usual design practice of using forty reinforcement diameters for the bond length.
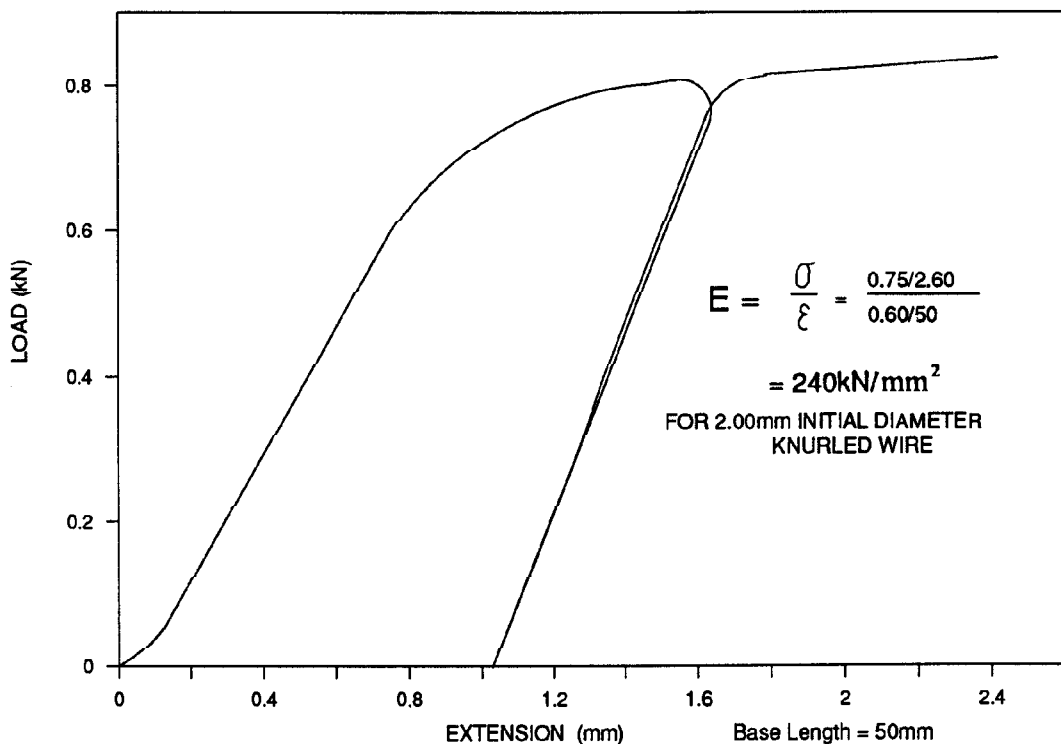
Figure 4.9 Load deformation plots of black annealed wire.

The prototype reinforcement cages were fabricated using an automatic welding machine which would spot weld wire junctions. Tests with spot welded model reinforcement indicated no loss of strength due to welding if the arc temperature was carefully controlled. This method was therefore adopted. Two reinforcement cages were constructed for each pipe to provide inner and outer steel and they can be seen in Plate 4.5. These were attached using short lengths of wire which also acted as placement spacers to maintain reinforcement cover depths. Reinforcement cages were constructed to the dimensions shown in Figure 4.10.
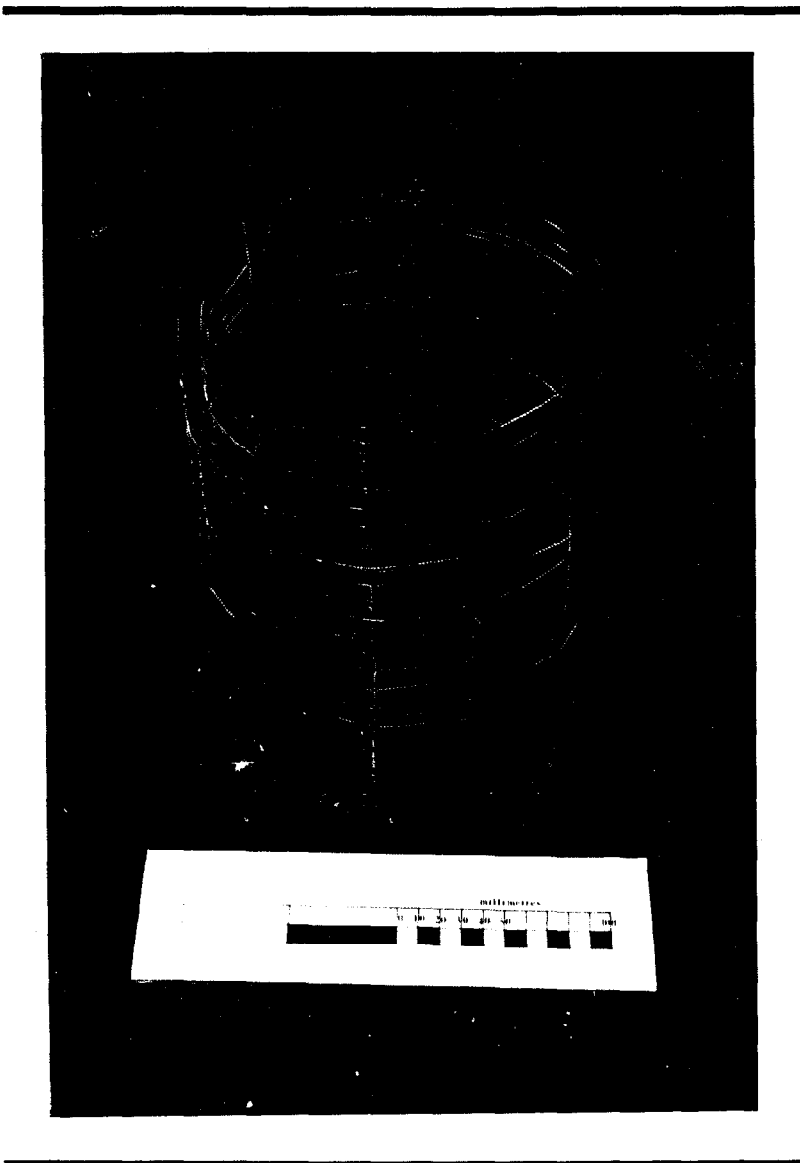
Plate 4.5 A typical model reinforcement cage.
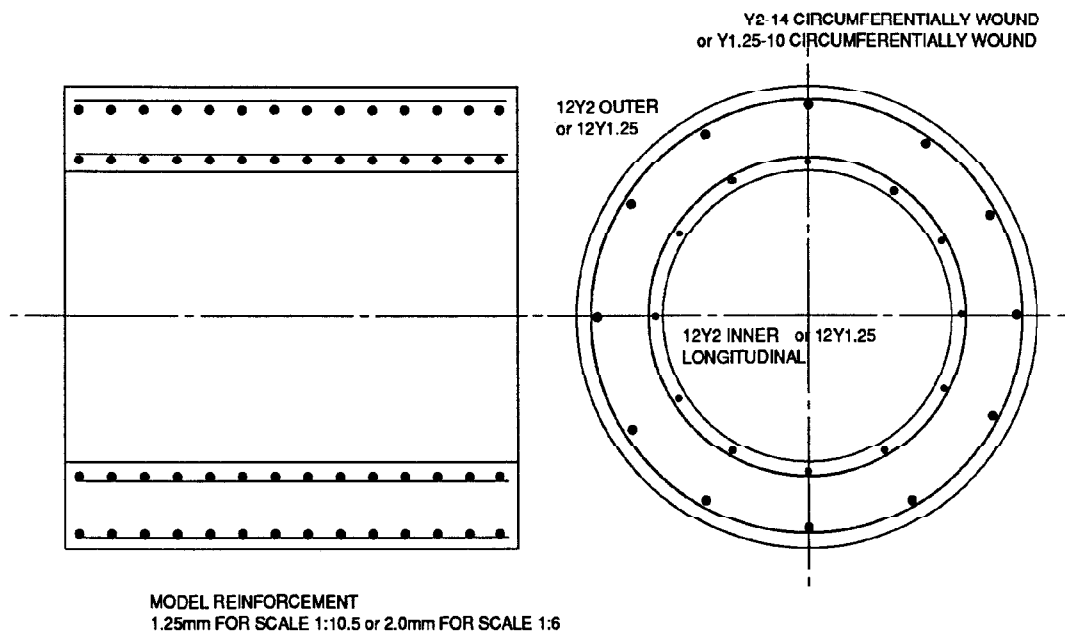
Figure 4.10 Reinforcement cage arrangements.

4.3 Joint sealing rings

True geometric modelling of the more complex profiled and finned sealing ring used for steel collar jointed pipes has not been possible. All model sealing rings were made from 'O' ring cord cut to length and glued to form a ring. Various diameters; 1.8mm; 2.4mm; 3.0mm; 3.5mm; were used to provide seals on the various diameter and scaled joints. The 'O' ring cord was cut to a length which provided a sealing ring requiring 2% extension in total length to reach its jointed diameter.

CHAPTER 5

SAND CHAMBER TESTS

5.1 Introduction

The progress of the overall programme of research is presented as Figure 5.1. This began with tests on pairs of pipes, axially loaded in the testing chamber filled with sand, (Figure 3.1), which could be stressed at the boundaries. The tests were designed to provide some knowledge of the behaviour of axially loaded hollow concrete cylinders. The variables introduced during the programme allowed for the testing of deflected pipes and different soil stresses surrounding the pipes. Testing began with unreinforced plain ended pipes and progressed to introduce firstly reinforcement and later, joint profiles. In all tests the sand used was Leighton Buzzard 14/25, some details of which are given in the next section.

THREE YEAR RESEARCH PROGRESS
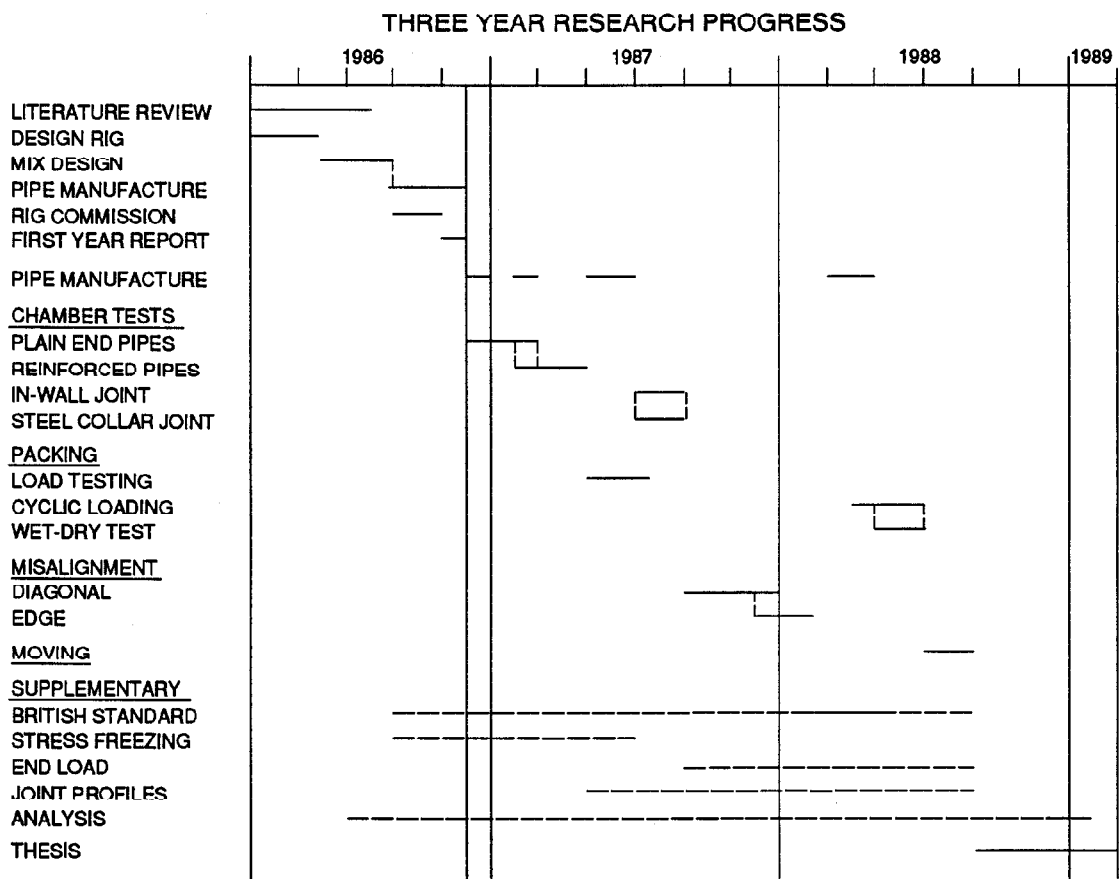
Figure 5.1 Test Programme.

5.2 Leighton buzzard 14-25 sand

An investigation was carried out to assess the properties of the sand. Previous research at Oxford University provided invaluable specialist information which may be required at a later stage. The characteristic tests on the sand resulted in the following information:-

Relative Density in the Chamber	$I_D = 85 - 88\%$	
Minimum Voids Ratio	$e_{min} = 0.49$	
Maximum Voids Ratio	$e_{max} = 0.78$	
Particle size distribution	$< 1.40mm$	100%
	$< 1.18mm$	84.7%
	$< 600\mu m$	1.2%
	$< 300\mu m$	0.2%
	$< 150\mu m$	0.05%

5.3 Pipe tests

A series of thirty one tests were conducted in the sand chamber and are summarised in Table 5.1. Thirteen tests were carried out on plain end unreinforced pipes. The pipes had walls of different thickness representing external diameter to wall thickness ratios of 8:1 and 14:1 and internal diameter to wall thickness ratios of 6:1 and 12:1. Pipes were initially tested surrounded by sand in the test chamber but without boundary stresses applied. The pipes were deflected to various initial alignments relative to each other.

PIPE TYPE	No.	DATE	PIPE WALL THICKNESS	σ_v kPa	σ_h kPa	ALIGNMENT	REMARKS
	1	26.11.86	Thick	0	0	Straight	
	2	2.12.86	Thin	0	0	Straight	
	3	8.12.86	Thick	0	0	0.25^0 up	
UN-	4	11.12.86	Thin	0	0	0.25^0 down	
REIN-	5	11.12.86	Thick	0	0	0.5^0 down	
FORCED	6	20.1.87	Thick	110	40	0.5^0 left	
	7	21.1.87	Thin	110	40	0.5^0 left	
PLAIN	8	23.1.87	Thin	110	40	1^0 right	
END	9	30.1.87	Thick	110	40	1^0 right	
	10	3.2.87	Thin	50	50	0.5^0 right	
	11	4.2.87	Thick	50	50	0.5^0 left	
	12	6.2.87	Thick	50	50	1^0 right	
	13	9.2.87	Thin	50	50	0.5^0 right	
	14	5.3.87	Thin	0	0	0.5^0 right	
REIN-	15	6.3.87	Thick	0	0	0.5^0 right	
FORCED	16	9.3.87	Thick	160	55	1^0 right	
	17	16.3.87	Thin	160	55	1^0 right	
PLAIN	18	19.3.87	Thick	110	40	1^0 right	Repeat 9
END	19	20.3.87	Thin	110	40	1^0 right	Repeat 8
	20	30.3.87	Thin	50	50	0.5^0 right	
	21	10.4.87	Thick	50	50	0.5^0 right	
	22	22.4.87	Thick	200	73	1^0 right	
	23	23.4.87	Thin	200	73	1^0 right	
IN	24	20.7.87	Thin	50	50	0.5^0 right	
WALL	25	21.7.87	Thick	50	50	0.5^0 right	
REIN-	26	22.7.87	Thick	160	55	1^0 right	
FORCED	27	23.7.87	Thin	160	55	1^0 right	
STEEL	28	28.7.87	Thick	50	50	0.5^0 right	Repeat 11,21,25
COLLAR	29	29.7.87	Thin	50	50	0.5^0 right	Repeat 10,13,20,24
REIN-							
FORCED	30	30.7.87	Thick	160	55	1^0 right	Repeat 16,26
	31	31.7.87	Thin	160	55	1^0 right	Repeat 17,27

Table 5.1 Summary of soil chamber test initial conditions.

Test No.	0°	30°	60°	90°	120°	150°	180°	210°	240°	270°	300°	330°
1			INT				INT				INT	
2			INT				INT				INT	
3			INT				INT				INT	
4			INT				INT				INT	
5			INT				INT				INT	
6			INT				INT				INT	
7			INT				INT				INT	
8												
9				INT				INT				INT
10				INT/EXT						EXT		
11				INT/EXT						EXT		
12				INT/EXT						EXT		
13				INT/EXT						EXT		
14				INT				INT				INT
15				INT				INT				INT
16				EXT						INT/EXT		
17				EXT						INT/EXT		
18				EXT						INT/EXT		
19				EXT						INT/EXT		
20				3No.EXT								
21				EXT						INT/EXT		
22				EXT				EXT				EXT
23				EXT				EXT				EXT
24				INT/EXT						INT		
25				INT/EXT						INT		
26				INT/EXT						INT		
27				INT/EXT						INT		
28				INT/EXT						INT		
29				INT/EXT						INT		
30				INT/EXT						INT		
31				INT/EXT						INT		

INT = internal strain gauge   EXT = external strain gauge
Positions of strain gauges are referenced in degrees starting with zero at the bottom of the pipe and moving clockwise around the circumference

Table 5.2 Positions of strain gauges.

During the first tests some of the pipes were cracking. It was not until the full axial load capacity of the rig had been applied and the test stopped, that post test inspection of the pipes revealed extensive cracking. It was found that once the pipes had cracked (as seen in Plate 5.1) they were continuing to sustain increasing axial load. It was apparent that a method was required to inspect the pipes visually for the onset of cracking. Once a pipe has cracked it is no longer capable of performing its long term functions. A post-mortem examination of data may reveal onset of failure but a method of determining failure by visible cracking during the test was required so that once the pipe was visibly failing the test could be stopped.

Plate 5.1 Cracking of unreinforced model concrete pipes (Test 4).

After investigations into the various methods of obtaining a continuous visual inspection of the internal walls of the pipes, a method using a spot light for illumination and a mirror to obtain a view was chosen. Tests could now be stopped as soon as cracking was observed.

A summary sheet for each test was prepared as shown in the example in Figure 5.2. Data recording and transducer positions were noted together with initial test arrangement details. Typical data recording during this test series included measurements using eight LVDT's for pipe position; three LVDT's for joint gap; ten electrical resistance strain gauges for concrete surface strains; five pressure cells for test chamber boundary conditions and a load cell for jacking load. Notations for transducer positions are summarised in Figure 5.3.

Programmes were written to record test data which allowed initial (zero) readings to be taken. During a test each transducer was scanned four times every second and data were recorded after preset load increments, usually 2.5kN, had been passed.

Testing progressed to introduce reinforced pipes and joint profiles into the programme. With each new type of pipe initial arrangements were reproduced and tests repeated to enable valid comparisons to be made.

DATE: 2·1·7·87	DATA FILE: TEST 25	TEST No. 25

PIPE: (Thick)/Thin̶   (Reinf)/Un̶rein̶f   Plai̶n̶/In Wall̶/Steel̶

ALIGNMENT Line   ○   Level ○·5° RIGHT

BOUNDARY STRESS   vert. 50kPa   horz. 50kPa

MAX. APPLIED LOAD   202·33   **kN**

REMARKS

INSTRUMENT POSITIONS

ELEV.

PLAN

NOTES:		ZERO	ST. GAUGE
Data Files Zero 25· DAT before jointing	1	−7583	17 long ⎫ 270
Zero 25A· DAT after jointing	2	1601	18 ang ⎬ INT
	3	1940	19 cir ⎭
	4	2137	20 long ⎫ 90
	5	922	21 ang ⎬ INT
	6	−4047	22 cir ⎭
	7	−1595	23 long ⎫ 90
	8	−10231	24 ang ⎬ EXT
	9	−108	25 cir ⎭
	10	−3711	26 dummy
3·5mm ⌀	11	12924	31

Figure 5.2 Test summary sheet.
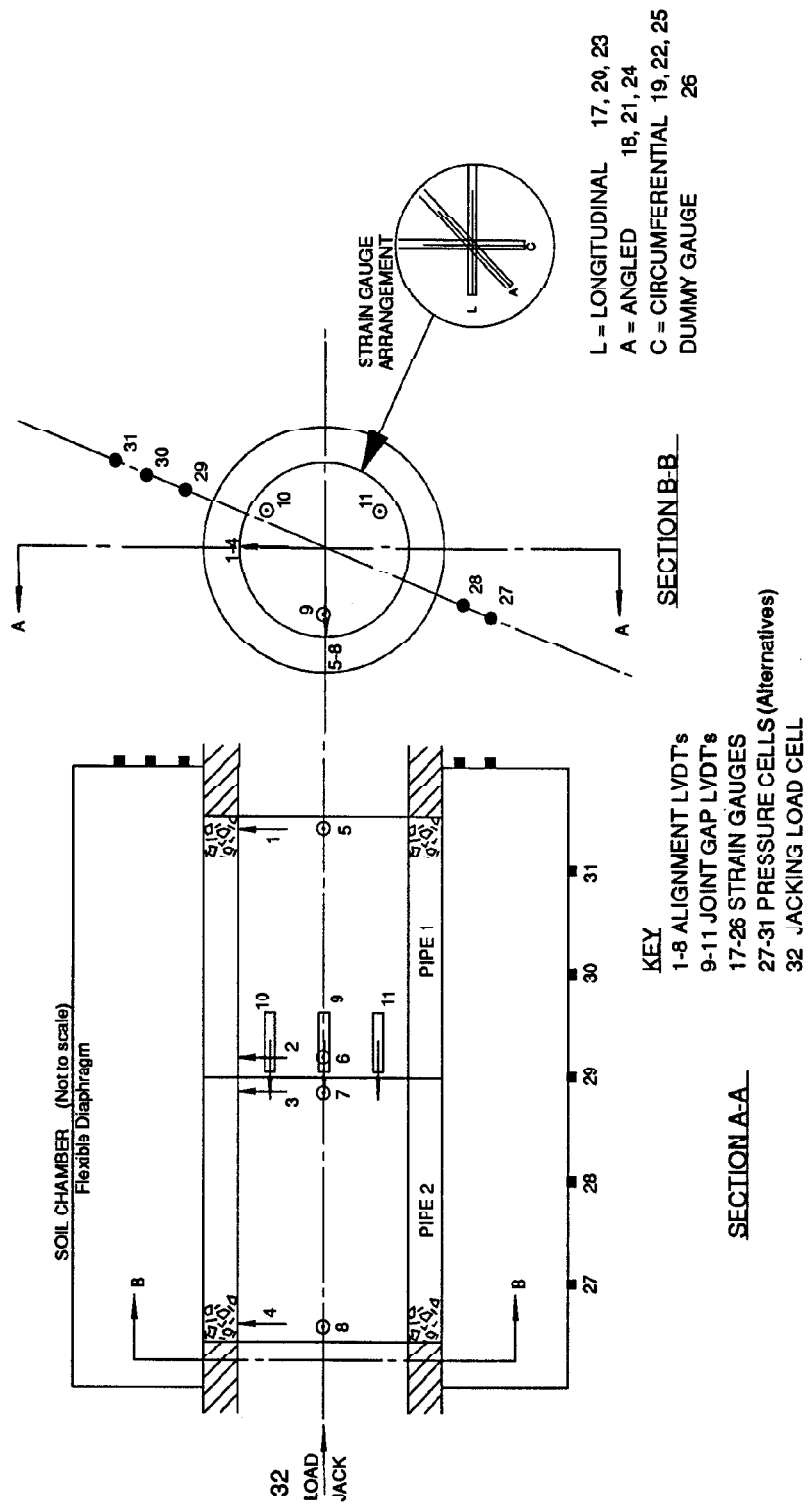
Figure 5.3 Notations for transducer positions.

SECTION B-B

STRAIN GAUGE ARRANGEMENT

L = LONGITUDINAL   17, 20, 23
A = ANGLED   18, 21, 24
C = CIRCUMFERENTIAL 19, 22, 25
DUMMY GAUGE   26

SOIL CHAMBER   (Not to scale)
Flexible Diaphragm

PIPE 1

PIPE 2

SECTION A-A

KEY
1-8 ALIGNMENT LVDT's
9-11 JOINT GAP LVDT's
17-26 STRAIN GAUGES
27-31 PRESSURE CELLS (Alternatives)
32 JACKING LOAD CELL

LOAD
JACK

5.4 Results of the tests

5.4.1 Vertical and horizontal positions

Data were recorded which monitored the vertical and horizontal positions of the two pipes under load at their individual ends. The transducers were mounted at the positions shown in Figure 5.4.
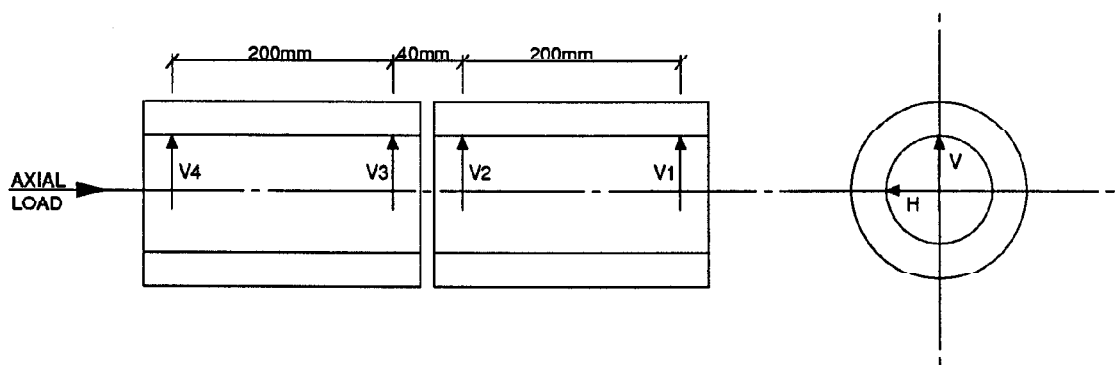
Figure 5.4 Positions of LVDT's measuring pipe alignment.

The transducers were fixed to a 40mm diameter bar which was secured at each end. Initial readings on the LVDT's were taken using a straight edge to enable geometrical analysis of the orientations of the pipes. Using this information the horizontal and vertical alignment of the internal diameters of the pipes could be calculated. These can be related to line and level readings taken on a full scale pipejack. Further calculations of the three dimensional orientation of consecutive pipes resulted in information about the maximum angular deflection and theoretical contact position between the two pipes. These calculations are summarised below:-

1. All readings are corrected to give pipe position relative to the zero datum line.

$$H1 = H1 - H1_{zero}$$

$$V1 = V1 - V1_{zero} \quad etc.$$

2. *Alignment of each pipe is calculated.*

$$ALH_1 = H1 - H2$$

$$ALV_1 = V1 - V2$$

$$ALH_2 = H3 - H4$$

$$ALV_2 = V1 - V2$$

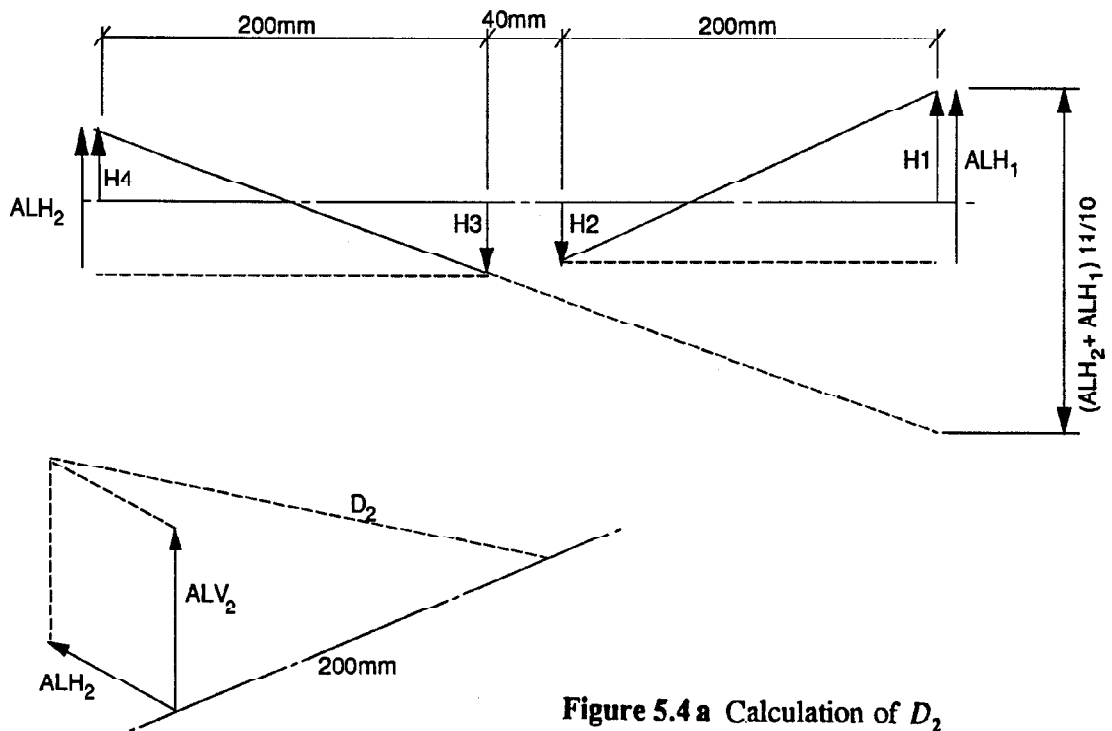3. *The diagonal length between triangulation points is calculated.*

Figure 5.4 a Calculation of D_2

The length of the diagonal on pipe 2 is

$$D_2 = \frac{11}{10} \sqrt{((ALH_2)^2 + (ALV_2)^2 + 200^2)}$$

The length of the diagonal on pipe 1 is

$$D_1 = \frac{11}{10} \sqrt{((ALH_1)^2 + (ALV_1)^2 + 200^2)}$$

Total horizontal displacement between ends of the pipe

$$ALH_T = \frac{11}{10}(ALH_2 - ALH_1)$$

Total vertical displacement between ends of the pipe

$$ALV_T = \frac{11}{10}(ALV_2 - ALV_1)$$

Total diagonal length between extreme ends of the pipes

$$D = \sqrt{((ALH_T)^2 + (ALV_T)^2 + (440)^2)}$$

Deflection angle between consecutive pipes

$$\beta = \cos^{-1}\left(\frac{-D^2 + D_2^2 + D_1^2}{2.D_2.D_1}\right) \qquad \ldots\text{Eq 5.1}$$

Analysis and visual inspection of the early deflected pipe tests indicated that sand was entering the gap between pipe ends, preventing full realignment of the pipes. This resulted in axial load transfer at positions away from the theoretical contact point and crushing of sand grains. Some spalling of concrete (shown in Plate 5.2) at the areas of sand penetration was visually evident. Whilst this would be true modelling of the situation at full size in granular materials, it was considered necessary to limit sand ingress into the pipe joint gap. This was satisfactorily achieved with the use of strips of masking tape.
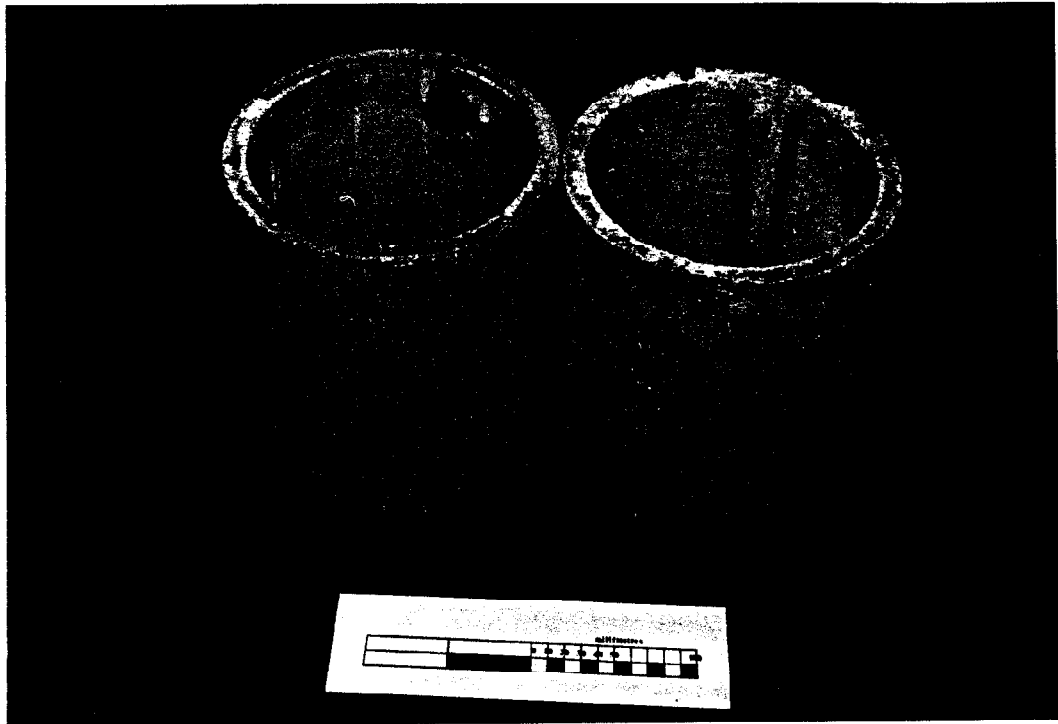
Plate 5.2 Spalling at common plain end of pipes (Test 14).

Results of changes in pipe alignment are presented in graphic form by plotting either angular deflection or location of point of contact against applied axial load. Graphs from three tests are presented in Figure 5.5. The tests had the same initial deflection angle of 0.5^0 horizontally and boundary stress conditions of 50kPa vertical and 50kPa horizontal and the data were taken from the results of Tests 20, 25 and 29. The only intended difference between the tests was the type of pipe being tested; Test 20 was on a thin walled, plain ended pipe; Test 25 was on a thick walled, in wall jointed pipe and Test 29 was on a steel collared, thin walled pipe: all pipes were identically reinforced.

The plot in Figure 5.5a shows how all the pipes attempt to align themselves but as alignment is occurring so Figure 5.5b shows that the point of contact between the pipes is changing. Test 29 maintains almost the same point of contact during the test but does not fully align itself, possibly

due to the ingress of sand into the joint or the ends of one of the pipes not being square. The probability of non square ends is also shown due to the larger than intended initial deflection angle on this test.
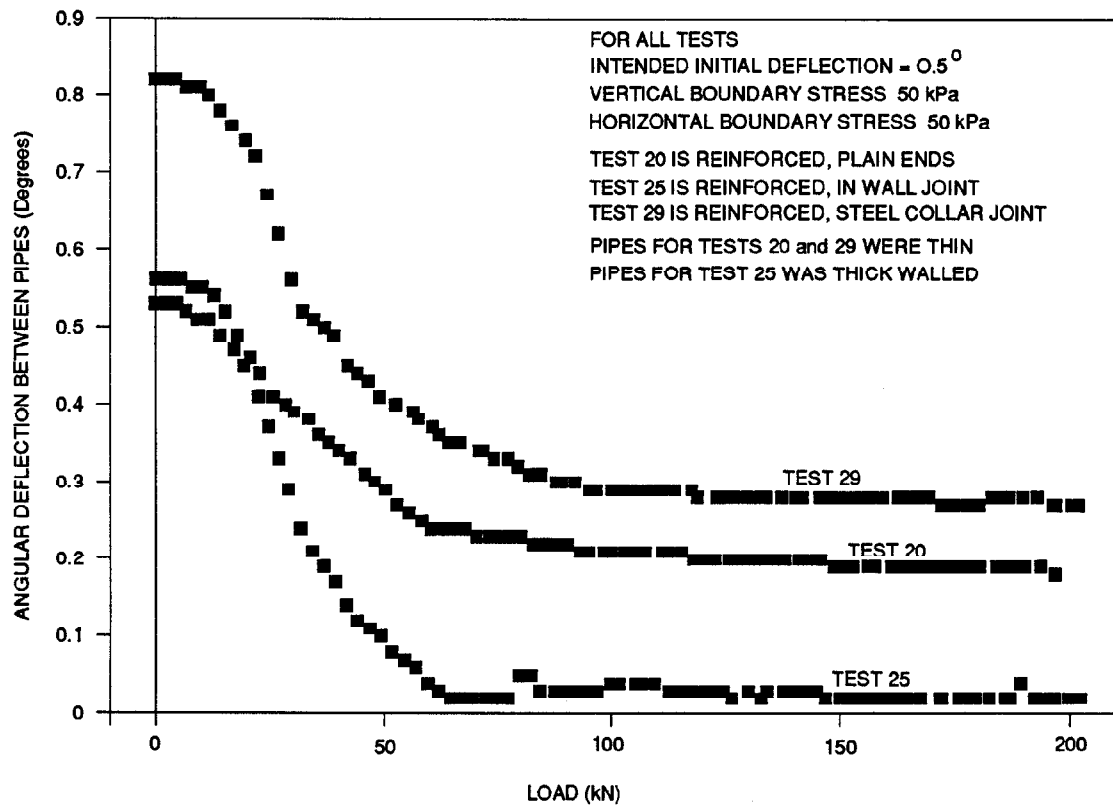

Figure 5.5a Alignment of pipes.

Pipes used in Test 20 do not fully align but the position of contact changes from the left hand side to the top of the pipes. The pipes from Test 25 align themselves and the position of contact between the pipes changes from the left side of the pipes to the right side quite suddenly at about 70kN of applied axial load.

One problem noted throughout this test series was that pipes were aligning themselves or reaching a point when no further change of alignment was occurring, but the pipes had not visibly failed. The research was aimed at assessing jacking loads of misaligned pipes and investigating the different failure modes. This is not possible if the pipes are always moving to an 'aligned' position.
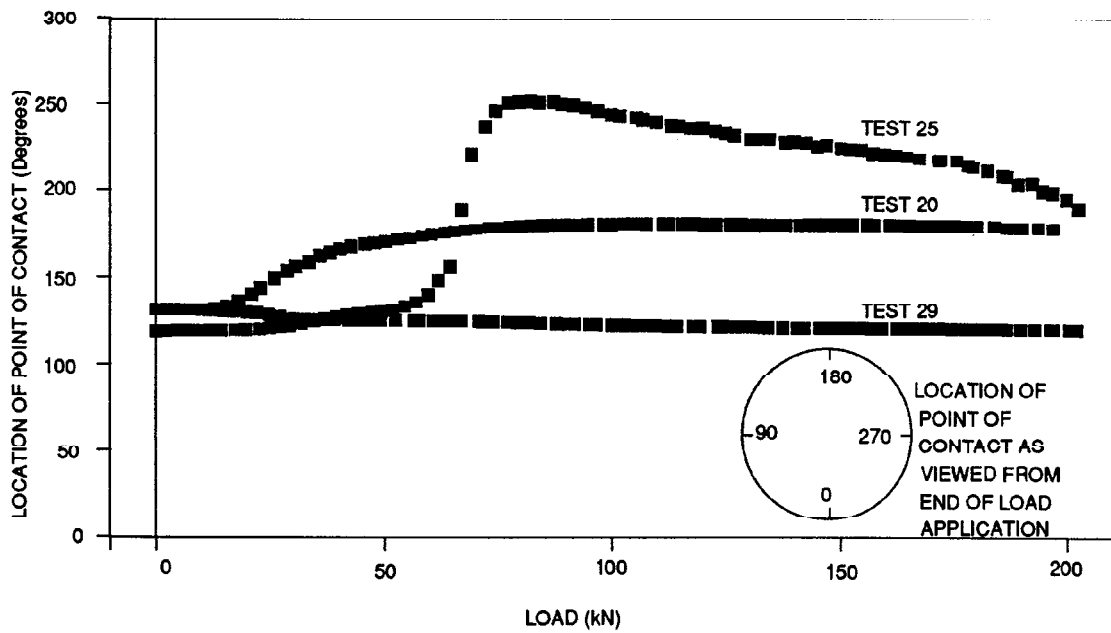
Figure 5.5b Location of point of contact between pipes.

Throughout this test series it proved difficult to compare tests. Even when initial conditions were identical, pipes moved differently during the test and it is therefore important to assess the three dimensional orientation changes of consecutive pipes before attempting to interpret test results.

5.4.2 Joint gap

The previous assessment of pipe deflection was measured relative to the model pipes' internal surfaces. This method of analysis takes no account of manufacturing tolerances and the possibility of pipe ends not being square relative to the internal surface. To obtain an assessment of pipe end squareness, three LVDT's were mounted spanning the common joint between the two pipes. The LVDT's had their zero datum readings taken in free air with one pipe placed on top of the other. Changes in the measured joint gap at the start of testing and during loading would enable analysis to be made of the contact point relative to the pipe end squareness. This can be compared to the deflections obtained from the alignment LVDT's.

Measurements of the changes of joint gap between the pipes for Tests 20, 25 and 29 are presented in Figure 5.6 and can be compared to the deflection data shown in Figure 5.5.

Joint gaps recorded during Test 20 all tended towards a reading of -0.2mm compared with the joint gap 'zero' reading taken when no axial load was applied. The gap was uniform around the pipes' circumference and the point of contact was recorded at the top of the pipes. Before the application of axial load the pipes had a joint gap difference of 0.9mm which agreed with the previously calculated angle of deflection of 0.52^0 between pipes. Joint gap values recorded during Test 25 indicated that the gap on the right of the pipe became much less than that on the left. This can be compared to the data recorded of the points of contact which also moved from the left to the right of the pipe. However, data recorded during Test 29 show the joint gap close to the bottom of the pipe to be the only position at which the gap is changing by a significant amount. During this test the point of contact remained on the left side of the pipe. There appears to be no logical explanation for the changes in the joint gaps recorded.
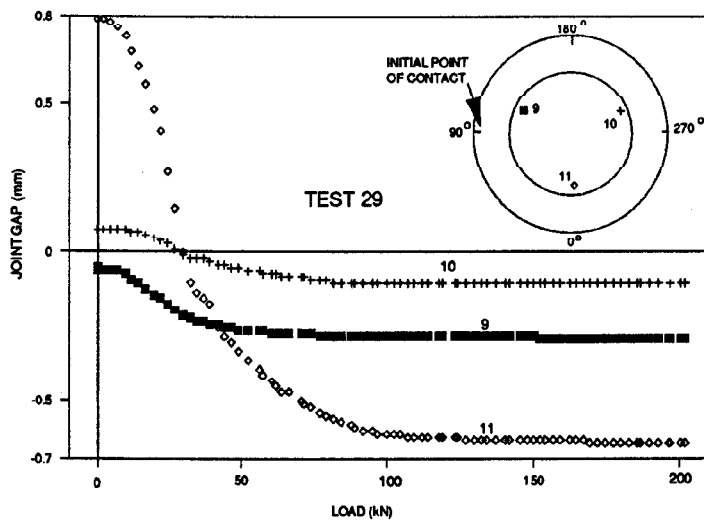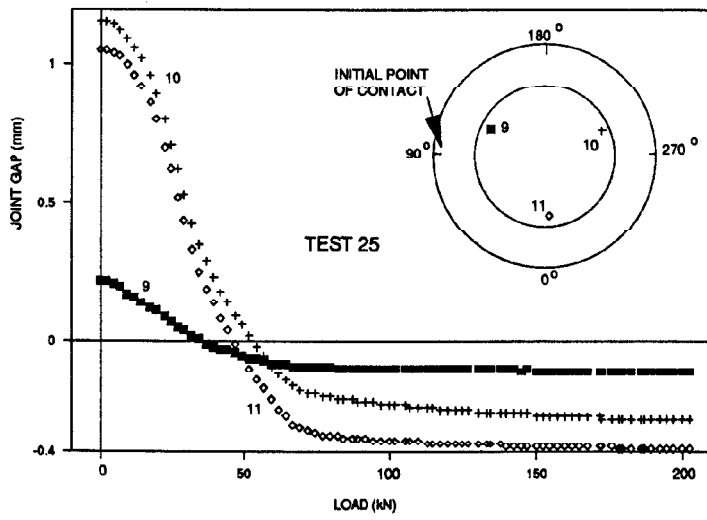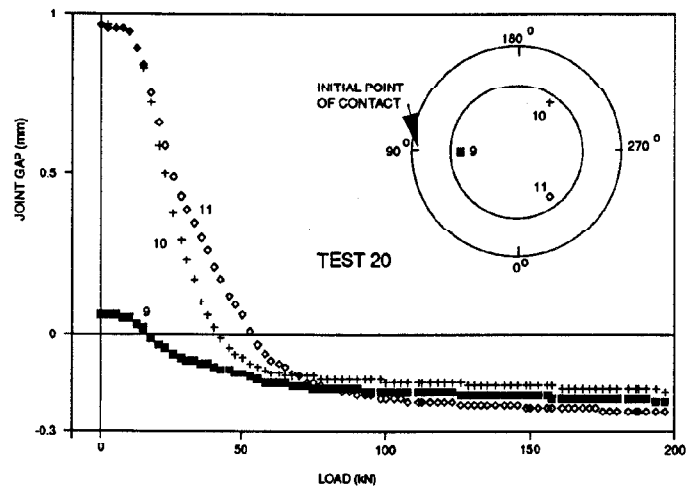
Figure 5.6 Variation of joint gaps.

Sand Chamber Tests 5-17

5.4.3 Pressure cells

The pressure cells were clamped in the chamber wall with their measuring diaphragms flush with the inside surface of the wall. In this test series they were mounted in a straight line vertically below the centre line of the pipes and at 100mm centres. Using results from Test 25 the pressure distribution shown in Figure 5.7 is observed.
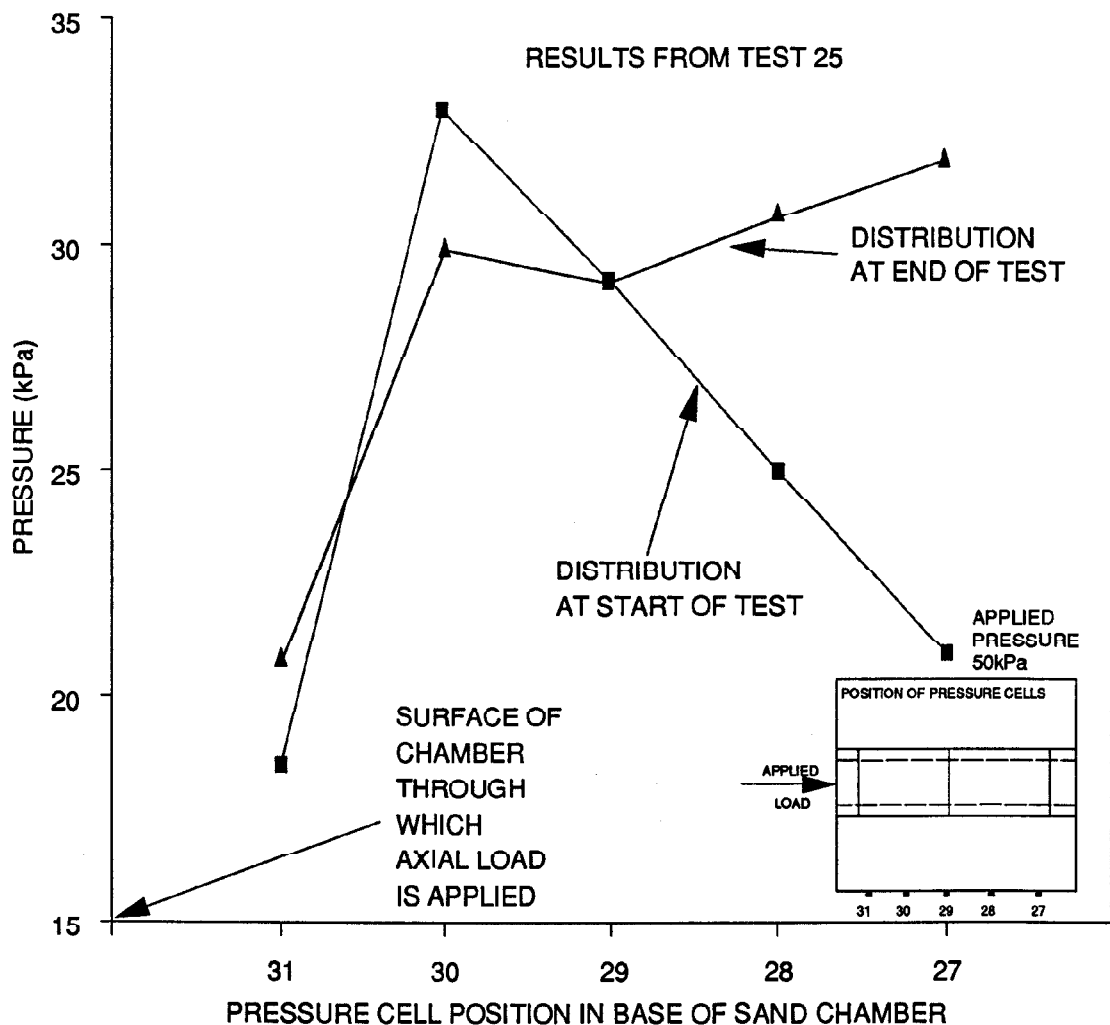

Figure 5.7 Distribution of pressure cell readings for Test 25.

The plots indicate how total sand stresses change during the test. Stresses measured on the transducer nearest the jacking ram change very little and stresses measured furthest from the

jacking ram increase significantly as jacking load is applied. This suggests that interaction between the pipes and the sand is influencing measurements at the boundary, which in turn must have influence on the pipes' interaction with the sand.

5.4.4 Electrical resistance strain gauges (ERSG's)

The ERSG's were glued to the concrete 30mm from the ends of the pipes (15mm for jointed pipes). Gauges were positioned at various circumferential positions relative to the point of contact and either inside or outside the pipe. They were always attached to the end of the first pipe which was nearest to the second pipe. Their positions on the pipe have been summarised in Table 5.2 and position references are to angular positions as viewed from the end of load application.

5.4.4.1 Principal strain analysis and sign convention

ERSG rosettes were mounted on the concrete surface with the individual gauges at 45^0 and three gauges to each rosette. They were mounted with one gauge longitudinal, parallel to the pipe's central axis, one gauge at 45^0 to this and the third gauge circumferentially around the pipe. The individual gauges are referred to as L. A and C respectively.

Another separate single gauge was mounted close to the pipes but on a 100mm concrete cube. This was used as a dummy gauge and was to allow for temperature or excitation voltage variations. Strain gauge readings were recorded with the pipes placed vertically in free air to obtain comparable datum readings. Calculation of principal strains and their orientation was carried out using the strain gauge data and Mohr's circle for strains. The analysis and sign conventions used are listed below:-
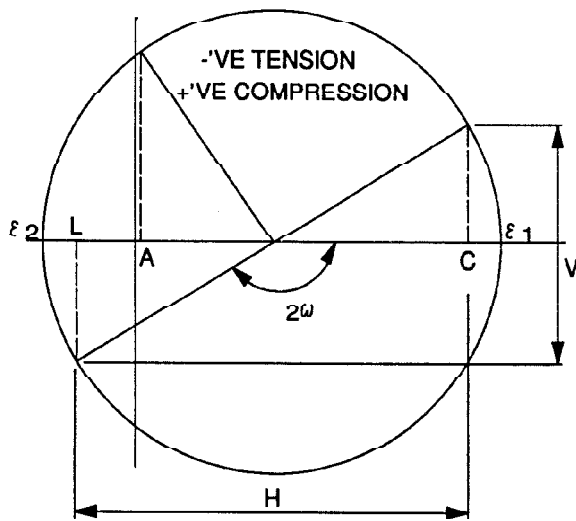
$$\frac{\varepsilon1 + \varepsilon2}{2} = \frac{L + C}{2}$$

$$V = L + C - 2A$$

$$H = C - L$$

$$\varepsilon1 = \frac{L + C}{2} + \frac{\sqrt{H^2 + V^2}}{2}$$

$$\varepsilon2 = \frac{L + C}{2} - \frac{\sqrt{H^2 + V^2}}{2}$$

Major principal strain = $\varepsilon1$

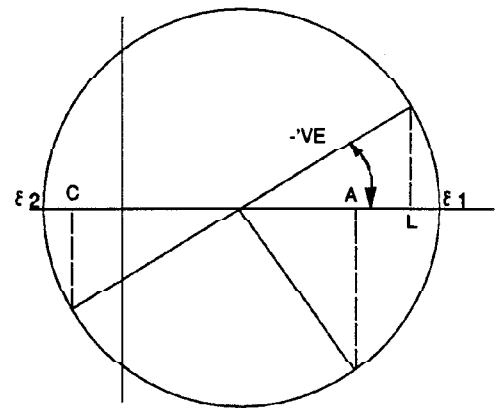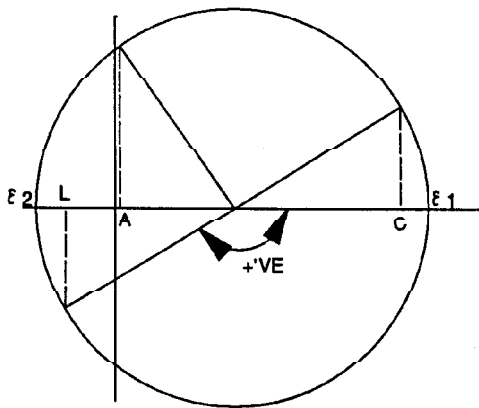Minor principal strain = $\varepsilon2$

Figure 5.7a   Sign Convention

The direction of the major principal strain was measured positive anti-clockwise and negative clockwise from the longitudinal strain gauge.

5.4.4.2 Strain gauge results

Comparison of the strain readings at gauge positions around the circumference of the pipe gives clear evidence of changes of loading conditions at the gauge. The complexity and interaction of various loads applied to the pipe during this test series and the pipes constantly changing their orientation means that strain data from the various tests was not suitable for worthwhile comparisons between tests.

Strain readings for each individual test can be explained when the changes in orientation of the pipes are considered. Results from Test 25 are analysed using the Hooke's Law relationship below and are presented by plotting major and minor principal stress magnitudes and their directions against applied axial load in Figure 5.8.

$$\sigma_1 = \frac{E(\epsilon1 + \nu\epsilon2)}{1 - \nu^2} \text{ etc. for plane stress} \qquad ...\text{Eq 5.2}$$

During Test 25 the initial point of contact was on the left side of the pipes close to the position of rosettes 2 and 3. The stresses calculated for these rosettes indicate a principal compressive stress on the inside of the pipe wall which began at an angle of 45^0 to the length of the pipe and which gradually changed to an alignment of 20^0 to the longitudinal axis and had a magnitude of $24N/mm^2$. The data recorded on the outside of the pipe at the same position showed tensile stresses whose major principal measurement tended to be directed along the length of the pipe The maximum tensile stress was $6N/mm^2$ at the end of the test directed around the circumference of the pipe.

Data recorded at rosette position 1 indicated that stresses did not change at its position until an axial load of 80kN was applied to the pipes. This agreed with the data presented in Figure 5.5 which showed that the point of contact between the pipes changed to the right hand side, where rosette 1 was mounted. From this stage onwards principal compressive stresses were recorded
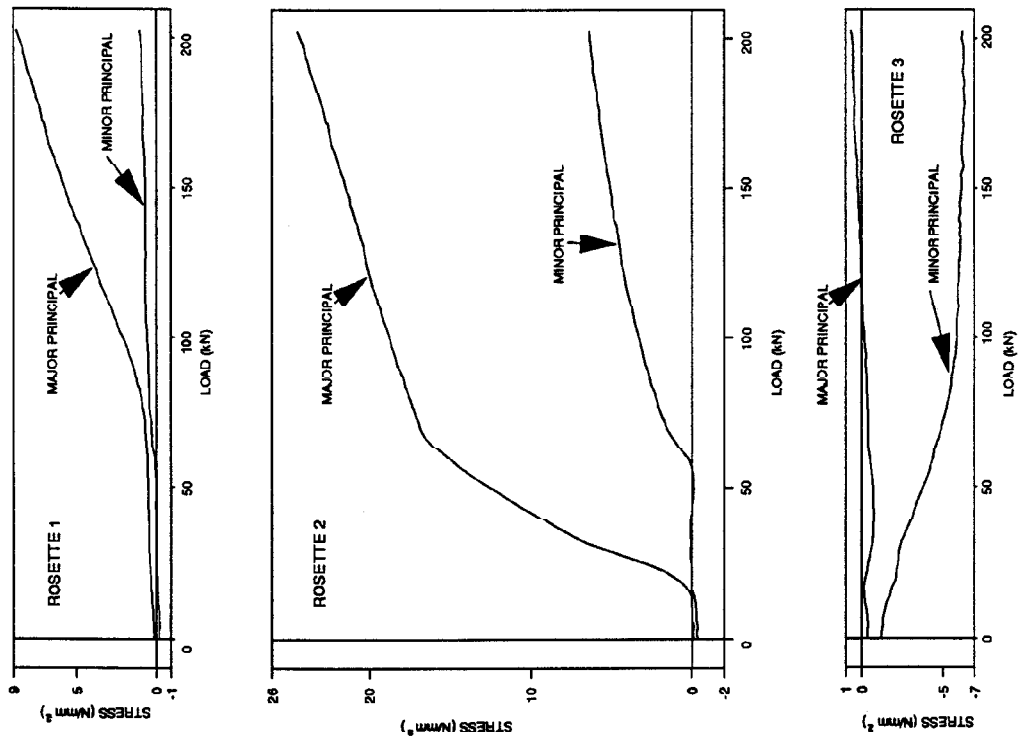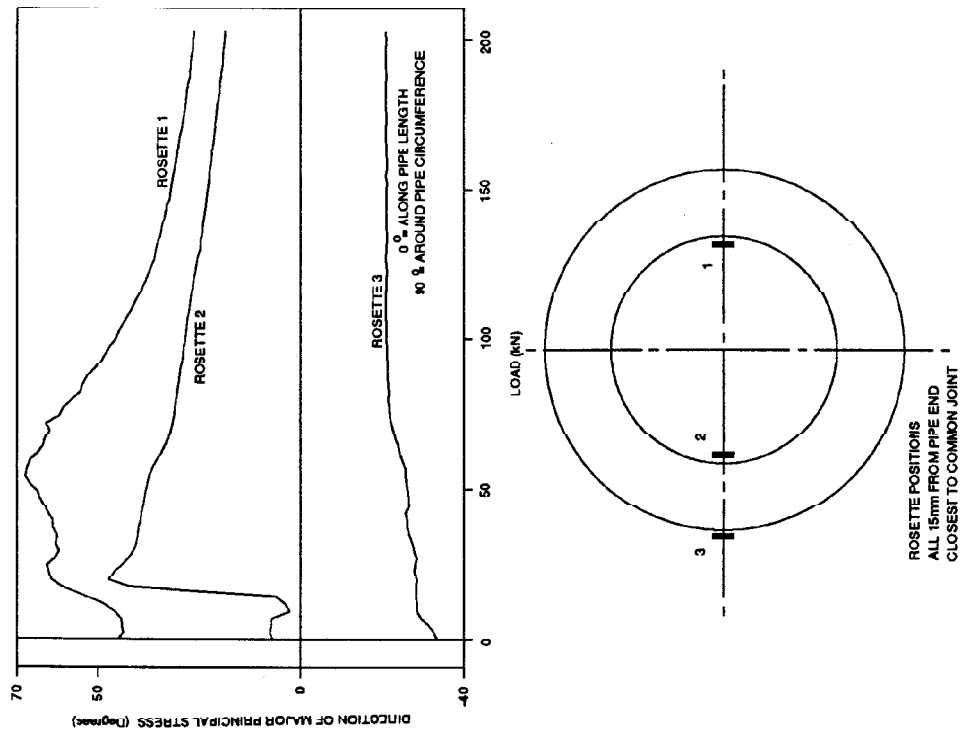
Figure 5.8 Principal stress readings from Test 25.

which were orientated at 45^0 changing to 25^0 to the longitudinal axis of the pipes. The compressive stresses were accompanied by a relatively small minor compressive stress around the pipes' circumference. The magnitude of the major compressive stress was $9N/mm^2$ at the end of the test. This indicated that even though the point of contact was recorded as having moved around to this side of the pipe a greater compressive stress was still being transferred between pipes on their left hand side.

5.4.5 Changes of deflection angle between pipes

The graph presented in Figure 5.9 plots changes of pipe alignments for Tests 14 to 23. The plot shows how all the pipes have reached a stage where their alignments have stopped changing. On initial inspection it appears that the rate of realignment might be associated with the magnitude of stress induced at the boundaries of the sand. This possibility is examined in Section 9.2.

ALIGNMENT BETWEEN PIPES   TESTS 14-23

BOUNDARY STRESS N/mm^2

TEST No.		VERT.	HORZ.
14	0.5	0	0
15	0.5	0	0
16	1.0	160	55
17	1.0	160	55
18	1.0	110	40
19	1.0	110	40
20	0.5	50	50
21	0.5	50	50
22	1.0	200	73
23	1.0	200	73

Figure 5.9   Pipe alignments.

Sand Chamber Tests 5-23

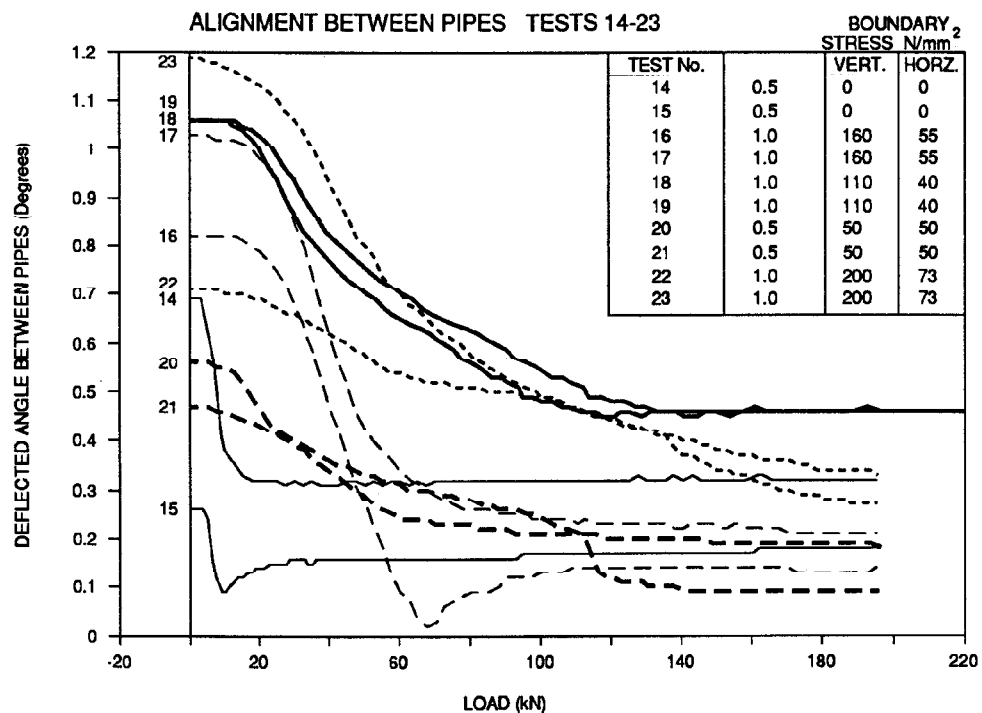## 5.5 Summary

The following points are summarised or noted from this series of tests:-

1. All the pipes came to an aligned position during the test. The research requires testing of pipes whilst they are in a misaligned position.

2. It is important to assess the three dimensional orientation of pipes to enable full interpretation of the results.

3. Compression of the concrete occurs at the pipe joint as the joint gap appears to have a negative value when axial load is applied.

4. The introduction of reinforcement prevented the earlier failure that occurred due to longitudinal cracking of the pipe.

5. No joint packing materials were used.

6. Ingress of soil into the pipe joint can cause problems due to spalling of the concrete.

7. No significant difference was noted when joint profiles were introduced into the tests.

8. The complex loading arrangements means analysis of stress and strain is only possible on an individual test basis.

CHAPTER 6

MISALIGNED PIPE TESTS

6.1 Introduction

The chamber tests described in the previous chapter were not totally satisfactory due to the influence of the flexible membrane boundaries. Inspection of the test results revealed that all pipes tested in a deflected orientation were aligning themselves as axial load was applied. The pipes were aligned before any measurements or visual signs of failure were recorded. This research aims at providing information about axial load capacity of pipes when they are deflected and it was clear that this was not going to be possible in the soil chamber. The compression rig in which the soil chamber was clamped was adjustable and the supplementary apparatus detailed below was designed and manufactured to maintain pipes in a deflected position as axial load was increased.

6.2 Misalignment apparatus

The soil test chamber was designed for testing pipes in sand, providing full circumferential interaction between model pipes and the soil. This modelled the situation that might occur in granular soils but pipejacking in cohesive soils and rocks creates a very different interaction between pipe and soil. In all pipejacking operations it is usual to excavate a hole 6-10mm larger in diameter than the outside diameter of the pipe being installed. This provides

assistance when steering the pipeline and a void into which lubricants can be injected. In the instance of rock or cohesive soils, which are substantially self supporting in the short term, the pipe would be in contact with the ground at a few external areas only.

The misalignment apparatus shown in Figure 6.1 and Plate 6.1 was designed to model this situation with a limited area of contact. Large yokes were manufactured from duraluminium which is flexible enough to deform when subjected to large loads. The yokes were machined with a diameter modelling the typical overbreak of a pipejack. Contact between the yoke and pipe before loading was theoretically a thin longitudinal strip, but as axial load was applied to the apparatus so both the pipe and yoke deformed and the width of the contact increased.

The yokes were attached to adjustable tension rods by hinged connections allowing the yoke to remain square to the pipes' external wall. The yokes could be adjusted from one test to the next to test at different angles of initial misalignment. The tension rods were instrumented with strain gauges to measure the normal reaction force between the pipe and yoke.
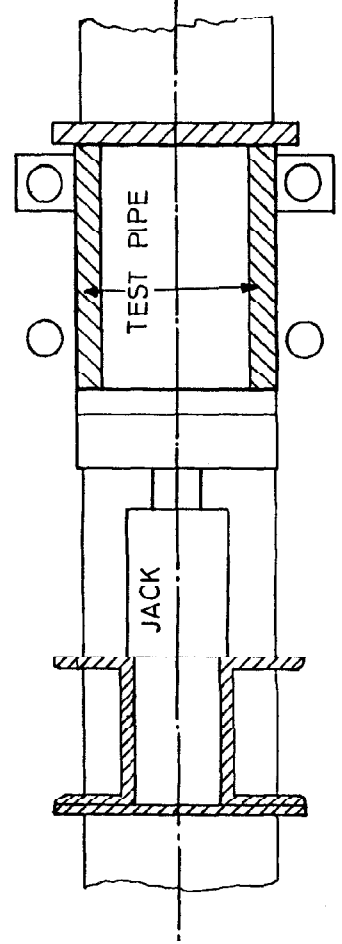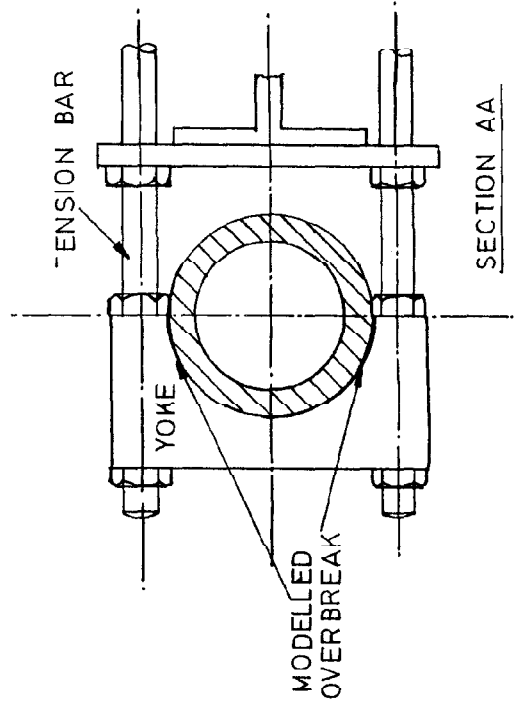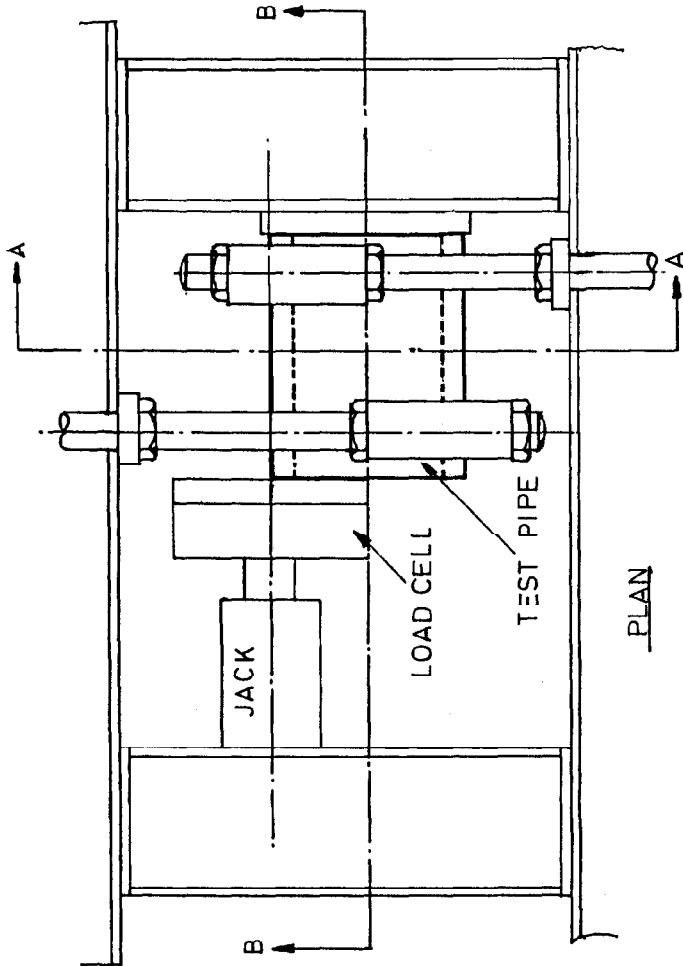
Figure 6.1 Misalignment apparatus general arrangement.
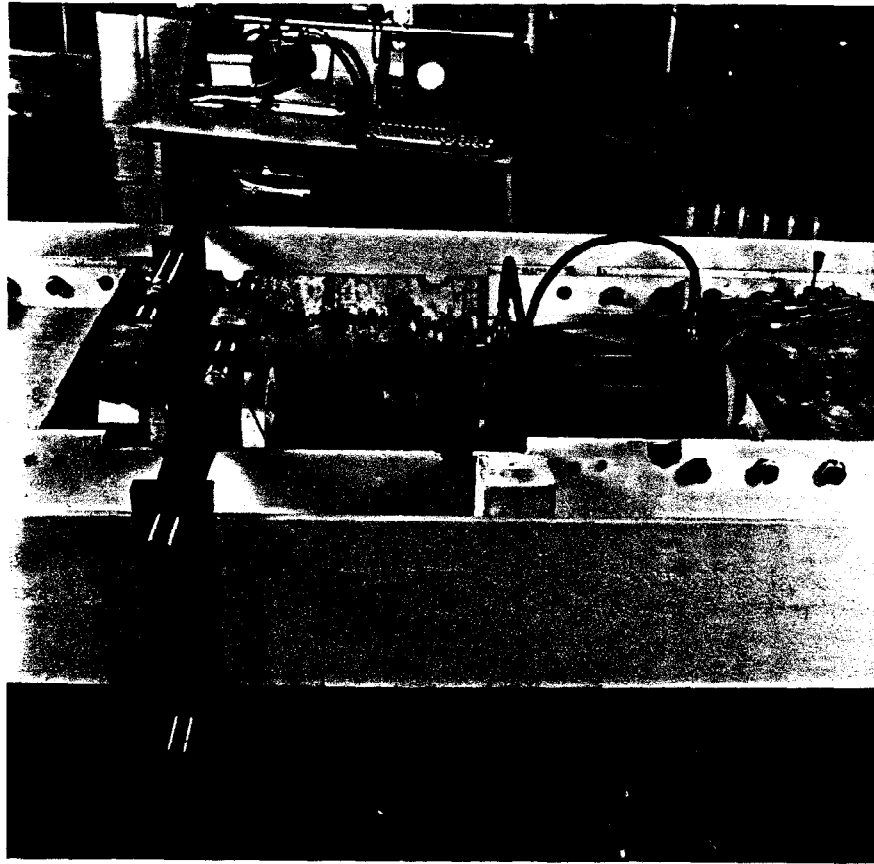
Plate 6.1 A general view of the misalignment test arrangement.

The yokes could be arranged to provide support to the pipe which would model three different circumstances occurring on prototypes. Initially, pipes were tested with yoke and jacking load positioned as shown in Figure 6.2a which modelled the situation which would occur when a straight pipejack deviated from its intended line and was subsequently corrected. In this circumstance the axial load would be transferred diagonally between opposite corners of the pipe. The second misalignment condition modelled was for pipejacking around curves when the load would be transferred along one edge of the pipe and the ground would prevent the pipe from continuing in a straight line as shown in Figure 6.2b. Finally pipes were tested modelling axial load distribution over the full end area of the pipes.
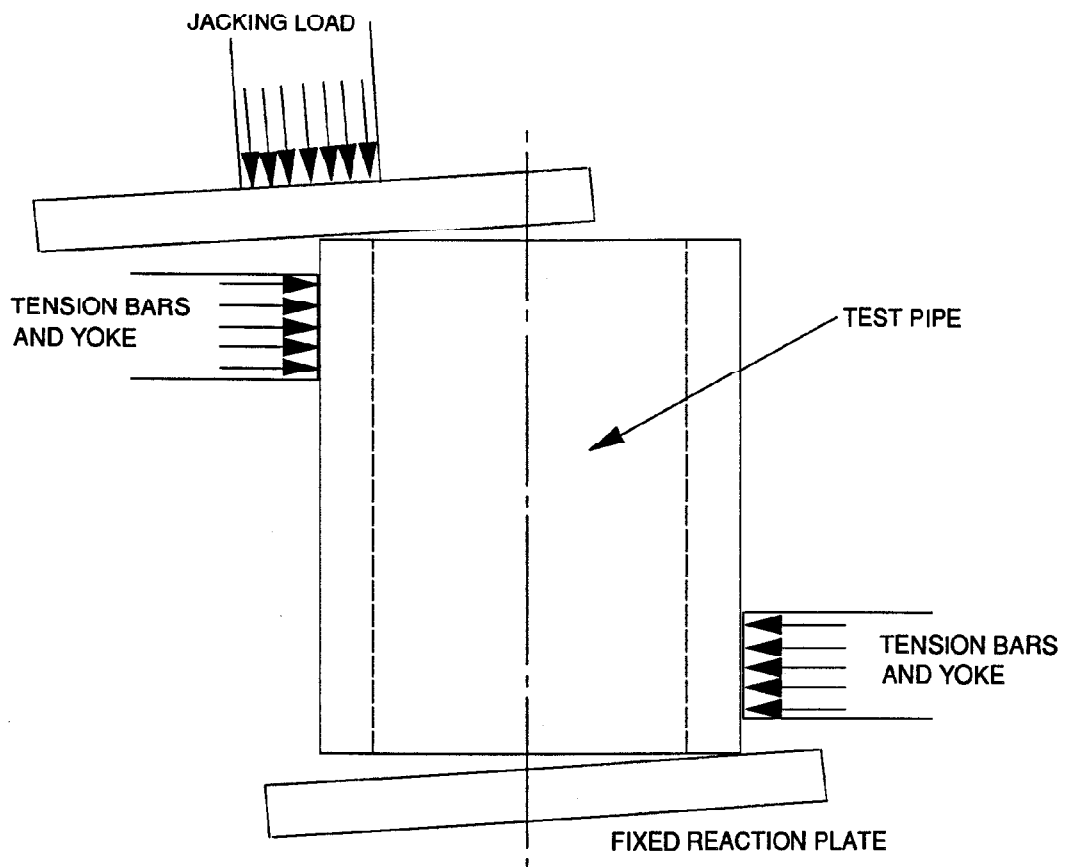
Figure 6.2a Loading arrangement for diagonal tests.

The tension bars were clamped to the main frame of the testing rig and the reaction plates and jacks in the rig were designed to allow their orientation to each other to be adjusted. The end yoke and one jack were moved close together and pipes were tested individually.

JACKING LOAD

TENSION BARS
AND YOKE

TEST PIPE

TENSION BARS
AND YOKE

FIXED REACTION PLATE
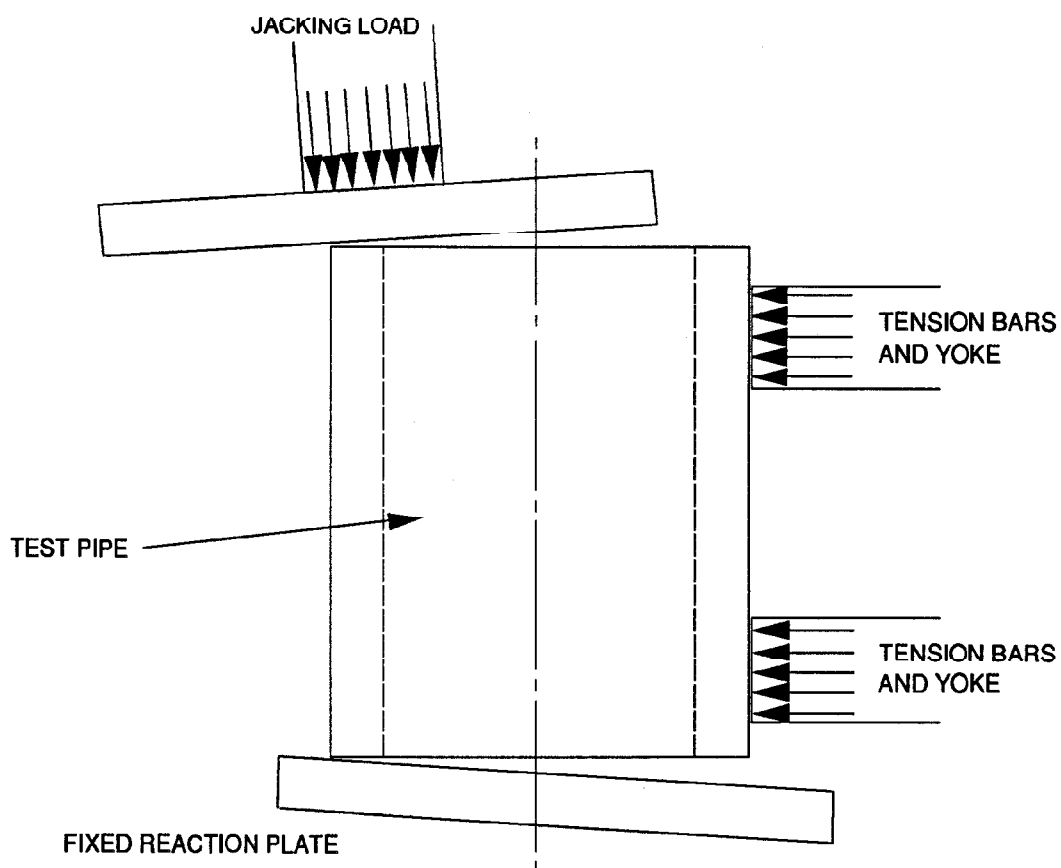
Figure 6.2b Arrangement for edge loading tests.

6.3 Test procedure

Pipes were restrained from alignment in a deflected position at two points by yokes attached to tension bars that were known to be flexible. Measurement of the tension bars' movements under test loads was achieved by replacing model concrete pipes with a steel cylinder that was considered rigid. The steel cylinder was axially loaded using the tension bars and yokes to provide various deflected angles. The movement of the yokes was recorded using dial gauges and the system was loaded and unloaded several times.

Having established that the flexibility and rigidity which the yokes provided were suitable a series of 24 tests was carried out. The parameters at the start of each of these tests are summarised in Table 6.1; both thick and thin walled pipes were tested with various initial deflections.

During this test series transducers were mounted as shown in Figure 6.3 and listed in Table 6.2. A load cell was used to monitor axial load, the tension bars were instrumented to measure loads on the yokes and LVDT's were mounted on a fixed rod inside the pipe. The LVDT's measured changes in horizontal and vertical diameters each end of the pipe and movements of the pipe. LVDT's were also mounted at one end of the pipe to measure changes in the angle between the pipe end and the plane of the end plate. Electrical resistance strain gauge rosettes were mounted at various circumferential positions midway along the pipes' length. The test was monitored using software that continually read all channels and recorded at preset load increments. During testing, pipes were monitored visually and any crack or damage marked and noted as they were seen.

A review was carried out after the first five tests had been conducted. This resulted in the manufacture and use of ball and cup connectors between the tension bars and yokes to allow the yokes to pivot. These accommodated rotation of the yokes to the alignment of the pipe thus maintaining a strip contact rather than bearing on one edge of the yoke.

TEST No.	PIPE REFER-ENCE	PIPE TYPE	INITIAL DEFLECTION (Degrees)	MAXIMUM LOAD APPLIED (kN)
MA1	H25	Thin In Wall	0.64	94
MA2	H31	Thin In Wall	3.00	45
MA3	H34	Thin In Wall		28
MA4	H35	Thin In Wall		39
MA5	H36	Thin In Wall		39
MA6	H39	Thick In Wall	1.20	80
MA7	H34	Thick In Wall	1.70	70
MA8	H32	Thick In Wall	1.10	60
MA9	H33	Thick In Wall	2.28	60
MA10	H43	Thick In Wall	1.28	100
MA11	H40	Thick In Wall	0.43	110
MA12	H44	Thick In Wall	0.60	110
MA13	H40	Thin In Wall	0.21	103
MA14	H44	Thin In Wall	1.03	40
MA15	H30	Thin In Wall	2.08	35
MA16	H43	Thin In Wall	1.59	37
MA17	H41	Thin In Wall	Square	158
MA18	H42	Thin In Wall	Square	204
MA19	H53	Thin Steel	0.86	204
MA20	H51	Thin Steel	1.72	174
MA21	H41	Thick In Wall	1.72	64
MA22	H42	Thick In Wall	0.86	203
MA23	H53	Thick Steel	1.72	204
MA24	H45	Thick Steel	Square	204

Table 6.1 Summary of misaligned pipe tests.

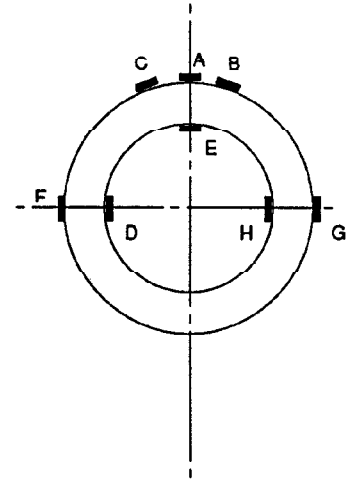| Test No.	A	B	C	D	E	F	G	H
MA1								
MA2								
MA3								
MA4	A1		C2		E3			
MA5								
MA6	A1	B2	C3					
MA7	A1	B2	C3					
MA8	A1	B2	C3					
MA9	A1	B2		D3				
MA10	A1	B2			E3			
MA11	A1	B2		D3				
MA12	A1	B2			E3			
MA13	A1					F3	G2	
MA14	A1					F3	G2	
MA15	A1					F3	G2	
MA16	A1					F3	G2	
MA17						F2	G1	H3
MA18						F2	G1	H3
MA19						F2	G1	H3
MA20						F2	G1	H3
MA21						F2	G1	H3
MA22						F2	G1	H3
MA23						F2	G1	H3
MA24						F2	G1	H3

Figure 6.4

Strain gauge positions.

Table 6.2 Position of strain gauge rosettes.
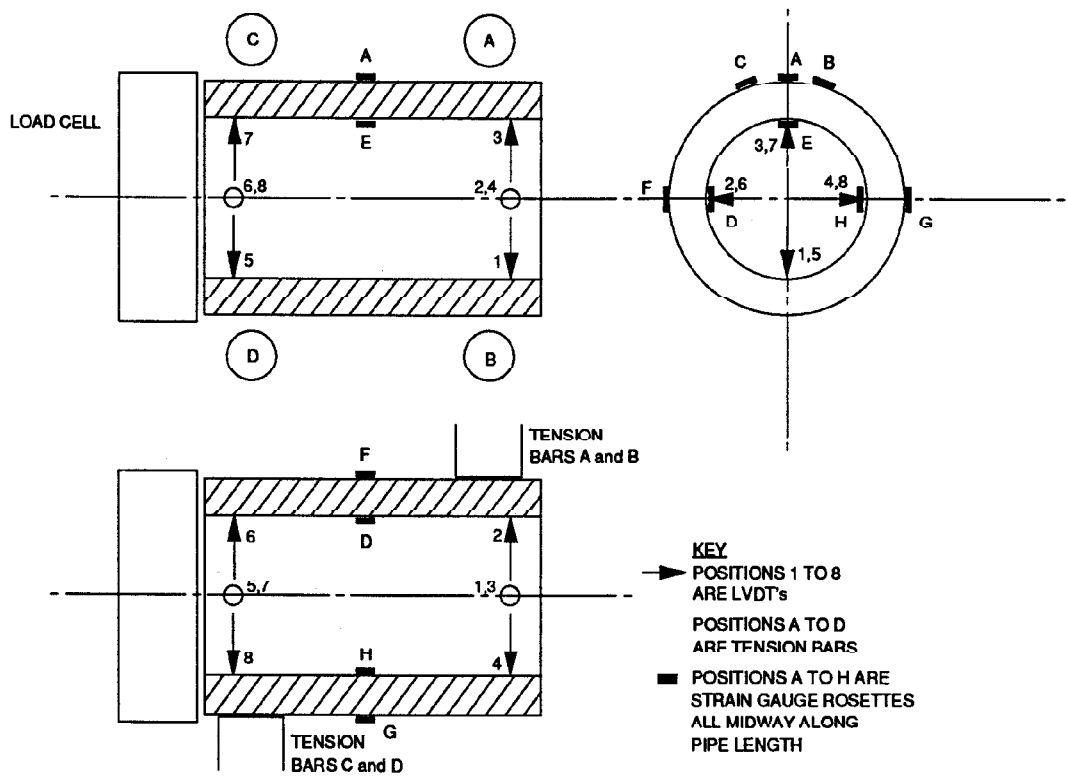
Figure 6.3 Positions of transducers.

The pipes tested were all reinforced and had a variety of joint profiles on their ends and only the most extreme end surfaces were loaded. This meant that for in wall jointed pipes loading was only possible on approximately one third of the cross sectional area of the pipe which sometimes led to local crushing of the spigot or socket.

Axial loading was gradually increased during the tests until either substantial cracking had occurred, the concrete at the joint had crushed or the load capacity of the apparatus had been reached.

A total of 24 tests, with the two modes described earlier in Section 6.2 were carried out. Sixteen pipes were tested with loading applied diagonally across opposite corners and eight pipes had axial load applied down one edge of the pipe or to the pipe's full end area. Results from the two types of tests will be presented individually in the next two sections.

6.4 Diagonal axial loading results

The arrangement of load application and yokes for this test series is presented in Figure 6.2a. Data were recorded of applied axial load, movement of the pipe, load reaction at the yokes and strains in the concrete. Presentation of the results will assess the changing pipe alignment and geometry and the affect of applied axial load and reactions induced in the tension bars. Strains recorded will be assessed and used to give an indication of stress distribution at the mid length cross-section of the pipe. During this presentation pipes will be referred to as either thick or thin walled indicating the two different scales used in modelling.

6.4.1 Deformations of the pipe

Measurements of the deforming pipe were taken using LVDT's to monitor the orientation of the end of the pipe and changes to the internal dimensions. The positions of the transducers have been presented in Figure 6.4 and data recorded from them can be used to calculate the orientation of the pipe.

Before the test was set up, readings were taken from the three transducers at the end of the pipe whilst the pipe was placed vertically on a flat plane. These indicated the measurements which would be recorded if the pipe's end deflection angle was zero and the readings were used as a datum. The pipe was placed in the test position and data collected from all the transducers. The initial deflection angle at the end of the pipe could be calculated and also used as a datum angle for the orientation of the internal surface of the pipe. As load was

applied to the pipe, changes in the pipes' orientation could be calculated for each set of readings taken. The calculated values of the pipes' deflection angles are presented in Figure 6.5 by plotting changes in the deflection angle of the internal surface of the pipe against applied axial load. The figure shows how realignment of the pipes began to occur. Pipes with initially small deflection angles stopped changing their orientation as was the case in Tests 6, 10, 12 and 14, whilst pipes with large angles at the start of testing were still realigning themselves when the test was stopped.

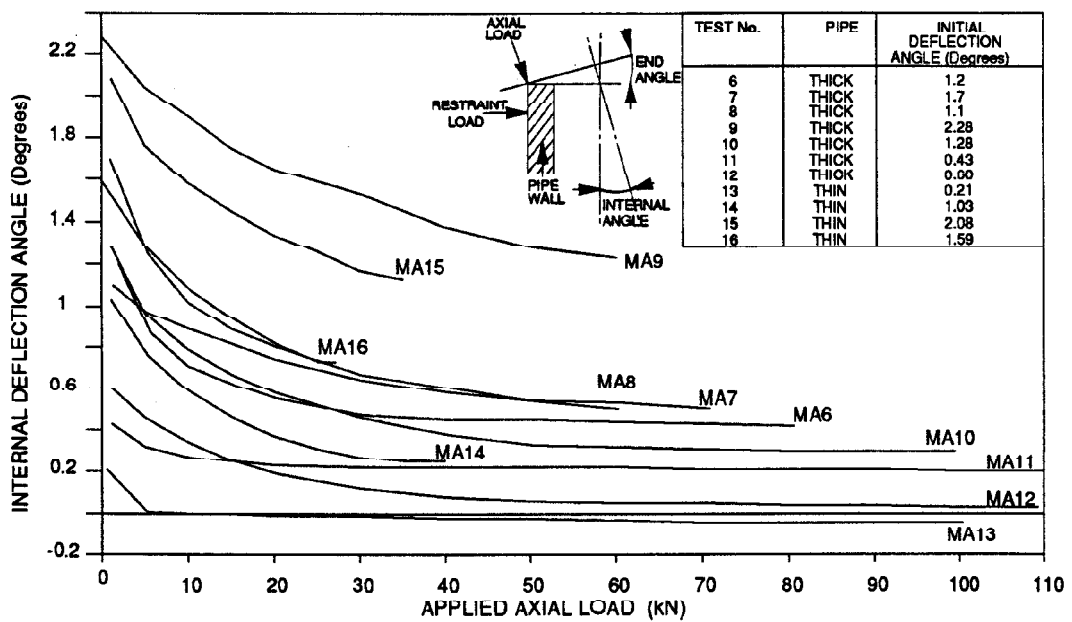| TEST No.	PIPE	INITIAL DEFLECTION ANGLE (Degrees)
6	THICK	1.2
7	THICK	1.7
8	THICK	1.1
9	THICK	2.28
10	THICK	1.28
11	THICK	0.43
12	THICK	0.00
13	THIN	0.21
14	THIN	1.03
15	THIN	2.08
16	THIN	1.59

Figure 6.5 Rotation of pipe during loading.

Only one of the calculated deflection angles was plotted in Figure 6.5. It is useful to examine and compare both internal diameter orientation and pipe end orientation. The changes of the angles are presented in Figure 6.6 where it can be seen how the angle of the end of the pipe changes more quickly than the internal surface angle. When looking at a plan view of the pipe it appears rectangular in shape before testing commences. The different rates of deflection changes measured as the test progressed show how the pipe deforms and becomes the shape of a parallelogram when viewed in plan.
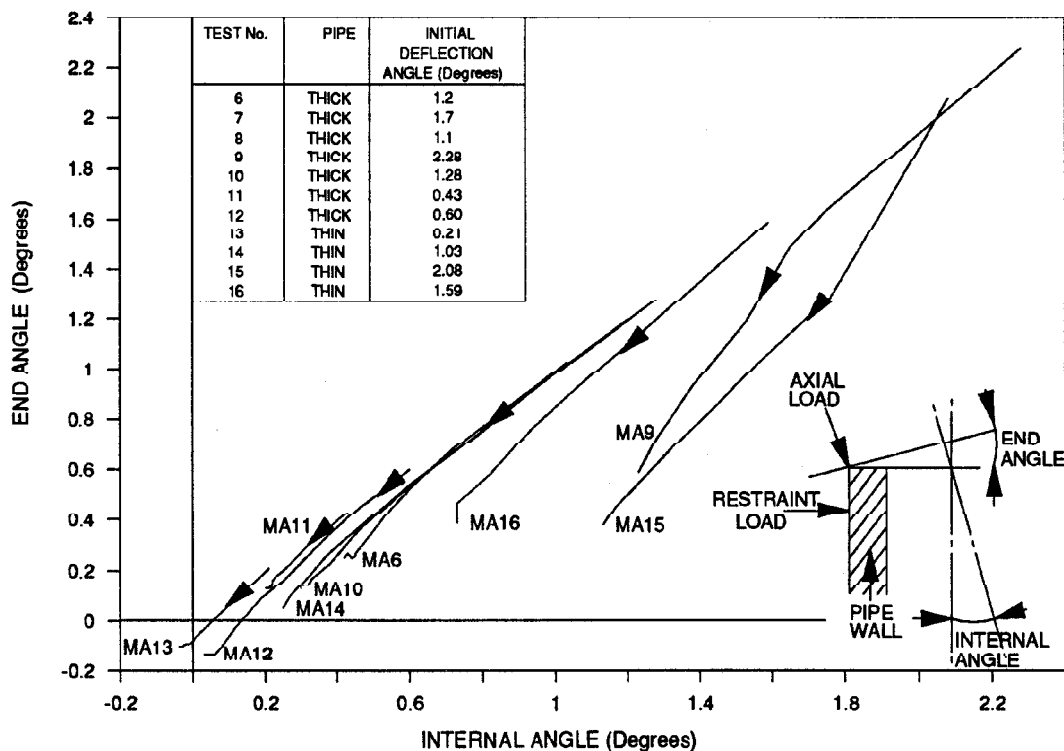
Figure 6.6 Deformation of pipe during loading.

TEST No.	PIPE	INITIAL DEFLECTION ANGLE (Degrees)
6	THICK	1.2
7	THICK	1.7
8	THICK	1.1
9	THICK	2.29
10	THICK	1.28
11	THICK	0.43
12	THICK	0.60
13	THIN	0.21
14	THIN	1.03
15	THIN	2.08
16	THIN	1.59

The difference between the internal surface and end angles is the change of angle at the corners of the parallelogram. These differences of angle were examined and can be related to axial load applied and the deflection of the pipe at the start of testing. The data recorded are presented in Figures 6.7a and 6.7b. These show for either thick or thin pipes how the difference between the measured angles becomes greater (which indicates more pipe deformation) for larger initial angles of deflection. In the Figures the positions at which cracks were first visibly noticed are marked. For the limited number of tests conducted this would seem to indicate that for thin pipes cracking occurs at a consistent load level and is not affected by deflection angles, and for thick pipes the point at which cracking first appears is related to deflection angle and not affected by applied load.
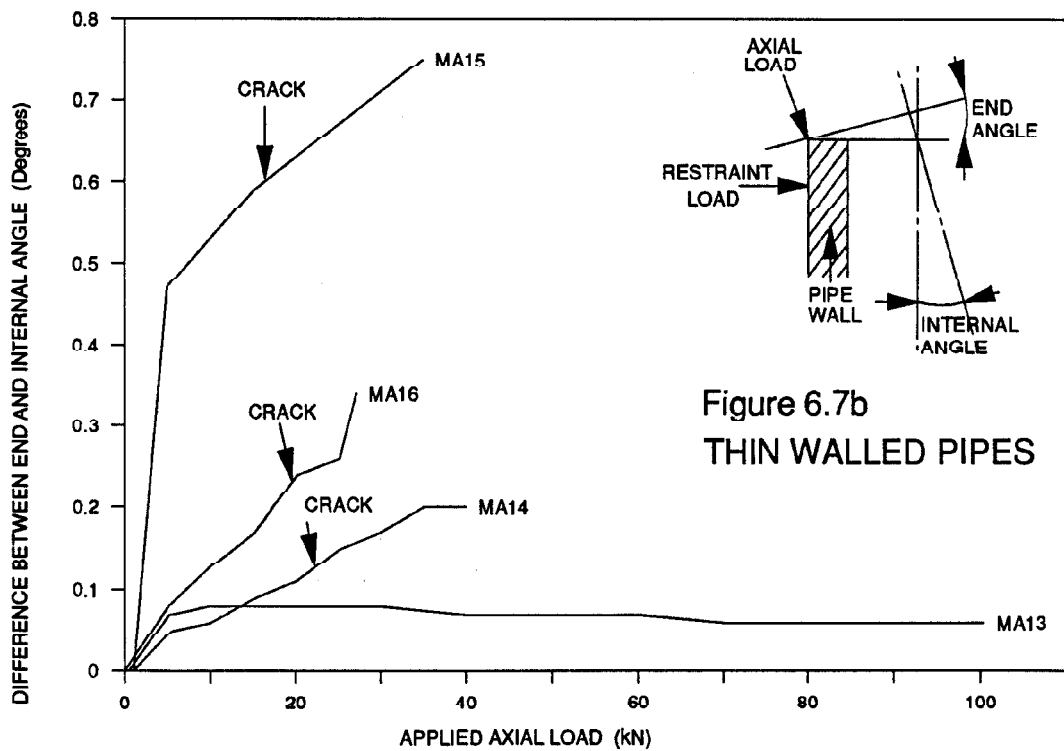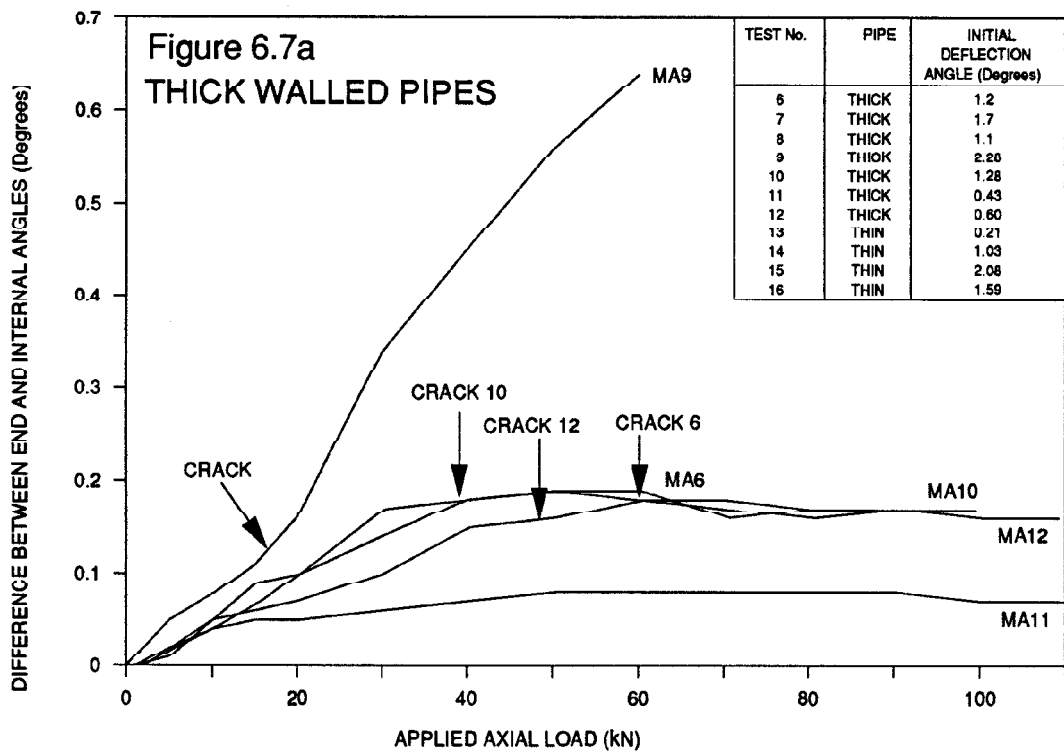
Misalignment Tests 6-13

Figure 6.7 Deformation of pipe compared to applied axial load.

Data recorded from the LVDT's mounted to measure the internal surface position of the pipe can be used to assess changes of pipe diameter. The data were examined for changes in both vertical and horizontal diameters. Analysis of the readings taken showed how the pipe expanded in the vertical plane and contracted in the horizontal plane. Changes of diameter were very small but in general it could be shown that the pipe end nearest the application of load experienced greater diameter changes than the opposite end of the pipe. An attempt was made to use the diameter changes to assess circumferential strains in the pipe, but results were not consistent and no agreement was found with strain gauge data.

6.4.2 Affect of pipe yokes

The yokes were attached to tension bars which were instrumented to enable recording of loads reacting against them. More detailed analysis is presented in Chapter 9 but a simple assessment of the statics of the test arrangement gives an indication of the loads expected in the tension bars, neglecting deflection angles and shear forces due to friction.
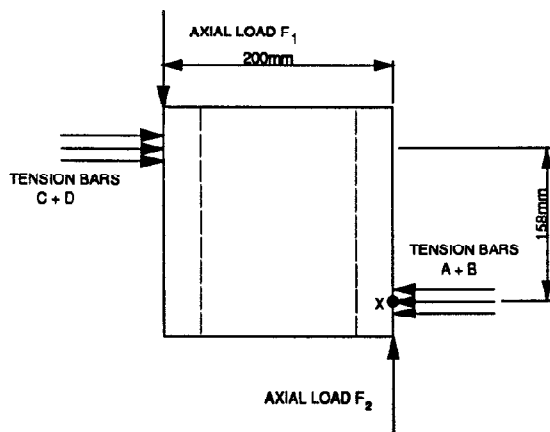
Resolving Forces

$$F_1 = F_2$$

$$C + D = A + B$$

Moments about X

$$(C + D)158 = F_1(200)$$

$$C + D = 1.27\, F_1$$

$$C = D \text{ and } A = B$$

due to symmetry

The analysis was examined by plotting applied load (F_1) against either tension bar load (C + D) or tension bar load (A + B) in Figure 6.8. Imposed on the figure is the theoretical relationship and also that obtained for testing a hollow steel cylinder, assumed to be rigid. Two points are clear from the graph; firstly, tension bar loads are linearly related to applied load while pipe deflections are changing. When the deflection angles become static no further increase in tension bar load is recorded. Secondly, the simple relationship presented above holds for the steel cylinder but for microconcrete pipes this is not the case. A different relationship between axial and tension bar loads appears to exist for concrete pipes. In general terms the following relationships can be approximated before pipes' deflection angles stop changing:-

$$\text{for simple theory} \qquad C + D = 1.27\,F_1 \qquad \text{...Eq 6.1}$$

$$\text{for steel cylinder} \qquad C + D = 1.29\,F_1$$

$$\text{for thin walled pipes} \qquad C + D = 0.56\,F_1$$

$$\text{for thick walled pipes} \qquad C + D = 0.46\,F_1$$

This would suggest that for the analysis of concrete pipes, the shear forces at the loading points and changes of deflection angles need to be taken into account.

Measurements were recorded from both the pairs of tension bars and the occurrence of shear forces can be examined by analysis of the tension bar readings. If no shear forces or friction were occurring the test would have been totally symmetrical and the tension bars loaded equally. This was found to be true for the hollow steel cylinder but results from the model concrete pipes presented in Figure 6.9 show how the tension bar loads are lower in rods A and B than the loads in rods C and D. This indicates shear forces between the pipe and yoke are affecting the results of the model concrete pipe tests. Tension loads in the bars furthest
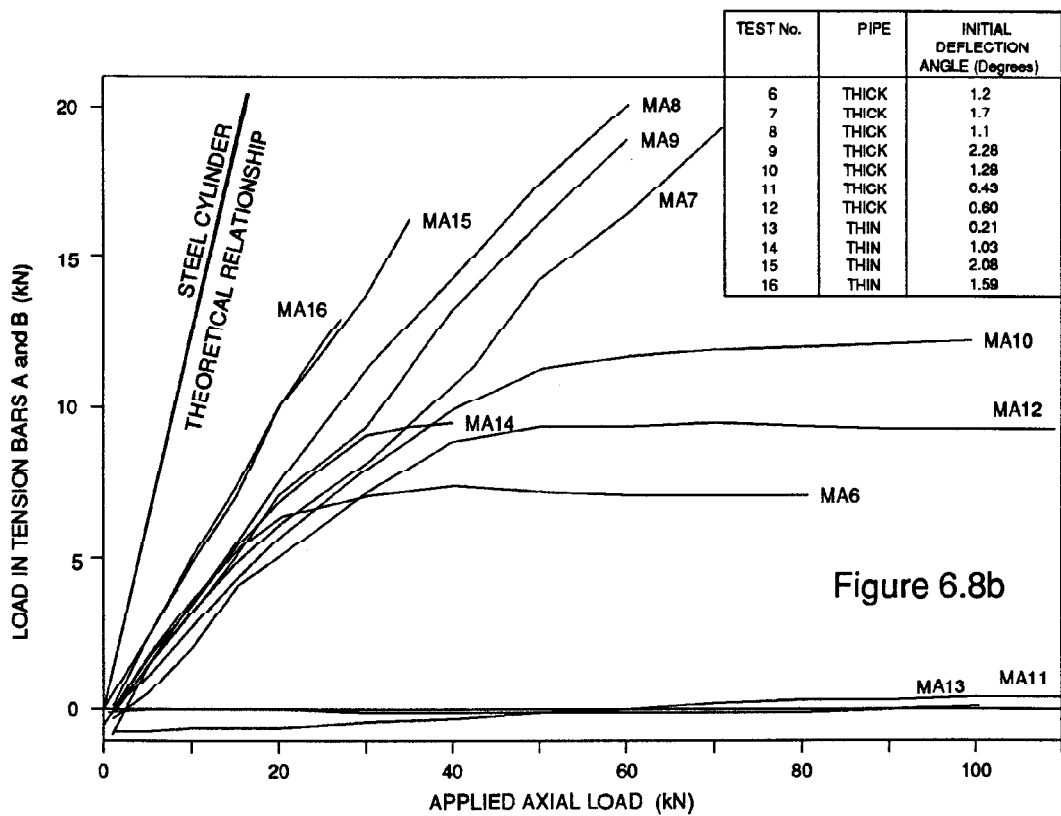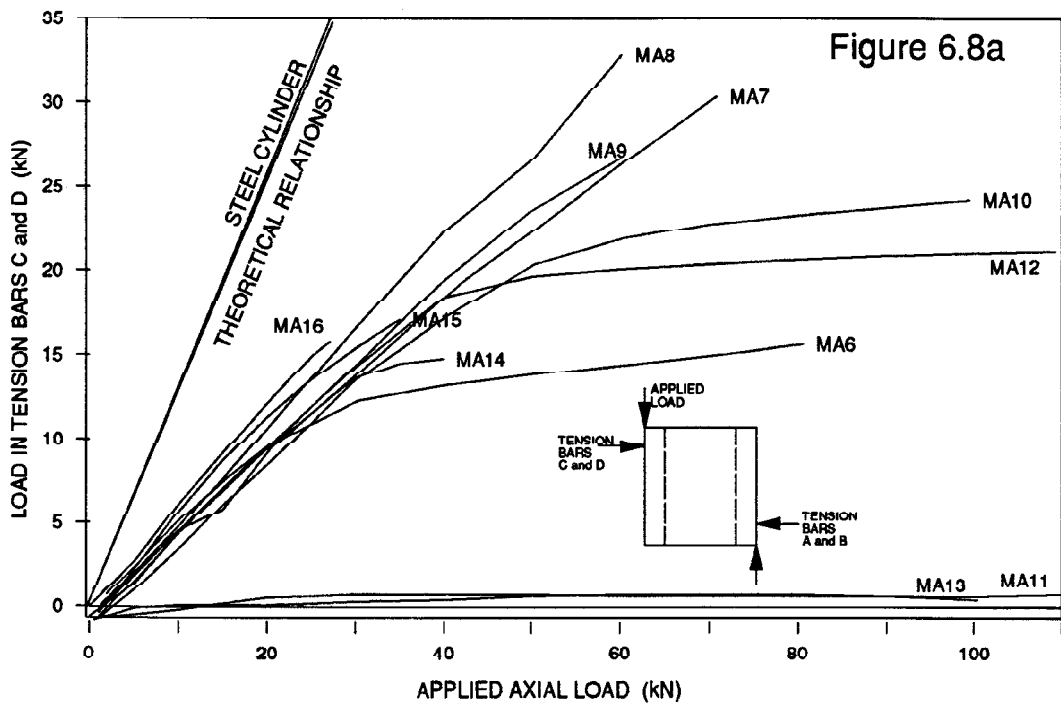
Figure 6.8 Comparison between tension bar loads and applied axial load.

from the load application are reduced by between 50% and 90% of the loads in the closest tension bars. The Figure indicates that the tension bar loads might be related to deflection angles. For larger initial deflections the loads measured in the pairs of bars are closer to the simple theoretical value than for smaller deflections when larger differences in tension bar loads occur. A plot of the variation of tension bar loads with changes of deflection angle was prepared but it took the same form as Figure 6.5 and was therefore not presented.

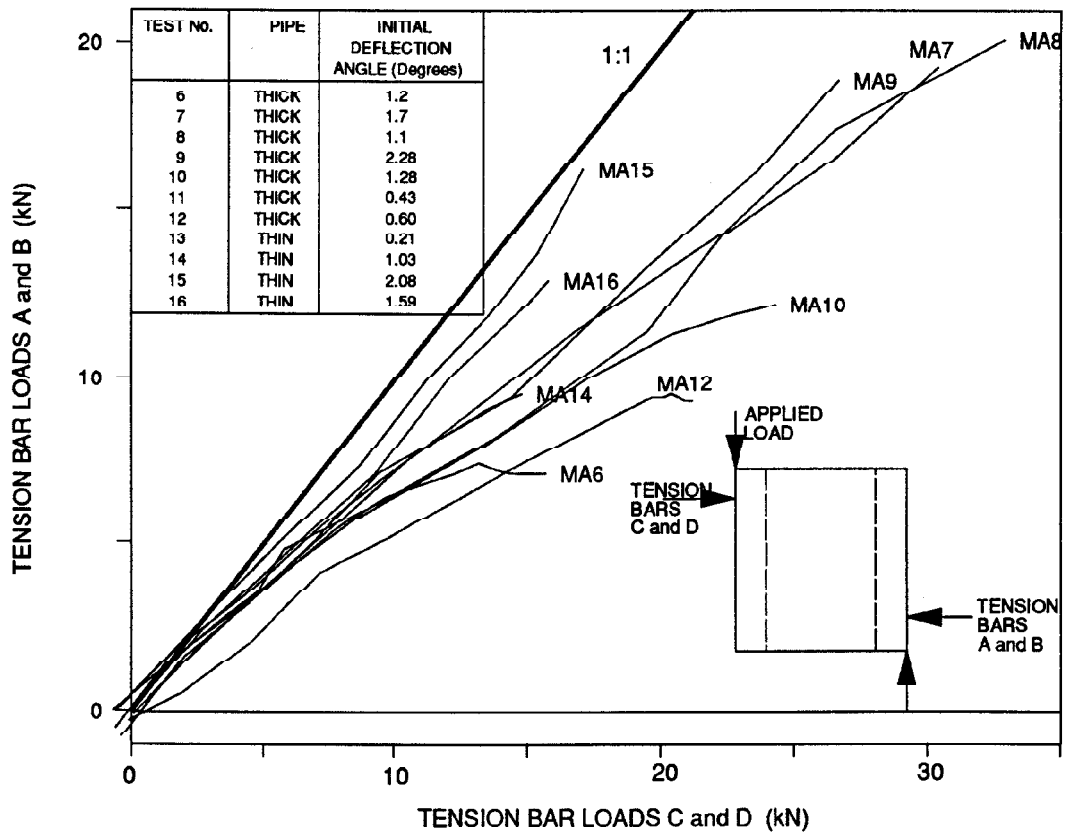| TEST NO.	PIPE	INITIAL DEFLECTION ANGLE (Degrees)
6	THICK	1.2
7	THICK	1.7
8	THICK	1.1
9	THICK	2.28
10	THICK	1.28
11	THICK	0.43
12	THICK	0.60
13	THIN	0.21
14	THIN	1.03
15	THIN	2.08
16	THIN	1.59

Figure 6.9 Comparison between opposing tension bar loads.

If pipes with small initial deflection values are considered there would be no tendency for the pipe to rotate and axial load would be transferred directly to the reaction load without

inducing any load onto the yokes. This indicates that pipejacking thrust loads are influenced by pipe deflections and interaction of the pipe with the ground. Therefore errors of excavation alignment during pipe installation should be avoided.

6.4.3 Strain gauge readings

Surface mounted electrical resistance strain gauge rosettes were used to monitor strains induced in the concrete at the various positions listed in Table 6.2. The use of gauges configured as forty-five degree rosettes enabled calculation of the magnitude and direction of principal strains.

Tests on thick walled pipes had gauges generally at the same position on the outside of the pipe in a direct line between the axial load application and axial reaction support (position A in Figure 6.10). This is the position where the early tests showed the first visible signs of cracking. The gauges were measuring tensile strains with maximum strains of -200μE before gauge failure or concrete cracking. The readings are presented in Figure 6.10 but show no noticeable trend other than that they are always tensile strains. The readings during Test 8 are of particular interest as one of the gauges was seen to have a crack running through its measuring wire. The crack in the concrete was first visible at 38kN of axial load and the strain gauge indicates failure at 36kN of axial load. This gives some indication as to how soon before the cracks are visible they can be detected with the strain gauge. Principal strains were orientated in line with the central axis of the pipe and around the circumference of the pipe with the largest tensile strains recorded around the pipes' circumference. Cracking was occurring at forty-five degrees and was therefore in association with the maximum shear strain.

Strain gauges were also mounted on the inside of the pipes at rosette position E to monitor the difference in strains recorded on opposite faces of the pipe wall. The internal strain gauges
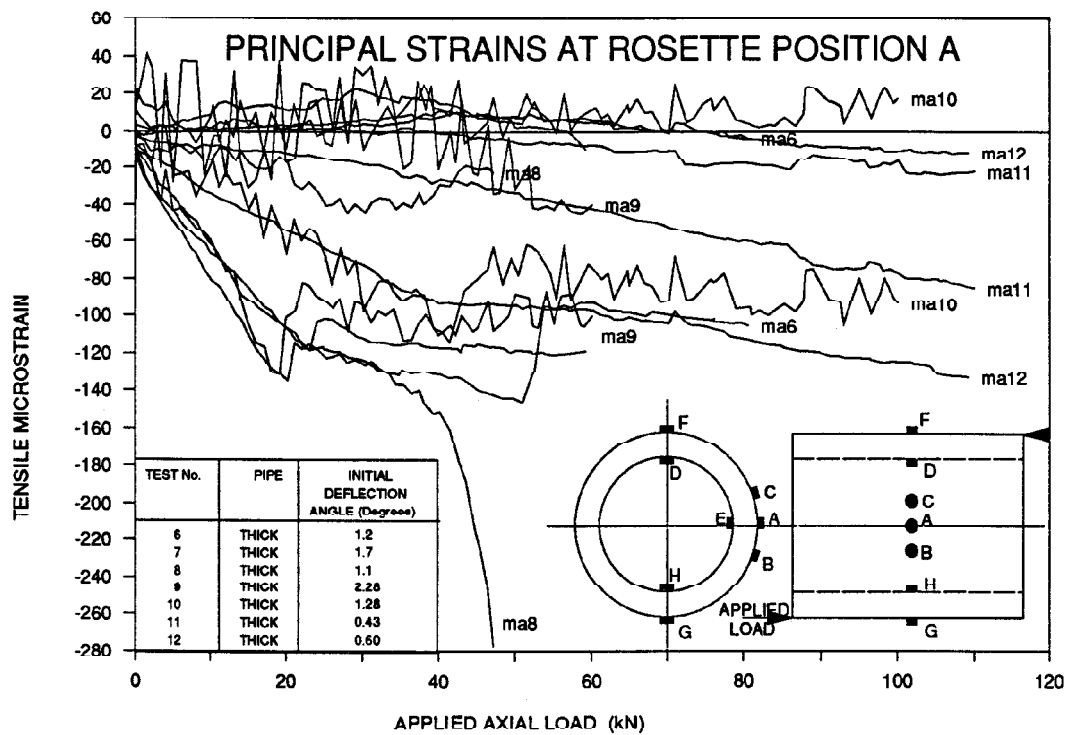
Figure 6.10 Principal strains at rosette position A.

were measuring compressive major principal strains in a line between the axial load application and reaction. The compressive strains were up to $300\mu\varepsilon$ within the elastic range of the concrete representing a major principal stress of $9N/mm^2$ diagonally across the inside of the pipe as opposed to a principal tensile stress of $-5N/mm^2$ on the outside face of the pipe orientated around the circumference of the pipe.

Positions of strain gauges were altered when thin walled pipes were tested and they were mounted at ninety degree intervals around the outside of the pipe. Gauges on the line between the position of axial load application and reaction (rosette position A) all measured tensile strains as they did on the thick walled pipes. Shear strain was larger for greater initial deflection and the highest recorded tensile strains at any given axial load were found in tests with the greatest initial deflection angles, as presented in Figure 6.11.
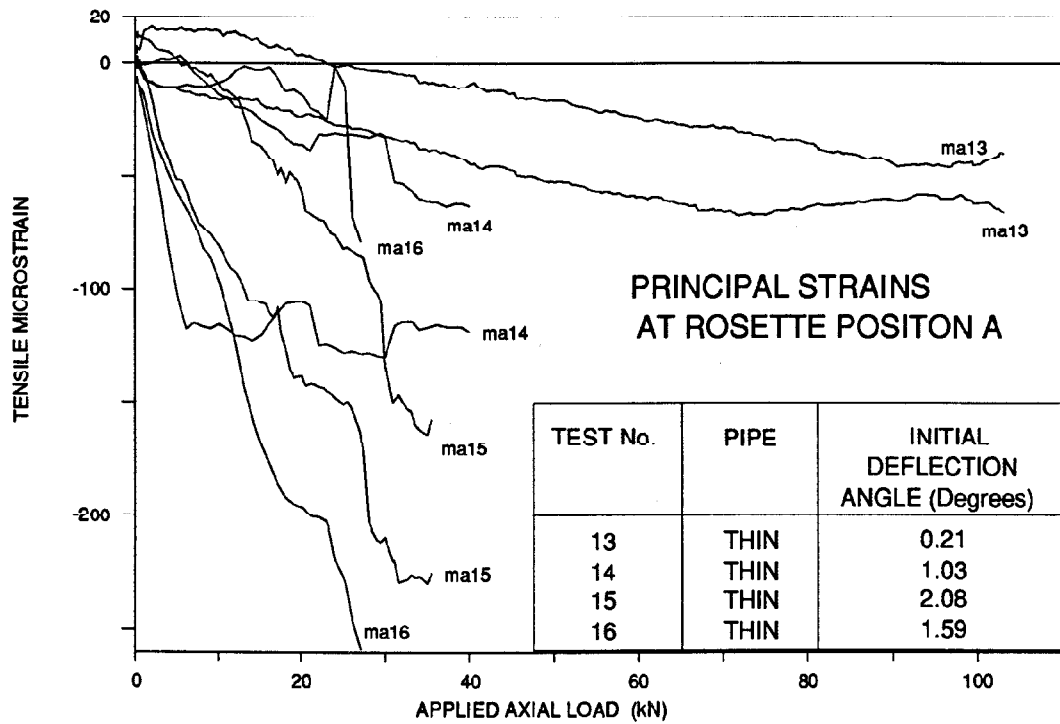
**PRINCIPAL STRAINS
AT ROSETTE POSITON A**

TENSILE MICROSTRAIN

ma13
ma13
ma14
ma16
ma14
ma15
ma15
ma16

APPLIED AXIAL LOAD (kN)

TEST No.	PIPE	INITIAL DEFLECTION ANGLE (Degrees)
13	THIN	0.21
14	THIN	1.03
15	THIN	2.08
16	THIN	1.59

Figure 6.11 Principal strain readings at rosette position A.

Strain gauges mounted on the pipe on a line perpendicular to the position of load application (rosette position G) are presented in Figure 6.12. These gauges are measuring compressive major principal strains in alignment with the direction of load application. Test 13 is of interest because the pipe was tested with no initial deflection angle and a maximum compressive stress of $27N/mm^2$ was recorded but longitudinal stresses were not the same at all rosette positions around the pipes' circumference which indicates that the loading was not symmetrical.
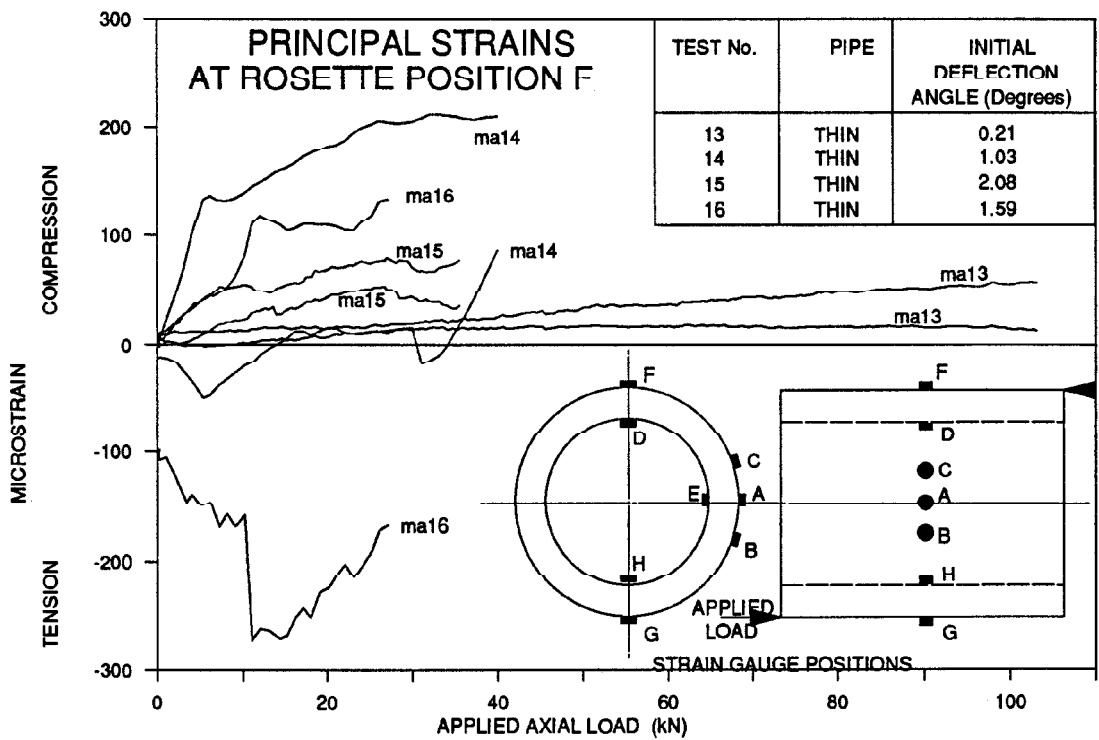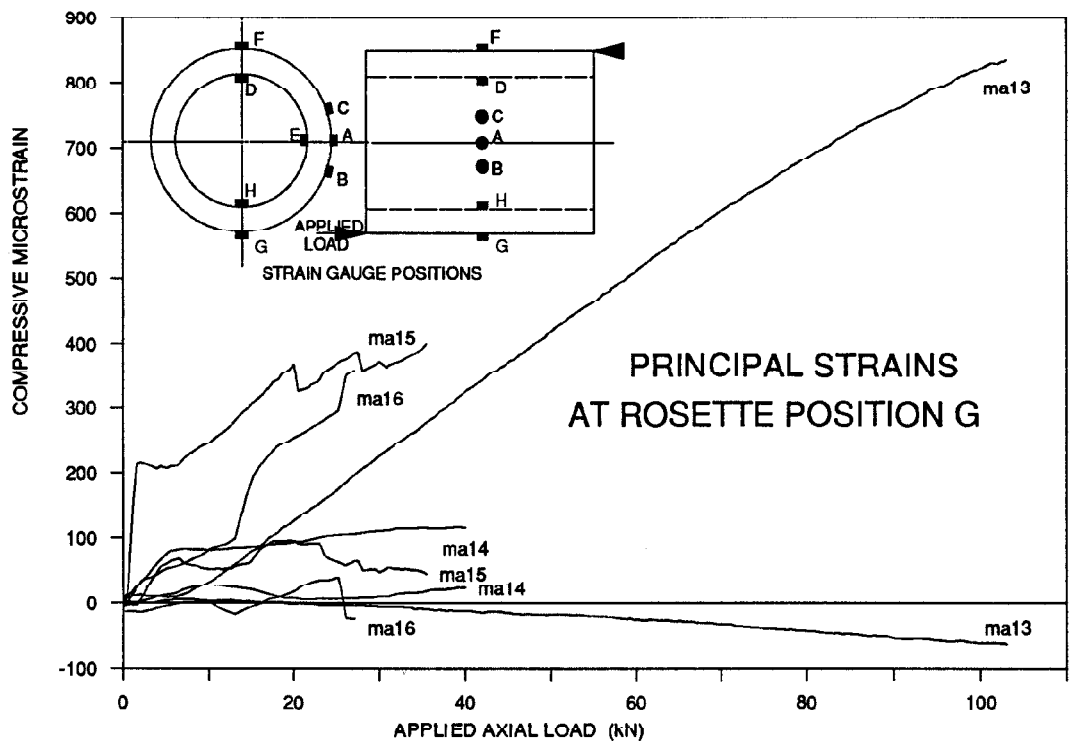
Figure 6.12 Principal strain readings at gauge positions G and F.

6.4.4 Failure modes

Three distinctly different modes of failure were experienced during the diagonal loading tests. Firstly, diagonal cracks occurred on the outside of the pipe in a line between the axial loading points as seen in Plate 6.2. These were due to excess shear strains being encountered and these cracks were always the initial type of failure experienced when deflection angles were large.

Secondly, if deflection angles were not large, failure would occur as a result of excessive compressive stresses at the axial loading points of in wall jointed pipes as shown in Plate 6.3 due to the smaller available cross-sectional area at which load could be applied.
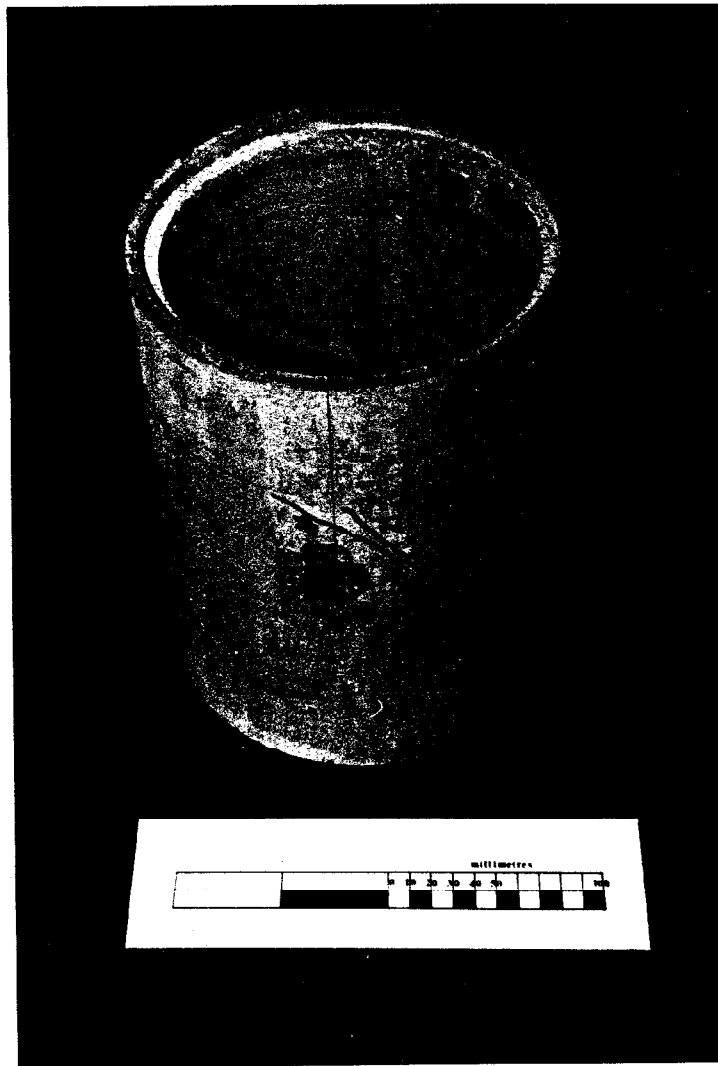
Plate 6.2 Diagonal cracking occurring during Test 14.

Thirdly, it was noted that on examination of pipes after testing, some had experienced failure due to a single longitudinal crack which was on the inside surface of the pipe and positioned parallel to the line of contact between the pipe and yoke attached to the tension bars C and D. This is the same failure mode as that experienced on a British Standard pipe crushing test. The crack was associated with loads measured in the tension bars of 30kN for the thick walled pipes and 17kN for the thin walled pipes. These loads were much greater than those applied when carrying out the British Standard tests on the model pipes where typical ultimate

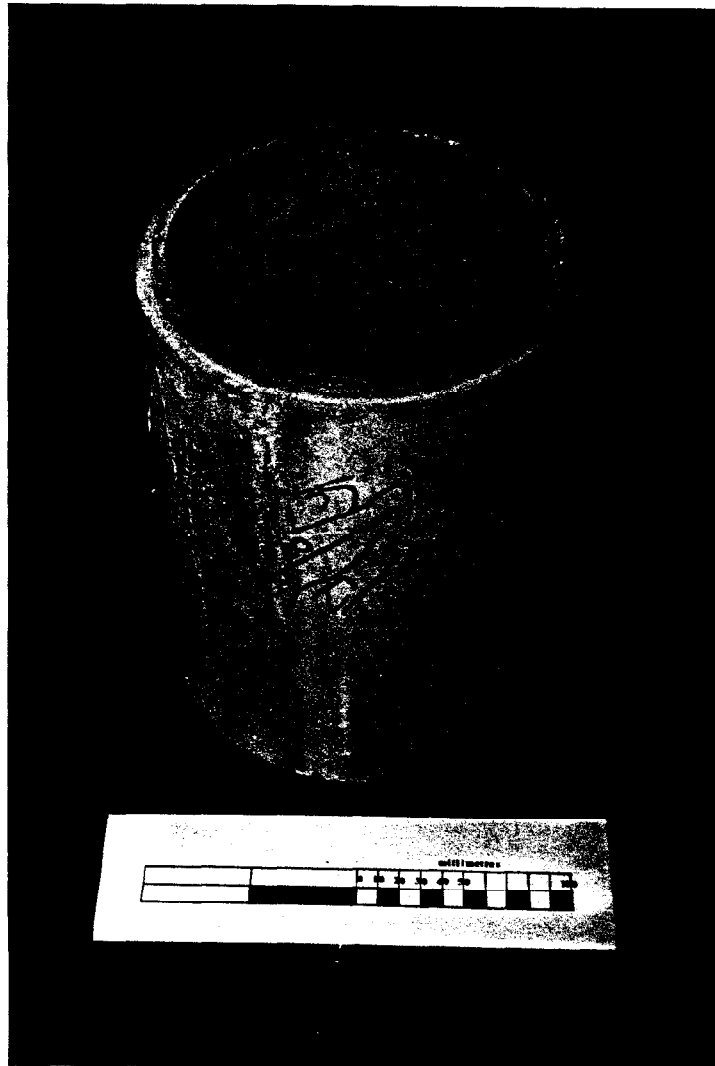**Plate 6.3** Diagonal cracking and joint crushing from Test 15.

load values were 8kN for thick walled pipes and 4.5kN for thin walled pipes but with loads applied over the full length of the pipe. This difference is believed to be due to the effects of the loads being concentrated on a short length of the pipe and compressive axial loads restraining the pipe.

6.5 Edge loading results

The arrangement of loading applied to the pipes during this test series has been shown in Figure 6.2b and is modelling pipes being pushed around a curve. Three different angles of deflection at the joint were tested; 0^0; 0.86^0 and 1.72^0. On a full size pipejack these deflections are equivalent to:-

1   Straight pipejacks (0^0).

2   900mm internal diameter, 2.44M long pipes on a radius of 165M (0.86^0).

3   900mm internal diameter, 2.44M long pipes on a radius of 82M (1.72^0).

4   900mm internal diameter, 1.1M long pipes on a radius of 75M (0.86^0).

5   900mm internal diameter, 1.1M long pipes on a radius of 37M (1.72^0).

6   1800mm internal diameter, 2.44M long pipes on a radius of 167M (0.86^0).

7   1800mm internal diameter, 2.44M long pipes on a radius of 83M (1.72^0).

Note should be taken that before pipes are installed on a radius, consideration needs to be given to the watertightness and integrity of the pipe joints especially at large deflection angles.

In this test series the yokes against the sides of the pipe were attached to tension bars and positioned to prevent lateral movement of the test pipe. However, when axial load was applied the tension bars measured no load as the friction between the axial loading platens and the pipe was sufficient to prevent significant lateral movement of the pipe. It would be necessary on a prototype pipejack to consider the shear stress capabilities of the pipe joints.

During the studies a construction site was visited where pipes were being installed on a horizontal radius and one pipe had begun to fail due to shearing at the joint causing one pipe to move sideways relative to the next pipe.

6.5.1 Deformations of the pipe

During the analysis of this test series it was found that results were best considered by assessing movement of the pipe within the test rig and changes of the pipe's diameter. Deflection angles were not providing any useful information about changes in the pipes' shape or position. Diagrammatic representation of the pipe's movements and changes of diameters during various tests are presented in Figure 6.13.
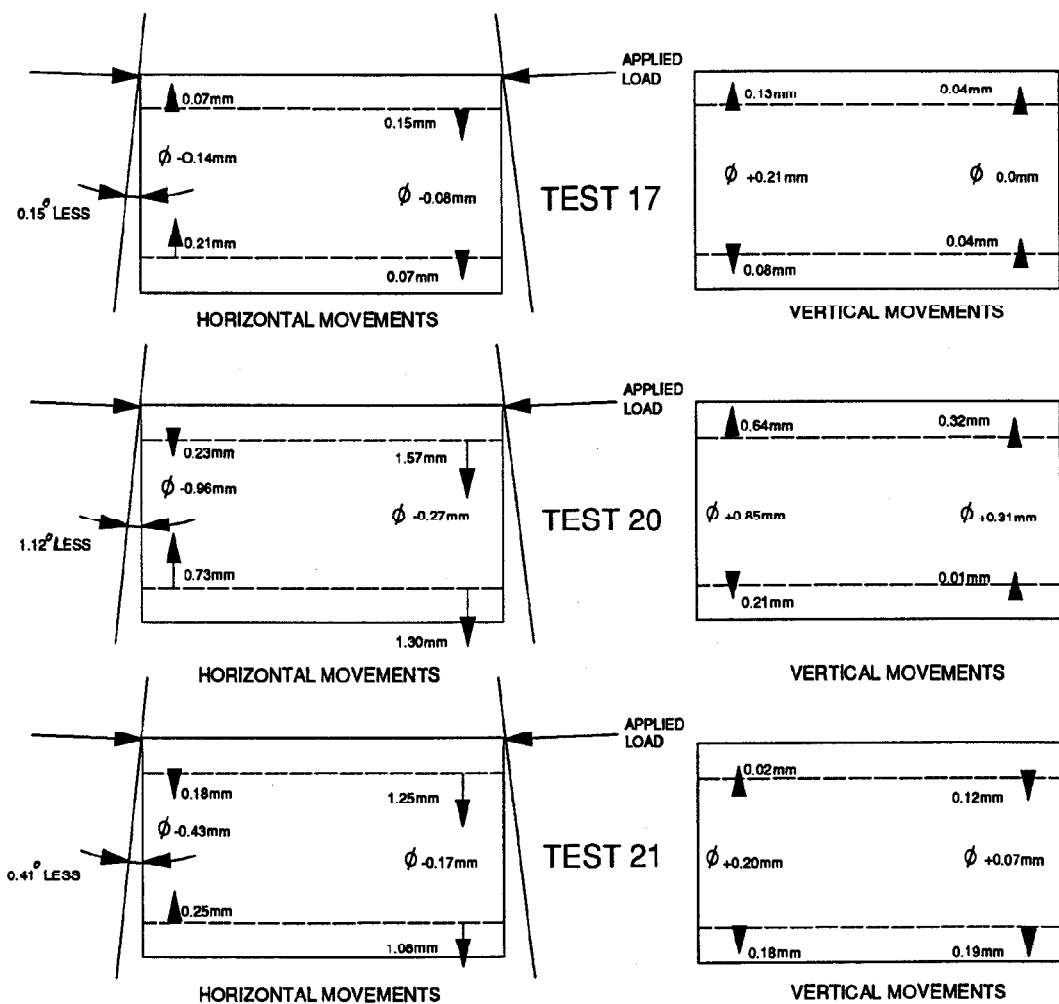

Figure 6.13 Pipe movements and changes of diameter.

The pipejacking fraternity refer to the ends of jacking pipes as either the leading end or the trailing end. The leading end of a pipe is nearest to the destination and the trailing end is nearest to the thrust pit.

The deformations of pipes during the edge loading tests were consistently different for each end of the pipe. The trailing end of the pipe experienced smaller diameter changes but larger lateral movements. The leading end of the pipe had diameter changes of up to four times those of the trailing end, the largest differences occurring with largest angular deflections of the pipe.

The pipes loaded without any angular deflection i.e. with loading on the full circumferential end area, experienced insignificant shape changes or movements. Thin pipes with the largest deflection angles had diameter changes of +1.0mm (0.6%) vertically and -1.0mm horizontally on the leading end of the pipe, whilst thin pipes without deflection angles had diameter changes of less than 0.1mm. Thick pipes experienced diameter changes of less than 0.05mm with no joint deflection and up to ±0.4mm for initial pipe deflections of 1.72^0.

6.5.2 Strain gauge readings

Electrical resistance strain gauge rosettes were mounted in the same position on pipes for all the tests. The rosettes were positioned halfway along the pipe length at three positions; two were perpendicularly in line under the axial load platen either internal (rosette H) or external (rosette G) and the third rosette was externally 180^0 around the circumference (rosette F) of the pipe from the first two gauges. Major and minor principal strains were calculated from the data recorded during testing.

The strain readings showed major principal compressive strains along the length of the pipe which were always larger as deflection angles were increased; they are presented in Figure

6.14. Minor principal strains were very small in comparison and are not plotted; they were orientated around the circumference of the pipe. The magnitudes of strains were not very sensitive to the deflected angle at which load was applied to the pipe.

It is interesting to compare the level of strain readings recorded. It was found that the two gauges mounted on opposite faces of the pipe's wall were measuring compressive strains that were consistently almost double on the inside face compared to those on the outside face. Figure 6.15 presents a plot of the ratios between these two gauges and average values are given in Table 6.3. It is interesting to note that the magnitude of the strains were not very sensitive to the initial misalignment angles at which the pipes were set.
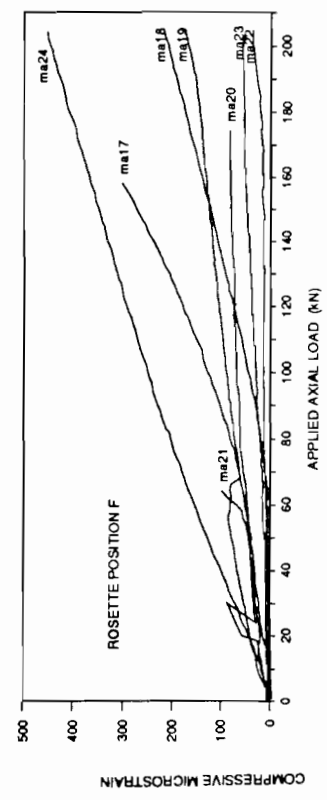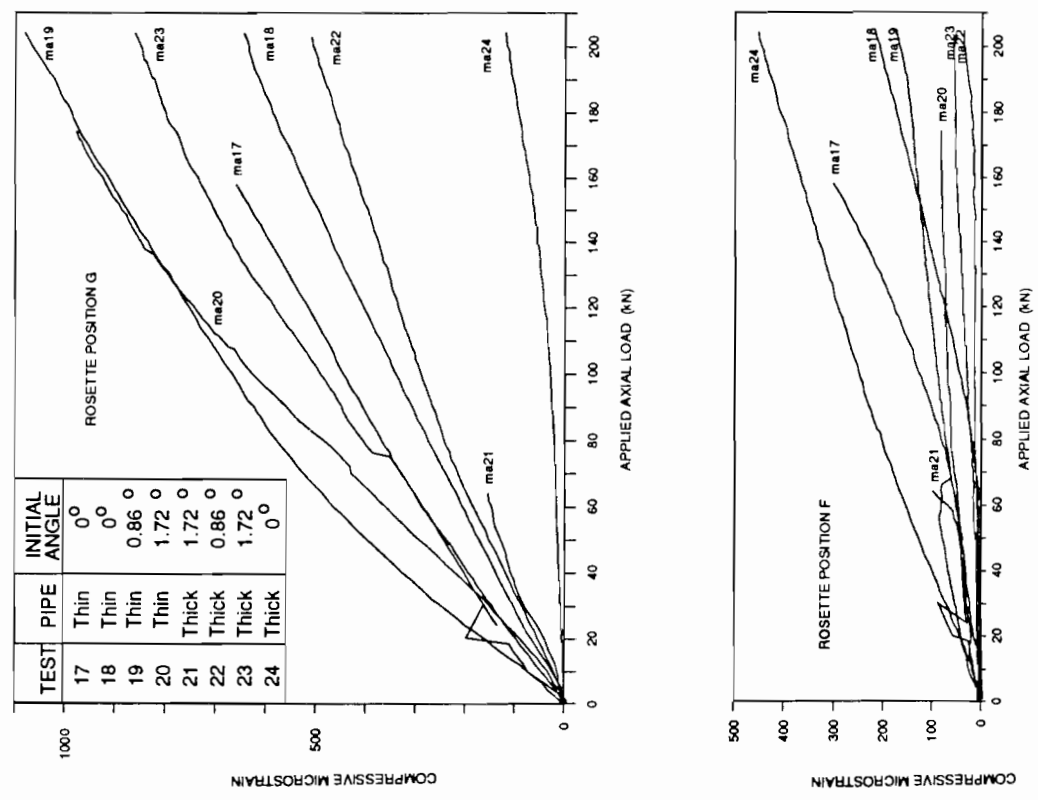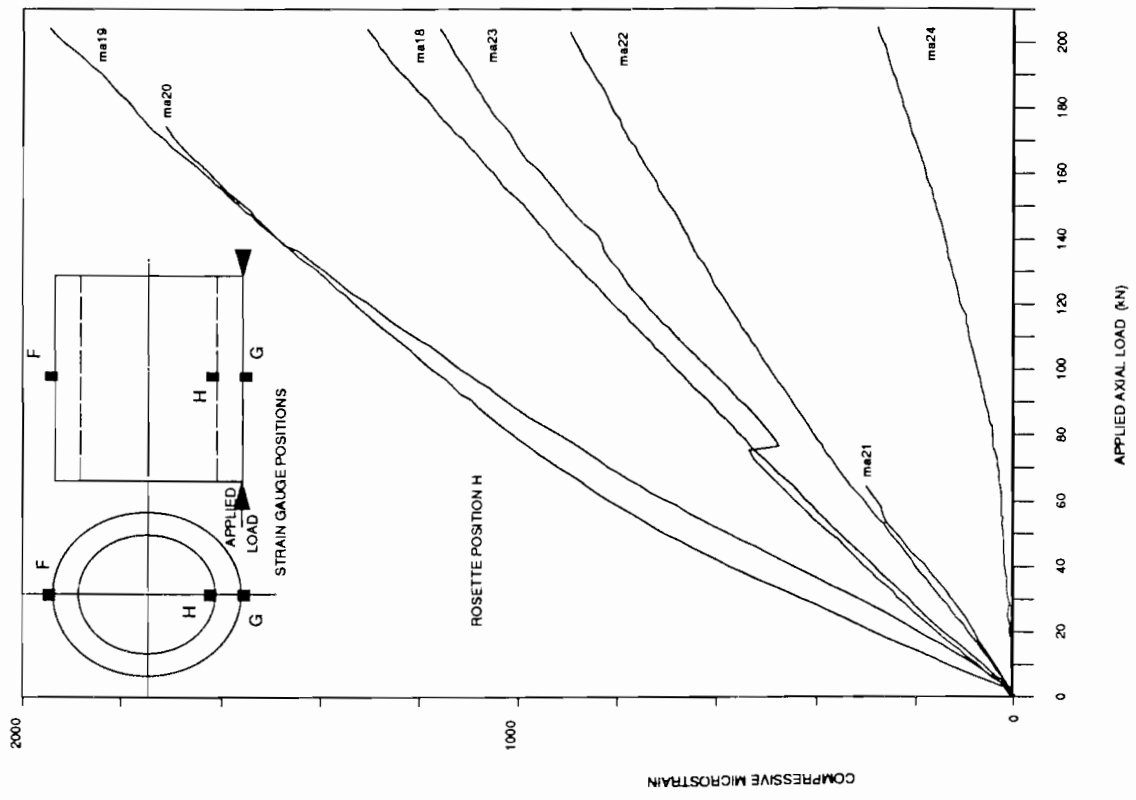
Figure 6.14 Variation of strain readings at various positions on the pipe.
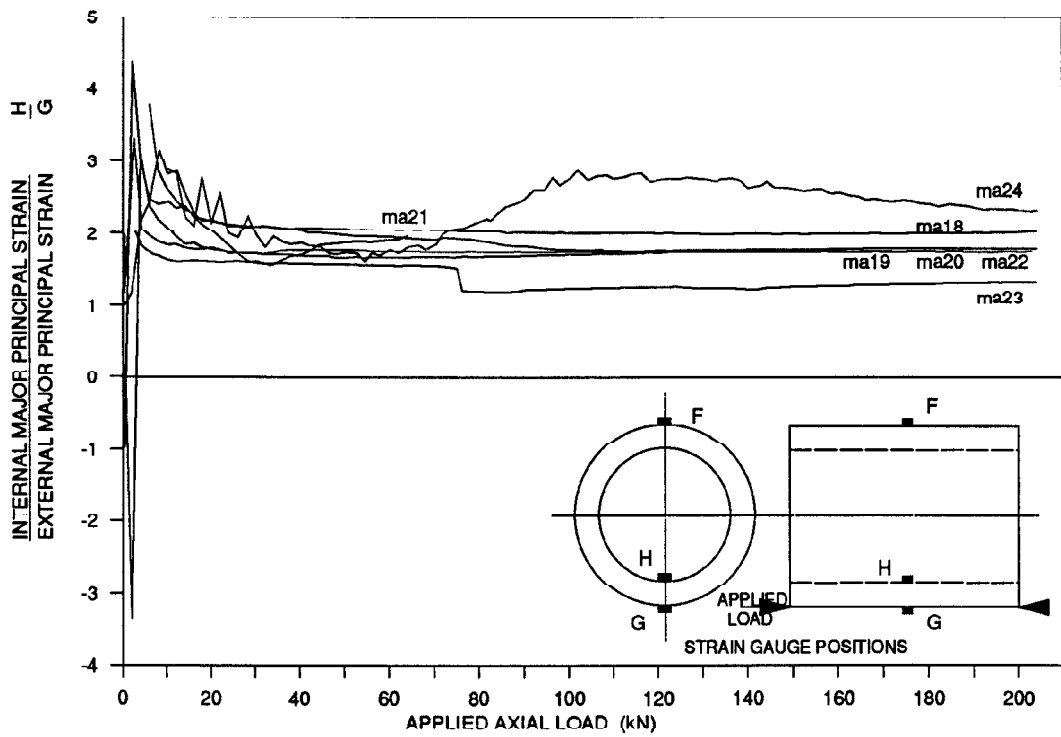
Figure 6.15 Ratio between internal and external principal strains.

Test No.	ε3/ε1 (major internal / major external)	Deflection Angle (Degrees)
17		0
18	2	0
19	1.8	0.86
20	1.8	1.72
21	1.9	1.72
22	1.8	0.86
23	1.4	1.72
24	2.3	0

Table 6.3 Ratio between internal and external longitudinal strain measurements.

Major and minor principal stresses were calculated using Hooke's Law and a sample of principal stresses from Test 19 are plotted in Figure 6.16. The Figure also includes a plot of the orientation of the major stresses during the test. The stresses in Test 19 were greater than experienced in any other tests and it can be seen that principal compressive stresses at rosette position H are above 60N/mm².

Figure 6.16 Principal stresses calculated from Test 19.

Strains measured 180^0 around the pipe's circumference were found to be significant only when load was applied to the full circumferential end area. The stresses presented from Test 19, for this rosette position F, indicated a compressive stress of $6N/mm^2$ orientated at an angle between 30^0 and 50^0 to the pipe's longitudinal axis.

6.5.3 Failure modes

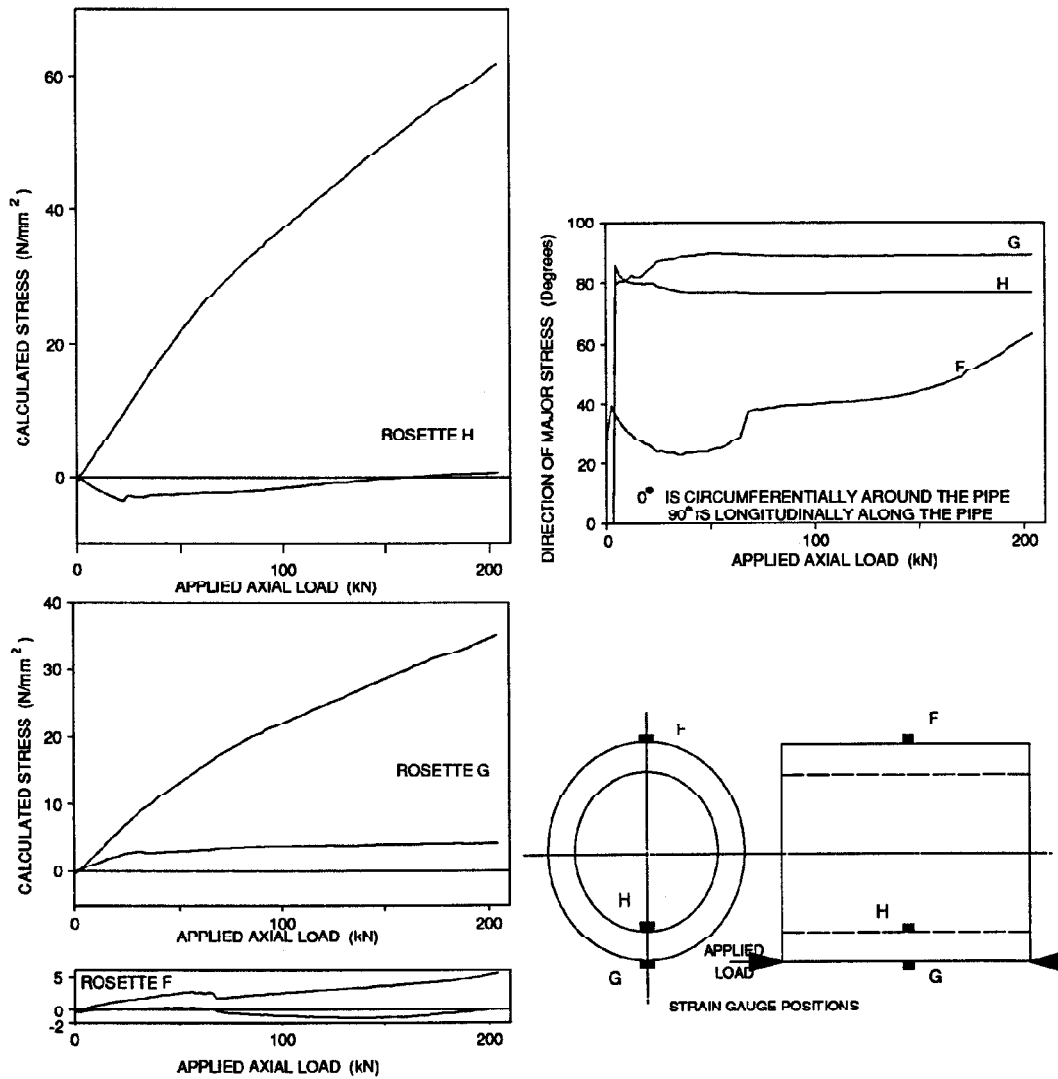A summary below in Table 6.4 gives details of tests conducted and visual signs of failure:-

Test No.	Pipe Type	Deflection Angle (Degrees)	Load Applied (kN)	Failure Mode
17	Thin	0	158	Crushed pipe joint.
18	Thin	0	204	
19	Thin	0.86	204	
20	Thin	1.72	174	138kN longitudinal crack; 174kN crushed joint.
21	Thick	1.72	64	64kN in wall joint crushed
22	Thick	0.86	203	
23	Thick	1.72	204	160kN longitudinal crack
24	Thick	0	204	160kN slight spigot spalling

Table 6.4 Summary of failure modes.

The failure of pipes in this test series was explosive with no advance warning. The pipes were usually failing due to crushing of the joint as seen in Plate 6.4 and a wedged shape piece of concrete was being driven between the reinforcement cages of the pipe. This failure

is the same mode as experienced during compressive strength testing of concrete cubes and is due to excessive compressive load being applied to the end of the pipe causing failure due to shearing.
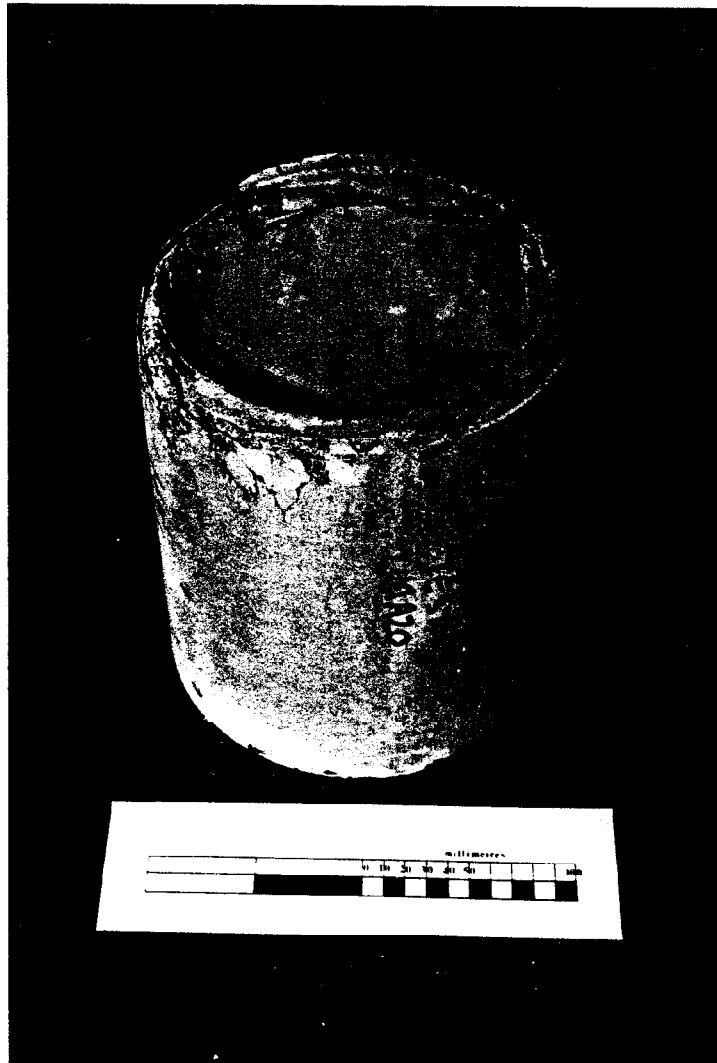

Plate 6.4   Crushing of the pipe end during Test 20.

6.6 Summary of misalignment tests

1   Different types of failure modes have been experienced due to compressive, tensile, shear and bending failure.

2   Changes in the diameter of the pipe were not usually significantly large and would be difficult to measure accurately in a full size pipejack except when jacking around curves.

3   Measurements in the tension rods gave an indication of the normal pipe/soil interaction loads that might be expected and the advantage of excavating a straight hole into which the pipes could be jacked.

4   Changes in deflection angles during the diagonal loading tests revealed useful information about the pipe deformation and how the deflected angles between pipes decreased as increased axial load was applied.

5   Stresses calculated from diagonal loading test results indicated that external tensile stresses were measured and were greatest around the pipe's circumference. At the same position on the pipe, internal stresses were compressive and largest on the diagonal between loading points.

6   Stresses calculated during edge loading tests also showed significant differences between measurements on the internal and external surfaces of the pipe. All major compressive stresses were orientated longitudinally along the pipe but their magnitude was twice as high on the internal surface compared to the external surface.

CHAPTER 7

JOINT PACKING MATERIAL

7.1 Introduction

Packing materials are recommended for use in jacking pipe joints but no details of their nature or exact positioning in the joints were available when this research commenced. The packing material is used as an aid to distribute areas of high stress concentrations over larger pipe end area and thereby reduce the maximum stress level. In the past packing materials have been used intermittently by some pipejacking contractors and totally avoided by others. When packing materials have been used they have been associated with attempts to stop spalling of the concrete at the pipe joint.

The aim of this series of tests was to assess the advantages and disadvantages associated with the use of packing materials. The tests would lead to recommendations on the use of materials, the nature of the material to be used, how thick it should be and where it should be placed. The materials were assessed under cyclic load conditions and tested in various conditions: as purchased; saturated; saturated and then room dried.

The ideal material is considered to be one that compresses greatly when loaded and recovers its thickness when unloaded, and a material that does not induce tensile strains in the concrete that are any greater than those associated with the axial load applied. The packing material

should have a Poisson's ratio in compression near to zero. It is emphasised that these are ideal requirements and properties and the aim of the test programme was to find the packing material most able to meet the requirements.

Loading of packing material should be between concrete surfaces to simulate the friction between packing material and pipe end that would be experienced in practice. Part of the function of the joint packing material is believed to be prevention of stress concentrations created by high points on the concrete surface. This is especially relevant to the trowel finished end of a vertically cast pipe.

7.2 Test programme

A series of cyclic loading tests was carried out to test various prototype packing materials used in jacked pipe joints. The tests were conducted using 100mm sided concrete cubes as loading media with packing material sandwiched between them. The concrete cubes were instrumented with electrical resistance strain gauge rosettes. Load was applied using an hydraulic jack and the arrangement of the test equipment and transducer positions are shown in Figure 7.1 and Plate 7.1.
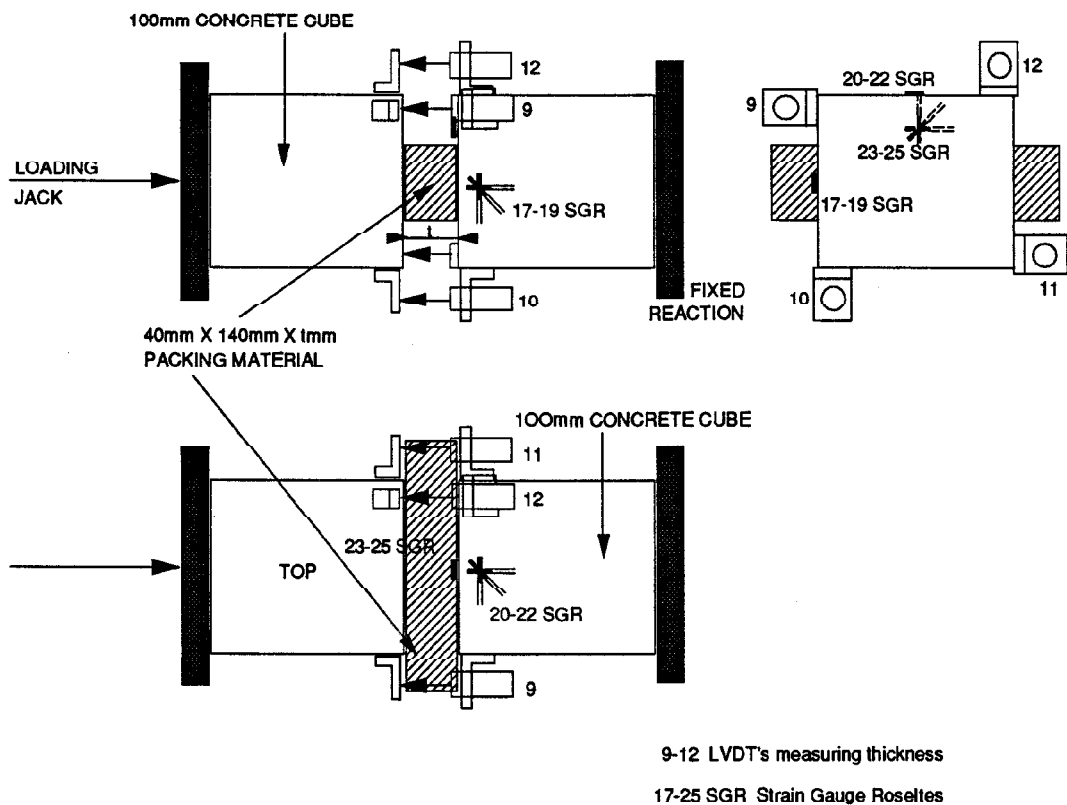
Figure 7.1 Arrangement of equipment and transducer positions.

Three electrical resistance strain gauge rosettes were used to monitor magnitude and direction of principal strains. Four LVDT's monitored the gap between the concrete cubes and hence the compression and recovery of packing material thickness. The four LVDT's also enabled assessment of any eccentricity in the loads applied. Initially a large number of different materials was tested and further experiments were conducted on selected materials as a result of these initial tests. Tests were carried out on the following material types and thicknesses:-

6mm, 12mm, 18mm and 25mm exterior grade plywood

12mm good one side shuttering plywood

12mm and 18mm chipboard

12mm softboard

6mm, 12mm and 18mm dense fibreboard

3mm hardboard

18mm planed timber

12mm and 18mm blockboard

Plate 7.1 Apparatus for cyclic loading of joint packing materials.

All the materials were loaded cyclically using the mechanism drawn in Figure 7.2. This mechanism controls the hydraulic jack by moving the control handle using a linkage and cam driven by a mot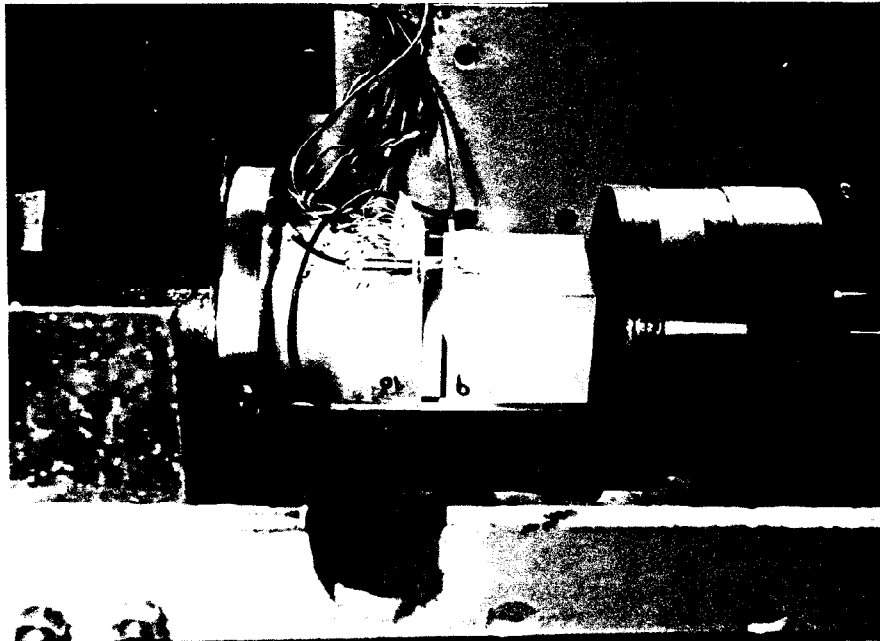or. The profile of the cam and motor speed provided a cyclic duration of 152 seconds during which the packing was loaded for 10 seconds.

CAM FOLLOWER

NEUTRAL

RETRACT   **EXTEND**

**CONTROL
LEVER**

CAM

**SHAFT
CONNECTED
TO MOTOR
DRIVE**

**ADJUSTABLE
LINKAGE**

**HYDRAULIC
RAM**

**CONTROL
BLOCK**

MOVEMENT PRODUCED BY CAM

TOTAL CYCLE TIME = 152 Secs.

0-10 Secs. LOAD
10-11 Secs. UNLOAD
11-25 Secs. NEUTRAL
25-27 Secs. RETRACT
27-150 Secs. NEUTRAL
150-152 Secs. EXTEND
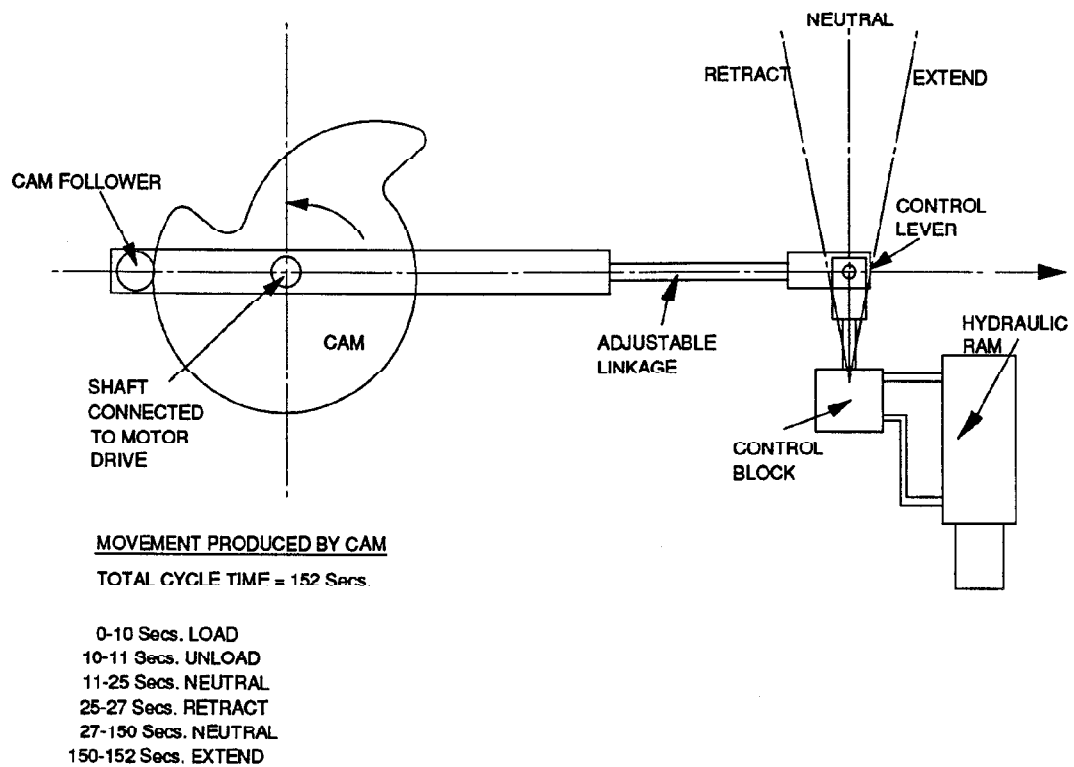
Figure 7.2   Cyclic loading apparatus.

A programme was written which enabled data to be recorded during 40 second time intervals and allowed recording of data before, during and after loading. Data were recorded during every load application for the first ten applications of load and thereafter recordings were made every tenth cycle. The first and last cyclic load applications were carried out manually and allowed data to be recorded as load was being increased and decreased. This data recording process   gave a clear indication of how the properties of the packing materials changed during the application of approximately 360 load/unload cycles.

Following initial testing, further cyclic loading was carried out on the following materials at the stated stress levels and material conditions:-

Stress	Material	Condition	Initial Thickness
50N/mm^2	Dense fibreboard	As supplied	18mm, 12mm, 6mm
	Chipboard		18mm
	Exterior grade plywood		18mm, 6mm
15N/mm^2	Dense fibreboard	As supplied	18mm, 12mm, 6mm
	Chipboard		18mm, 12mm
	Exterior grade plywood		18mm. 6mm
	German chipboard		22mm
15N/mm^2	Dense fibreboard	Saturated	18mm, 12mm, 6mm
	Chipboard		18mm, 12mm
	Exterior grade plywood		18mm, 12mm, 6mm
	German chipboard		22mm
	Softboard		10mm
15N/mm^2	Dense fibreboard	Saturated then	12mm, 6mm
	Chipboard	room dried	18mm, 12mm
	Exterior grade plywood		18mm, 12mm, 6mm
	German chipboard		22mm
	Softboard		10mm

Data recording the changing densities and thickness of packing materials were recorded while the materials were being saturated and dried and are presented in Figures 7.3a and 7.3b.
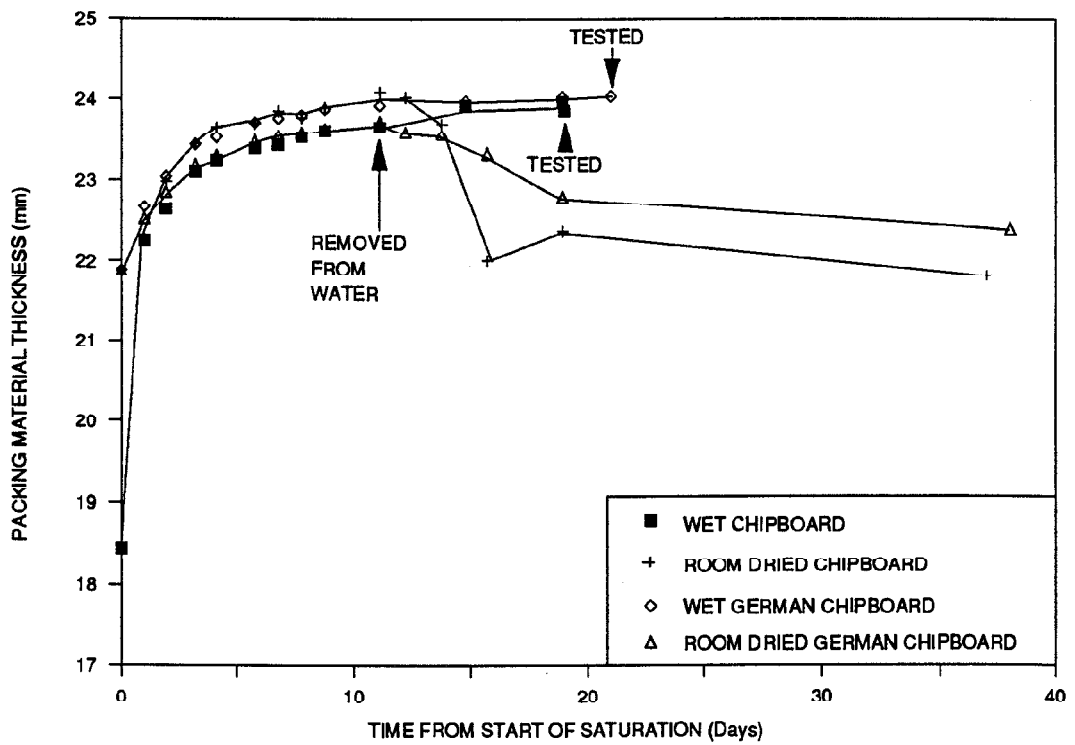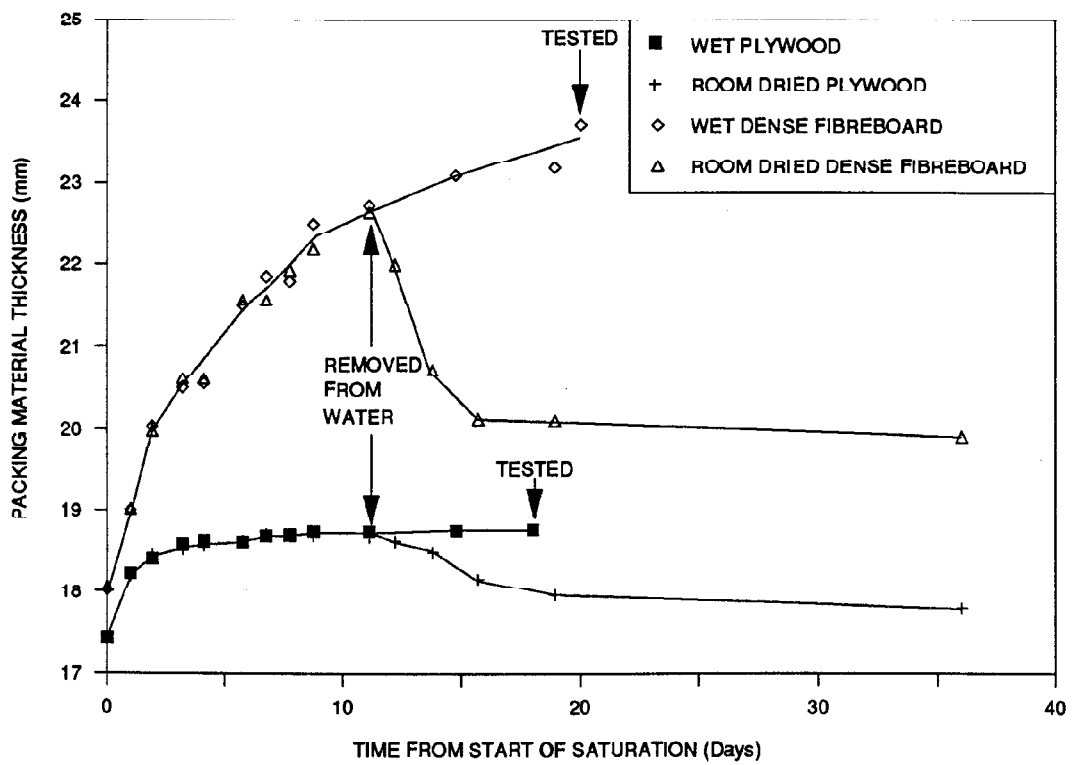
Figure 7.3a Thickness of packing materials whilst being saturated.
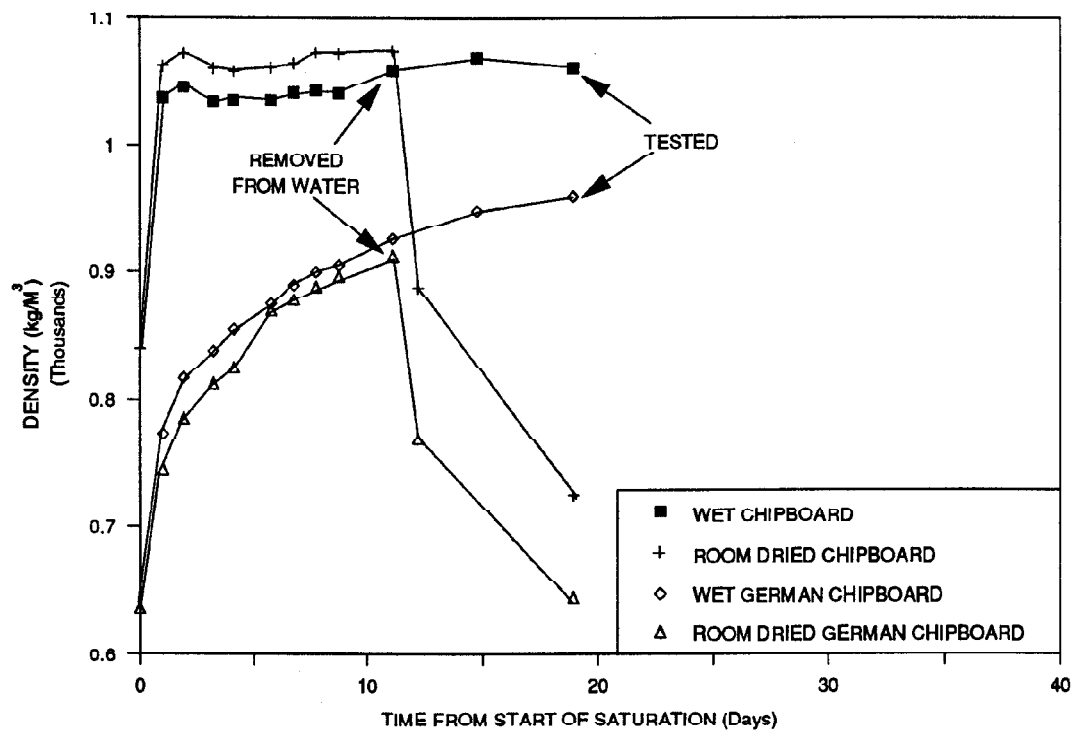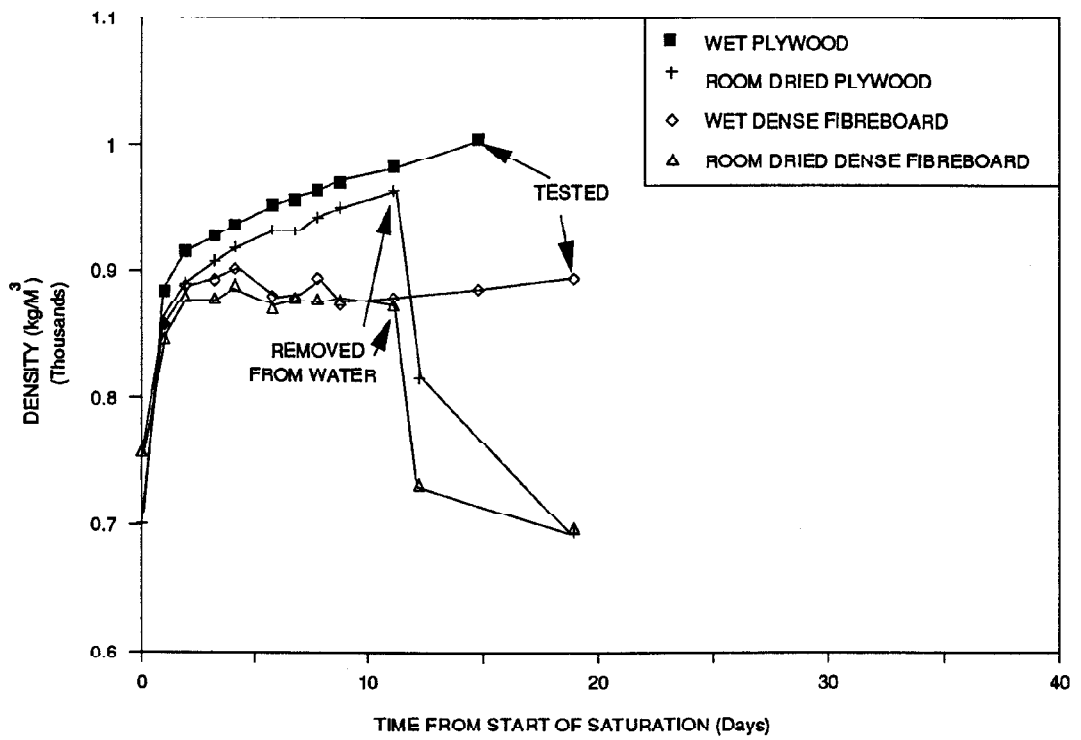
Figure 7.3b Densities of packing materials whilst being saturated.

Effects of stress concentrations applied to concrete have been researched previously by Williams (1979), whose report reviews current analytical procedures and presents results from a test programme to assess the concrete's ability to sustain high stresses over limited load areas. Various types of material were used and all tests were loaded to failure. Figure 7.4 presents results showing how the concrete bearing stress is increased as the load area is decreased. Bearing stress can be up to four times the concrete compressive strength before failure occurs. Included in the report are details of the effects of loading onto a trowelled surface which can reduce the concrete bearing stress to half the value compared with the loading of flat surfaces. The results from these tests are of some use to the current research but take no account of distributed stresses; all the bearing stresses applied were concentrated and uniform.
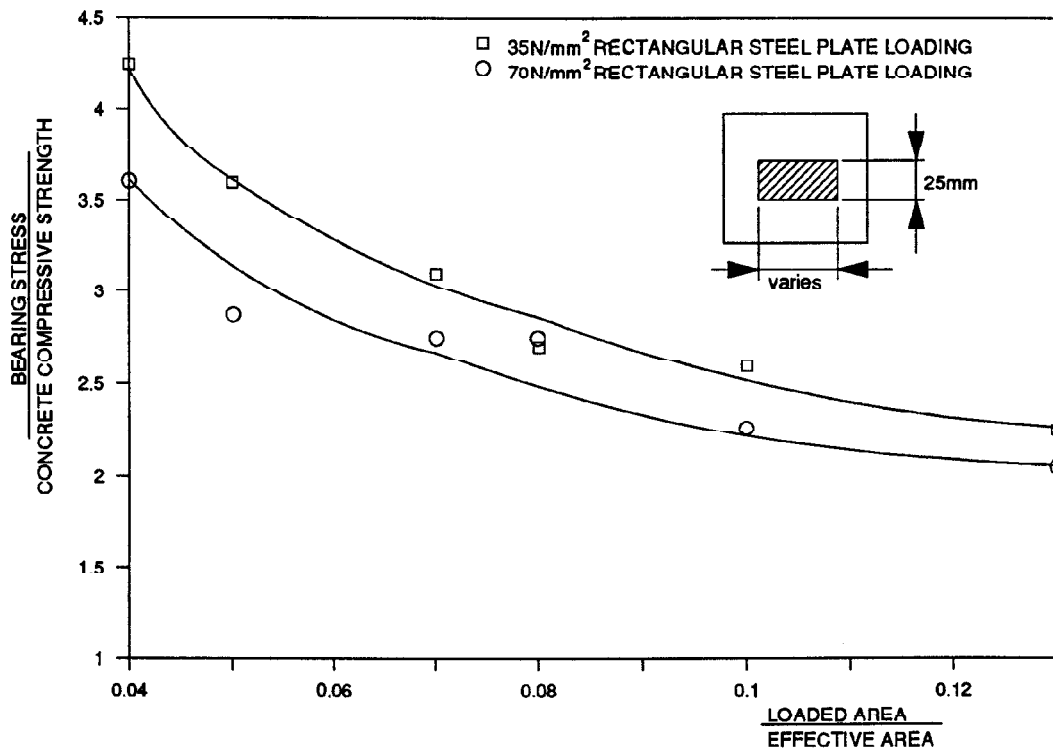
Figure 7.4 Plot of ultimate bearing stress variations (Williams 1979).

7.3 Results

Examination of the initial cyclic loading test results revealed several points of interest. It was clear that packing materials were being permanently deformed (Plates 7.2 and 7.3) and the material properties were totally different after one load application had been performed compared with the properties of the material before testing began. Consideration of the conditions in which the packing material would be used led to all analysis being carried out on results recorded subsequent to the application of the first load.
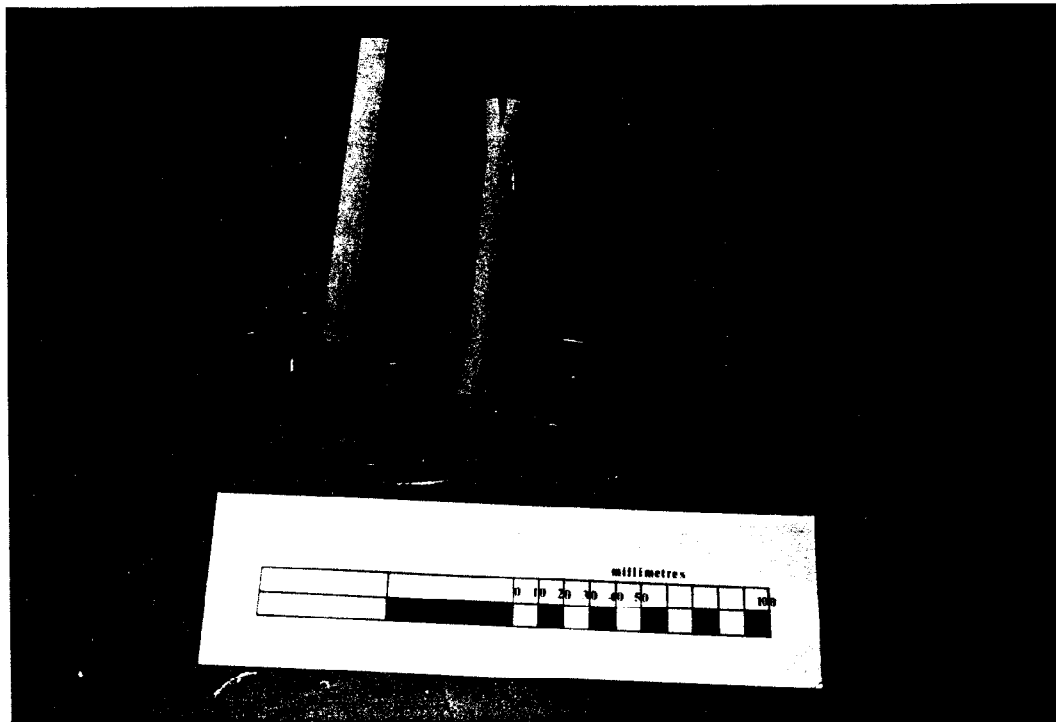
Plate 7.2 Typical joint packing materials.

Some of the initial materials tested were immediately ruled out of the subsequent test programme. 18mm thick planed timber compressed along the direction of its grains rather than
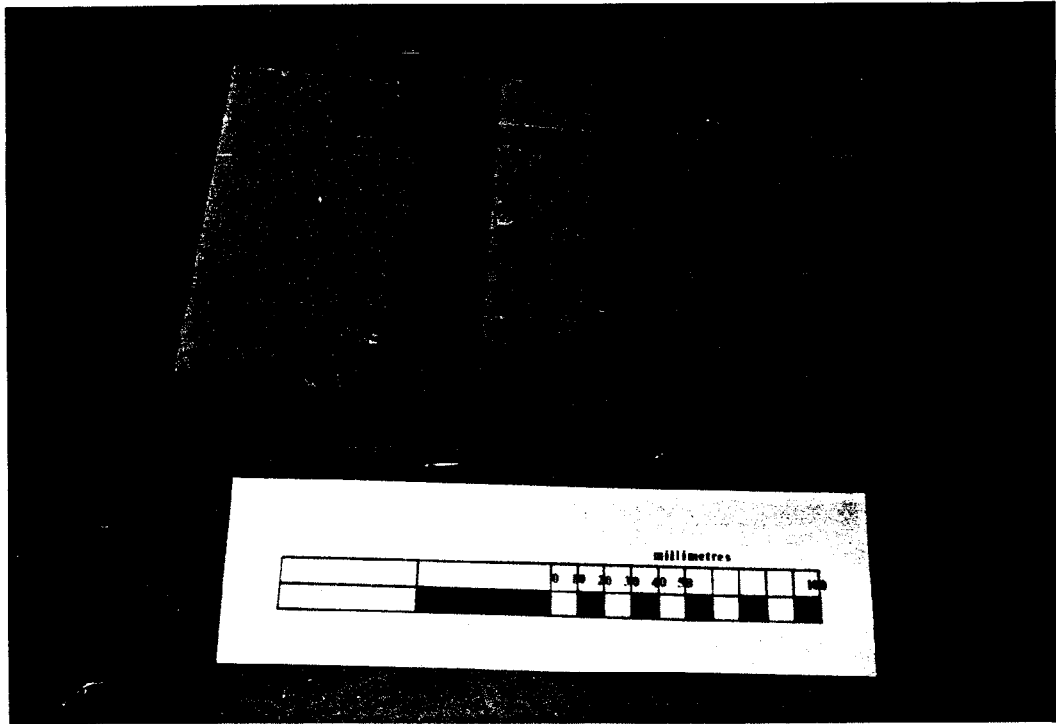
Plate 7.3 Typical joint packing materials.

in the direction of load application which led to displacement of one concrete cube relative to the other. The timber was chosen as knot free and was not considered to be a viable proposition for a packing material.

Blockboard disintegrated on application of load and was not tested further; hardboard was obtained in 3mm thickness only and was not compressible; 12mm softboard compressed to 4.5mm and then resembled dense fibreboard. Good one side shuttering plywood compressed unevenly due to many gaps in the ply as it had been laminated. Further testing and analysis was carried out on dense fibreboard, plywood and chipboard.

7.3.1 Stress/strain relationship

Data have been processed to give details of the stress and strain conditions induced in the packing material. Stress is obtained by dividing the load applied to the packing material by the area of material under compression and load is assumed to be distributed uniformly. Strain is the change in thickness of the material since it was first loaded divided by its original thickness. Plots similar to those presented in Figure 7.5 were obtained, but these plots do not present the information in a suitable format.
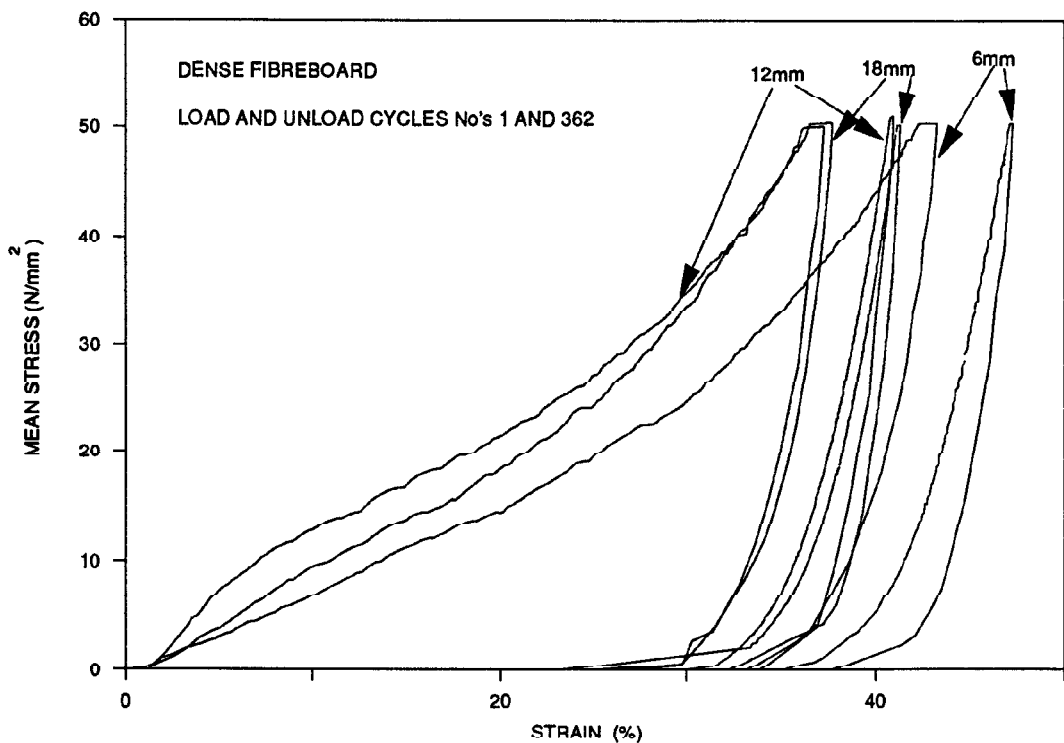
Figure 7.5 Stress/strain plot for dense fibreboard.

The graphs were re-drawn to plot strain as a change in thickness during the current load cycle divided by thickness of packing material at the start of the cycle. The new graphs are

presented in Figure 7.6, but thicker packing materials appear to be strained to a lesser extent than thin materials, yet are more compressible overall and therefore better at distributing stress concentrations.
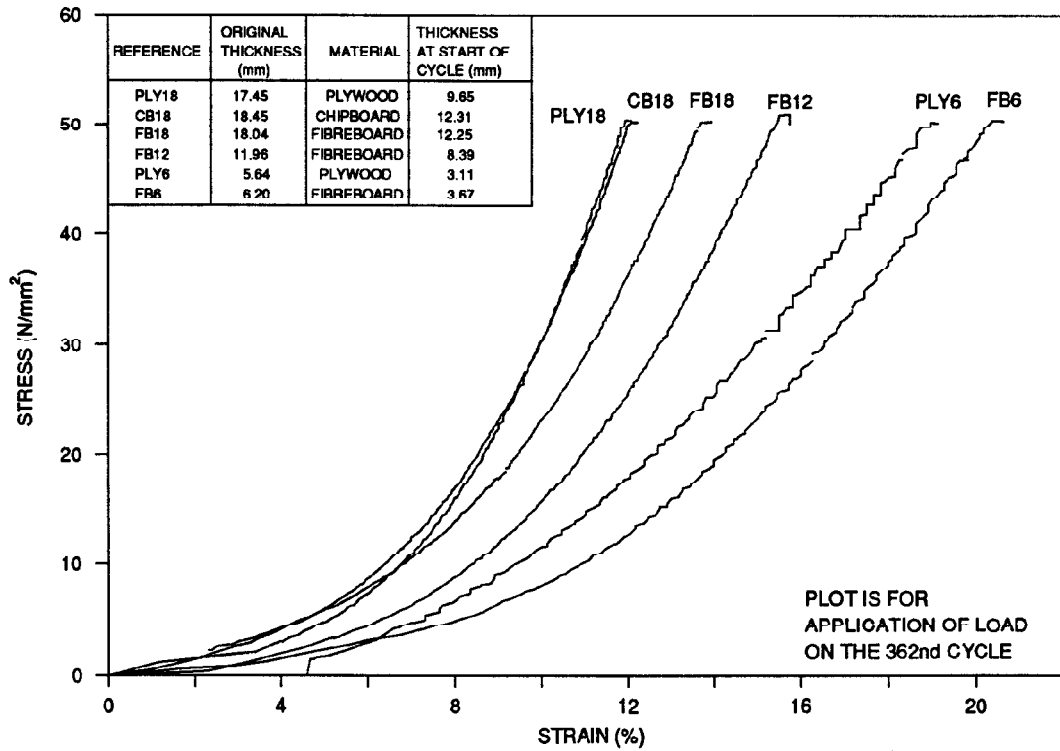
Figure 7.6   Stress/strain plots for 362 load cycles.

If the compressive properties of the packing material are the only consideration, the material with maximum compression is required. This is not evident from the stress/strain plots presented and the data are replotted as compression in millimetres during the current load cycle against induced stress in Figure 7.7.

The first of these plots shows clearly the greater compressibility of thicker packing materials. The second plot shows the differences for similar thickness packing materials and depicts 18mm dense fibreboard as the most compressible material.
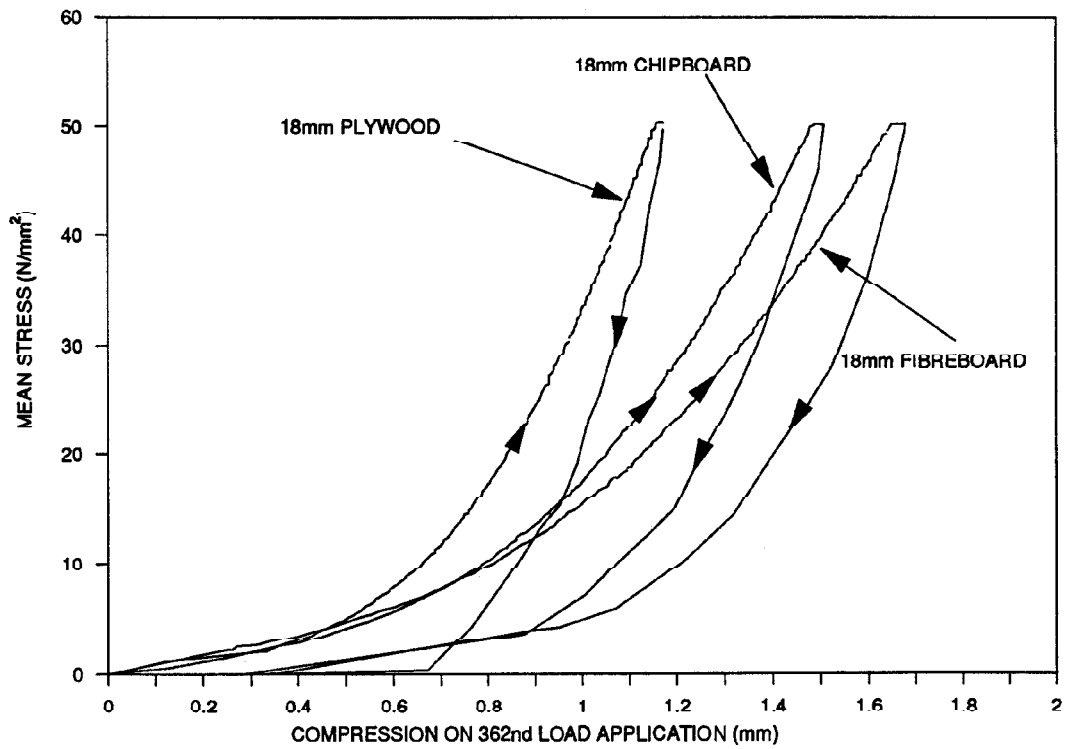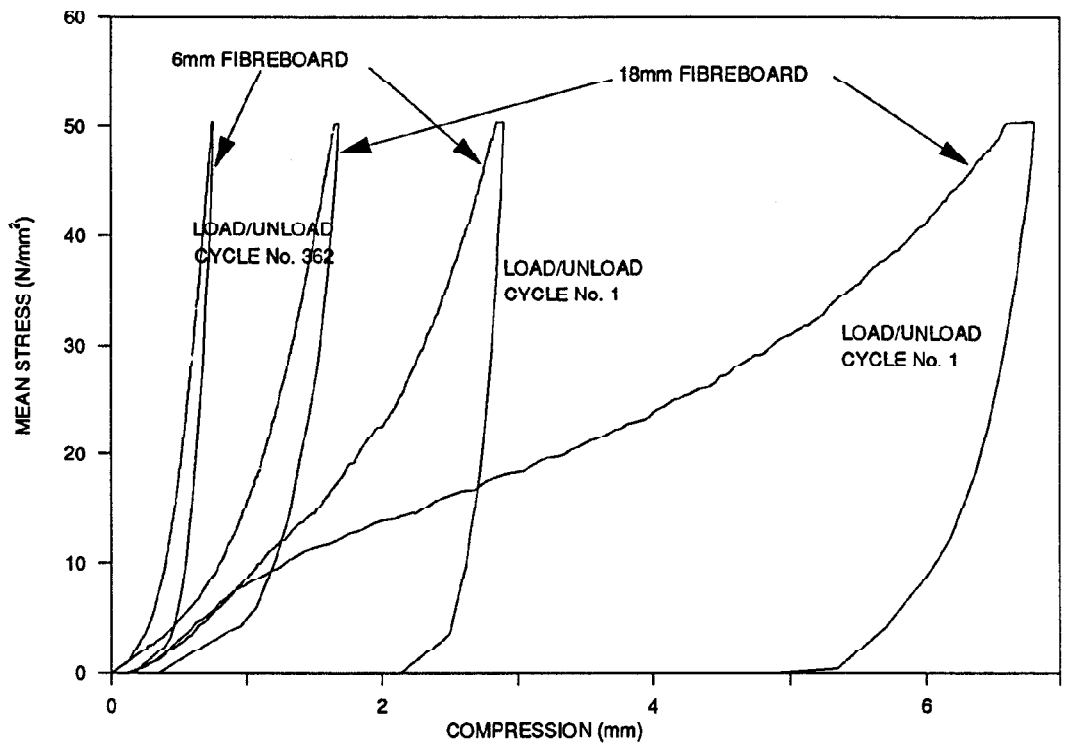
Figure 7.7 Stress/compression plots for various packing materials.

7.3.2 Effect of cyclic loading

A graph plotting time against load is presented in Figure 7.8 and indicates the magnitude and duration of load applied during a typical joint packing material test. The effect of cyclic loading on a pipejack is important due to the method of pipe installation. Many of the pipes are loaded a large number of times during installation i.e. on a 100 metre long pipejack without an interjack station the average number of load applications to the pipes is 200. If an intermediate jacking station is used it is likely that pipes nearest to it will be subjected to an even larger number of load cycles and the largest magnitudes of load.

The tests on the packing materials showed how the material properties changed during the application of a large number of load cycles. A graph showing how the material is compressed and recovers its thickness to a lesser extent with each load application is presented in Figure 7.9. The behaviour was much more noticeable in tests on saturated materials due to drying out of the material during the test; the duration of each test was fifteen hours.
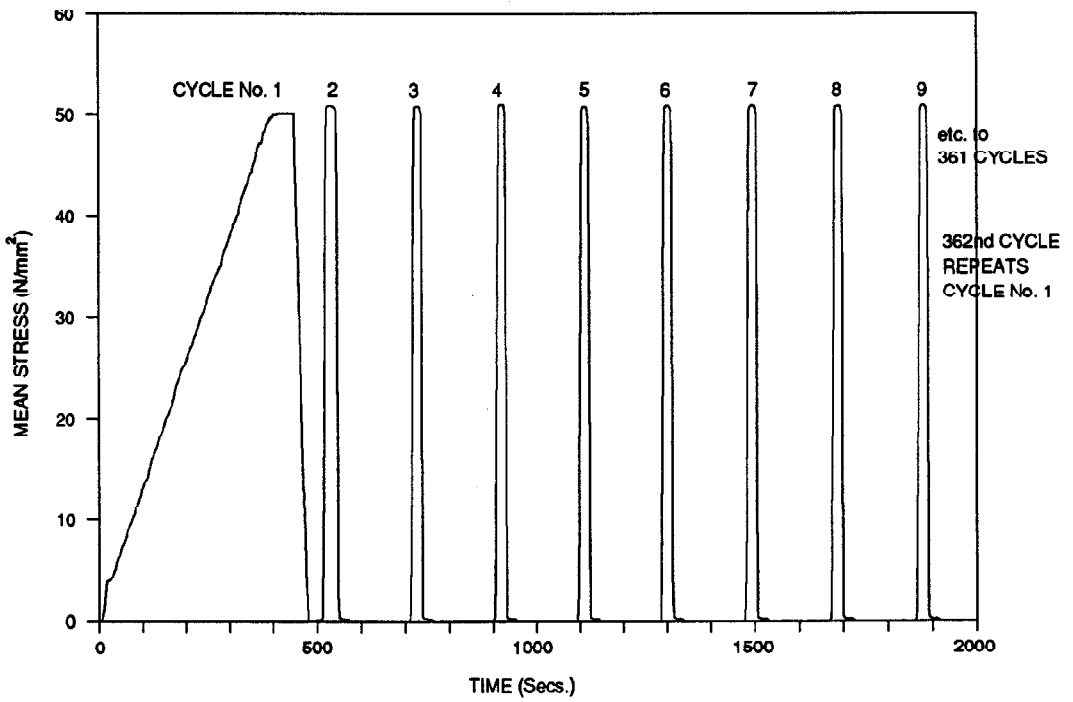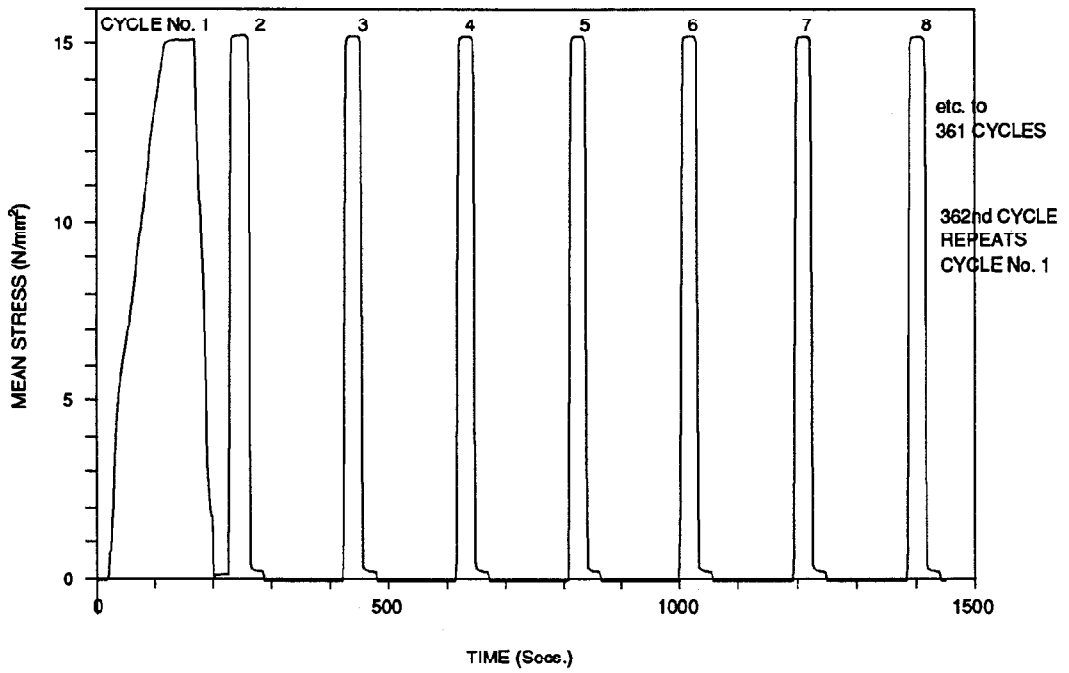
Figure 7.8 Duration of load applications for cyclic loading.
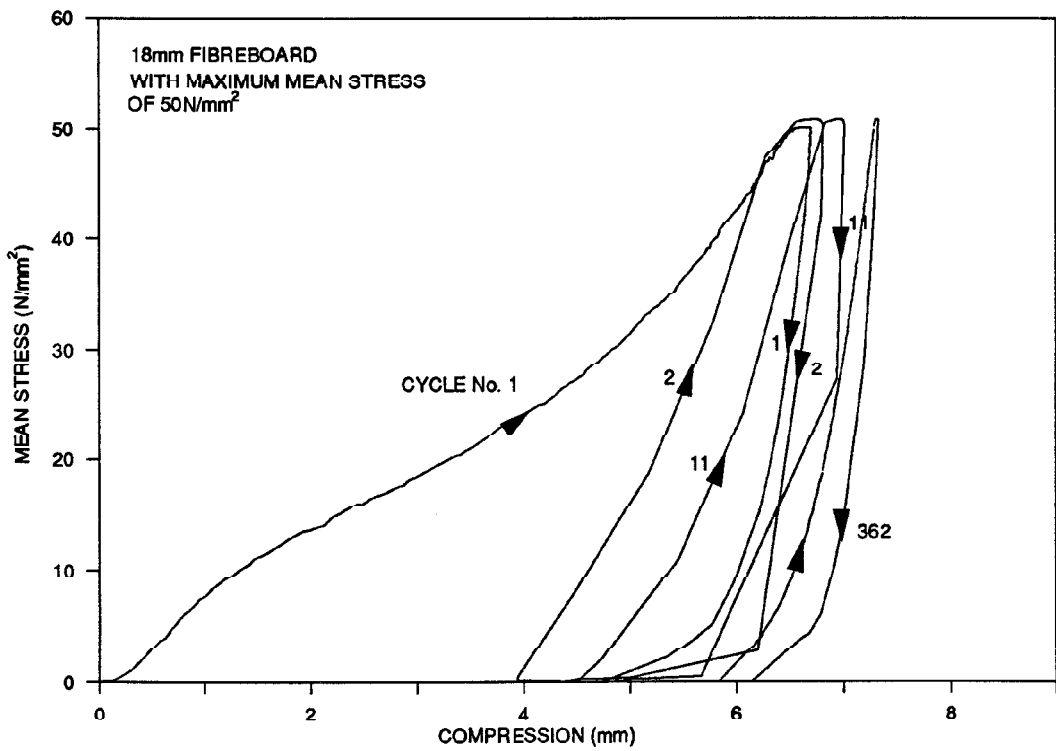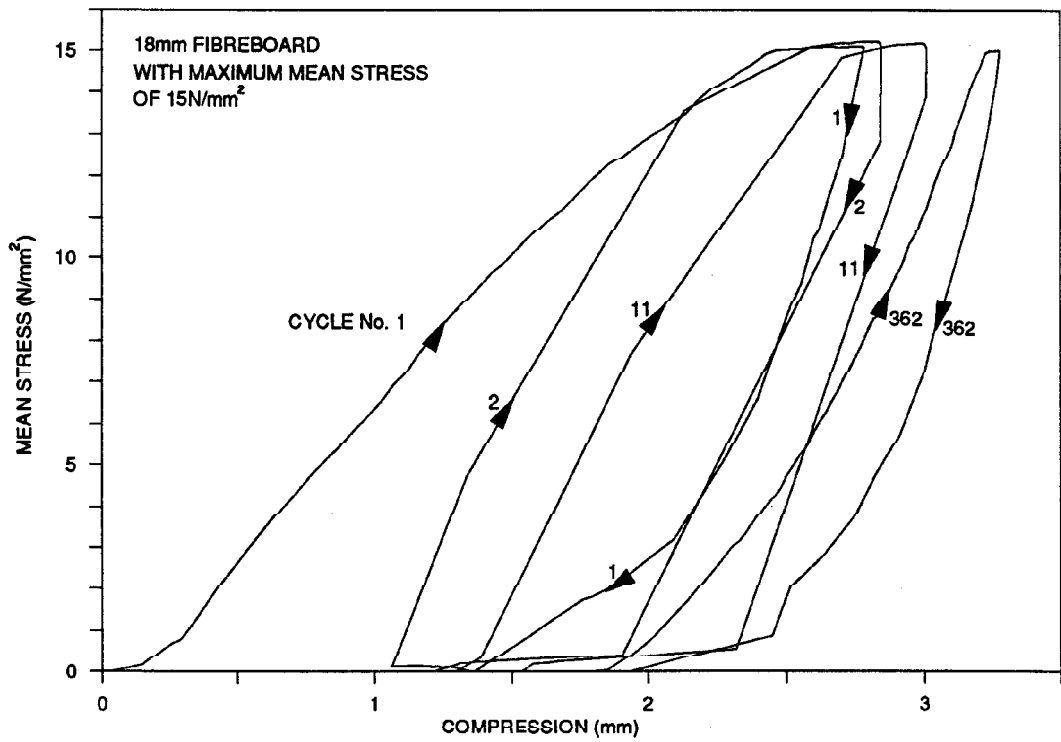
Figure 7.9 Effect of cyclic loading on compression of dense fibreboard.

7.3.3 Variation of packing material thickness

During the test series different initial packing material thicknesses were tested and the difference in their behaviour under compression loads can be seen in Figure 7.7 where more compression is shown to take place in thicker materials. It is not until the geometry of a jacking pipe is considered that the effects of different compressions of packing materials can be fully appreciated.

When considering pipes in a straight line with perfectly square ends relative to each other, the packing material compression and hence its thickness have no effect on the distribution of stress concentrations because stress is uniform. It is not until pipes are considered whose ends are not square, even and aligned that the requirements of the packing material compression need be considered. It could easily be argued that this is the circumstance on all pipejack joints and that ideally square pipes never occur.

Materials that are more compressible when subjected to high stresses are of most benefit in assisting distribution of stress concentrations. The ideal scenario would be to find a material that resulted in equal stresses over the pipes' end area whatever the magnitude of deflection between pipes or unevenness in pipe end profile. This is clearly impossible to achieve, so a material that has a lot of compressibility in order to distribute stresses over as great an area as possible is required. To give some indication as to how deflected pipes affect the compressive requirements of the packing material Table 7.1 can be examined. The table details variations in pipe joint gaps related to angular deflections and further quotes typical measurements of horizontal line and/or vertical level on a prototype jack that would be associated with the particular deflection angle. When reading the table, the deviations quoted are maxima   over the length of one pipe assuming the previous pipe is exactly on the proposed centreline at both ends and that the pipe ends are square to each other. Deviations for line or level assume that the other has no deviation and figures for line and level assume both have equal deviations from the intended centreline.

Angular Deflection (Degrees)	Maximum internal joint gap difference (mm)			Equivalent Line and/or Level deviations (mm)					
				Line or Level only			Line and Level		
	150 mm I.D.	900 mm I.D.	1800 mm I.D.	232 mm long pipe	1100 mm long pipe	2440 mm long pipe	232 mm long pipe	1100 mm long pipe	2440 mm long pipe
0	0.00	0.00	0.00	0.00	0.00	0.00	0.00	0.00	0.00
0.025	0.07	0.39	0.79	0.10	0.48	1.06	0.07	0.34	0.75
0.05	0.13	0.79	1.57	0.20	0.96	2.13	0.14	0.68	1.51
0.075	0.20	1.18	2.36	0.30	1.44	3.19	0.21	1.02	2.26
0.1	0.26	1.57	3.14	0.40	1.92	4.26	0.29	1.36	3.01
0.15	0.39	2.36	4.71	0.61	2.88	6.39	0.43	2.04	4.52
0.2	0.52	3.14	6.28	0.81	3.84	8.52	0.57	2.72	6.02
0.3	0.79	4.71	9.43	1.21	5.76	12.78	0.86	4.07	9.04
0.4	1.05	6.28	12.57	1.62	7.68	17.04	1.15	5.43	12.05
0.5	1.31	7.85	15.71	2.02	9.60	21.30	1.43	6.79	15.05
0.75	1.96	11.78	23.56	3.04	14.40	31.94	2.15	10.18	22.58
1	2.62	15.71	31.42	4.05	19.20	42.59	2.86	13.58	30.11
1.25	3.27	19.63	39.27	5.06	24.00	53.23	3.58	16.97	37.65
1.5	3.93	23.56	47.12	6.07	28.80	63.87	4.29	20.36	45.18

Table 7.1 Comparison between angular deflections between pipes and typical line and level surveys on pipejacks.

7.3.4 Changes of material densities during saturation and drying

Whilst packing material was being saturated totally immersed in water, regular measurements were being taken of the changes in thickness and weight occurring; the data are presented in Figure 7.3.

The difference between the materials' properties when immersed in water can be seen by comparing German chipboard to chipboard. The chipboard readily absorbed water and became more dense than water whereas the German chipboard appeared to be more resilient to water absorption and never attained a greater density than water. Dense fibreboard and chipboard retained some of their increased thickness once they were removed from the water and dried.

The changes of densities of other materials fell between that of dense fibreboard and German chipboard. Ordinary chipboard became frail when saturated and began to disintegrate if it was not carefully handled.

7.3.5 Effect of material conditions

The test results were greatly influenced by the history of atmospheric conditions which the packing material had experienced. It was important to test the material in the various conditions to simulate possible treatment and conditions the material might be subjected to on a construction site. It is possible that the packing material would be left in the open air, saturated in a pipejack with water running in the invert or saturated by ground water on the external face of an in wall jointed pipe.

The differences in the compressive properties of the material experienced during the tests are presented in Figure 7.10 where it can be seen how saturated materials are much more

compressible than materials which have not been treated. Packing material which has been saturated and then dried at room temperature returns to the same thickness when compressed as material that had not been saturated but has more thickness recovery when unloaded. These behaviours were found to be the case for all materials tested and clearly demonstrate that the saturation of the packing material is not detrimental to the compressive behaviour or integrity. If it were practically possible, saturation of packing material would be a distinct advantage in distributing jacking loads over larger areas.
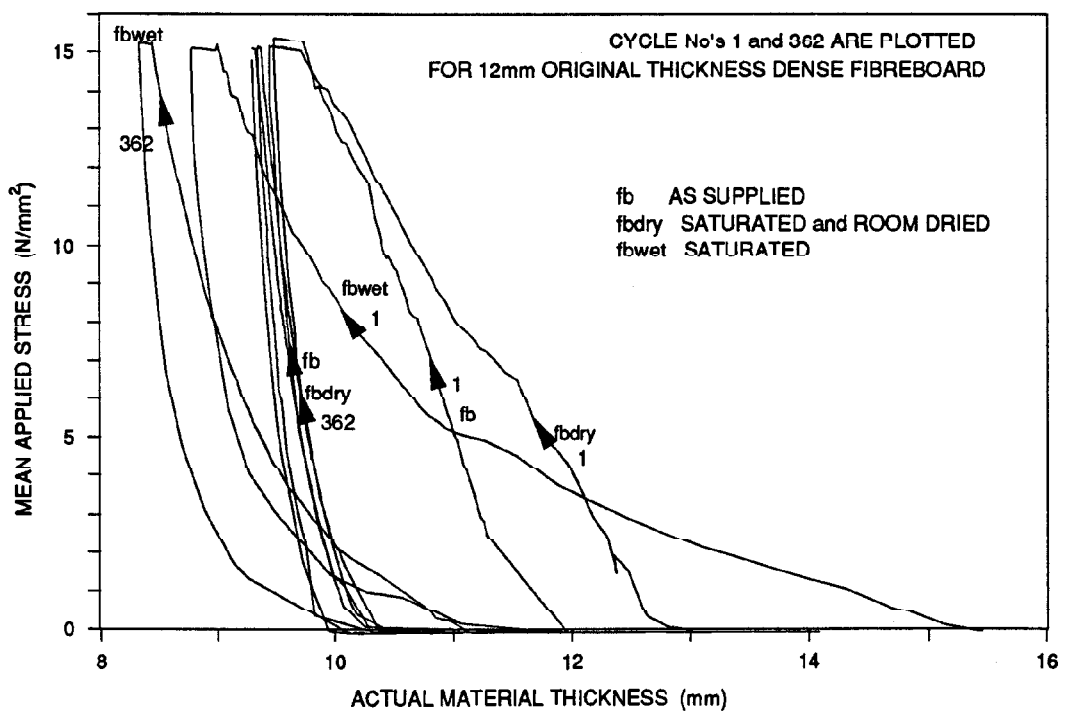
Figure 7.10 Effect of material condition on compression characteristics.

7.3.6 Differences between materials

The materials disregarded at the early stage of this test series were presented in Section 7.3; they were generally degrading when compressed. Comments in this section will be about dense fibreboard, chipboard and plywood.

Analysis of the results has been carried out on data from the last load cycle applied and the compression of the packing material has been analysed to provide data on jacking load capacity. These data have been based on assumed maximum allowable stresses and have been calculated for packing material on a 1200mm external diameter and 900mm internal diameter pipe. The author assumes that the full end area of the pipe is used for load transfer and are presented in Figure 7.11 and Figure 7.12 by comparing stress distributions for various angular deflections between pipes and relating these to total jacking loads. It can be seen that as joint deflections increase so load is rapidly concentrated onto a small area of the end of the pipe and hence results in reductions in jacking load capacity. Distribution of stresses on the end of a pipe is the same for a given distance from the edge of the pipe irrespective of pipe diameter, but increased end area results in larger jacking loads being acceptable.

Consideration of joint profiles and rebated packing material is presented in Chapter 9. It takes into account the pipes' elasticity as this will increase the end area available for load transfer.

At this stage it can be commented that dense fibreboard gives greatest capacity for transmitting jacking forces between pipes and for distributing concentrations of stress. Saturated packing material is beneficial but perhaps not practicable. In general, water enhances the ability of a packing material to distribute load and the material is beneficial towards distribution of loads on pipe ends which are not square.

JACKING LOAD CAPACITY OF PACKING MATERIALS
ON MISALIGNED 900mm INTERNAL DIAMETER PIPES
WITH MAXIMUM ALLOWABLE STRESS OF 15 N/mm^2
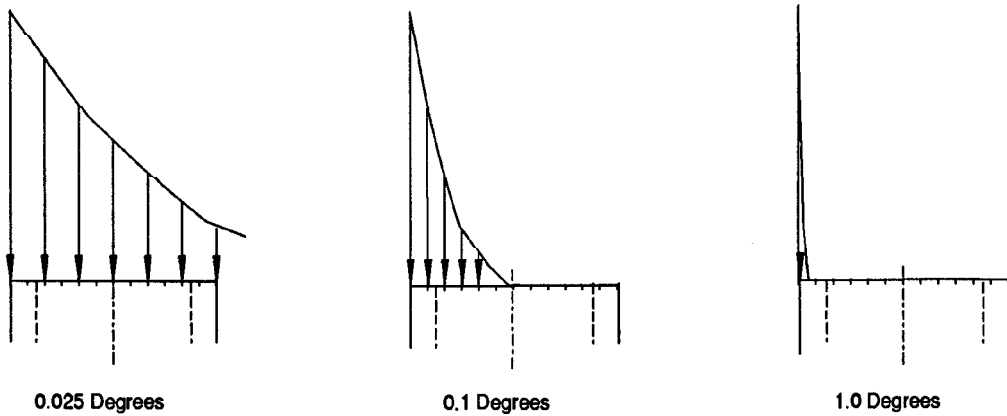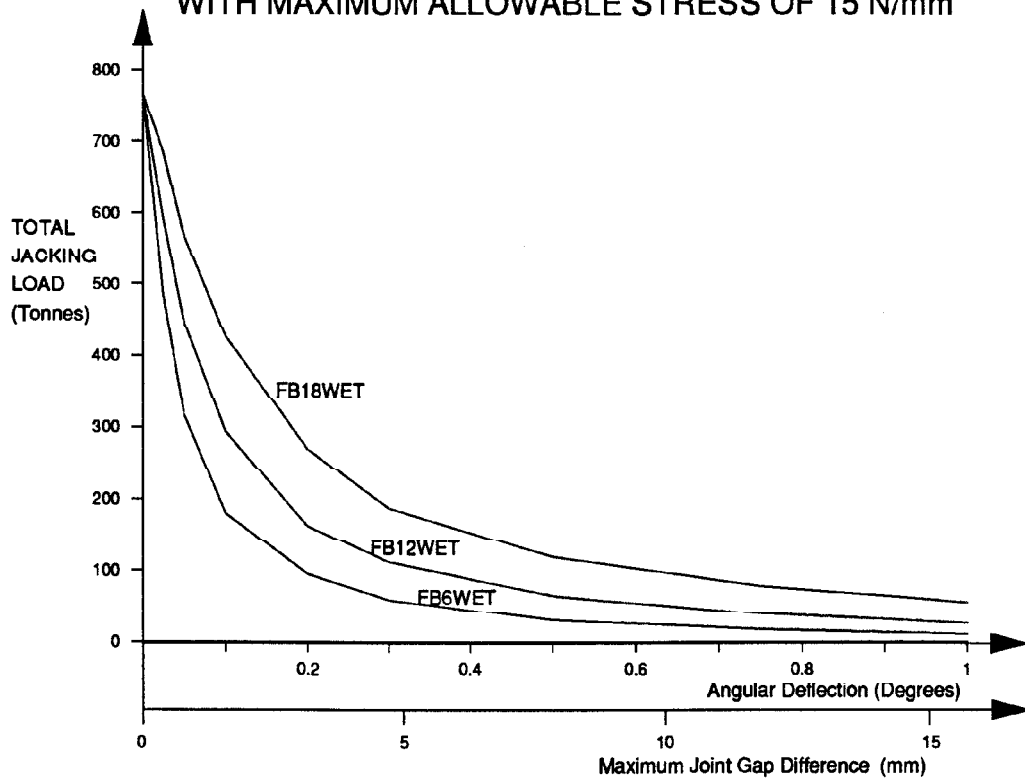
Distribution of Load at stated Angular Deflections

Figure 7.11 Jacking load capacity of a 900mm internal diameter pipe.

Typical Stress Distribution on Pipe Ends
for various Angular Deflections between Pipes

ANGULAR DEFLECTION (Degrees)	PIPE INTERNAL DIAMETER		
	900 mm	1800 mm	
	Maximum Internal Joint Gap		
	Differential (mm)		(b-a)
0.0	0.0	0.0	0.0
0.025	0.4	0.8	0.8
0.05	0.8	1.6	1.6
0.1	1.6	3.1	3.1
0.2	3.1	6.3	6.3
0.3	4.7	9.4	9.4
0.5	7.8	15.7	15.7
0.75	11.8	23.6	23.6
1.0	15.7	31.4	31.4

Angular Deflection = 0.00

Maximum 15 N/mm² Stress

Stress N/mm²

Position x (mm)
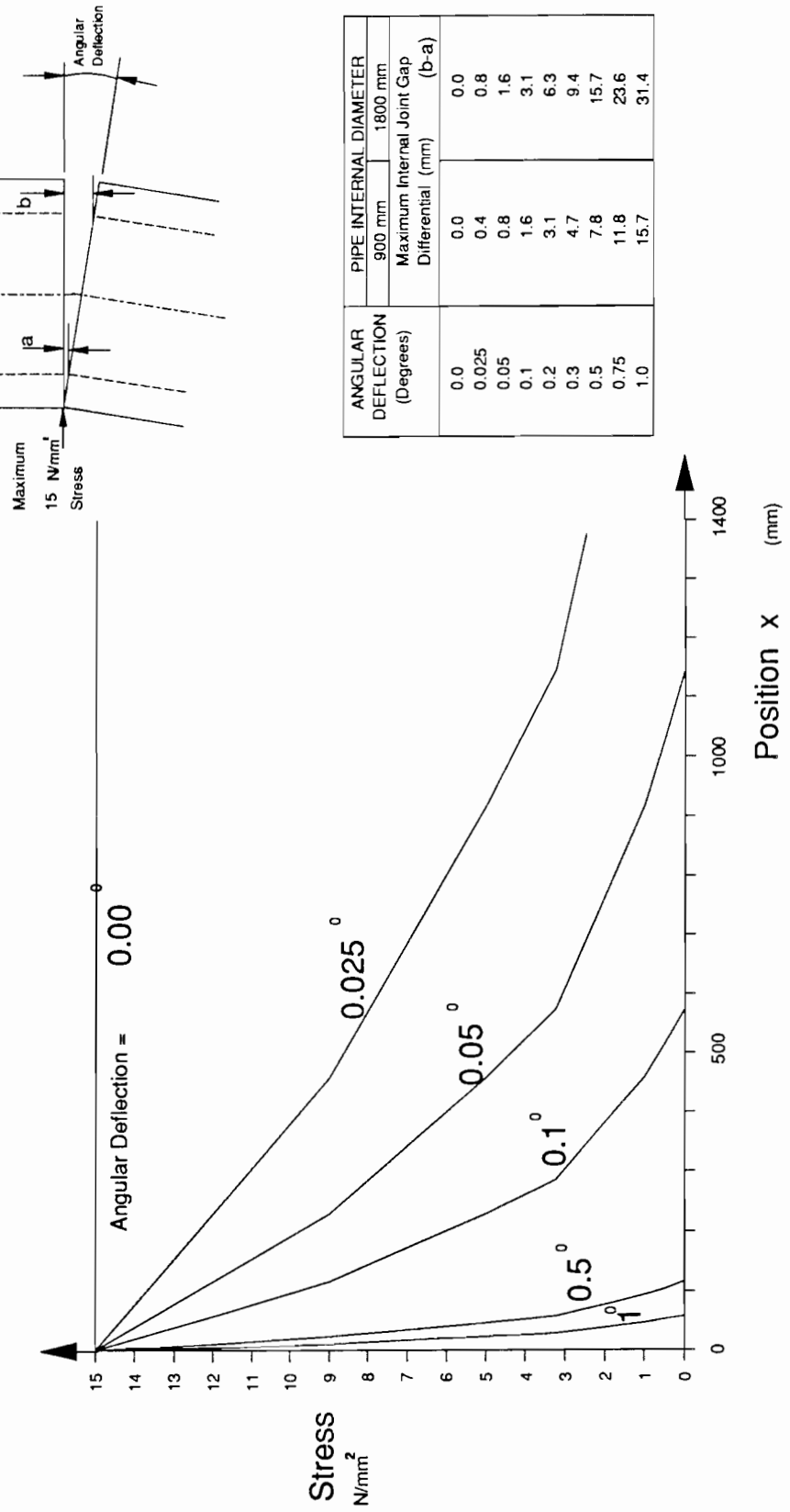
Figure 7.12 Stress distribution for various angular deflections.

Effects of packing material properties on deflected pipe joints should be related to deflections measured relative to the pipe end squareness. This gives the best indication of the magnitude of joint gap the packing material must bridge in order to transfer load. Squareness of the pipe end is thus a very important factor in considering a pipe's jacking capacity. It should be noted that pipes complying to end squareness tolerances of the British Standard could have a joint gap of up to 8mm on a 900mm internal diameter pipe. This equates to a deflection of 0.5 degrees even before pipes are deflected relative to each other. The British Standard also allows for pipe squareness to be 4mm across the wall thickness as shown in Figure 7.13.

DIMENSIONS ARE APPLICABLE
TO A 900mm INTERNAL DIAMETER PIPE

± 4mm SQUARENESS
TOLERANCE

± 4mm TOLERANCE CAN
BE INCLINED IN
EITHER DIRECTION

4mm SQUARENESS
TOLERANCE
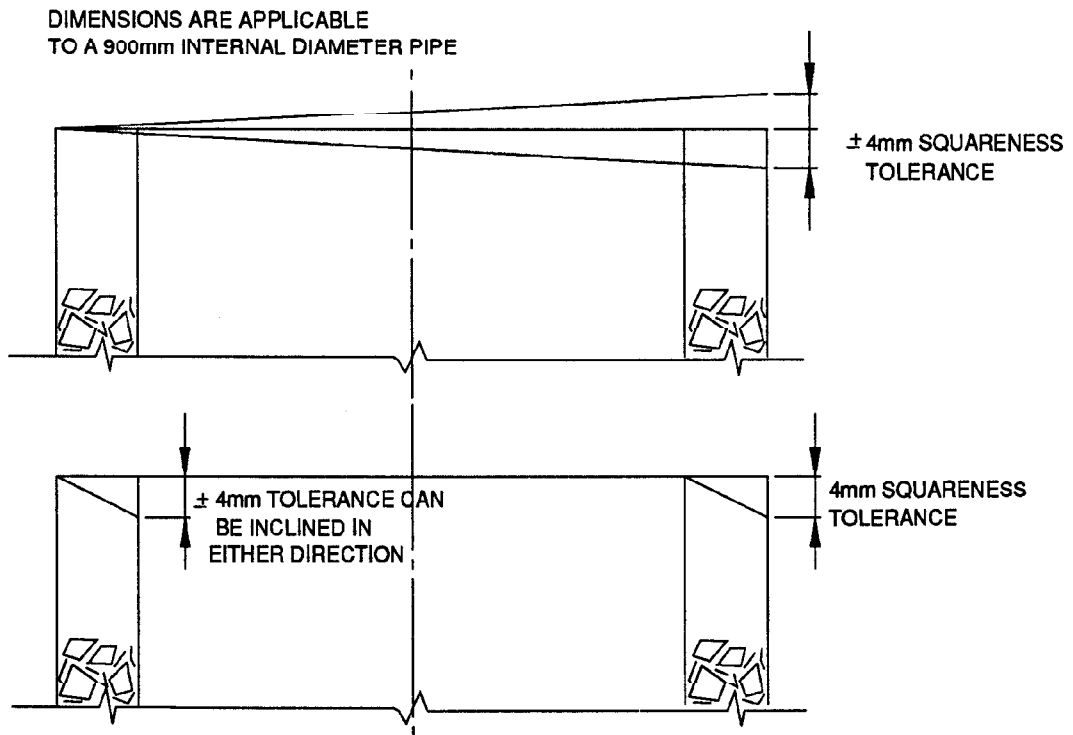
PICTORIAL REPRESENTATION OF BRITISH STANDARD SQUARENESS
TOLERANCES AND HOW IT IS POSSIBLE FOR THEM TO MAGNIFY
DEFLECTION ANGLES BETWEEN CONSECUTIVE PIPES

Figure 7.13 Conflict between British Standard squareness tolerances.

Materials chosen to best suit these compressive requirements have been listed in Table 7.2 with the most compressible, dense fibreboards, appearing at the top of the table. The table is calculated with all materials allowed the same maximum stress and lists materials in order of their ability to transmit axial load with a deflection of 0.2 degrees at the joint. Almost the same order would appear in the table independent of stress level or deflection angle.

MATERIAL	LOAD CAPACITY OF PACKING MATERIAL (Tonnes)								
	ANGULAR DEFLECTION (Degrees)								
	0	0.025	0.05	0.1	0.2	0.3	0.5	0.75	1
* FB1850	2572	1738	1189	689	374	245	129	71	47
* CB1850	2572	1615	1042	588	310	196	99	53	35
FB18WET	766	685	567	426	269	187	119	78	56
* FB1250	2572	1523	938	523	266	162	79	42	28
CB18WET	766	629	516	384	239	166	106	68	49
CVBWET	766	636	522	393	256	177	112	75	54
FB12WET	766	627	479	317	177	123	72	44	29
* PLY1850	2572	1371	820	451	222	132	63	33	22
PLY18WET	766	603	462	307	169	118	69	41	27
FB12W	766	595	447	295	163	113	65	39	26
PLY12WET	766	586	444	293	162	112	65	39	26
FB12WET3	766	577	439	291	161	111	66	39	26
FB12WET	766	575	437	290	160	111	65	39	26
CB12WET	766	577	434	285	157	109	63	38	25
* PLY650	2572	974	547	280	114	62	29	15	10
CVBCHIP	766	515	359	216	116	76	41	23	15
FB1815	766	545	380	214	118	77	40	21	14
CVBDRY	766	515	357	208	113	75	40	23	14
* FB650	2572	912	506	257	108	60	28	14	9
CVBCHIP2	766	511	356	209	113	75	41	22	14
CB18DRY	766	494	328	187	99	64	32	17	11
FB6W	766	474	319	183	97	63	33	18	12
FB6WET	766	486	317	180	95	60	31	17	11
CB1815	766	482	305	170	90	55	27	14	9
PLY18DRY	766	415	263	143	72	44	22	11	7
PLY1815	766	421	258	142	71	44	20	11	7
CB12DRY	766	409	248	136	68	40	19	10	7
FB12DRY	766	428	247	138	66	38	18	9	6
FB1215	766	407	234	130	63	36	17	9	6
CB1215	766	388	221	122	58	33	15	8	5
PLY6WET	766	381	215	119	56	32	15	8	5
FB6DRY	766	324	180	95	40	22	10	5	3
FB615	766	316	175	91	39	21	9	5	3
PLY12DRY	766	307	170	89	39	22	10	5	3
SOFTWET	766	272	149	76	32	18	8	4	2
PLY6DRY	766	238	132	64	24	13	6	3	2
SOFTDRY	766	229	124	61	24	13	6	3	2
PLY615	766	229	127	61	23	12	5	3	2

NOTE : All materials tested to maximum stress level of 15 N/mm^2 unless marked with "*". Those marked with the asterisk were tested to 50 N/mm^2.
All data are calculated for a 900mm internal diameter, 1200mm external diameter pipe assuming full end area contact.

KEY

MATERIAL TYPE

FB – Doneo Fibrobord
CB = Chipboard
PLY = Plywood
SB = Softboard

APPLIED STRESS
(N/mm^2)

FB | 18 | 50 | WET
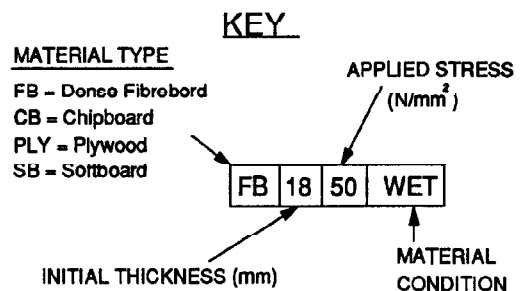
INITIAL THICKNESS (mm)

MATERIAL CONDITION

Table 7.2 Comparison of load capacities of various packing materials.

7.3.7 Strain gauge readings

Mounting positions of electrical resistance strain gauge rosettes have been shown in Figure 7.1. Analysis has been carried out to find principal strain magnitudes and directions and concrete stresses can be assessed below the elastic limit of the concrete. Figure 7.14 presents data plotting measured maximum and minimum principal concrete stresses compared to stress applied by the hydraulic jack. The maximum compressive concrete stresses were always found to be measured in alignment with the direction of load application immediately beneath the packing material. Tensile stresses are a potential problem with a concrete pipe; the magnitude of tensile stress measured during tests on dense fibreboard did not exceed the tensile strength of the concrete.
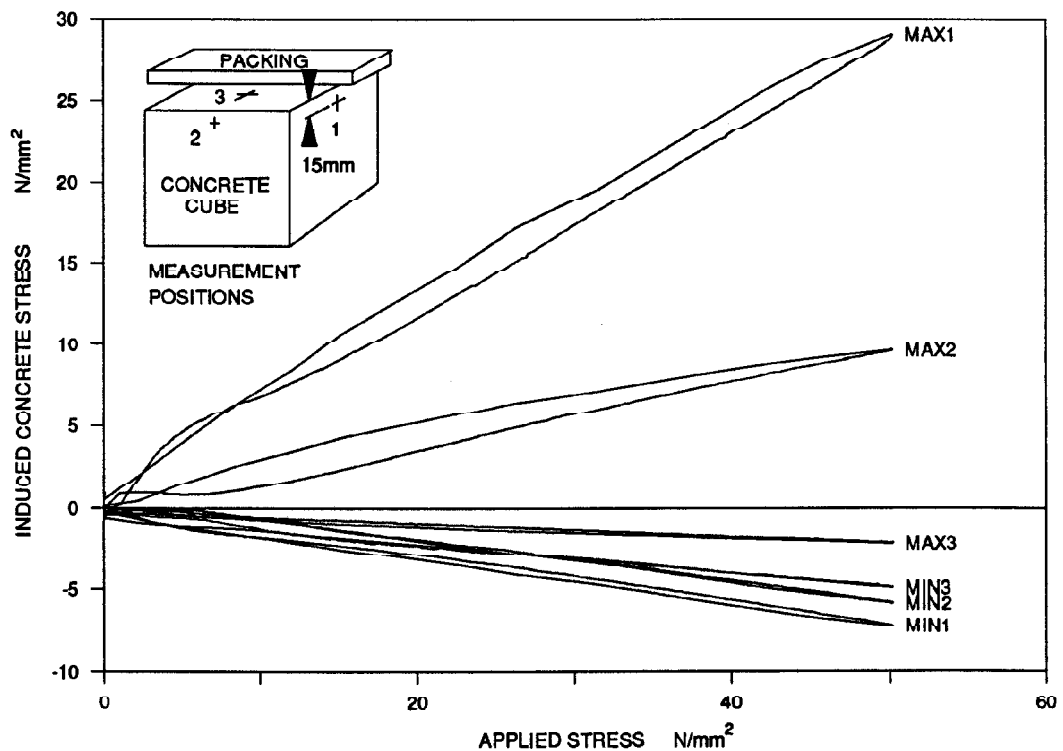
Figure 7.14 Induced stresses in the concrete for 18mm dense fibreboard.

7.3.8 Tensile strain distribution

A series of tests was conducted to assess the tensile strain distribution in the concrete. Positioning of the packing material was varied so that the effect of its position relative to the edge of the concrete could be assessed. Arrangement of instrumentation and some data obtained are presented in Figure 7.15 and Figure 7.16.

Figure 7.15 Typical distribution of tensile strains induced on concrete cubes.

As packing material was brought closer to the edge of the concrete, tensile strain readings peaked at a distance of 30mm from the concrete/packing interface. Theory on distances to

this peak strain suggest it is related to the breadth of the packing material used, Williams (1979), by dividing the packing width by the square root of 2. This calculates to 28mm which agrees closely with the experimental results.
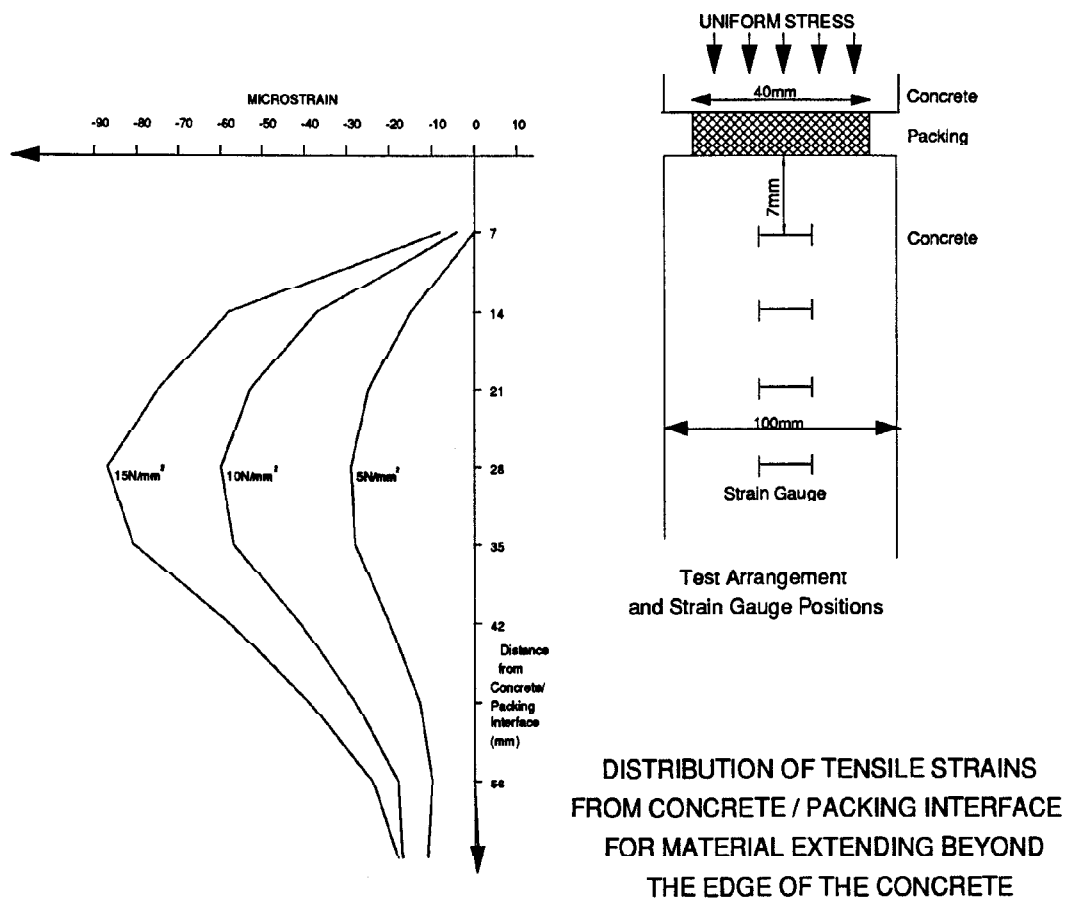
7.4 Stress distribution at joints

An accurate full analysis of stress distribution at pipe joints needs to take into consideration concrete elasticity, joint profile and packing material type and condition. Analysis has been carried out for in wall and steel collar joints with packing material placed in typical positions. The analysis and results are presented in Chapter 9.

In general it can be seen how jacking load capacity increases as the joint deflection between pipes becomes less. Stress is very concentrated when deflection angles are large.

A summary of packing material test results would suggest that:-

1   Thick packing materials are most beneficial.

2   Deflection angles greater than 0.20^0 combined with high axial loads are to be avoided; angles are to be measured with load applied and do not allow for any pipe elasticity.

3   Wet materials improve load transfer capabilities by up to three times.

4   Cyclic loading conditions need to be considered due to permanent packing material compression.
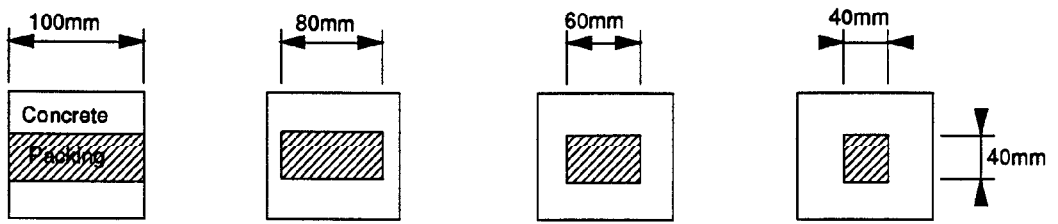
Cross Sections on X-X

Elevation
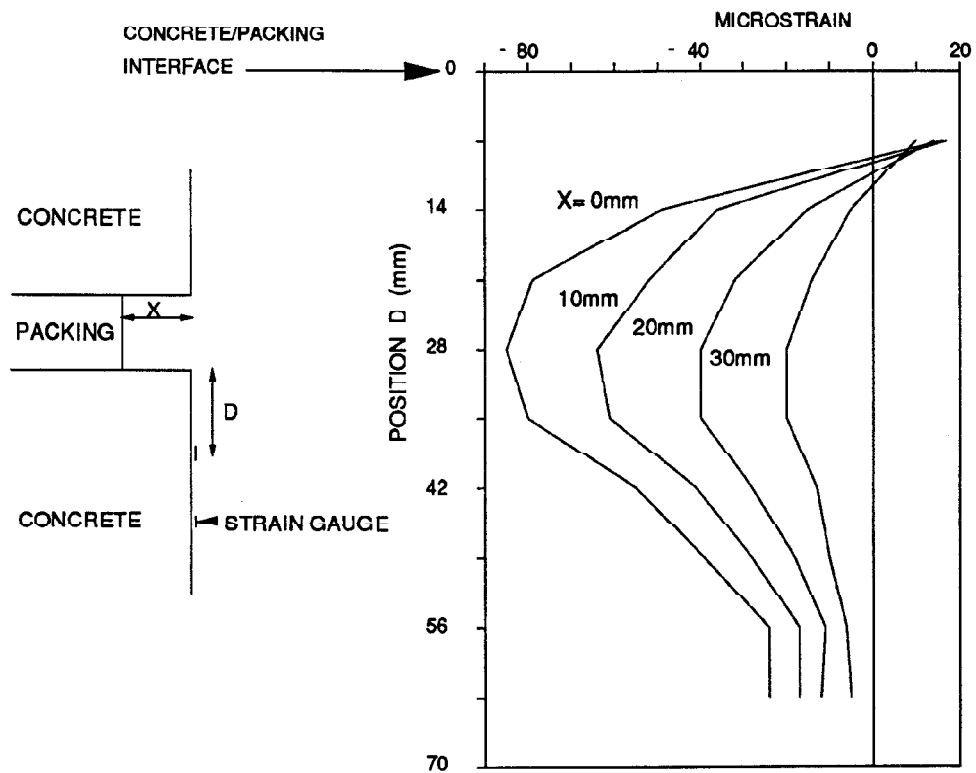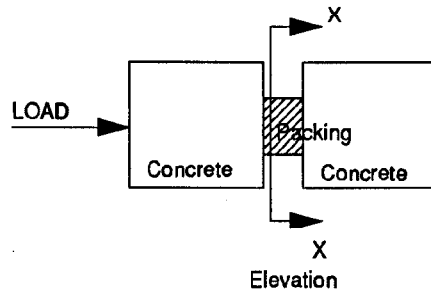
DISTRIBUTION OF TENSILE STRAIN READINGS
FOR JOINT PACKING MATERIAL REBATED FROM CONCRETE FACE
WITH AN APPLIED STRESS OF 15N/mm^2

Figure 7.16 Effect of position of packing material.

7.5 Profiled packing material

Samples of a polymer packing material were obtained and tested. The material was being supplied to a development project in Yorkshire, managed by ARC Concrete Limited, Decon Engineering Company Limited and Yorkshire Water Authority. The packings were produced by injection moulding and were profiled to provide initial contact in the centre of the wall thickness of the pipe as shown in Figure 7.17. Measurements of the cross-section of the material indicated a radius of 87.5mm for each of its surfaces. Analysis of the compression under the loading arrangement illustrated in Figure 7.1 indicated the contact widths shown in Table 7.3.
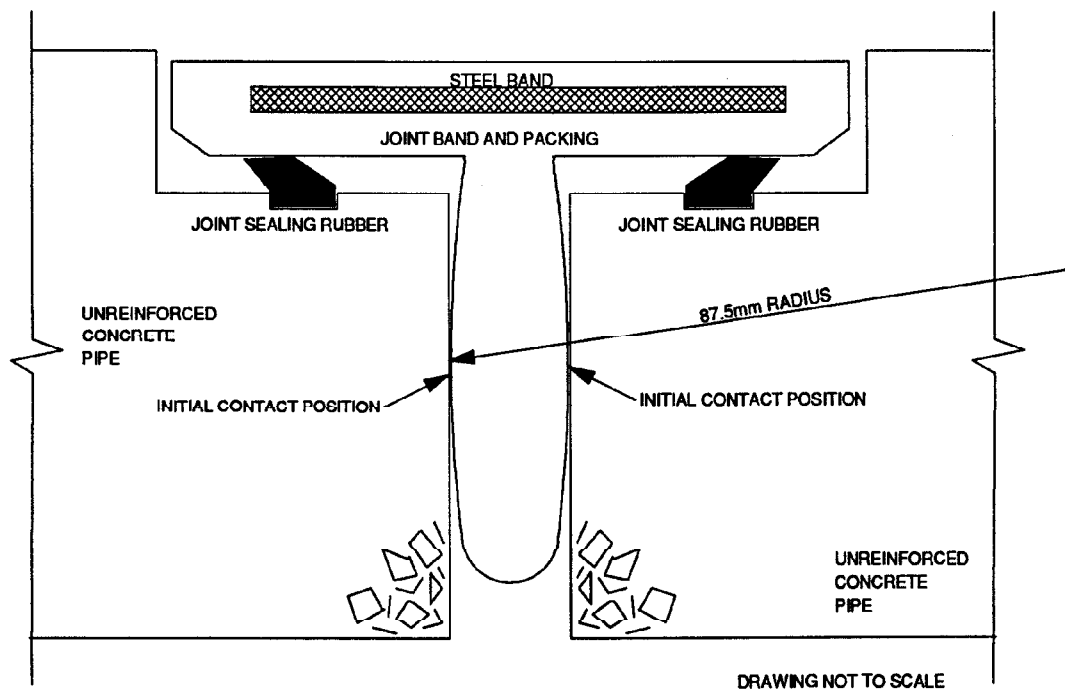
Figure 7.17 Profiled joint collar and packing material.

Results from the tests on this profiled packing material highlight again the importance of assessing the material under cyclic loading conditions. Whilst the material was initially

Material compression from start of current load cycle (mm)	Contact width (mm)	Mean stress during first cycle (N/mm^2)	Mean stress during 142nd cycle (N/mm^2)
0	0	0	0
0.5	20	11.7	
0.73	24	19.5	
0.77	25	21.6	5.2
0.85	26	23.4	8.6
0.89	26.4		12.4
0.95	27		16.1
1.0	27.5		19.5
1.05	28		21.5

Table 7.3 Contact widths for profiled packing material.

87.5mm radius on its surface, 140 load cycles of 200kN on a 100mm length permanently deformed the material and it then had a surface radius of 219mm. This affects the stress distribution across the packing material width and is studied in more detail in Section 9.8.

CHAPTER 8

MOVING PIPES

8.1 Outline

A series of tests was planned in which the model pipes would be pushed through the sand filled test chamber. Previous tests in the chamber had been on static pipes and a comparison was required for the prototype installation methods when pipes would be moving through the soil. Pipes were manufactured for this test series as follows:-

> unreinforced plain end
>
> reinforced plain end
>
> unreinforced in wall joint
>
> reinforced in wall joint
>
> reinforced steel collar joint

Five pipes were required for each test and both thick and thin walled pipes were manufactured.

Instrumentation of the tests was limited to measurements of total soil boundary stresses, jacking load, reaction load, longitudinal pipe movement and time. It was hoped to develop relationships between jacking load and sand stresses and to investigate any particular problems with jacking pipes through the soil chamber. The author hoped that some comments

could be made on pipe to soil interaction and development of friction angles at the pipes' external surface even though the boundaries of the chamber would interfere. It was planned to push all pipes in straight lines and make no allowance for deflected pipes.

8.2 Test procedure

Frictional resistance as pipes passed through the ports in the chamber wall needed to be calibrated before pipes were tested in the sand filled chamber. This was done by pushing pipes through the chamber while it was in the test position but without any sand in the chamber. The top of the chamber was removed and pipes were supported on a straight edge as they passed through the air filled chamber. The straight edge maintained pipe alignment and did not allow self weight of the pipes to cause misalignment at the centre of the pipe string and added very little to the jacking resistance. Data were recorded as pipes were pushed through the air filled chamber monitoring jacking load and longitudinal movement of the pipe string. This enabled the frictional resistance through both chamber ports to be related to the position of the pipe string. The procedure for adding and removing pipes as they passed through the chamber is summarised in Figure 8.1. Once pipes had passed through the chamber they could be reused so long as there were no visible signs of damage.

Once the ports had been calibrated the pipes remained in position whilst the chamber was rotated, the end plate removed and sand poured around the pipes. The chamber was rotated to the test position and boundary stresses adjusted as required. Pipes were pushed through the sand filled chamber and data recorded as previously but with the addition of four total pressure cells monitoring sand pressure at the internal surface of the chamber wall. All the pressure cells were mounted in the end wall of the chamber on a radial from the pipe centreline as shown in Figure 8.2 and were mounted in the end wall furthest from the jack pushing the pipes. They could monitor pressures as the sand interacted with the pipes and as the sand was pushed towards the end wall. It was necessary to reduce the recorded jacking load to
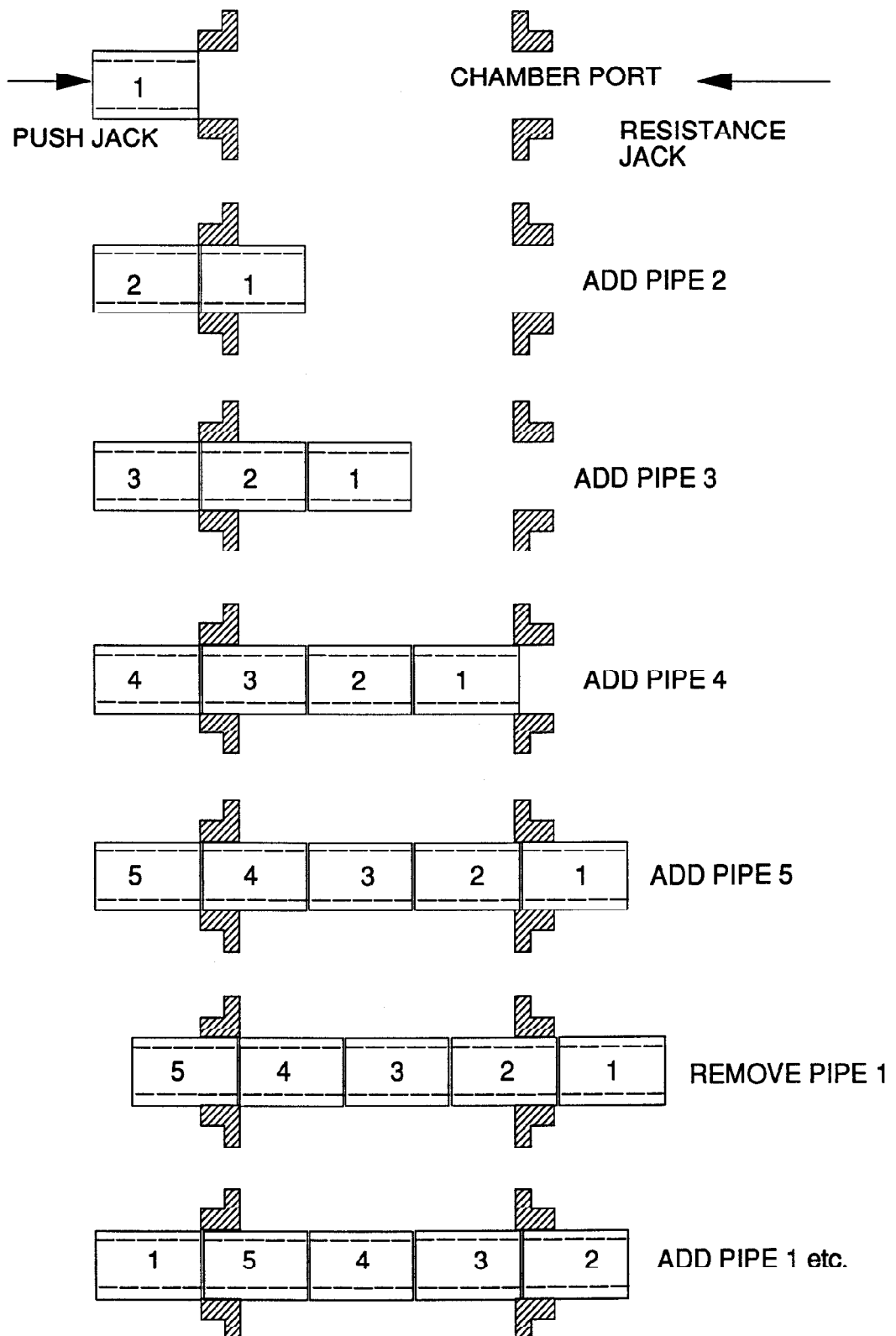
Figure 8.1 Sequence of pushing pipes through chamber.

allow for frictional resistance as the pipes passed through the chamber ports. This could be done by relating the pipe string's position to the previously recorded data for pushing the pipes through the empty chamber.
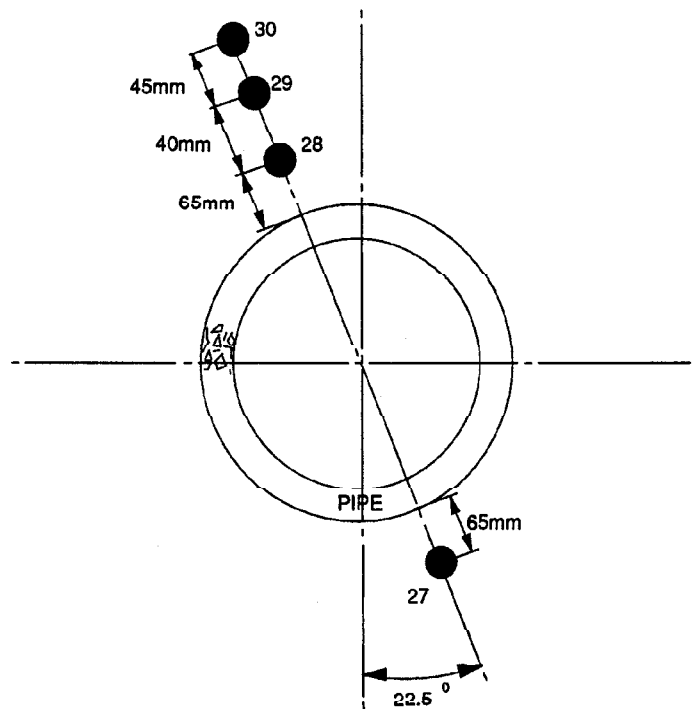

Figure 8.2 Position of total pressure cells.

Tests were carried out with different induced sand stresses and for various pipe types; a summary of tests is presented below:-

Test No.	Pipe Type	Boundary stress (vertical, horizontal) (kPa)
1	unreinforced; thick walled; in wall joint	0,0
2	reinforced; thin walled; in wall joint	0,0 variable resistance on second jack
3	unreinforced; thin walled; in wall joint	0,0; 40,40; 110,40; 160,55; 200,73; 0,0
4	reinforced; thin walled; plain end	0,0; 20,20; 50,20; 50,35; 75,35; 75,50; 75,75; 110,75; 150,75; 150,100; 200,100; 0,0
5	reinforced; thick walled; steel collar	0,0
6	reinforced; thin walled; steel collar	0,0
7	reinforced; thick walled; in wall joint	0,0

In addition to the jacking ram, a second ram was used to provide end resistance to movement of the pipe string rather than pushing with no end resistance. This was used to model pipes at various positions along a prototype pipejack and to take into account the different possible loading conditions. Load on the resistance jack was monitored using a pressure cell mounted in the hydraulic circuit; the pressure cell had previously been calibrated to relate oil pressure and ram position to the load resistance of the jack.

8.3 Results

Several problems were encountered while conducting this test series which are stated here and need to be taken into account when interpreting the test results.

The calculations of shear stresses, normal stresses and friction angles may have been unreliable due to error in measurement of normal stress caused by sand arching and due to sand grains caught between the pipes and ports in the chamber.

During the test crushed sand and abraded concrete collected near the exit port and was drawn into the tolerance gap between the pipe and chamber port as the pipe was moved. This caused the frictional resistance at the port to change during the test process and an attempt at correction was made by comparing final jacking forces to those at the start of the test.

Abrasion of the pipe surface (Plate 8.1) as it passed through the ports and the sand resulted in a reduction of pipe external diameter which in turn led to less frictional resistance at the ports but a larger gap for dust to enter. It proved difficult to jack unreinforced pipes without causing longitudinal cracking. This was assessed to be due to the high jacking forces required to overcome frictional resistance at the ports.

Pipes with steel collar joints proved almost impossible to push into the ports due to the close tolerance fit of the steel collar. When the steel collar met with the port wall any misalignment between the two caused the collar to deflect and forced the collar back along the pipe, eventually distorting the steel collar. Tests on the steel collared pipes were abandoned as even when the pipes were entering the chamber aligned, it was impossible to inspect the pipe as it entered the exit port.

One interesting point which came from the tests was the measure of frictional resistance as the pipes passed through the ports. This proved to be a very satisfactory way of testing the pipe's external diameter tolerance. This was particularly noticeable in two instances; often model pipes would have a slightly larger diameter one end and therefore encountered higher port entry resistance. It was also found that thick walled pipes had a slightly larger diameter than thin walled pipes. This is explained by the difference in the shrinkage of the pipes during curing due to the shorter hydration path.

Plate 8.1 A view of the abrasion that occurred during moving tests.
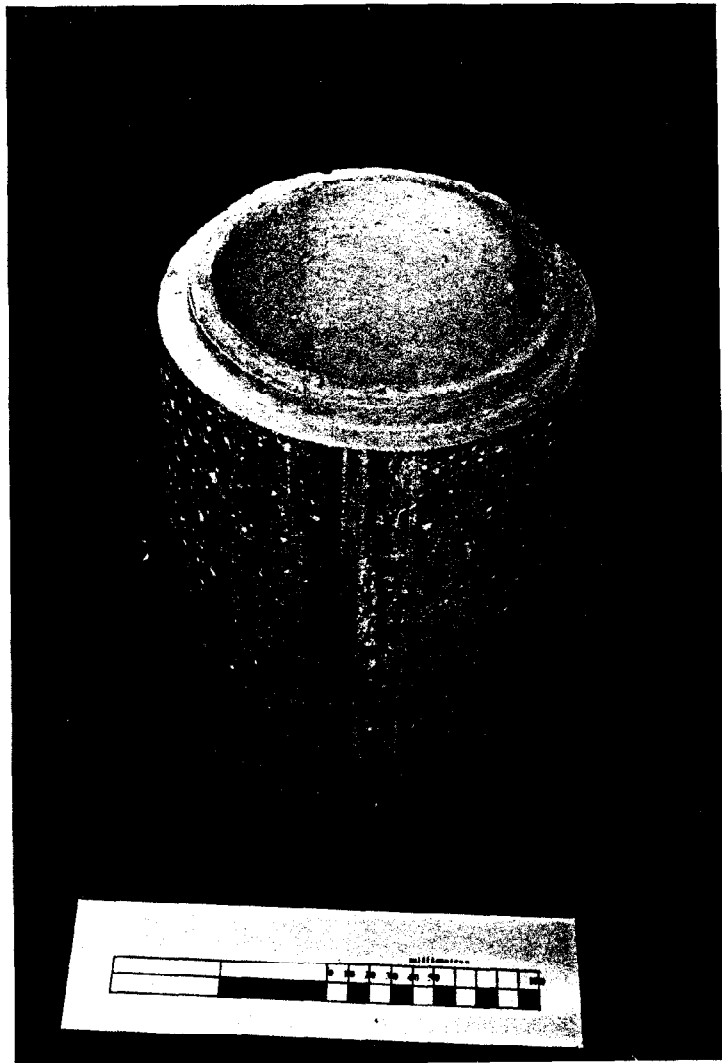
8.3.1 Resistance to jacking

The main result from this test series was a measure of friction forces at the pipe/soil interface. Some typical results without sand are first presented in Figure 8.3 where it can be seen how results can be corrected to allow for frictional resistance at the ports.
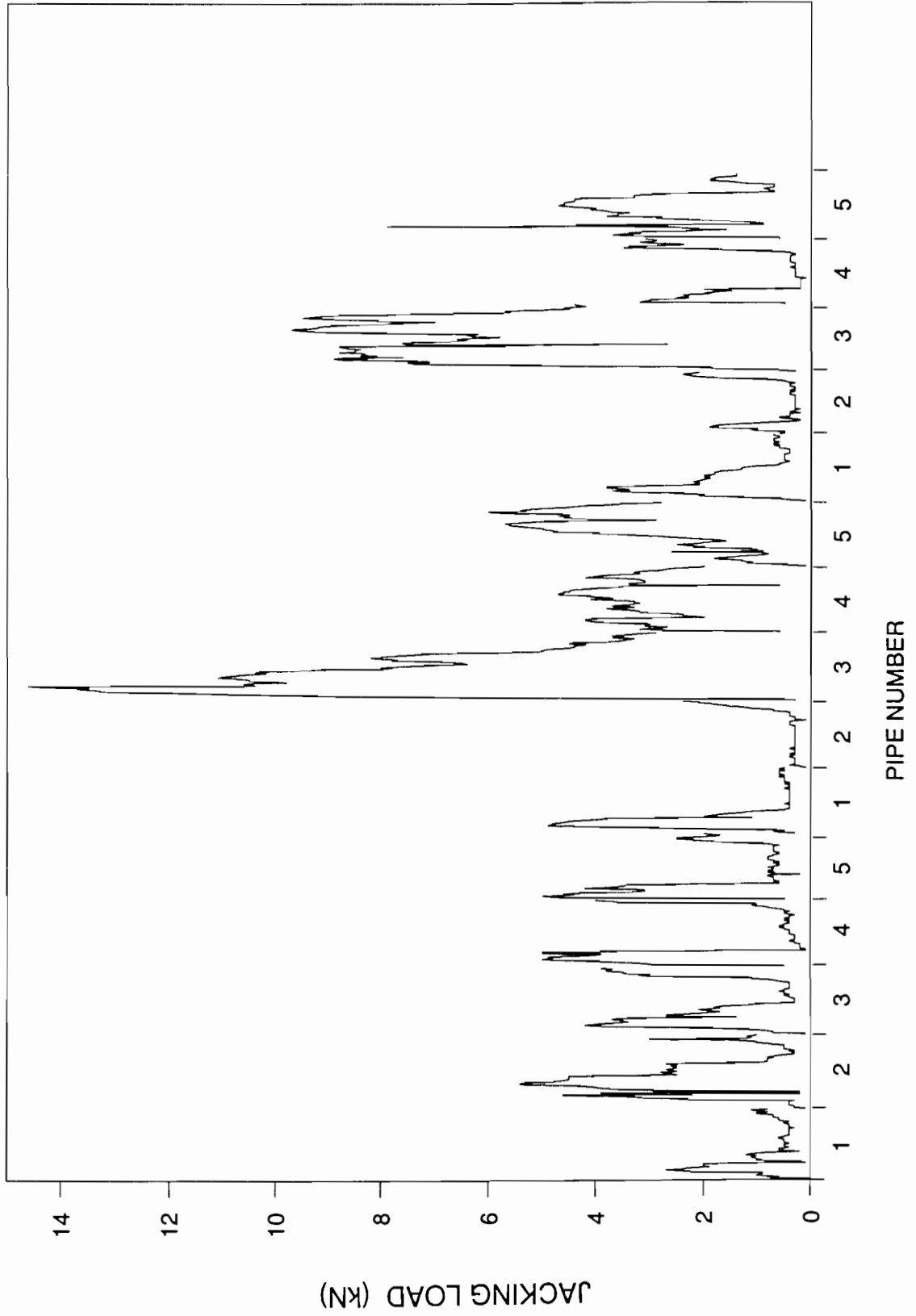
Figure 8.3   Resistance to jacking pipes through ports only.

Two of the tests were carried out to establish jacking resistance changes as the boundary stresses were increased. Results from these tests are presented in Figure 8.4 where the increase in total jacking resistance as total soil stresses are increased can be seen. The data are re-presented in Figure 8.5 by plotting mean sand stress against corrected jacking load. From this graph a linear relationship can be seen:- as boundary stresses increase so jacking forces are higher. It can be noted that the resistances encountered in the chamber are much higher than those experienced in practice. A typical frictional resistance in this type of sand at full scale would be expected to be $40kN/m^2$. Analysis of the data results in frictional resistance values of between 40 and $240kN/m^2$ of pipe external surface area. The high values are possibly due to dense sand surrounding the pipe in the laboratory sand chamber where as in practice pipes would be surrounded by loose sand which has fallen into the overbreak; this is discussed further in Section 9.5.

Stresses measured in the ground will be different from those in the chamber due to boundary conditions, arching, overbreak and pore pressure.
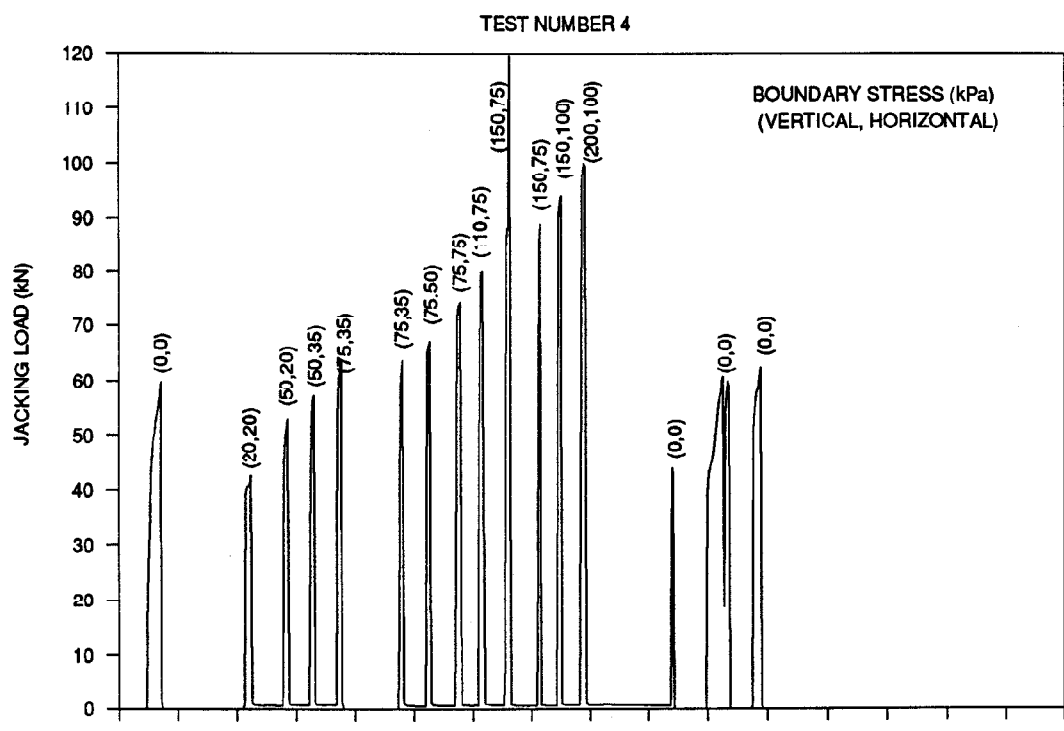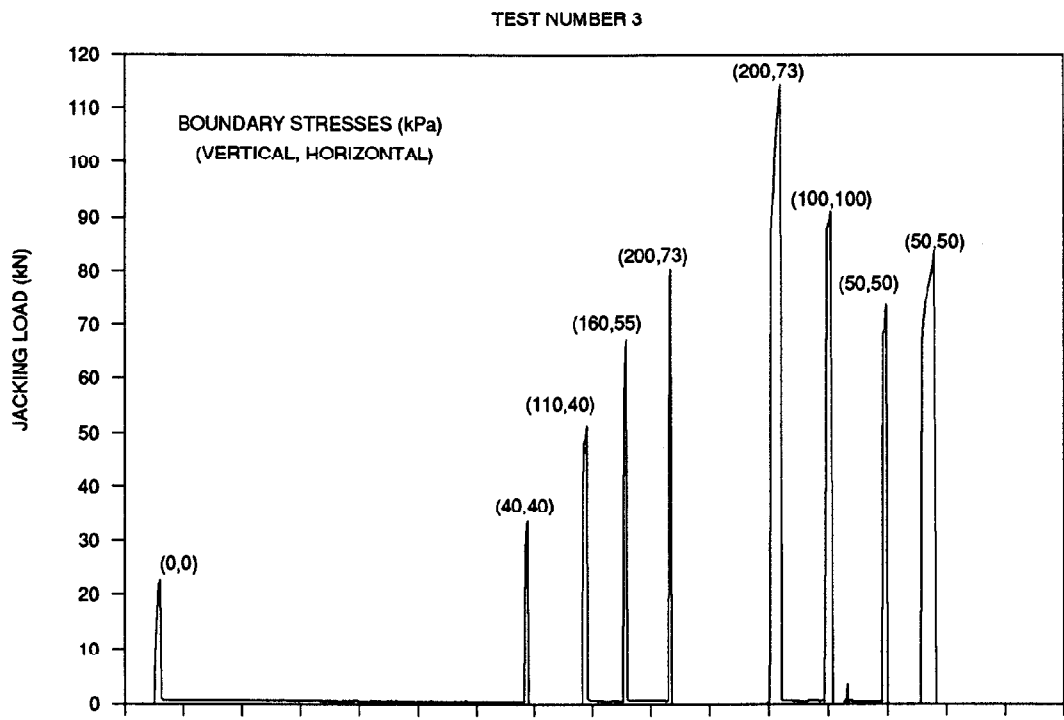
Figure 8.4 Change in jacking force as boundary stress is varied.
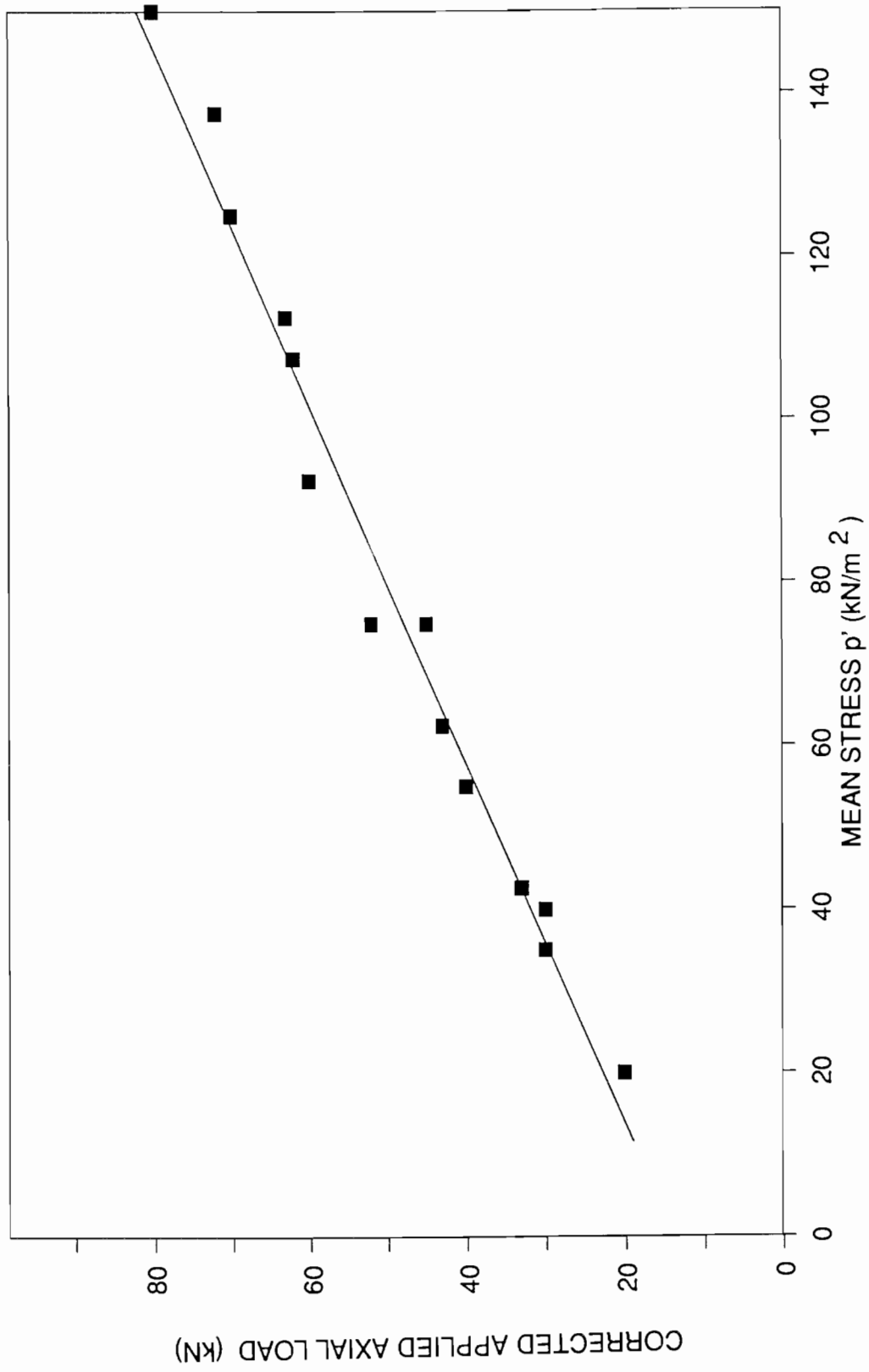
Figure 8.5 Relationship between jacking load and mean sand stress.

The reaction jack was used in one test only. The effect on the jacking load required to move the pipe string can be seen in Figure 8.6 as causing an increase in jacking force equal to the resistance applied. Note can also be taken of the increasing jacking resistance as the test progresses due to the ingress of fines in between the pipe and exit port.
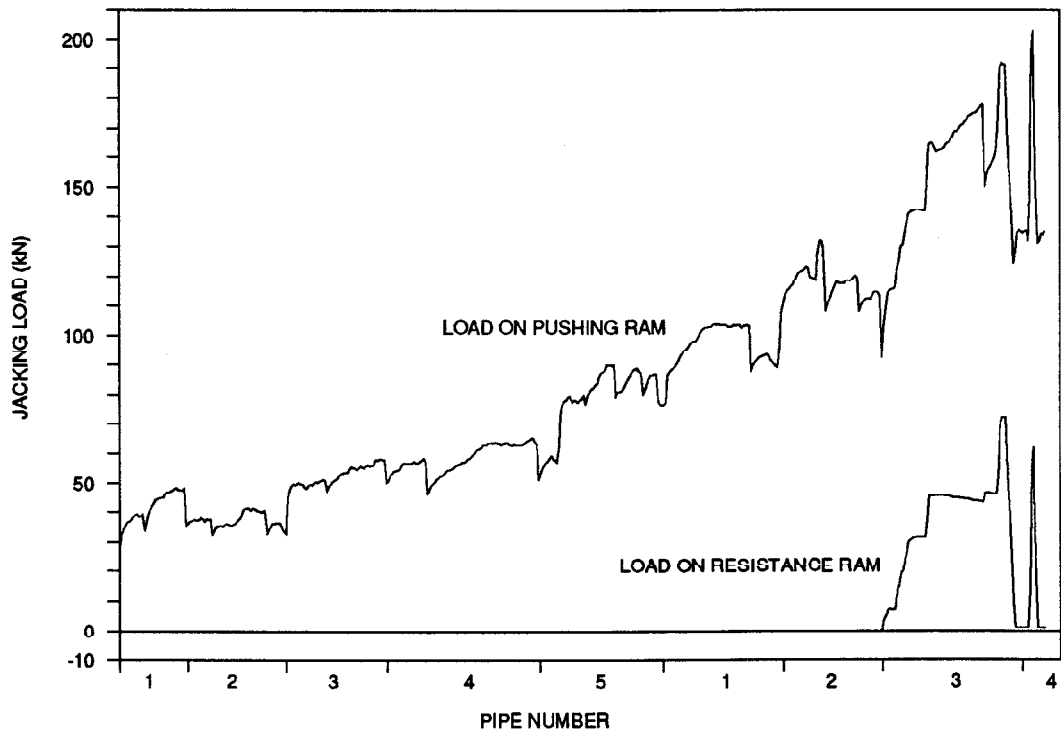
Figure 8.6 Effect of adding jacking resistance to movement.

8.3.2 Boundary pressures

Total pressure cells were mounted with their measuring diaphragms flush with the internal surface of the chamber wall towards which the pipes were being pushed. They were arranged on a radius away from the pipe as depicted in Figure 8.2. Data are represented in Figure 8.7 which plots the distribution of total pressure on the end wall as measured by the pressure cells. The influence of pipe movement can be seen as the data readings on cell number 28

increase significantly. The distribution shows how the top boundary and pipe movement influence the readings. It is believed in practice that there is a tendency for soil to drag and move as the pipe progresses. It can be seen in the pressure distribution plots how a zone of sand close to the top of the pipe was being pushed against the end wall of the chamber. Readings on pressure cell 27 under the pipe string never returned to their original values after boundary stresses were released. It is difficult to make any further valued comment or conclusions due to the closeness of the boundaries and confinement of the chamber. Some further analysis is presented in Chapter 9.
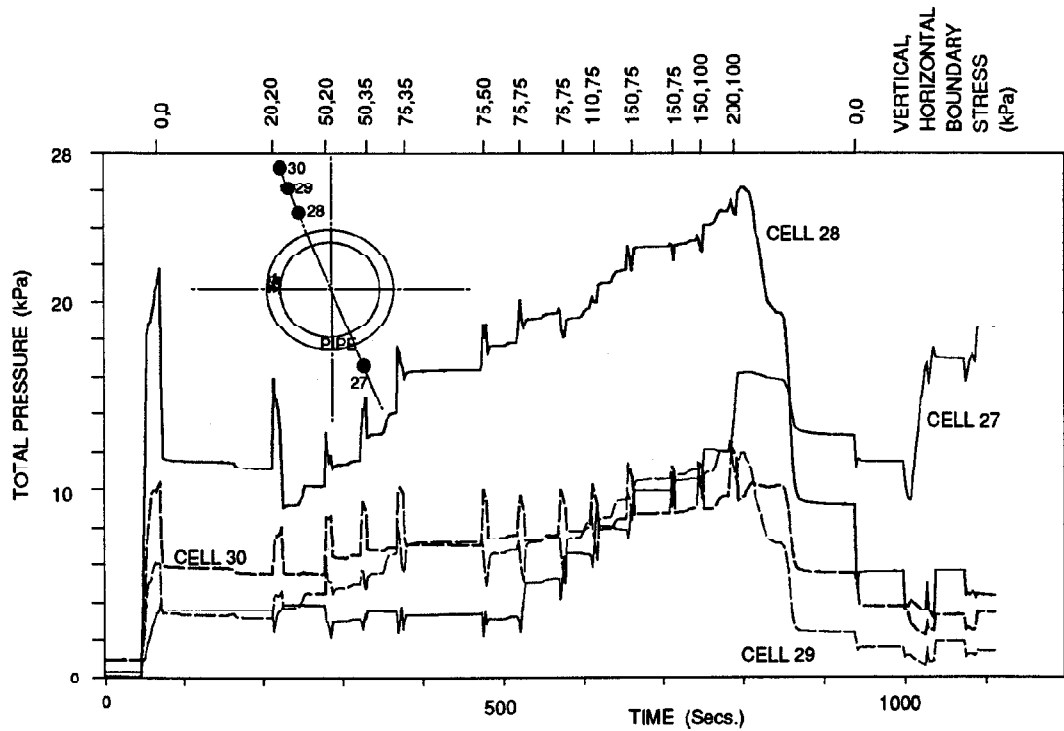
Figure 8.7 Total pressure cells, distribution of readings.

8.4 Summary

Some general comments can be concluded from the test series:-

1   Frictional resistances to jacking in the test chamber appeared unrealistically high.

2   Pushing pipes through the ports while monitoring axial load proved a very good measure of a pipes' external diameter tolerance.

3   Interaction between the pipe wall and sand appeared to result in a zone of dragging sand approximately one quarter of the pipe radius away from the external wall.

4   Soil stress level directly affected the frictional resistance to jacking.

CHAPTER 9

ANALYSIS AND DISCUSSION

9.1 Introduction

The results obtained from the four test series, chamber tests, misalignment tests, packing tests and moving pipe tests are discussed. Further analysis is carried out on some of the data obtained and the implications of the research for pipejacking are presented. A comparison with data from full-scale pipejacks is made in order to understand some of the pipe behaviours witnessed during the testing programme.

9.2 Realignment during chamber tests

The angle of deflection between the two pipes being tested in the chamber compared with the applied axial load was presented in Figure 5.9. Since conducting this initial series of tests, studies were carried out on moving pipes in the soil chamber. Results from the moving pipe tests gave an indication of friction forces between the pipes and sand. These values can be used to correct the axial load recorded during the chamber tests which was measured outside the chamber to the load applied at the common pipe joint in the centre of the chamber. It is also of interest to investigate the affect of applied boundary stress on the rate of

realignment. The results of the chamber tests are presented in Figure 9.1 which take into account these corrections and plots the corrected load per unit of external surface area divided by the applied boundary stress against the measured joint deflection.

BOUNDARY STRESS		TEST No.
VERT. (kPa)	HORZ. (kPa)	
160	55	16,17
110	40	18,19
50	50	20,21
200	73	22,23
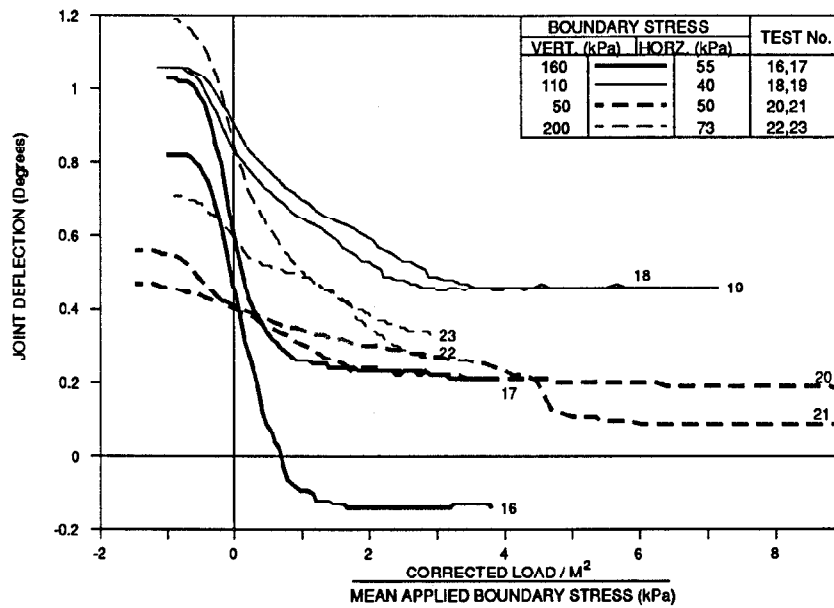
Figure 9.1 Changes in pipe alignment related to applied axial and soil stresses.

Two points of interest arise from this plot. Firstly, it appears that pipes were realigning themselves before load was applied at their common joint. This was possible but was not expected to be as prominent as shown in the graph and is probably due to the correction to axial load being too large. Secondly, the axial load applied to obtain alignment between the pipes does not appear to relate only to boundary stresses, as the positions when alignment occurs for different magnitudes of stress do not follow in order of increasing mean stress.

Results from pressure cell readings taken during testing indicated much lower stresses beneath the pipes than those applied at the flexible boundaries. It is possible to make an estimate of the distribution of stresses in the chamber by assuming a linear distribution of

vertical stress between the flexible boundary and the pressure cell. The data used for Figure 9.1 are presented in Figure 9.2 with this correction included together with some additional test results.

Results from the majority of the tests showed how the pipes never fully aligned themselves but maintained a deflection angle at their common joint due to the ingress of sand into the pipe joint. However, all the tests showed how the deflection angle between pipes stopped changing. All the tests indicated the occurrence of friction at the chamber ports as realignment did not take place immediately when measured axial load was applied which is represented by the initial straight section of each plotted curve.

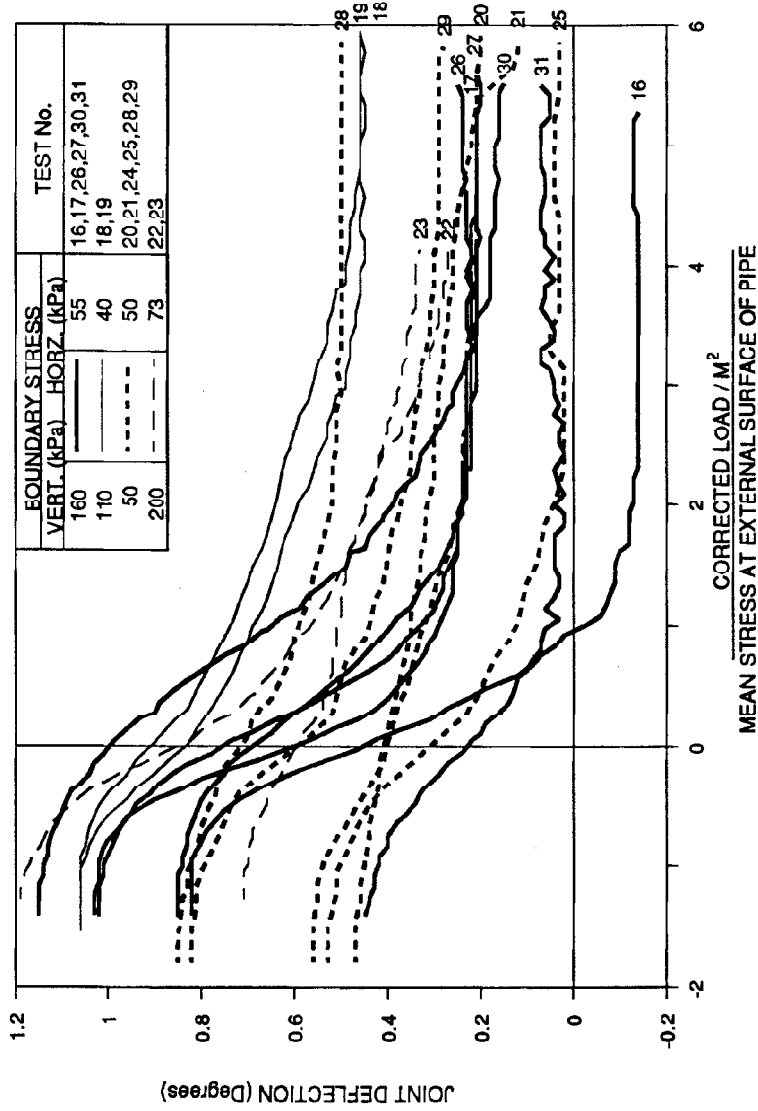**Figure 9.2** Changes in pipe alignment related to applied axial stress and soil stress on the pipe.

9.3 Changes of pipe alignment in practice

Changes in the alignment of pipes during jacking at full-scale can be examined by studying line and level records from pipejacks both during progress of the works and on completion of construction. Two examples are presented from pipejacks in ground conditions encountering either chalk or silts and gravels. Records were kept of the first pipe position as the pipejack advanced and of the pipeline position on completion of jacking. Ideally a record might also have been kept of the pipe position while jacking load was applied during construction to monitor changes of pipe position whilst subjected to axial load.

In the instance of pipejacking through chalk, 1200mm internal diameter pipes were being installed. The final position of the installed pipes were surveyed in order to carry out re-inverting works in the tunnel. Examination of the change in position of the pipes revealed two points; firstly, misalignment of the pipes had been maintained to the same extent as during construction; secondly, the misalignments had progressed along the length of the tunnel in the direction of installation by about 5 metres.

In contrast to the pipejack in chalk, works for the construction of a 900mm internal diameter pipejack encountering gravels and water bearing ground had a very different behaviour. Problems during construction of the pipejack required large thrust loads to be applied, but no larger than for the pipejack in chalk, and this resulted in straightening of the pipejack. A survey of the positions of pipes after construction revealed 75% of the pipes to be in a near perfectly straight line. It was only the pipes towards the excavation face that maintained their misalignments because they were subjected to less axial load. Data from this pipejack are presented in Figure 9.3.
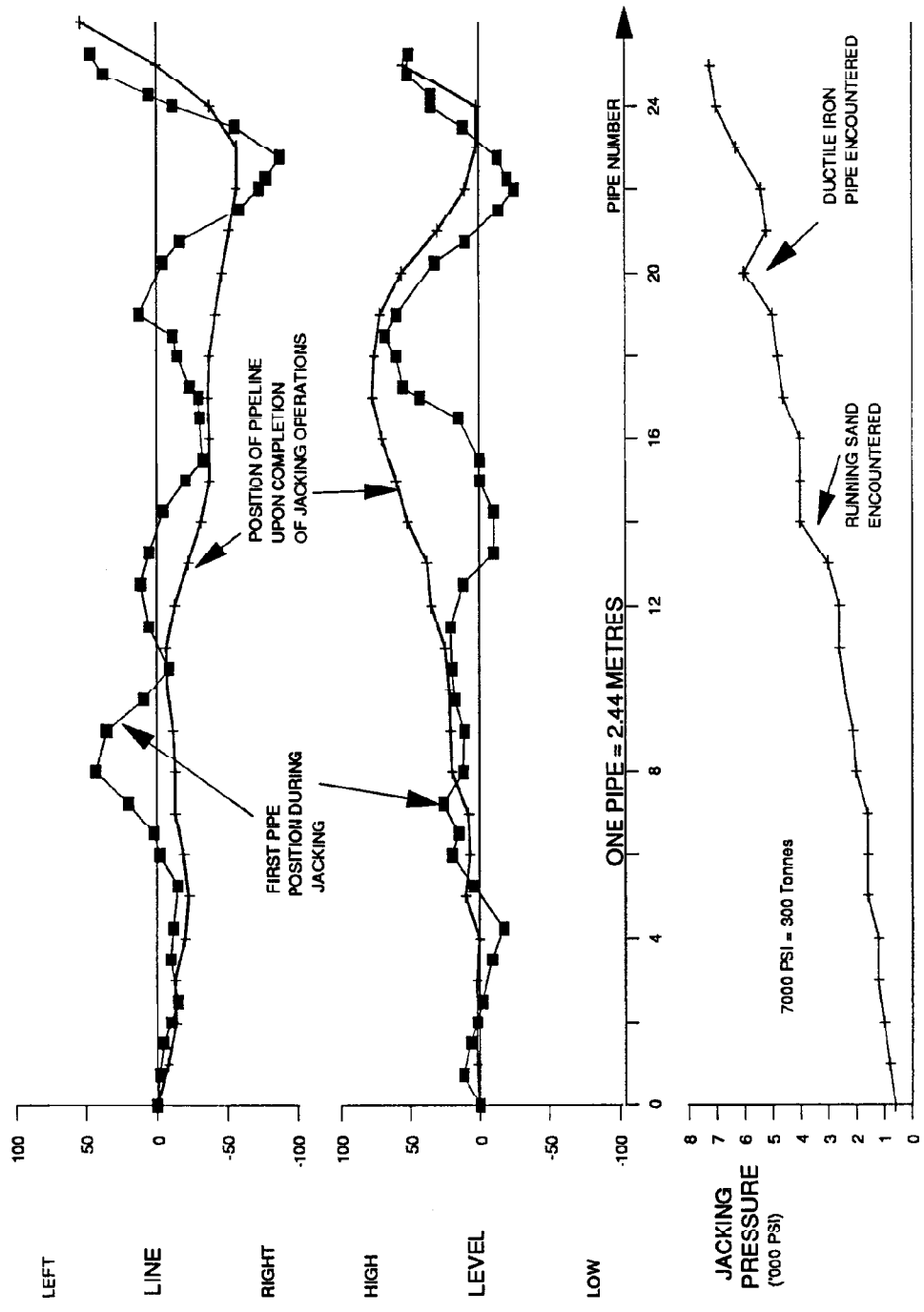
Figure 9.3 Variations of line and level from a 900mm diameter pipejack.

The two different behaviours described above can be related to the misalignment tests and the need for flexibility in the tension bar restraints during these tests. Study of the loads induced in the tension bars gives an indication of the resistance the ground around a pipejack must provide if realignment is prevented. Data are presented in Figure 9.4 by plotting pipe end deflection angle against the ratio of induced tension bar loads divided by applied axial load. This shows how with smaller deflection angle, less interaction occurs between the pipe and restraint and so less between the pipe and surrounding soil on a full-scale pipejack. It can be concluded from this evidence that for straighter pipejacks less force is required for installation.
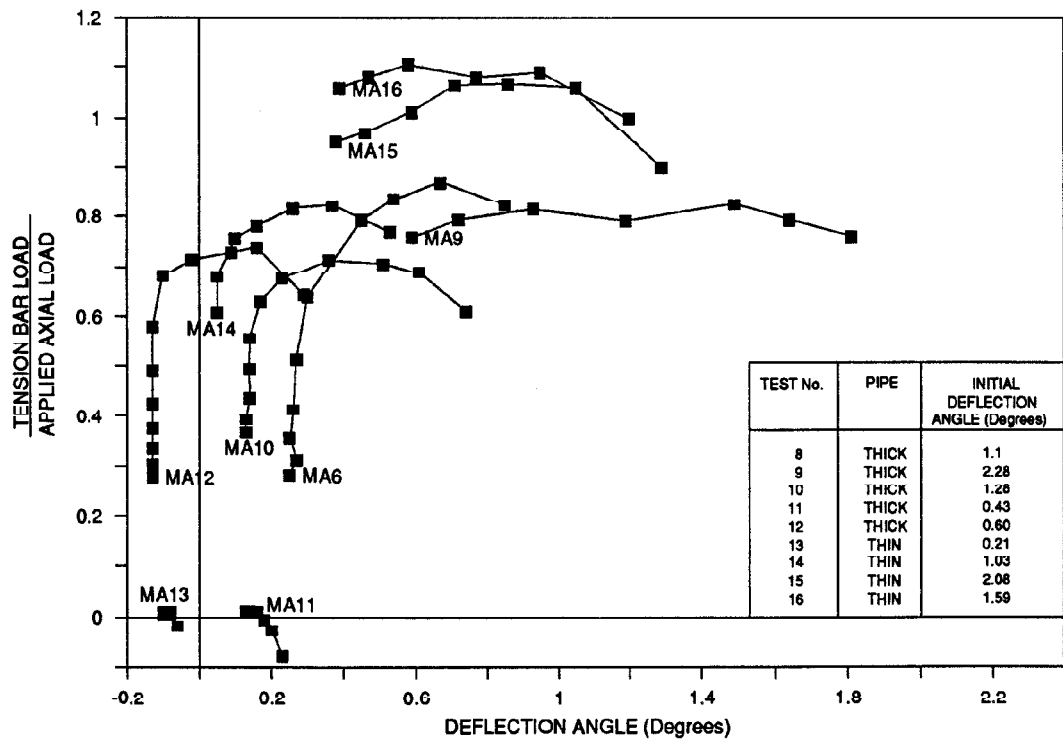
Figure 9.4 Change in ratio of applied axial load to total tension bar load as deflection angle changes.

9.4 Distribution of soil stress on the pipe

The theory for distribution of bending moments and circumferential forces in pipes is presented by Széchy (1967). However, to assess jacking loads during installation it is required to find the radial stress on the pipe and the angle of friction (δ) between the pipe and the surrounding soil.

Auld (1982) and the author presented analyses relating total jacking forces to soil stresses and pressure on the external surface of a pipe, but with no allowance taken for variations of total stress with depth below ground level. The initial analysis was presented in Section 2.6 and the following shows calculations for changing soil stress with depth below ground level.

Radial stresses on a pipe due to the imposed soil stresses can be deduced as shown below:-

$$\sigma_{vc} - \gamma R$$

$$K_0(\sigma_{vc} - \gamma R)$$

$$K_0 \sigma_{vc}$$

$$R$$

$$\sigma_{vc}$$

$$\sigma_{hc} = K_0 \sigma_{vc}$$

$$\alpha$$

$$\sigma_{vc} + \gamma R \sin \alpha$$

$$K_0(\sigma_{vc} + \gamma R \sin \alpha)$$

$$K_0(\sigma_{vc} + \gamma R)$$

$$\sigma_{vc} + \gamma R$$

σ_{vc} = total vertical stress at centroid of pipe
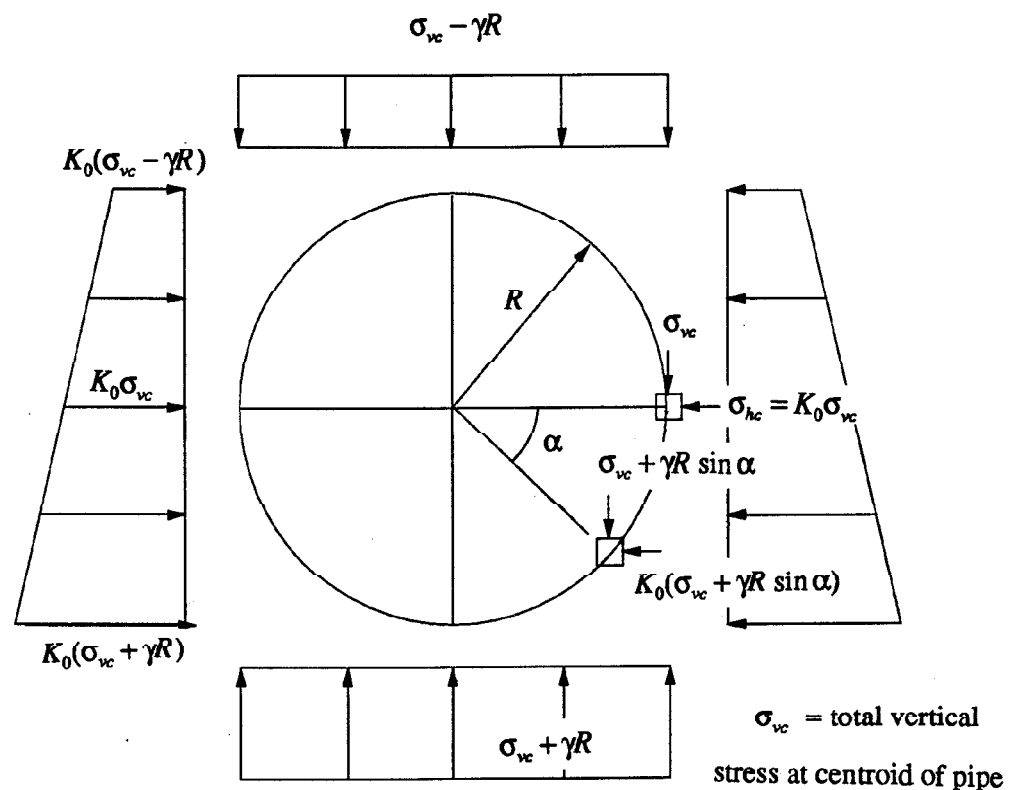
Figure 9.5a Soil stresses on a pipe.

Use Mohr's circle to find radial stress at any point.
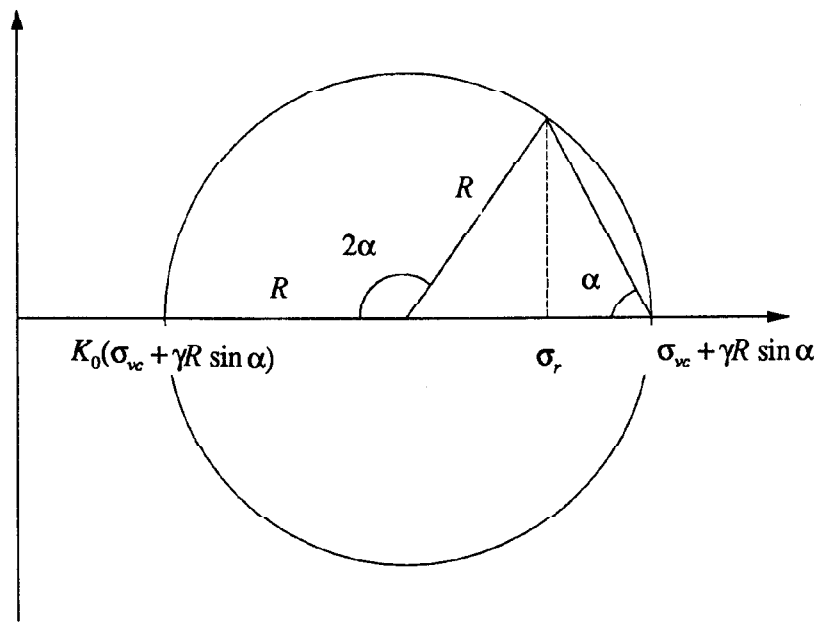
Figure 9.5b Mohr's circle of stresses on a pipe.

Radial stress at any point on the circumference of the pipe

$$\sigma_r = (\sigma_{vc} + \gamma R \sin\alpha)\left(\frac{1+K_0}{2}\right) + (\sigma_{vc} + \gamma R \sin\alpha)\left(\frac{1-K_0}{2}\right)\cos(\pi - 2\alpha)$$

$$\sigma_r = \left(\frac{\sigma_{vc} + \gamma R \sin\alpha}{2}\right)(1 + K_0 - (1 - K_0)\cos 2\alpha)$$

For

$$\alpha = \frac{\pi}{2} \qquad\qquad \sigma_r = (\sigma_{vc} + \gamma R)$$

$$\alpha = 0 \qquad\qquad \sigma_r = \sigma_{vc} K_0$$

$$\alpha = -\frac{\pi}{2} \qquad\qquad \sigma_r = (\sigma_{vc} - \gamma R)$$

Total load imposed on a pipe can be found by integrating:-

$$P_{TOTAL} = 2 \int_{-\frac{\pi}{2}}^{\frac{\pi}{2}} \sigma_r R \, d\alpha$$

$$= \int_{-\frac{\pi}{2}}^{\frac{\pi}{2}} R(\sigma_{vc} + \gamma R \sin\alpha)(1 + K_0 - (1 - K_0)\cos 2\alpha) d\alpha$$

$$= R \int_{-\frac{\pi}{2}}^{\frac{\pi}{2}} \sigma_{vc}(1 + K_0 - (1 - K_0)\cos 2\alpha) + \gamma R \sin\alpha(1 + K_0) - \gamma R(1 - K_0)(\sin\alpha\cos 2\alpha) d\alpha$$

$$= R\left[\sigma_{vc}(1 + K_0)\alpha - \sigma_{vc}(1 - K_0)\frac{\sin 2\alpha}{2} - \gamma R \cos\alpha(1 + K_0) + \gamma R(1 - K_0)\left(\frac{\cos 3\alpha}{6} - \frac{\cos\alpha}{2}\right)\right]_{-\frac{\pi}{2}}^{\frac{\pi}{2}}$$

$$P_{TOTAL} = \pi R \sigma_{vc}(1 + K_0) \qquad\qquad ...Eq\ 9.1$$
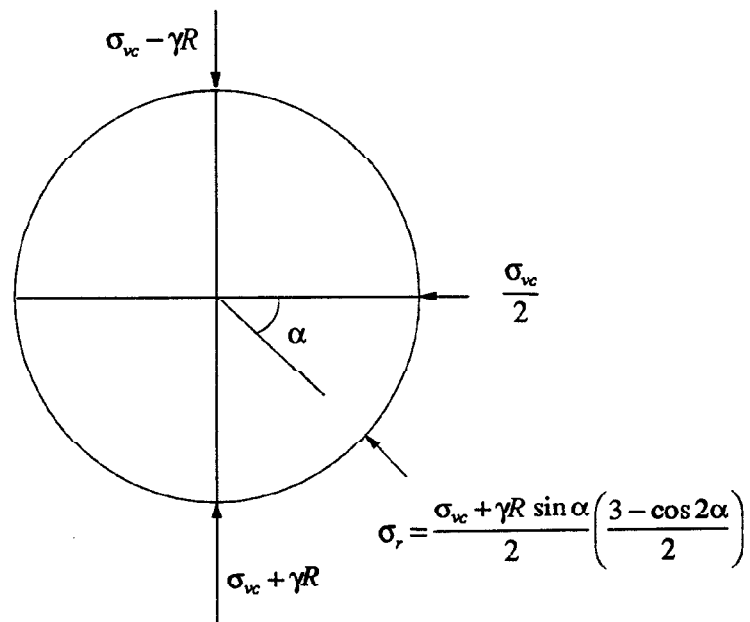
Figure 9.5c Stress distribution on a pipe for $K_0 = 0.5$
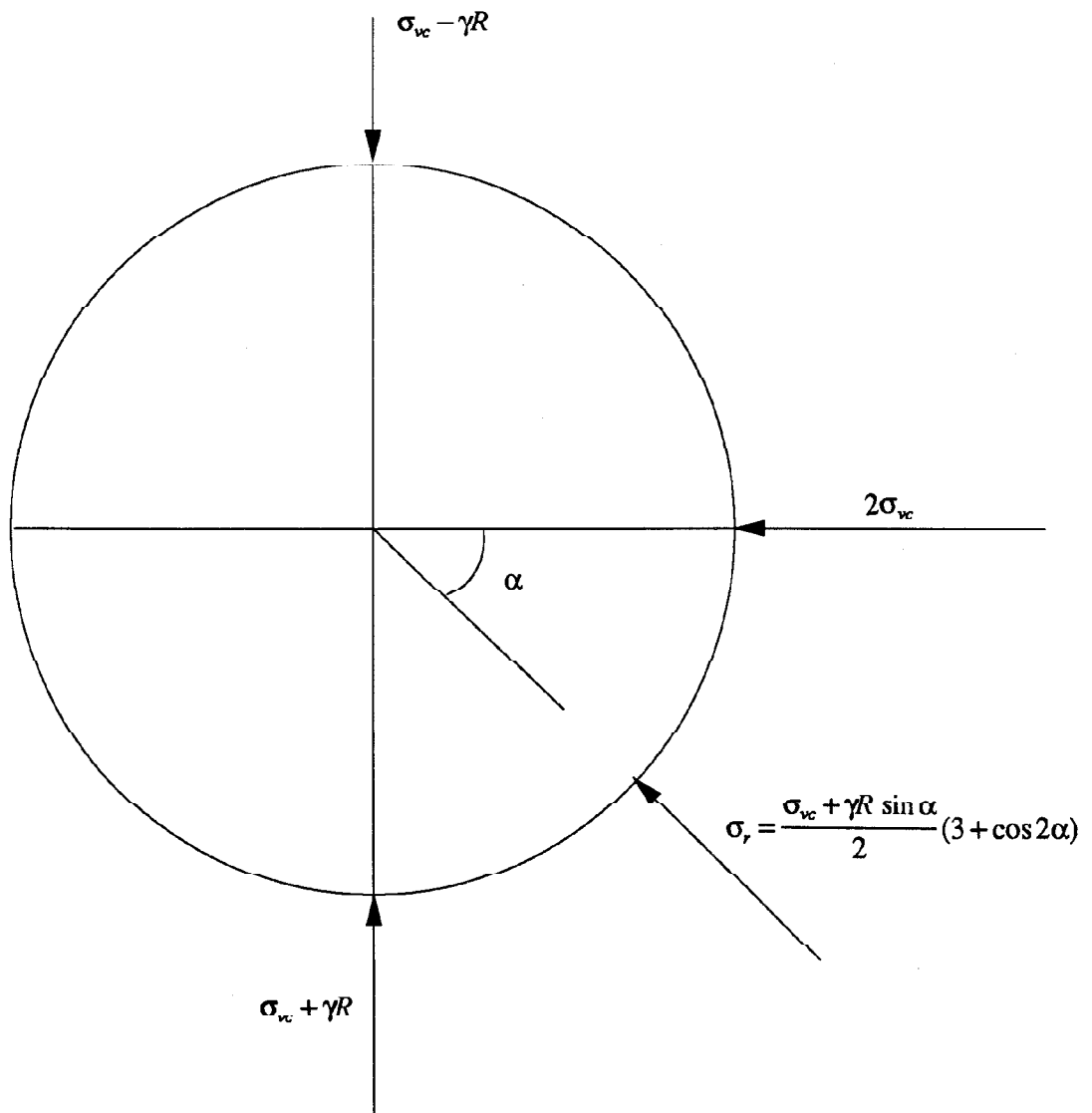
Figure 9.5d Stress distribution on a pipe for $K_0 = 2$

In the above analysis self weight of the pipe and its contents have been neglected. The jacking force required to push the pipe is found by relating frictional resistance, F, to the total pressure on the pipe and the angle of friction between the pipe and soil, δ.

$$F = P \tan \delta \qquad \text{...Eq 9.2}$$

where δ has previously been assumed as 0.7 of the angle of internal friction, ϕ , of the surrounding soil. This can be related to the prediction of jacking forces that were experienced in the moving pipe tests and is discussed in Section 9.5.

9.5 Angle of friction between sand and pipe

Reference is made to the graph in Figure 8.5, plotting mean sand stress against axial load on the pipes for data obtained during moving pipe tests. Whilst the data points appear to indicate a linear relationship between mean sand stress and jacking load, study of some literature suggests this may not be a correct assumption. Tomlinson (1969) presents a table relating angle of friction (δ) at the pipe/soil interface to the soil friction angle (ϕ) by the following constants for concrete to sand interfaces:-

Surface Finish	δ/ϕ for dry sand
smooth (made in metal formwork)	0.76
grained (made in timber formwork)	0.88
rough (cast on ground)	0.98

Table 9.1 Typical values of δ/ϕ from Tomlinson (1969).

However, study of more recent literature shows that the value of soil friction angle varies as mean soil stress changes. Bolton (1986) presents data showing that the variation can be attributed to dilatancy of the sand by the formula:-

$$I_R = I_D(10 - \ln p') - 1$$

where I_R = relative dilatancy index

I_D = relative density of sand

p' = mean sand stress

and $\phi - \phi'_{crit} = 5I_R$

where ϕ'_{crit} = critical state friction angle for Leighton Buzzard 14/25 sand = 35^0
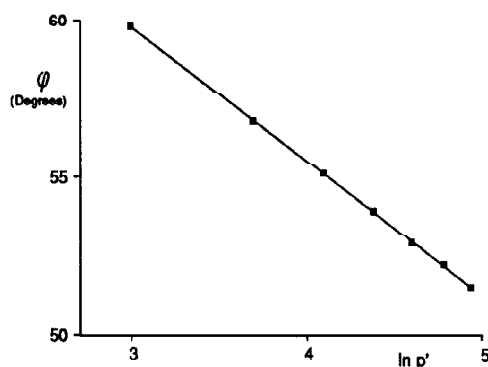
Soil friction angle can be linearly related to the logarithm of mean sand stress as shown in Figure 9.6 for a constant relative density of sand.

$\phi = 5(I_D(10 - \ln p') - 1) + \phi'_{crit}$

Figure 9.6 Relationship between ϕ and $\ln p'$.

Using Bolton's relationship for the relative dilatancy index and calculating values of soil friction angle at different levels of mean stress, it can be deduced that either the angle of friction between pipe and sand varies with soil stress level to maintain a constant ratio between δ and ϕ or the constants quoted by Tomlinson are dependent on mean sand stress for a constant δ value.

The data points plotted in Figure 8.5 are now assessed with the possibility that a linear relationship does not occur between the mean sand stress and applied axial load. The data are presented in Figure 9.7 where it can be seen that a curved line can be drawn between the data points. A second curve is plotted in the same figure which corrects mean soil stress at the boundaries of the test chamber to the estimated soil stress at the pipe/sand interface by interpolation using pressure cell readings as described in Section 9.2. The angle of friction

between the pipe and the soil is the inverse tangent of the axial load divided by the mean sand stress, which varies as the mean soil stress changes. Values of the angle of friction between the pipe and sand calculated from this gradient are tabulated below:-

Mean sand stress p' (kN/m²)	Soil friction angle φ (degrees)	Angle of friction δ between the pipe and sand. (degrees)	
		using boundary stresses	using estimated stress on pipe
20	59.8	64.5	68.6
40	56.8	61.7	66.3
60	55.1	59.9	64.9
80	53.9	58.3	64.1
100	52.9	56.5	62.9
120	52.2	55.0	62.1
140	51.5	53.7	60.5

Table 9.2 Comparison between values of φ and δ.

The curve obtained from the estimated mean stress at the pipe/sand interface appears to be the most reasonable calculation for finding the angle of friction at the interface. This would indicate that in the sand chamber the ratio between the angle of friction at the pipe/sand interface and the friction angle of the sand is 1.18. It is not possible for values of δ/φ to be greater than unity. It is therefore suggested thatinterferencefrom the close boundaries of the chamber and friction at the ports contributed significantly to increases in the axial load.

A comparison with the constants presented by Tomlinson would suggest a value of δ/φ of 0.76 should have been expected while δ/φ = 0.70 is usually used by pipejackers. A possible
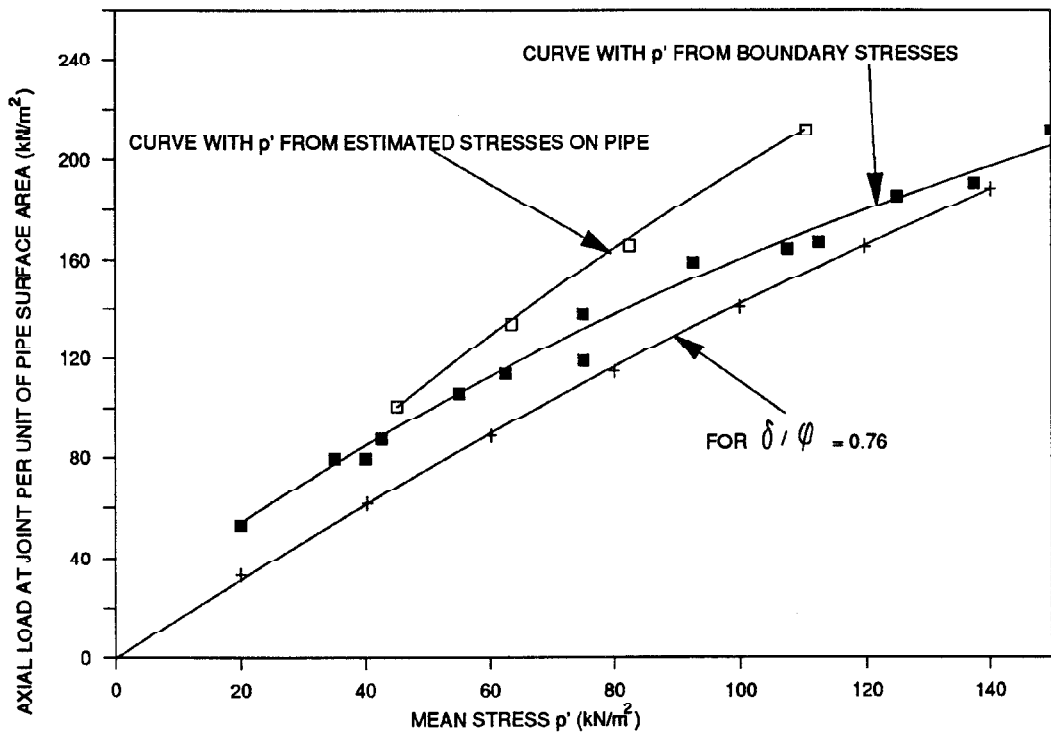
Figure 9.7 Variation of angle of friction between pipe and sand as mean stress level changes.

explanation for this discrepancy is that stresses develop in the sand as the pipe moves due to the interaction between the pipe and sand and the actual stresses imposed on the pipe became greater than estimated. The values quoted by Tomlinson are suggested design values and are likely to be lower bound. A curve is plotted in Figure 9.7 which is the theoretical relationship for δ/φ = 0.76 calculated as shown in the table below:-

p' (kN/m²)	φ (Degrees)	δ(forδ/φ= 0.76) (Degrees)	Axial Force F = P tan δ = p'πR2 tan δ (kN/m)
20	59.8	45.4	12.7
40	56.8	43.2	23.6
60	55.1	41.9	33.8
80	53.9	40.9	43.5
100	52.9	40.2	53.1
120	52.2	39.7	62.6
140	51.5	39.1	71.5

Table 9.3 Values of jacking force.

It can be concluded that for calculation of jacking forces in the test chamber a value of δ/φ of 1.18 should be used and estimates of stresses on the pipe should be made.

Following the paper presented by Bolton (1986) a discussion was published, Bolton (1987), by Tatsuoka suggesting that for values of mean stress below 150kPa further verification would be needed to prove the relationships used above. The discussion by Tatsuoka was based on experiments using Toyoura sand and suggested that when mean stresses were below 150kPa the friction angle of sand was constant. The author considers a reasonable case has been presented to justify the curved lines presented in Figure 9.7 for analysis of this research. It is noted that for the instance of predicting jacking forces it is the upperbound value of δ/φ that would usually be used.

9.6 Stresses measured at the chamber boundary during moving pipe tests

Palmeira (1987) conducted pull-out tests in a large cubical chamber on a number of reinforcement geotextiles. He presents data recorded from pressure cells mounted in the chamber wall through which the test samples were being pulled. A comparison of data recorded by Palmeira to the pressure cell data recorded during the jacked pipe tests is shown in Figure 9.8 and shows a much lower horizontal stress to bond stress ratio occurring for jacked pipe tests. The distribution of horizontal stresses is similar but the chamber used in the jacked pipe tests was much smaller and there was interference from the boundary walls.

The difference between Palmeira's work and this research is that Palmeira was testing under plane strain conditions and the pipejack tests were nearly axisymmetric. An analysis of the shear stresses on the pipe compared to the pressures and total loads on the end wall of the chamber might be expected to reveal comparable data. However, large differences occur which might be attributed to interference from boundaries of the chamber. It is more significant that very large pressures on the end wall of the chamber in close proximity to the outside of the pipe and large friction forces in the chamber ports due to the ingress of sand as the testing progressed, might have been occurring.
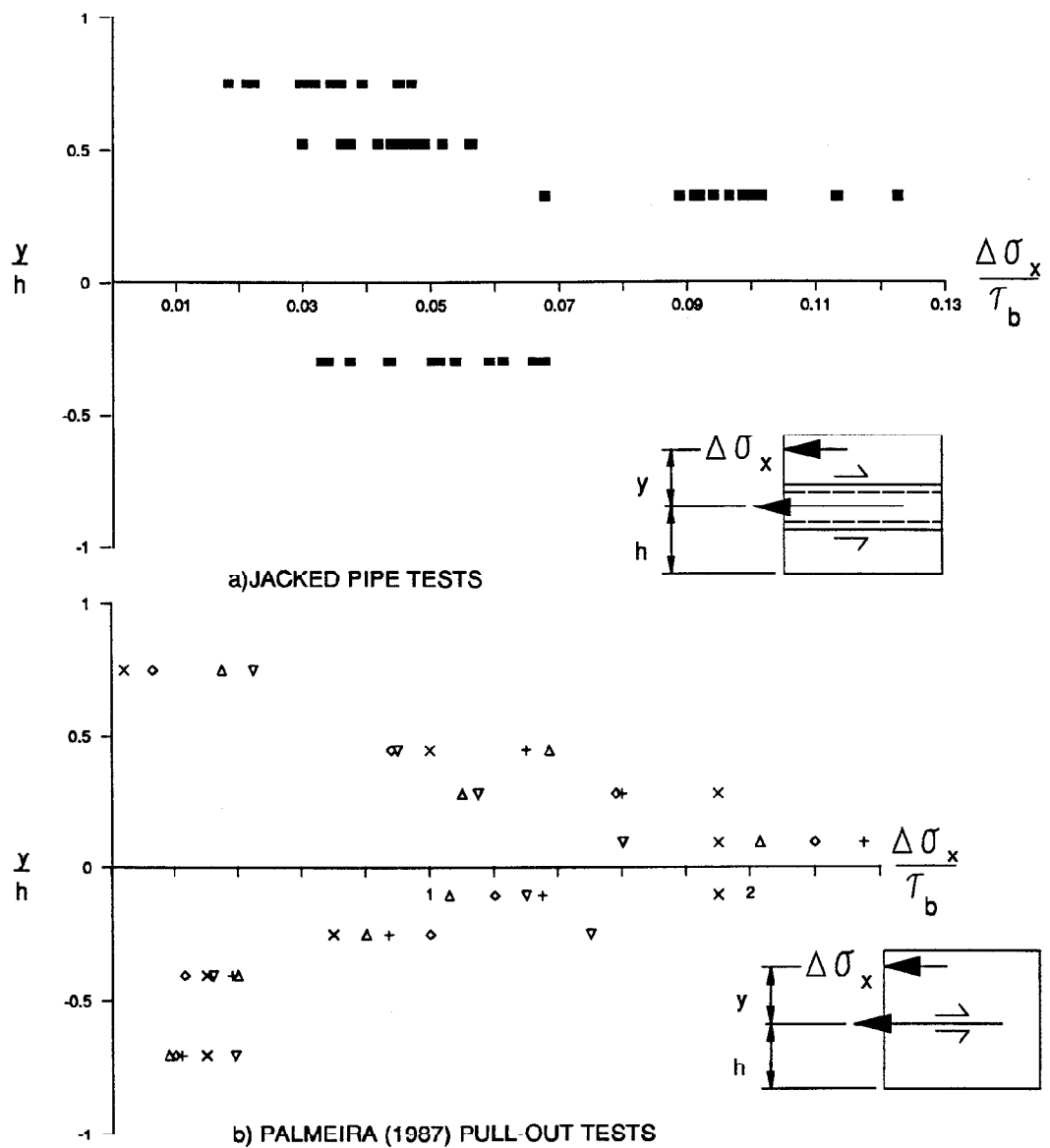
Figure 9.8 Comparison between boundary stresses for jacked pipe tests and pull-out test data obtained by Palmeira (1987).

9.7 Joint packing materials

Joint packing materials were not used in the model pipe tests; all testing has been on full-size prototype packing materials and analysis has been applied to a typical pipe of 900mm internal

diameter. The analysis and data presented in this Section apply only to the ability of a pipe joint to transmit axial jacking forces as a result of the type of packing material used and do not consider the possible failure of the pipe.

Data obtained during packing material tests were presented in Chapter 7 and are used here to assess total jacking loads when a maximum allowable compressive stress level was imposed at the pipe joint. Initially only the packing material was considered compressible and each test material was assessed for its capability of distributing stresses over as great an end area of the pipe as possible. These load capacities have been calculated for various materials and were presented in Table 7.2.

Elasticity of the pipe is considered next and reference has been made to Boresi and Sidebottom (1932) who have considered a thick walled cylinder subjected to axial loads. Change in length of the cylinder was considered due to uniform end loading by using the simple elastic formula

$$\Delta l = \sigma l / E$$

where
σ = stress on pipe end

E = elastic modulus

l = length of cylinder

Δl = change of length of cylinder

This simple relationship is used by the author in the consideration of deflected jacked pipes by assessing compression of narrow longitudinal slices of the pipe which are assumed to be subjected to uniform axial stress as shown in Figure 9.9. The effect of considering pipe elasticity is that axial stress is distributed over a greater end area of the pipe and hence more axial load can be applied within any given limiting stress level. The profile of stress distribution is not altered but is applied to a greater width of the pipe. The resulting compression of the pipe and packing material is exaggerated and shown in Figure 9.10.
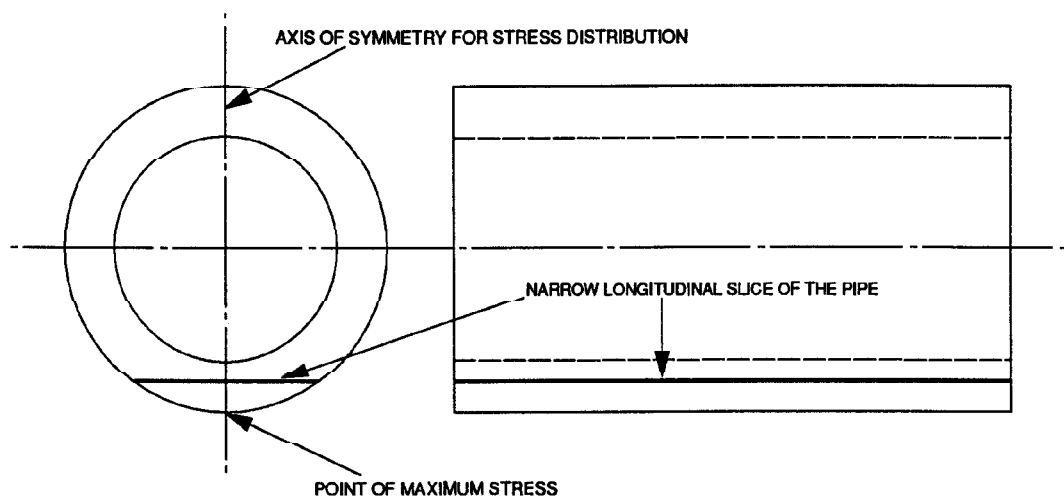
Figure 9.9 Longitudinal slice of the pipe subjected to uniform stress.

The league table of results presented in Table 7.2 is reassessed to take into consideration pipe elasticity. The results indicate that axial load capacity of the pipe is increased and some specific results are presented in Table 9.4. Looking at 18mm thick dense fibreboard for a 900mm internal diameter jacking pipe, where a pipejacking contractor would usually install a thrust rig capable of applying a jacking force of 300 tonnes but expects to use only 200 tonnes before installing an intermediate jacking station, the following can be stated:-

If the maximum allowable stress is $15N/mm^2$ and the packing material is dry then the joint deflection can be 0.2^0. However, if the allowable stress is $50N/mm^2$ with the same material, joint deflection can now be in excess of 0.5^0 for the same axial load capacity. It is noted that this consideration is for a packing material which is dry and that if the material becomes wet axial load capacity is increased. It is assumed that pipe ends are perfectly square when calculating axial load capacities and allowable joint deflections.
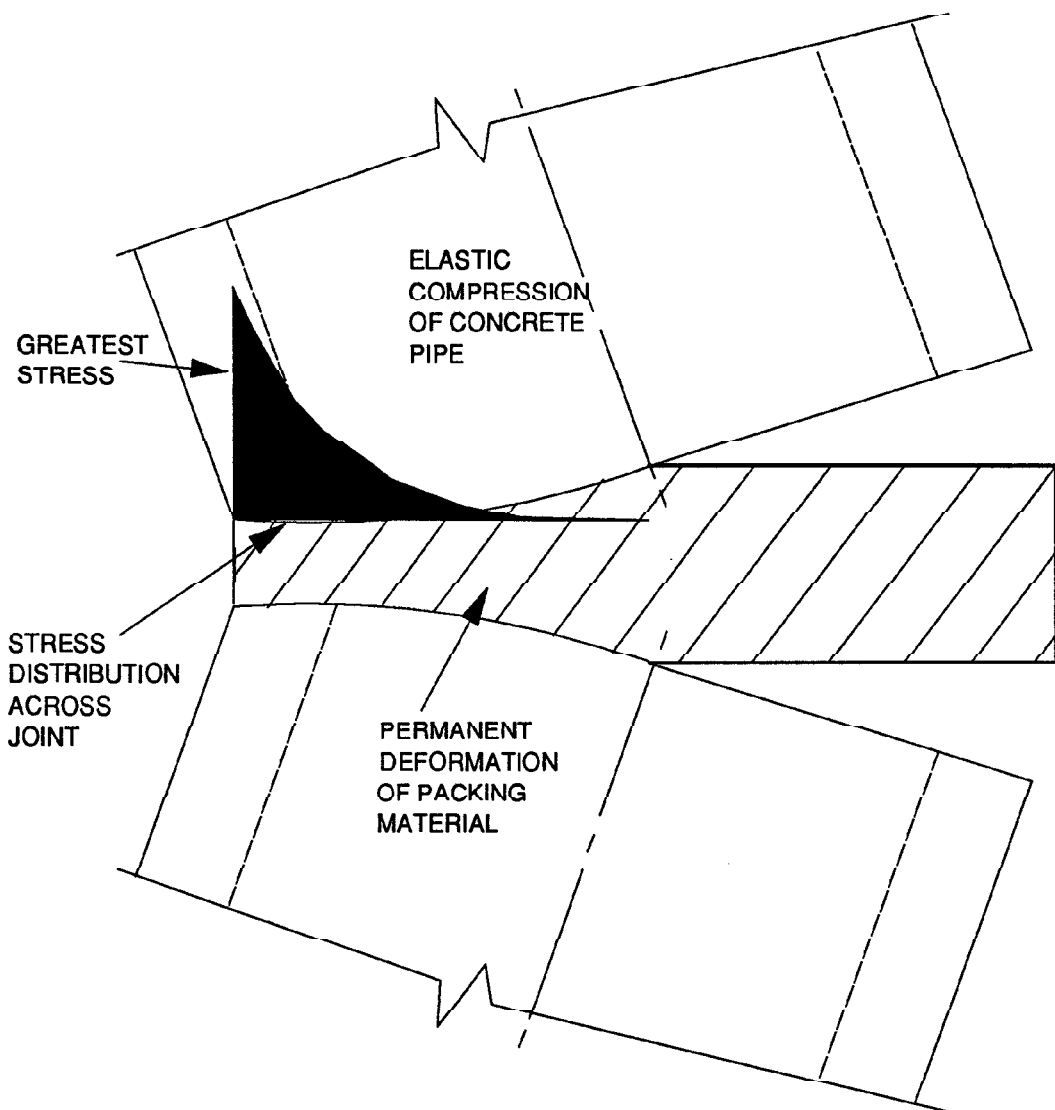
Figure 9.10 Exaggerated deformations of pipe and packing material.

The load that pipe manufacturers specify can be applied when jacking pipes is governed by a maximum end stress of 10-15N/mm² and they state that it should be evenly distributed; the author suggests that consideration of local concentrations of stress would change this requirement. Williams (1979) presented data shown in Figure 7.4 which suggests that small areas of concentrated stress are acceptable with up to four times the stress level that might usually be considered. It is argued that a stress level of 50N/mm² on a small area can be tolerated.

| Material Type | Allowable Axial Load (Tonnes) | | | | | | | | |
| | Deflection Angle between Pipes (Degrees) | | | | | | | | |
	0	0.025	0.05	0.1	0.2	0.3	0.5	0.75	1
FB1850	2572	1900	1485	1010	606	419	253	163	115
CB1850	2572	1806	1386	920	542	368	221	141	99
PLY1850	2572	1763	1297	840	488	328	192	121	86
FB1815	766	585	470	309	171	121	72	44	29
CB1815	766	532	393	241	131	89	51	29	20
PLY1815	766	471	329	195	104	69	38	22	14

This Table can be compared with the values quoted in Table 7.2 which did not allow for elasticity of the pipe. The values quoted assume pipe ends are square and the values are allowable axial loads for pipes with maximum allowable stresses as stated in the material type of either $15N/mm^2$ or $50N/mm^2$.

Table 9.4 Allowable axial loads allowing for elasticity of pipes.

All the data and load capacities presented in this section have been derived by considering a jacked pipe with the total end area of the pipe available for transmitting axial load. Pipes used for jacking are required to be watertight and have a joint profile and sealing ring to provide this. In the United Kingdom the in wall and steel collar joints shown in Figure 2.2 are usually used. Provision of this type of joint reduces the available end area for transmitting axial load. It is recognised in the pipejacking industry that rebating joint packing materials from the edge of the pipe prevents superficial damage. The axial load applied to the pipe is now considered allowing for the reduced end area and rebated materials on 900mm internal diameter pipes with either in wall or steel collar joints. The effect of the reduced available area is to decrease allowable jacking loads by between 10% and 20% compared with those quoted in Table 9.4.

Another consideration is that it is possible, in saturated ground conditions, for packing materials on the outside of a sealing ring used in an in wall jointed pipe to become wet and hence improve jacking capacity. On a steel collar jointed pipe the packing material is always on the inside of the joint sealing ring and cannot become wet in water bearing ground.

9.8 Profiled joint packing materials

There has been some speculation in the pipejacking industry during recent years about the possible use of profiled packing materials or pipes with ends that have a radius curve across the width of the pipe wall. The incentive behind this idea is the belief that jacking loads might best be transferred from pipe to pipe through the middle section of the wall thickness. However, the main endeavour should be to distribute axial load over a large end area of the pipe and this is no better achieved with radius pipe ends than with flat pipe ends or flat packing material. If the only objective is to maintain contact stresses to the middle section of the pipe wall this can be done equally well with flat packing materials of restricted width.

The author has conducted some studies on the possible use of profiles on pipes or packing materials. Results of tests on a profiled packing material were presented in Section 7.5. Further studies have been conducted into contact stresses at pipe joints with the use of radius profiles and reference has been made to literature presented by Johnson (1985) and Roark and Young (1976). Theoretical contact stresses at joints have been examined for concrete to concrete contact and for a packing material sandwiched between radius curved concrete surfaces. Details of the data obtained are presented in Table 9.5. No allowance has been made for pipes with ends that are not square or for pipes that have an angular deflection between them.

For a 900mm internal diameter pipe with concrete to concrete contact:-

Total axial load (kN)	Load/M on a 1050mm diameter (kN)	Maximum induced stress $\sigma_c = 0.591\sqrt{\frac{FE}{d}}$ (N/mm^2)		Contact width $b = 2.15\sqrt{\frac{Fd}{E}}$ (mm)	
		d = 100mm	d = 1000mm	d = 100mm	d = 1000mm
500	152	130	41	1.49	4.71
1000	303	183	58	2.10	6.65
1500	455	224	71	2.58	8.15
2000	606	259	82	2.97	9.40
2500	758	290	92	3.32	10.51
3000	909	317	100	3.64	11.51

For an 1800mm internal diameter pipe with concrete to concrete contact:-

Total axial load (kN)	Load/M on a 1950mm diameter (kN)	Maximum induced stress $\sigma_c = 0.591\sqrt{\frac{FE}{d}}$ (N/mm^2)		Contact width $b = 2.15\sqrt{\frac{Fd}{E}}$ (mm)	
		d = 100mm	d = 1000mm	d = 100mm	d = 1000mm
1000	163	134	42	1.54	4.88
2000	326	190	60	2.18	6.89
4000	653	269	85	3.09	9.76
6000	979	329	104	3.78	11.95
8000	1306	380	120	4.36	13.80
10000	1632	425	135	4.88	15.43

where d = end radius on pipe; F = applied load in kN/M; E = elastic modulus of concrete

$$= 31.7 \text{kN/mm}^2.$$

Table 9.5 Maximum stresses and contact widths for radius pipe ends without packing material.

It can be seen that maximum contact stresses are very high even in the ideal position with contact all around the circumferential end area of the pipe. Figure 9.11 shows how induced stresses and contact width vary as the radius on the pipe end is changed.

Now studying the case of packing material sandwiched between the concrete surfaces the following analysis is presented, using formulae from Roark and Young (1976):-

$$\text{Maximum induced stress} \quad \sigma_c = 0.798\sqrt{\frac{F}{k_d C_E}} \quad \text{...Eq 9.3}$$

where

$$C_E = \frac{1-v_1^2}{E_1} + \frac{1-v_2^2}{E_2}$$

F = applied load in kN/M

$E_1 = 31.7 kN/mm^2$

$v_1 = 0.22$ for concrete

E_2 and v_2 vary depending on packing material and stress level applied

and

k_d = end radius times two

Contact width

$$b = 1.60\sqrt{F k_d C_E} \quad \text{...Eq 9.4}$$

An example is calculated for 18mm dense fibreboard with maximum induced stresses of 15N/mm² and 50N/mm².

At 15N/mm², E_2 = 0.45kN/mm² and v_2 = 0.22, the applied axial load would be 1516kN/M of pipe mean circumference with a pipe end radius of 1000mm and contact width is 80.6mm.

At 50N/mm², E_2 = 0.1375kN/mm² and v_2 = 0.22, the applied axial load would be 54578kN/M of pipe mean circumference with a pipe end radius of 1000mm and contact width is 871mm.

This particular application of the analysis is limited due to the restricted wall thickness of the pipe as an 871mm contact width is clearly not possible when the pipe wall thickness is limited to 150mm. The analysis assumed semi-infinite materials were being loaded. With
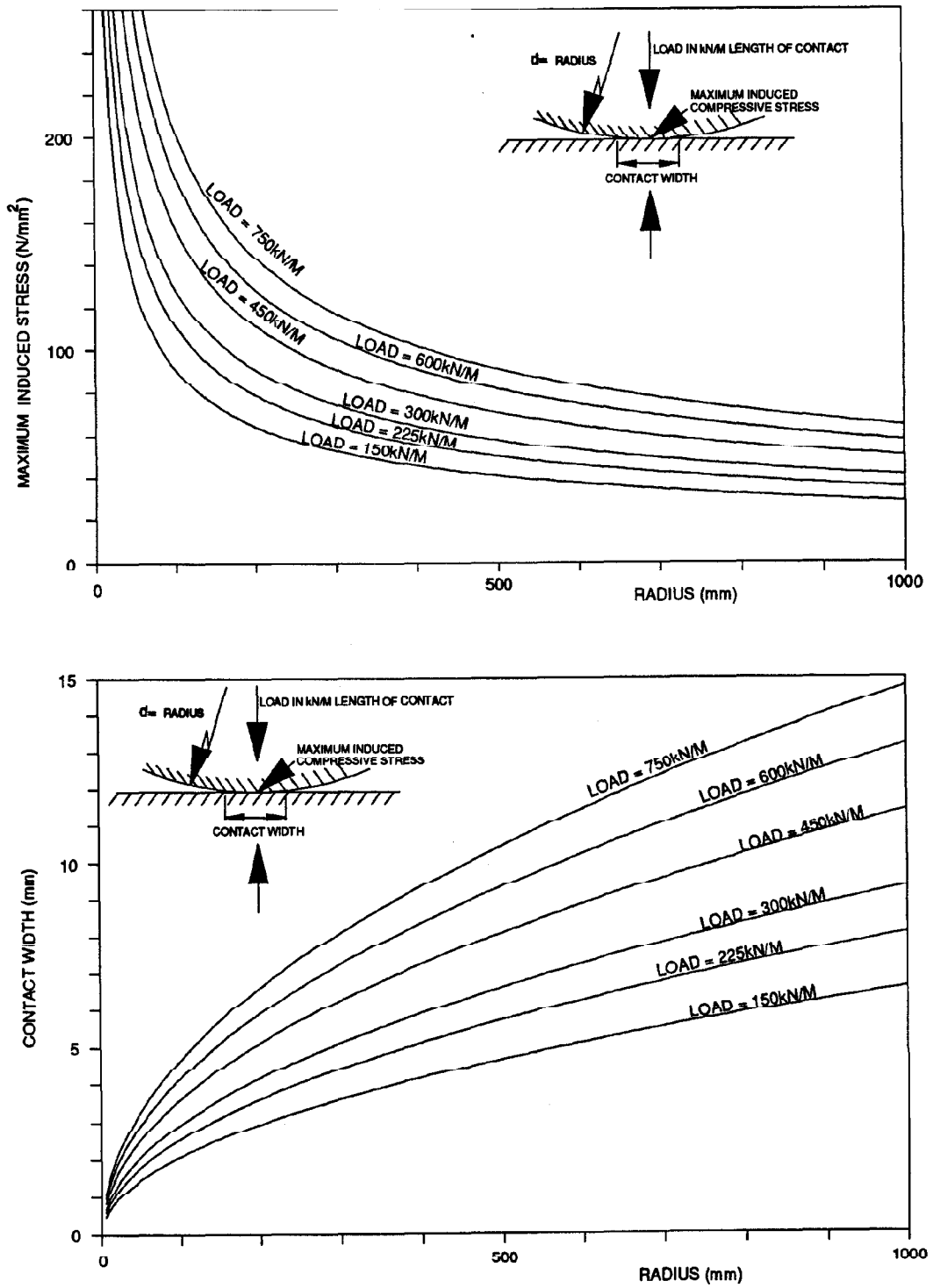
Figure 9.11 Variation of induced stresses and contact width for varying pipe end radii.

the restricted wall thickness imposed the maximum allowable stress of $50N/mm^2$ would reduce the maximum load but a comparison of the figures above to those obtained in Table 9.5 shows clearly the major benefits that can be achieved when using packing materials.

9.9 British Standard crushing tests

A number of tests was conducted during the progress of the research in accordance with clause 18.3 of BS 5911: part 4 (1986 draft). The test arrangement is shown in Figure 9.12 and the tests were used as a check on the repeatability of the quality of manufactured pipes. The control tests were all conducted to find the ultimate load capacity of the model pipes with results of 4.5kN for thin walled pipes and 8kN for thick walled pipes.

Figure 9.12   Test arrangement and strain gauge positions on British Standard crushing tests.

The British Standard requires inspection at various loads during a test for the occurence and width of cracks. At the required increments a feeler gauge is used to check the crack width.

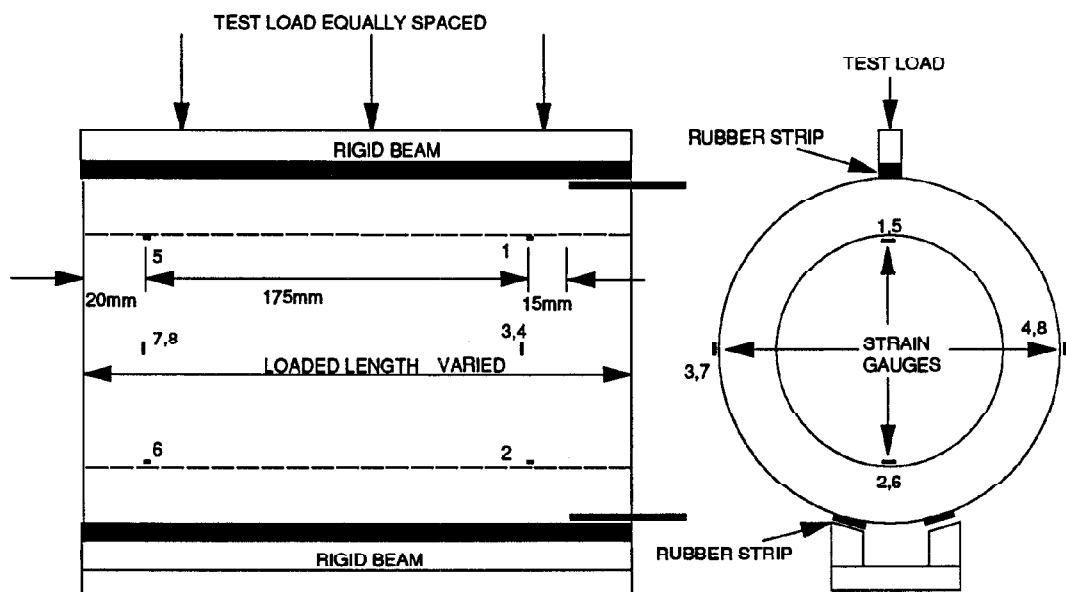It was not possible to use this inspection method on model pipes due to the effects of scaling and pipes were therefore instrumented with strain gauges. Rates of loading were scaled as were 'no crack', proof and ultimate load requirements as presented in Table 4.4.

Roark and Young (1976) present formulae for maximum and minimum bending moments induced in pipes and their positions. Some model pipes used for this research had strain gauges attached to measure the induced strains at the areas indicated by Roark and Young. The moments at the crown, M_c, and springing point, M_s, are related to the applied load, P, and the mean radius of the pipe, R, by the following constants:-

$$M_c = 0.318 \, P \, R$$
$$M_s = 0.182 \, P \, R$$

...Eq 9.5

Thus, the ratio of the magnitudes of M_c to M_s under elastic loading for this test should be 1.75. Results obtained from strain gauge readings corresponded closely with this figure as can be seen in Figure 9.13. Combining these relationships with elastic bending formulae allows an estimate of the apparent elastic modulus of the pipe material to be made. The values of apparent elastic modulus obtained are presented in Table 9.6 and the values generally over estimate elastic modulus of the concrete by a factor of two compared with the value of $31.7 kN/mm^2$ obtained from British Standard tests in accordance with BS 1881: part 112: 1983. Similar over estimates were found by Milligan (1988) for unreinforced concrete and clay pipes with internal diameters of between 225mm and 600mm.
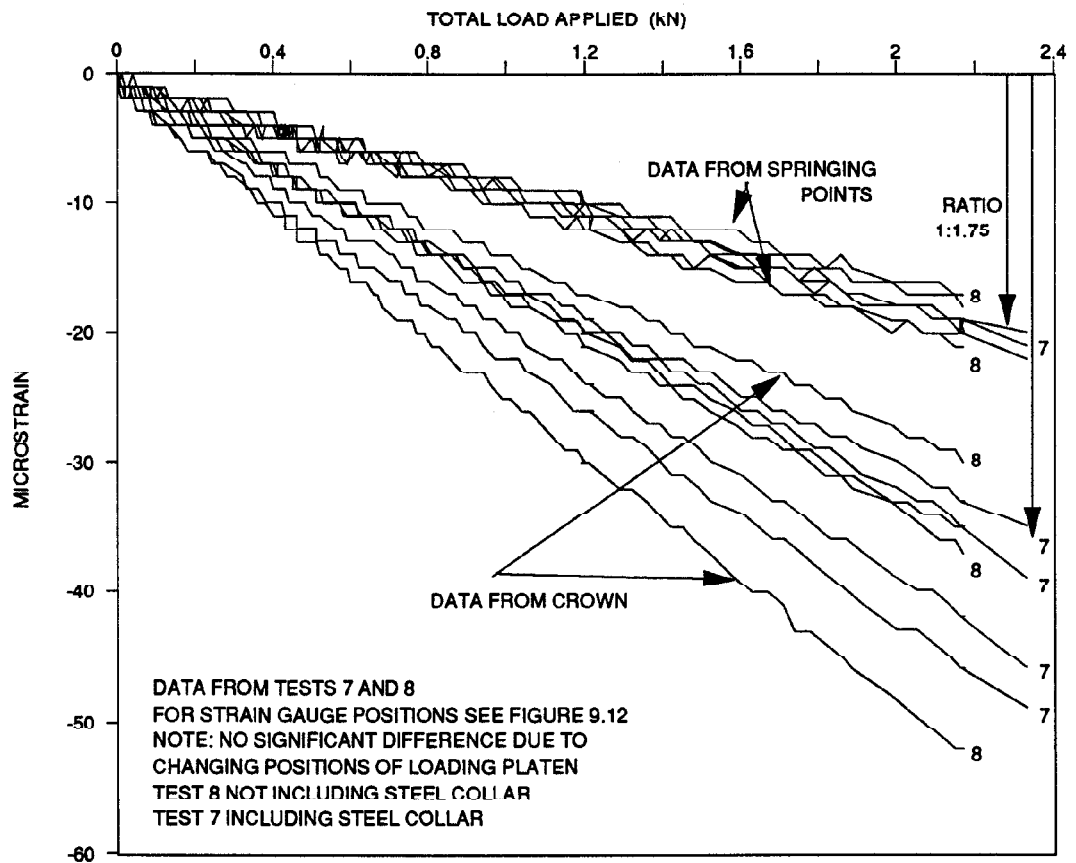
Figure 9.13 Strain gauge readings from British Standard crushing tests.

Another area of interest was the affect of steel collars on the test results. This was assessed by placing the loading platens on either the full length of the pipes including the steel collar or on the concrete surface only. The strain gauge readings recorded are presented in Figure 9.13 and it appears that positioning of the loading platen does not significantly affect the results.

Test No.	Pipe wall thick- ness	Elastic modulus at crown (kN/mm^2)	Elastic modulus at springing (kN/mm^2)
1	thin	94.7	89.0
2	thin	64.2	60.0
3	thick	41.2	21.4
4	thick	49.0	31.8
5	thick	61.8	70.8
6	thick	65.5	70.8
7	thick	74.2	77.2
8	thick	57.8	63.7

Table 9.6 Values of apparent elastic modulus from crushing test results.

CHAPTER 10

CONCLUDING REMARKS

The work presented in this dissertation is the first stage of an overall programme that is to continue with fieldwork monitoring. It has begun with laboratory based model experiments which will be correlated to pipe behaviour on construction sites during the next phase of the research. The complete programme is being conducted with close cooperation and interaction from industrial partners who have invaluable information and experiences to contribute.

A review of pipejacking and construction site practice was presented in Chapter 2 which highlighted the details of the system and where further research was required. This dissertation has detailed a laboratory based model test project that has investigated pipe behaviour, effects of deflection between consecutive pipes, use of joint packing materials and predictions of the angle of friction at the pipe/soil interface.

During the initial test series it was discovered how pipes align themselves when subjected to high axial loads. This has been related to alignment of pipes on pipejacks carried out in granular materials. The effect of ingress of sand into pipe joints, causing spalling of the concrete, was noted. The importance of assessing pipes in their three dimensional orientation has been presented and how this can be related to typical line and level measurements on pipejack construction sites.

The tests continued to assess the pipes' axial load capacities when they were restrained in a misaligned position as might be the instance when jacking in rock or stiff cohesive materials or jacking around curves. Failures of the pipes were observed due to cracking and crushing attributed to compression, tension, shear or bending failure dependent on the loading geometry. Pipes were instrumented with strain gauges to give details of magnitudes of stress induced in them. It was noted how very different distributions of stress occur on the internal and external surfaces of the pipe. With loading applied along one edge of the pipe the major principal compressive stresses were double on the inside face of the pipe compared to the outside of the pipe. However, if axial loading was applied diagonally across a pipe, significant tensile strains were measured on the external surface of the pipe orientated around the pipe's circumference. These were accompanied by major principal compressive strains on the inside surface of the pipe but in alignment between the loading positions. Most significantly initial cracking was on the outside of the pipe and associated with measured maximum shear strains.

Significant forces were measured in tension bars which were used to measure the modelled interaction between the pipe and surrounding soil. It was seen how these forces were occurring with high deflection angles and were relatively small or had stopped changing when deflection angles became small. The occurrence of shear forces at the positions where yokes restrained the pipes was noted. It seems reasonable to conclude from this evidence and the results of moving pipe tests that any deviation from line or level on a pipejack would significantly contribute to increased jacking loads.

During the misaligned pipe tests measurements were taken of changes in the shape of the pipes. The changes in pipe diameter were found to be significant when loading along one edge of the pipe and it may prove possible to measure these in the field exercise that is to follow this initial stage. When diagonal loading was applied to the pipes, changes in the shape of the pipe occurred, distorting the pipe to the shape of a parallelogram when it was viewed perpendicularly to the plane of loading.

A large number of different types of joint packing materials has been tested and the results analysed to predict theoretically allowable jacking loads on pipes for different deflected angles. The most suitable packing material was dense fibreboard and it was found that the material became much more suitable for distributing jacking loads when it became wet. The parameters for the ideal packing material were assessed by its ability to distribute load concentrations over as large an end area of the pipe as possible whilst not inducing excessive tensile stresses in the concrete. It is noted that the packing material plays an important role in distributing stress concentrations caused by irregularities of the end surface of a pipe or any lack of end squareness that might have occurred during manufacture. The effects of cyclic loading are very important to enable full assessment of packing materials as they are permanently deformed as soon as they have been loaded and unloaded once. After the first load cycles the materials tested had little change in stress/strain compression characteristics unless stress magnitudes were increased.

It is suggested that it would be in the best interests of pipejacking if manufacturers were to supply packing material already attached to the ends of pipes before deliveries were made to site. This would not only enable a standard to be maintained throughout the industry but would aid the positioning of packing material on the pipe which has proven to be significant in the prevention of superficial damage.

Comments have been made about the ability of concrete to be subjected to local areas of high concentrations of stress and how pipe manufacturers' recommendations of mean stress levels distributed over the full end area of the pipe are perhaps a little ambiguous.

The advantages of using joint packing material have been presented and 18mm thick dense fibreboard is recommended as the most suitable from the selection of materials tested. It is advantageous for the material to become wet and essential to assess cyclic loading when

comparison is made with other materials. The research to date has not highlighted any significant difference in the performance of either in wall or steel collar jointed pipes, although each pipe joint type has specific applications for which it is suitable.

The ability of a pipe to sustain axial load has been theoretically analysed based on the test results. From these studies it was found that a 900mm internal diameter pipe with 18mm thick dense fibreboard packing material should be able to sustain likely jacking loads with a deflection angle of 0.5^0 and an allowable maximum stress of $50N/mm^2$. It is important that deflection angles of pipes are measured with axial load applied as they are in a different orientation compared with pipes which are not loaded. This must be monitored in the fieldwork project to assess the extent of lateral pipe movement when subjected to jacking loads. A theoretical approach to assessing the use of radius profiled ends and/or packing material has been made but requires further analysis to allow for the finite thickness of pipe walls.

Some experiments were conducted to assess the effect of moving pipes through the sand filled chamber and to estimate the angle of friction at the pipe/soil interface. This was found to be dependent on the level of stresses applied to the boundary of the chamber. Some discussion has been presented about the likely changes of friction angle as mean stress magnitudes change based on Bolton's (1986) paper and the subsequent discussion. The jacking resistances in the chamber appeared unrealistically high perhaps due to the inability to model the overbreak that would normally occur during construction. This led to dense sand surrounding the pipe whereas on a prototype pipejack it is more likely that material around the pipe would be loose.

During the progress of this test series the frictional resistance at the chamber ports was measured whilst pushing pipes through them, to enable correlation and allowance for this

friction when pushing pipes through the sand filled chamber. Pushing the pipes through the chamber ports while monitoring axial load was found to be an efficient method of measuring the pipes' external diameter deviations.

Studies have been presented analysing the distribution of radial stresses around the pipe due to the loading from the soil and how this can be used to predict resistance to jacking. The importance of an accurate assessment of mean soil stress and the angle of friction at the pipe/soil interface has been noted in order to predict the jacking load. Studies have been conducted by other authors, Haslem (1986) and O'Reilly and Rogers (1987) to assess the effects of line and level deviations on the prediction of jacking load. This research has reinforced the importance of maintaining near perfectly straight pipejack lines during installation in order to minimise jacking forces.

The remarks conclude with some recommendations and discussion about how the research programme might influence pipejack monitoring and site control. Appropriate fieldwork measurements to be made in the future research are discussed and an approach to a new British/European Standard test for assessing a pipe's ability to be jacked is outlined.

It has become clear that it is not sufficient to monitor only line and level if high axial loads are being applied and large deviations of angle between pipes are being experienced. It is necessary to account for and measure deflection angles between pipes and squareness of pipe ends. The simplest method of carrying out this monitoring seems to be by measurements of the joint gap between consecutive pipes, measured at various points around the circumference. The fieldwork exercise should be able to correlate measurements of joint gap to line and level deviations, deflection angles, load distribution at the joint and compression of packing material.

Discussions with the industrial sponsors of the research have highlighted the importance of both contractor and client using only personnel experienced in pipejacking for day to day

supervision of construction. The personnel should be acquainted with the various methods of excavation and working in different ground conditions, the importance of accurate and regular monitoring and prediction of problems before they arise. It is important to use tunnel excavation labour experienced specifically with pipejacking in order to avoid line and level deviations that have occurred when using insufficiently trained or supervised labour. The importance of trained labour and management, both from the contractor and client, cannot be overlooked.

Further work is required to assess the effects of many high axial load cycles applied to pipes close to intermediate jacking stations.

It is suggested that the required British Standard works test to assess axial load capacity of jacking pipes could be developed from the test series on misaligned pipes. Perhaps, at this stage it is time for testing of full-size pipes in a suitable compression machine, the same machine to be used by all pipe manufacturers.

As previously stated this project was part of a continuing programme of research which will soon commence with the monitoring of some pipejacks in the field. The immediate areas of interest that would benefit from research during the field exercise are detailed below:-

1   The prime consideration will be to monitor distribution of stresses in the pipejacking system. How is load transferred from pipe to pipe and how does the surrounding ground interact? What are the distribution of stresses on the outside of the pipe and what shear stresses are developed at the pipe/soil interface?

2   Confirmation of the distribution of stresses in full-size misaligned pipes, correlated to those found in misaligned pipe tests in the laboratory.

3   Monitoring of the use of dense fibreboard packing material, its compression and distribution of stresses at pipe joints.

4   Suitable instrumentation and transducers should be installed to allow for long term monitoring, although this will not be the prime consideration in their design.

5   It would be useful to assess the different loading conditions imposed on pipes at the leading end and trailing end of pipejacks and also in the vicinity of intermediate jacking stations.

6   Correlation can be carried out with the laboratory results and data to determine design safety factors that could be used to prevent the occurrence of pipe damage.

7   The use of lubricants in pipejacking and the closure of overbreak onto the pipes can be assessed. It will be important to monitor carefully soil conditions and for at least one of the monitored pipejacks to include an extensive site soil investigation, before, during and after installation.

8   The reuse of instrumented pipes is worthy of consideration.

9   Measurements of lateral movements of pipes when subjected to axial load should be carried out.

10   Manufacturers should now be able to proceed with development of a more suitable Standard test to assess a pipe's ability to sustain jacking load.

The research programme would benefit from an attempt to model mathematically the pipejacking system in axisymmetry or preferably in three dimensions. This would complement the overall programme, perhaps confirming some of the results found in the laboratory and to be found in the fieldwork. It is suggested that the numerical modelling would begin with attempting to assess the misaligned pipe tests by analysing individual pipes and would progress to model a string of pipes in a soil. It would be interesting to attempt to correlate between experimental and numerical results, magnitude and direction of the concrete strains on the internal and external walls of the pipe.

REFERENCES

American Concrete Pipe Association, (1960). Jacking Reinforced Concrete Pipelines. Virginia, U.S.A.

Auld, F. A., (1982). Determination of Pipe Jacking Loads. Paper presented at Pipe Jacking Conference, Manchester.

Bassett, R. H., (1979). The Use of Physical Models in Design. Proceedings of the 7th European Conference on Soil Mechanics and Foundation Engineering, Brighton. Vol. 5 pp 253-270.

Bieganousky, W. A. and Marcuson, W. F., (1976). Uniform Placement of Sand. Journal of the Geotechnical Engineering Division, ASCE. Vol. 102. No. GT3.

Bolton, M. D., (1986). The Strength and Dilatancy of Sands. Geotechnique 36, No. 1, pp 65-78.

Bolton, M. D., (1987). The Strength and Dilatancy of Sands. Geotechnique 37, No. 2, pp 219-226.

Boresi, A. P. and Sidebottom, O. M., (1932). Advanced Mechanics of Materials. Wiley and Sons, Inc. New York.

British Constructional Steelwork Association Ltd. and Constructional Steel Research and Development Organisation, (1978). Structural Steelwork Handbook. Properties and Safe Load Tables.

British Standard 1881: (1983). Methods of Testing Concrete. British Standards Institute. London.

British Standard 5500: (1985). Specification for Unfired Fusion Welded Pressure Vessels. British Standards Institute, London.

British Standard 5911: Part 4 (1986 Draft). Precast Concrete Pipes and Fittings for Drainage and Sewerage: Specification for Jacking Pipes with Flexible Joints. British Standards Institute, London.

British Standard 8110: (1985). Structural Use of Concrete. British Standard Institute, London.

Byles, R., (1983). Streeter Pushes to Pipe Jack Record on Poole Sewer. New Civil Engineer, 30th June, pp 18-19, London.

Clarke, N. W. H., (1968). Buried Pipelines. A Manual of Structural Design and Installation. McLaren and Sons, London.

Clarkson, T. E. and Thompson, J.C., (1983). Pipe Jacking: State-of-the-Art in U.K. and Europe. Journal of Transport Engineering Division. Vol. 109(1) pp 57-72.

Code of Practice 110: Part 1 (1972). The Structural Use of Concrete, superseded by BS 8110 (1985). British Standard Institute, London.

Cole, J. M., (1986). 2.1 Metre Diameter Pipe Jack at Greenwich. Paper presented at Pipe Jacking Conference, London.

Concrete Pipe Association - personal communication.

Concrete Pipe Association of Australia, (1983). Pipe Jacking bulletin.

Craig, R. N., (1983). Pipe Jacking. A state-of-the-art review. Construction Industry Research and Information Association. Technical Note 112.

Dewar, J. D., (1964). The Indirect Tensile Strength of Concrete of High Compressive Strength. Technical Report No.377. Cement and Concrete Association, London.

Donnel, L. H., (1976). Beams, Plates and Shells. McGraw-Hill.

Drennon, C. B., (1979). Pipe Jacking State-of-the-Art. Journal of Construction Division, ASCE. Sept. 1979 pp 217-223.

Dumbleton, B., (1988). Record Pipejack Run Slows to a Halt. New Civil Engineer, 21st July, London.

Durden, J. A., (1982). Overcoming Jacking Pressures. Paper presented at Pipe Jacking Conference, Manchester.

Erntroy, H. C., (1960). The Variation of Works Test Cubes. Research Report No. 10. Cement and Concrete Association, London.

Evans, D. J. and Clark, L. A., (1978). A Machine for Cold Rolling Deformed Reinforcing Bars for Model Tests. Magazine of Concrete Research. Vol.30 No.102 pp 31-34.

Evans, D. J. and Clarke, J. L., (1981). A Comparison between the Flexural Behaviour of Small Scale Microconcrete Beams and that of Prototype Beams. Technical Report No.542. Cement and Concrete Association. London.

Haslem, R. F., (1986). Pipe Jacking Forces: from Theory to Practice. Proceedings of Infra-structure, Renovation and Waste Control Centenary Conference, pp 173-180. N.W. Association, Institute of Civil Engineers.

Hornung, K., Karlsruhe, K. S., Waldbronn, R. L. and Villmar, A. P., (1987). Berechnung und Konstruktion von Vortiebsrohren nach DVGW GW 312/ATV A 161. Beton-und-Stahlbetonbau No. 10 and 11, Berlin.

Hough, C. M., (1974). Concrete Pipe Jacking in the U.K. Tunnels and Tunnelling. Vol. 6 No.3.

Hough, C. M., (1986). Progress in Pipe Jacking Standards. Conference Proceedings. Pipe Jacking Association, London.

Hughes, B. P. and Chapman, G. P., (1966). The Deformation of Concrete and Microconcrete in Compression and Tension with Particular Reference to Aggregate Size. Magazine of Concrete Research. Vol. 18 No. 54.

Johnson, K. L., (1985). Contact Mechanics. University Press. Cambridge.

Kirkland, C. J., (1982). The Need for Research. Paper presented at Pipe Jacking Conference, Manchester.

Last, N. C., (1985). Notes on Seminar for Cone Penetration Testing in the Laboratory. Department of Civil Engineering, Southampton University.

Milligan, G. W. E., (1986). Current Research in Pipe Jacking. Conference Proceedings. Pipe Jacking Conference, London.

Milligan, G. W. E., (1988). Comparison of Load-Strain Performance of Clay and Concrete Pipes. Report to the Concrete Pipe Association, Leicester.

Newman, A., (1986). The Economics of Non-Disruptive Construction. Proceedings of the Pipe Jacking Association, London.

Noor, F. A. and Khalid, M., (1980). Deformed Wire Reinforcement for Microconcrete Models. Reinforced and Prestressed Concrete Models. Edited Garas and Armer. pp 103-118.

Noor, F. A. and Wijayasri, S., (1982). Modelling the Stress Strain Relationship of Structural Concrete. Magazine of Concrete Research. Vol. 34 No. 118 pp 25-34.

O'Reilly, M. P. and Rogers, C. D. F., (1987). Pipe Jacking Forces. Proceedings of the International Conference on Foundations and Tunnels. Vol. 2 pp 201-208. Edited McForde, Edinburgh Engineering Technics Press.

Palmeira, E. M., (1987). The Study of Soil-Reinforcement Interaction by means of Large Scale Laboratory Tests. Ph.D. Thesis, University of Oxford.

Peckham, G. A., (1987). The Joint Face Strength Test for Pipejacked Pipes. Final Year Report. University of Oxford.

Pipe Jacking Association - personal communication.

Pipe Jacking Association, (1981). A Guide to Pipe Jacking Design.

Pipe Jacking Association, (1986). Jacking Concrete Pipes. Pipe Jacking Association Design and Specification Bulletin No. 1.

Pomeroy, C. D., (1972). The Effect of Curing Conditions and Cube Size on the Crushing Strength of Concrete. Technical Report No. 470. Cement and Concrete Association, London.

Richardson, H. W. and Mayo, R. S., (1941). Practical Tunnel Driving. McGraw- Hill, New York and London.

Richardson, M. A., (1970). Pipeforcing: An Appraisal of Ten Years of Operation. Tunnels and Tunnelling. July 1970 pp 215-219.

Richardson, M. A. and Scruby, J., (1981). Earthworm System will threaten Conventional Tunnel Jacking. Tunnels and Tunnelling, April 1981 pp 29-32.

Roark, R. J. and Young, W. C., (1976). Formulas for Stress and Strain. McGraw-Hill, New York.

Sabnis, G. M., Harris, H. G., White, R. N. and Mirza, M. S., (1983). Structural Modeling and Experimental Techniques. Prentice Hall.

Sabnis, G. M. and Mirza, M. S., (1979). Size Effects in Model Concretes. Journal of Structural Engineering Division, ASCE. Vol.105. ST6. pp 1007-1020.

Shullock, S. H., (1982). Problems in Tunnelling by Pipe Jacking at Tilehurst. Journal of the Institute of Water Engineers and Scientists. April 1982 pp 151-153.

Széchy, K., (1967). The Art of Tunnelling. Budapest.

Tomlinson, M. J., (1969). Foundation Design and Construction. Pitman Publishing, London.

Tsui, S. H. and Mirza, M. S., (1969). Model Microconcrete Mixes. Structural Concrete. No. 223.

Waldron, P., Pinkney, M. W. and Perry, S. H., (1980). The Construction of a 1/12th Scale Prestressed Concrete Bifurcated Bridge Model. Reinforced and Prestressed Microconcrete Models. Edited Garas and Armer. Construction Press, Lancaster.

Wallis, S., (1982). West Feltham Pipe Jackers Push into the Future. Tunnels and Tunnelling. June 1982 pp 41-42.

Watson, T. J., (1987). Trenchless Construction for Underground Services. Construction Industry Research and Information Association. Technical Note 127.

Weiler, W. A. and Kulhawy, F. H., (1982). Factors Affecting Stress Cell Measurements in Soil. Journal of Geotechnical Engineering Division, ASCE. December 1982 GT12 pp 1529-1548.

White, R. N., (1983). Models for Structural Concrete Design. Handbook of Structural Steel. Edited Kong et al.

White, H., Moss, A. and Rowlands, E., (1988). Making Micro Work. Proceedings of the No-Dig Conference, Washington, U.S.A.

White, I. G. and Clark, L. A., (1980). Bond Similitude in Reinforced Microconcrete Models. Reinforced and Prestressed Microconcrete Models. Edited Garas and Armer. pp 67-75.

Williams, A., (1979). The Bearing Capacity of Concrete Loaded over a Limited Area. Technical Note 526. Cement and Concrete Association, London.

Williams, D. G. and Aalami, B., (1979). Thin Plate Design for In Plane Loading. Granada, London.

Winfield, R., (1986). The River Bullin Contract. Conference Proceedings. Pipe Jacking Association, London.

Winney, M., (1987). Scottish Pipe Push Mystery Prompts New Clay Joint Research. Underground Magazine, September 1987, London.

Winney, M., (1988 a). Berlin Pushes on Microtunnelling Innovation. Underground Magazine, September 1988, London.

Winney, M., (1988 b). Data Necessity. New Civil Engineer, 6th October, London.